

SEPTEMBER 1966

# STATISTICAL ANALYSIS OF THRUST VECTOR CHARACTERISTICS FOR ROCKET ENGINE CLUSTERS

Prepared for:

**NATIONAL AERONAUTICS AND SPACE ADMINISTRATION**  
**GEORGE C. MARSHALL SPACE FLIGHT CENTER**  
**Astrionics Laboratory**

(THRU) nm  
 (CODE) 28  
 (CATEGORY)

(ACCESSION NUMBER) 237  
 (PAGES) 28  
 (NASA CR OR TMX OR AD NUMBER)

UNDER CONTRACT NAS8-20211

GPO PRICE \$ \_\_\_\_\_

CFSTI PRICE(S) \$ \_\_\_\_\_

Hard copy (HC) 7.00

Microfiche (MF) \_\_\_\_\_

ff 653 July 65

**NORTHROP SPACE LABO**

6025 TECHNOLOGY DRIVE, HUNTSVILLE, ALABAMA 35805  
 TELEPHONE 837-0580  
 P. O. BOX 1484

167 18412

FACILITY FORM 602

4 STATISTICAL ANALYSIS OF THRUST VECTOR CHARACTERISTICS  
FOR ROCKET ENGINE CLUSTERS

Northrop/Huntsville Technical Memorandum No. 303

9 September 1966

by

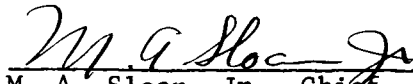
( J. W. Bradford  
F. L. Echols  
J. E. Hilliard  
W. E. Hinds  
L. R. Murdock

Prepared for:

National Aeronautics and Space Administration  
George C. Marshall Space Flight Center  
Astrionics Laboratory

Under Contract NAS8-20211

Reviewed and Approved by:

  
M. A. Sloan, Jr., Chief, Control Dynamics and Structural Dynamics Group

  
Dr. Steve S. Hu, Technical Director, Northrop/Huntsville

1 NORTHROP SPACE LABORATORIES  
HUNTSVILLE, ALABAMA 3

# FOREWORD

This report summarizes a technical study performed by Northrop Space Laboratories, Huntsville, Alabama, under Contract No. NAS8-20211 to the Astrionics Laboratory of the George C. Marshall Space Flight Center. Acknowledgement is extended to Messrs. H. Kennel and B. Wiesenmaier of the Guidance and Control Division for their sponsorship of and their many contributions to the study.

# ABSTRACT

This report documents a technical study undertaken to define a general solution for determining the statistical properties of the resultant thrust and moment vectors generated by a cluster of rocket engines. Ideally, the resultant thrust vector of a powered rocket vehicle with zero steering command should be directed along the longitudinal axis of the vehicle. The resultant thrust vector of an actual stage is a statistical quantity containing errors in both magnitude and direction. In addition the propulsion system in general applies an unwanted moment vector to the vehicle.

Although the attitude control system of a guided rocket automatically cancels any moment due to thrust misalignment, thrust alignment errors are important since such errors decrease the dynamic range of the actuation system and may cause degradation of vehicle performance both in atmospheric and exo-atmospheric flight.

Effort under this study was divided into two areas: (1) the derivation of a classical probability solution of the engine cluster problem, supported by a Monte Carlo simulation and (2) the statistical analysis of the resultant vector of actual engine clusters, based on information secured from engine manufacturers, engine and stage alignment personnel, etc.

The derivation of a frozen-time classical solution to the engine cluster problem, along with the statistical assumptions made, is given in the report. The solution is expressed in terms of a three-dimensional coordinate system embedded in the thrust frame and containing the thrust frame centerline as an axis. An interface is defined between the engine and the thrust frame such that a given engine type need be analyzed only once, regardless of the cluster



configuration in which it is used. Vector quantities are treated as triads and covariance matrices for the resultants are derived as explicit functions of the input tolerances. A different solution occurs for each of the following configurations: a single center engine, two engines side-by-side, and a ring of three or more equally spaced engines. Methods are given to combine the effects of several rings, thus extending the applicability of the solution to a wide class of geometries. In addition the solution is extended to include moments about a statistically located vehicle center of gravity. According to the results of the classical solution, variances of the resultant probability distributions are independent of the input shapes, provided the input variances and covariances are fixed.

The classical solution provides a means of optimizing the engine cluster geometry and input error budget. A number of the more obvious observations concerning geometrical and error budget optimization are listed in the report.

Extensive field investigations were conducted to obtain statistical and geometrical data on the H-1, J-2, and F-1 rocket engines and the corresponding Saturn stages in which they are used. Statistical models of each of these engines are presented based on static test firings, and complete analyses of the S-I and S-IC stages are given. Close agreement between the classical and Monte Carlo solutions was obtained in both cases.

Recommendations are made concerning both engine alignment procedure and additional research work.

# TABLE OF CONTENTS

<u>Section</u>	<u>Title</u>	<u>Page</u>
	ABSTRACT . . . . .	iii
	LIST OF FIGURES . . . . .	iv
	LIST OF TABLES . . . . .	ix
	DEFINITION OF SYMBOLS AND TERMS. . . . .	xi
I	INTRODUCTION . . . . .	1-1
II	TECHNICAL APPROACH . . . . .	2-1
III	COORDINATE SYSTEM AND TRANSFORMATION . . . . .	3-1
IV	CLASSICAL PROBABILITY SOLUTION OF AN ENGINE CLUSTER . . . . .	4-1
V	STATISTICAL OPTIMIZATION OF AN ENGINE CLUSTER . . . . .	5-1
VI	MONTE CARLO SIMULATION. . . . .	6-1
VII	CURRENT ALIGNMENT REQUIREMENTS AND TECHNIQUES FOR SATURN VEHICLE STAGES . . . . .	7-1
VIII	STATISTICAL MODELS FOR SATURN ENGINES AND STAGES . . . . .	8-1
IX	CONCLUSIONS . . . . .	9-1
X	RECOMMENDATIONS . . . . .	10-1
XI	REFERENCES. . . . .	11-1
	APPENDIX A. DERIVATION OF COORDINATE TRANSFORMATIONS . . . . .	A-1
	APPENDIX B. DERIVATION OF CLASSICAL SOLUTION . . . . .	B-1

# LIST OF FIGURES

<u>Figure No.</u>	<u>Title</u>	<u>Page</u>
1-1	EFFECTS OF THRUST VECTOR MISALIGNMENT ON A HYPOTHETICAL TWO-DIMENSIONAL ROCKET VEHICLE. . . . .	1-3
3-1	ENGINE CLUSTER COORDINATE SYSTEM . . . . .	3-2
4-1	COORDINATE SYSTEM USED FOR DERIVATION OF MOMENT ABOUT VEHICULAR C.G. . . . .	4-20
7-1	MODEL SPECIFICATION REQUIREMENTS . . . . .	7-4
7-2	ALIGNED ENGINE FOR S-I AND S-IB STAGES IN A VERTICAL STATIC CONDITION . . . . .	7-5
7-3	MODEL SPECIFICATION REQUIREMENTS . . . . .	7-7
7-4	ALIGNED ENGINE TO S-IC STAGE ORIENTATION IN VERTICAL STATIC CONDITION . . . . .	7-8
7-5	MODEL SPECIFICATION REQUIREMENTS . . . . .	7-10
7-6	ALIGNED ENGINE FOR S-II STAGE ORIENTATION IN VERTICAL STATIC CONDITION . . . . .	7-11
7-7	ALIGNED ENGINE FOR S-IVB STAGE ORIENTATION IN VERTICAL STATIC CONDITION . . . . .	7-11
7-8	BIPROPELLANT LIQUID-FUEL ROCKET ENGINE. . . . .	7-13
7-9	H-1 THRUST CHAMBER AND GIMBAL . . . . .	7-14
7-10	DOME-BEARING ASSEMBLY . . . . .	7-18
7-11	H-1 ENGINE ALIGNMENT STAND WITH INSTRUMENTS IN POSITION	7-22
7-12	H-1 ENGINE ALIGNMENT STAND BASIC GEOMETRY . . . . .	7-23
7-13	THRUST CHAMBER CALIBRATION FIXTURE. . . . .	7-24
7-14	PLACEMENT OF THRUST CHAMBER CALIBRATION FIXTURE, H-1 OUTBOARD ENGINE . . . . .	7-25
7-15	ALIGNMENT STAND AND WORK PLATFORM . . . . .	7-27
7-16	ENGINE ACCEPTANCE THRUST MEASURING SYSTEM SCHEMATIC .	7-29
7-17	F-1 ENGINE ACCEPTANCE TEST STAND SCHEMATIC. . . . .	7-30
7-18	TYPICAL STAGE SECTION . . . . .	7-33

LIST OF FIGURES (continued)

<u>Figure No.</u>	<u>Title</u>	<u>Page</u>
7-19	THRUST STRUCTURE ASSEMBLY. . . . .	7-34
7-20	S-IC STAGE VERTICAL ASSEMBLY TOOL. . . . .	7-36
7-21	STAGE TOOLING MARKS . . . . .	7-37
7-22	STAGE ALIGNMENT . . . . .	7-38
7-23	ENGINE-TO-STAGE ALIGNMENT, S-I STAGE . . . . .	7-40
8-1	LOAD CELL ARRANGEMENT, DYNAMIC TEST STAND, OUTBOARD H-1 ENGINE . . . . .	8-3
8-2	COORDINATE SYSTEM AND ACTUATOR POSITIONS, H-1 ENGINE .	8-6
8-3	SAMPLE PATTERN OF DYNAMIC THRUST AND MOMENT COMPONENTS, 836 kN (188 KIP) H-1 R&D ENGINE . . . . .	8-12
8-4	SAMPLE PATTERN OF DYNAMIC THRUST AND MOMENT COMPONENTS, 900 kN (200 KIP) H-1 R&D ENGINE . . . . .	8-13
8-5	COORDINATE SYSTEM, J-2 ENGINE. . . . .	8-16
8-6a	HISTOGRAMS OF DYNAMIC THRUST COMPONENTS, J-2 ENGINE .	8-21
8-6b	HISTOGRAMS OF DYNAMIC MOMENT COMPONENTS, J-2 ENGINE .	8-22
8-7	COORDINATE SYSTEM, F-1 ENGINE. . . . .	8-25
8-8a	HISTOGRAMS OF DYNAMIC THRUST COMPONENTS, F-1 ENGINE .	8-31
8-8b	HISTOGRAMS OF DYNAMIC MOMENT COMPONENTS, F-1 ENGINE .	8-32
8-9	THRUST FRAME GEOMETRY, S-I STAGE . . . . .	8-33
8-10	HISTOGRAMS FOR RESULTANT THRUST AND MOMENT VECTOR COMPONENTS, 500 MONTE CARLO TRIALS, NORMALLY DISTRI- BUTED INPUTS, S-I STAGE. (a) MAIN THRUST COMPONENT .	8-41
8-10b	SIDE THRUST COMPONENT ALONG PITCH AXIS . . . . .	8-42
8-10c	SIDE THRUST COMPONENT ALONG YAW AXIS . . . . .	8-43
8-10d	MOMENT ABOUT ROLL AXIS . . . . .	8-44
8-10e	MOMENT ABOUT PITCH AXIS . . . . .	8-45
8-10f	MOMENT ABOUT YAW AXIS. . . . .	8-46

LIST OF FIGURES (concluded)

<u>Figure No.</u>	<u>Title</u>	<u>Page</u>
8-11	THRUST FRAME GEOMETRY, S-IC STAGE. . . . .	8-47
8-12	TYPICAL PROBABILITY DENSITY FUNCTIONS FOR MOUNTING ERRORS, S-IC STAGE . . . . .	8-49
8-13	HISTOGRAMS FOR RESULTANT THRUST AND MOMENT VECTOR COMPONENTS, 1500 MONTE CARLO TRIALS, NORMALLY DISTRI- BUTED INPUTS (CASE 1) S-IC STAGE. (a) MAIN THRUST COMPONENT. . . . .	8-54
8-13b	SIDE THRUST COMPONENT ALONG PITCH AXIS . . . . .	8-55
8-13c	SIDE THRUST COMPONENT ALONG YAW AXIS . . . . .	8-56
8-13d	MOMENT ABOUT ROLL AXIS . . . . .	8-57
8-13e	MOMENT ABOUT PITCH AXIS . . . . .	8-58
8-13f	MOMENT ABOUT YAW AXIS. . . . .	8-59
8-14	HISTOGRAMS FOR RESULTANT THRUST AND MOMENT VECTOR COMPONENTS, 1500 MONTE CARLO TRIALS, NORMALLY DISTRI- BUTED INPUTS (CASE 2) S-IC STAGE. (a) MAIN THRUST COMPONENT. . . . .	8-61
8-14b	SIDE THRUST COMPONENT ALONG PITCH AXIS . . . . .	8-62
8-14c	SIDE THRUST COMPONENT ALONG YAW AXIS . . . . .	8-63
8-14d	MOMENT ABOUT ROLL AXIS . . . . .	8-64
8-14e	MOMENT ABOUT PITCH AXIS . . . . .	8-65
8-14f	MOMENT ABOUT YAW AXIS. . . . .	8-66
8-15	THRUST FRAME GEOMETRY, S-II STAGE. . . . .	8-68
8-16	THRUST FRAME GEOMETRY, S-IVB STAGE . . . . .	8-68
A-1	COORDINATE AXES AND TRANSFORMATION SEQUENCE . . . . .	A-2
A-2	TRANSFORMATION OF FORCES AND MOMENTS ACTING ON A RIGID BODY . . . . .	A-3
A-3	TYPICAL CENTER ENGINE MOUNTING . . . . .	A-3

LIST OF TABLES

<u>Table No.</u>	<u>Title</u>	<u>Page</u>
2-1	CONVERSION FACTORS USED IN THIS STUDY, ENGLISH UNITS TO INTERNATIONAL UNITS. . . . .	2-7
5-1	A COMPARISON OF RING RADIUS FOR RING AND CENTER ENGINE CONFIGURATIONS . . . . .	5-10
8-1	LOAD CELL READINGS DUE TO ENGINE THRUST, R&D H-1 ENGINE. . . . .	8-4
8-2(a)	DERIVED DYNAMIC FORCE AND MOMENT COMPONENTS, INBOARD R&D H-1 ENGINE (836 kN). . . . .	8-8
8-2(b)	DERIVED DYNAMIC FORCE AND MOMENT COMPONENTS, OUTBOARD R&D H-1 ENGINE (900 kN) . . . . .	8-9
8-3(a)	STATISTICAL PARAMETERS, 836 kN (188 kip) R&D H-1 ENGINE	8-10
8-3(b)	STATISTICAL PARAMETERS, 900 kN (200 kip) R&D H-1 ENGINE	8-11
8-4	MANUFACTURER'S DYNAMIC TEST DATA, J-2 ENGINE . . . . .	8-15
8-5a	ENGINE THRUST AND MOMENT COMPONENTS IN METRIC UNITS, J-2 ENGINE. . . . .	8-15
8-5b	ENGINE THRUST AND MOMENT COMPONENTS IN ENGLISH UNITS, J-2 ENGINE. . . . .	8-19
8-6	STATISTICAL PARAMETERS, J-2 ENGINE. . . . .	8-20
8-7	MANUFACTURER'S DYNAMIC TEST DATA, F-1 ENGINE . . . . .	8-24
8-8a	ENGINE THRUST AND MOMENT COMPONENTS IN METRIC UNITS, F-1 ENGINE. . . . .	8-28
8-8b	ENGINE THRUST AND MOMENT COMPONENTS IN ENGLISH UNITS, F-1 ENGINE. . . . .	8-29
8-9	STATISTICAL PARAMETERS, F-1 ENGINE. . . . .	8-30
8-10	NOMINAL VALUES AND TOLERANCES, ENGINE-TO-STAGE MOUNTING PARAMETERS, S-I STAGE . . . . .	8-35
8-11	ENGINE-TO-STAGE ALIGNMENT DATA, S-I STAGE . . . . .	8-37
8-12	STATISTICAL PROPERTIES, ENGINE TO STAGE MOUNTING PARAMETERS, S-I STAGE . . . . .	8-38
8-13	STATISTICAL INPUT MODEL, S-I STAGE . . . . .	8-38

LIST OF TABLES (Concluded)

<u>Table No.</u>	<u>Title</u>	<u>Page</u>
8-14	CLASSICAL SOLUTION FOR STATISTICAL PROPERTIES OF RESULTANT THRUST AND MOMENT VECTORS, S-I STAGE . . . .	8-40
8-15	MONTE CARLO SOLUTION FOR STATISTICAL PROPERTIES OF RESULTANT THRUST AND MOMENT VECTORS, S-I STAGE . . . .	8-40
8-16	NOMINAL VALUES AND TOLERANCES, ENGINE-TO-STAGE MOUNTING PARAMETERS, S-IC STAGE . . . . .	8-48
8-17	STATISTICAL INPUT MODEL, S-IC STAGE. . . . .	8-50
8-18	CLASSICAL SOLUTION FOR STATISTICAL PROPERTIES OF RESULTANT THRUST AND MOMENT VECTORS, S-IC STAGE, CASES 1 AND 2 . . . . .	8-55
8-19	MONTE CARLO SOLUTION FOR STATISTICAL PROPERTIES OF RESULTANT THRUST AND MOMENT VECTORS, S-IC STAGE, CASE 1.	8-53
8-20	MONTE CARLO SOLUTION FOR STATISTICAL PROPERTIES OF RESULTANT THRUST AND MOMENT VECTORS, S-IC STAGE, CASE 2.	8-60
8-21	MONTE CARLO SOLUTION FOR STATISTICAL PROPERTIES OF RESULTANT THRUST AND MOMENT VECTORS, S-IC STAGE, CASE 3.	8-60
8-22	NOMINAL VALUES AND TOLERANCES, ENGINE-TO-STAGE MOUNTING PARAMETERS, S-II STAGE . . . . .	8-69
8-23	NOMINAL VALUES AND TOLERANCES, ENGINE-TO-STAGE MOUNTING TOLERANCES, S-IVB STAGE. . . . .	8-69

DEFINITION OF SYMBOLS AND TERMS

MATHEMATICAL SYMBOLS

<u>Symbol</u>	<u>Definition</u>
c	Cosine
$\text{Cov}[X,Y]^*$	Covariance between random variables X and Y in operator form
$E[X]$	Expected value of random variable X in operator form
F	Force
M	Moment
N	Number of engines in a ring
R	Radius from cluster center to peripheral engine gimbal center projection in nominal gimbal plane
s	Sine
T	Tolerance boundary
u	Axis along engine centerline, positive in the direction of forward motion
v	Axis perpendicular to engine centerline, passing through nominal gimbal center and through a reference point of symmetry
$\text{Var}[X]$	Variance of random variable X in operator form
w	Axis completing the righthanded u v w - axis frame
x	Axis along cluster centerline, positive in the forward direction of travel; displacement along x-axis
y	Axis perpendicular to cluster centerline, lying in the nominal gimbal plane and passing through a reference point on the cluster; displacement along the y-axis
z	Axis completing the righthanded x y z - axis frame; displacement along z-axis
$\Gamma$	Nominal cant angle of a peripheral engine in the radial plane
$\gamma$	Small angle about w-axis through which engine must be rotated to assume ideal orientation
$\delta$	Small angle about v-axis through which an engine must be rotated to assume ideal orientation

\*Brackets used in mathematical expressions indicate function arguments



$\theta$	Angle in the nominal gimbal plane from positive y-axis to radial line, R, for a given engine
$\lambda$	Lagrange multiplier
$\mu_X$	Mean value of random variable X
$\rho_{XY}$	Linear corellation coefficient between random variables X and Y
$\sigma_X$	Standard deviation of random variable X
$\sigma_{XY}$	Covariance in subscript form between random variables X and Y
$\sigma_X^2$	Variance of random variable X in subscript form
$\psi$	Small angle about u-axis through which engine must be rotated to assume ideal orientation
$\approx$	"Approximately equal to"

#### Subscripts

F	Statistical parameter of a force
g	Center of gravity
M	Statistical parameter of a moment
o	Nominal part
u	Vector component along u-axis
v	Vector component along v-axis
w	Vector component along w-axis
x	Vector component along x-axis
y	Vector component along y-axis
z	Vector component along z-axis

ABBREVIATIONS AND DEFINITIONS

1. ATV - Actual thrust vector: The resultant force created by the burning propellants escaping from the engine thrust chamber.
2. Actuation plane: The plane defined by the actuator centerline and the thrust chamber centerline under zero deflection command.
3. Actuator attach point: The pivot point where the actuator attaches to the stage.
4. Cant angle: The angle formed by the extended engine centerline of a peripheral engine and the cluster centerline.
5. Center engine: An engine whose nominal thrust chamber centerline is collinear with the cluster centerline.
6. c. g. - Center of gravity.
7. DTV - Dynamic thrust vector: Estimate of the actual thrust vector as computed from the thrust measurements.
8. Engine centerline: A line perpendicular to the engine-to-stage mounting surface and passing through the point of intersection of the centerlines of the mounting surface keyways.
9. GTV - Geometric Thrust Vector: A line passing through the area centroids of the thrust chamber throat and exit planes. (H-1, J-2)
10. Gimbal bearing assembly: A mechanical assembly attaching the thrust chamber to the stage, and providing rotational freedom in pitch and yaw between the thrust chamber and stage.
11. Gimbal center: The point of intersection of the gimbal bearing axes.
12. Gimbal plane, engine: A plane containing the engine gimbal center and parallel to the engine-to-stage mounting surface.
13. Gimbal plane, stage: A plane containing the nominal gimbal centers of all engines.
14. Gimbal slide: A mechanical assembly which provides lateral adjustment of the thrust chamber with respect to the engine centerline.
15. Peripheral Engine: Any engine not located at the center of the cluster.
16. Pierce point: The point at which the thrust vector intersects the gimbal plane.
17. Pillow block, lower: That portion of the gimbal bearing assembly which attaches to the thrust chamber.
18. Pillow block, upper: That portion of the gimbal bearing assembly which attaches to the stage mounting surface.

19. Radial plane: A plane containing the cluster centerline and the gimbal center of a peripheral engine.
20. TCCL-Thrust chamber centerline: A line passing through the center of the engine injector face and the center of the exit plane.
21. Classical Solution: As used in this report, classical solution refers to the covariance matrix of the resultant thrust and moment vector components of an engine cluster. Each element of the matrix is expressed in Section IV as an algebraic formulation of input parameters.
22. TIR - total indicator reading: the diameter of the cylindrical tolerance zone of two or more concentric, regular features.

## SECTION I

### INTRODUCTION

#### 1.1 BACKGROUND

One of the important problems encountered in practical rocket flight is that of thrust vector misalignment. Ideally, the resultant thrust vector of a powered rocket vehicle with zero steering command should be directed along the longitudinal axis of the vehicle. In reality this resultant thrust vector is a statistical quantity which varies from instant to instant in both magnitude and direction due to the randomness of the propulsion process. Furthermore, the time average of the thrust vector will not be the ideal but will be "biased" in magnitude and direction due to sustained deviations in engine performance as well as mechanical alignment errors. To further complicate matters the propulsion system will in general apply not only the thrust vector but also an unwanted moment vector to the vehicle, tending to cause undesired rotations about the vehicle c.g.

Obviously thrust vector misalignment is a severe problem in unguided rockets, causing large deviations from the desired trajectory and in extreme cases tumbling and breakup of the vehicle. Indeed, the first work concerning the problem of thrust vector misalignment was prompted by development of small unguided rockets [G1]\*.

Fortunately, in guided rocket vehicles such as the Saturns, the onboard attitude control system automatically cancels any sustained moment due to thrust vector misalignment by applying an equal and opposite control moment.

---

\* Bracketed numerals denote corresponding references at the end of this report.

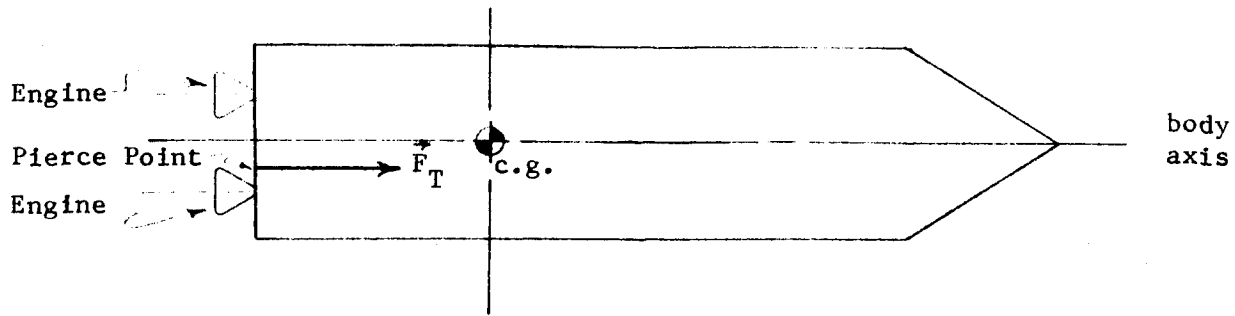
This is accomplished in any one of several ways such as gimbaling the main engines, positioning aerodynamic control surfaces, or firing auxiliary thrusters as in the case of roll control for the Saturn S-IVB stage.

## 1.2 EFFECTS OF THRUST VECTOR MISALIGNMENT

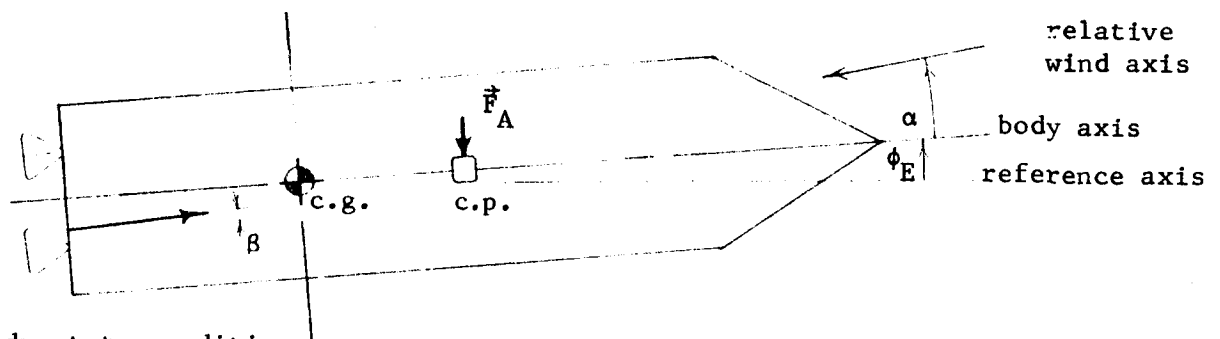
Although moments about the c.g. generated by thrust vector misalignment are automatically cancelled by the attitude control system, thrust vector misalignment is still an important consideration in guided rocket vehicles for several reasons.

(1) Thrust vector misalignment reduces the dynamic operating range of the attitude control system. Any gimbaling of engines to correct for moments caused by thrust vector misalignment lowers the remaining engine gimbal angle available for maneuvering.

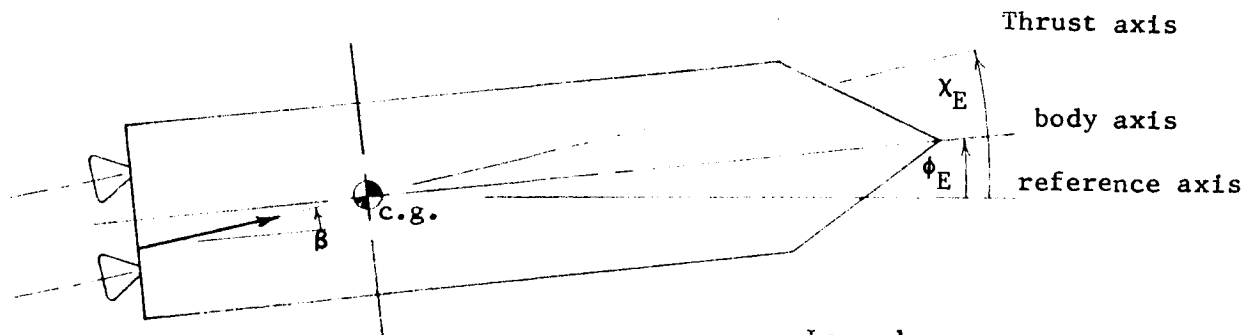
(2) One type of thrust vector misalignment reduces the maximum crosswind which can be withstood by a launch vehicle. Consider a case where the pierce point of the resultant thrust vector is displaced from the center of the gimbal plane, as shown in the simplified two-dimensional diagram of Figure 1-1(a). In order to maintain a stable pitch attitude during atmospheric flight, the control system must gimbal the engines in such a way that the summation of pitch moments about the c.g. is zero. This results in the quasi-steady state condition shown in Figure 1-1(b) where both gimble angle and angle of attack assume nonzero values such that the net control moment (algebraic sum of moments due to misalignment and gimbaling) is exactly cancelled by the aerodynamic moment. Aerodynamic loads on the vehicle structure are directly proportional to the total angle of attack resulting from both thrust



(a.) Pierce point error in resultant thrust vector



(b.) Quasi steady-state condition during atmospheric flight



(c.) Steady state condition during exo-atmospheric flight

Legend

- c.p. - center of aerodynamic pressure
- $\vec{F}_A$  - aerodynamic normal force
- $\vec{F}_T$  - resultant thrust vector
- $\alpha$  - angle of attack
- $\beta$  - Thrust deflection command
- $\phi_E$  - attitude error
- $\chi_E$  - Thrust axis error

Figure 1-1. EFFECTS OF THRUST VECTOR MISALIGNMENT ON A HYPOTHETICAL TWO-DIMENSIONAL ROCKET VEHICLE

misalignment and crosswind speed, and must be kept within structural limits. Consequently, any thrust misalignment of the type shown in Figure 1-1(a) directly reduces the maximum crosswind speed which can be withstood by the vehicle.

(3) Thrust vector misalignment can degrade the performance of closed-loop guidance. Closed-loop guidance during powered flight consists of directing the resultant thrust vector at all times such that the vehicle traverses an optimal trajectory from its present position to the desired target. In the practical implementation of guidance it is usually more convenient to direct the attitude of the vehicle rather than its thrust vector, based on the assumption that the thrust vector and the vehicle centerline are collinear. When a thrust vector pierce point error exists, the attitude control system will gimbal the engines to null any moment about the c.g. Once the vehicle is outside the atmosphere it will assume the attitude shown in Figure 1-1(c). Note that although the vehicle attitude is exactly as commanded by the guidance system, the line of action of the thrust vector is in error. The guidance system cannot sense the error directly and must rely on inertial velocity and position measurements from the navigation system to show the long-term effect of such an error. Hence, the vehicle will not in general fly the desired trajectory or reach the desired end conditions.

### 1.3 SOURCES OF THRUST VECTOR MISALIGNMENT

All contributions to thrust vector misalignment in an engine cluster may be divided into two categories: (1) geometrical errors and (2) thermodynamic phenomena within the combustion process. Geometrical errors are

those which cause the mechanical thrust chamber centerlines and gimbal points of the various engines within the operating cluster to be located at other than their nominal positions. Included are such items as dimensional errors within the engine and stage, structural compliance under thrust, and thrust chamber warpage due to temperature changes. Imperfections in the combustion process cause the dynamic thrust vector of an engine to depart from the thrust chamber centerline during hot firing. In addition, combustion imperfection accounts for errors in thrust magnitude and for nonzero roll moments about the thrust chamber centerline due to swirling of exhaust gases.

Geometrical and combustion uncertainties are each capable of producing all types of thrust vector misalignment in a multi-engine cluster: thrust vector magnitude and directional errors, pierce point errors, and roll moments about the cluster centerline.

#### 1.4 BASIS FOR STUDY

The study documented herein represents the first step<sup>\*</sup> in analyzing the thrust vector characteristics of engine clusters. The objectives of the study were as follows:

(1) Define a general solution for determining the statistical properties of the resultant thrust and moment vectors of an engine cluster, taking into account all tolerances affecting these vectors.

---

\* A DDC Literature Survey conducted by Redstone Scientific Information Center failed to produce any literature directly pertaining to thrust vector misalignment in engine clusters.



(2) Determine the influence of the shapes of input probability distributions on the resultant thrust and moment vectors.

(3) Determine the actual distributions of tolerances on existing hardware by conducting field investigations to secure information from engine manufacturers, personnel responsible for alignment procedures, etc.

(4) Construct a Monte Carlo simulation of the thrust vector problem and employ it in supporting the general solution.

(5) Evaluate results, draw conclusions, and make recommendations.

The Technical Approach pursued in the study is given in the following section and the pertinent results are discussed in Sections III through VIII. Conclusions and recommendations are presented in Sections IX and X. The lengthy derivations concerned with coordinate transformation (Section III) and the classical solution (Section IV) are postponed until the appendixes to avoid interrupting the main theme of the text. References on probability and statistics theory as well as all sources of hardware data are listed at the end of the report.

## SECTION II

### TECHNICAL APPROACH

#### 2.1 GENERAL

The technical approach taken in this study was selected as one showing the most promise of fulfilling the study objectives within the available time. A set of ground rules was established at the outset to delineate the scope of the investigation. The ground rules, study tasks, and analytical procedure are presented in the following subsections.

#### 2.2 GROUND RULES

The applicability of the study results is limited to engine clusters which conform to the following ground rules:

1. Engine Type. The cluster consists of engines of a single type.
2. Engine Symmetry. Each peripheral engine within the cluster is mounted symmetrically about a radial plane containing the cluster centerline and the engine gimbal point.
3. Gimbal Plane. The nominal gimbal points (or equivalent reference points for non-gimbaled engines) lie in the same plane for all engines constituting the cluster.
4. Canting. All engines constituting a clustered ring are assumed to have the same nominal cant angle.
5. Engine Independence. All engines within a cluster are statistically independent in performance and mounting errors.

6. Actuators. Analysis is limited to the case of zero gimbal command, with the actuators treated as stiff rods of zero deflection length.

No error sources are considered within the actuation or control systems.

Analysis was limited to consideration of steady-state operation of engine clusters. Transient behavior and stochastic analysis were omitted from the study. No attempt was made to analyze the combustion process of a rocket engine, but rather the analysis depends on the ability to measure engine performance. All solutions obtained in the study are valid for clusters conforming to the groundrules, and in some instances extend beyond these limits as noted in the explanations contained in Section IV.

### 2.3 STUDY TASKS

The following specific tasks were defined and performed under the study, based on the objectives, groundrules, and available field data.

1. Coordinate systems and transformations. General coordinate systems were defined for the cluster and the individual rocket engines. The necessary coordinate transformations were derived to express engine thrust and moment contributions in terms of the cluster coordinate system.
2. Classical probability solution. A classical probability solution was derived in which the variances of the resultant thrust and moment vectors were expressed as functions of engine performance and mounting error variances.
3. Monte Carlo simulation. A Monte Carlo simulation computer program was designed for use in supporting the classical solution.

4. Data acquisition. Pertinent data and information were gathered on the H-1, J-2, and F-1 engines and on the Saturn stages using these engines.
5. Tolerance distributions. Hardware performance and alignment data were analyzed to determine the shapes of the probability distributions of engine performance and mounting parameters.
6. Saturn stage analysis. The classical and Monte Carlo techniques were used to analyze the S-I and S-IC stages.
7. Documentation. Study results were documented in final report form along with all assumptions made.

#### 2.4 ANALYTICAL PROCEDURE

The fundamental study requirement was to develop a general probability solution applicable to a wide range of cluster configurations. To achieve maximum generality, it was decided to establish an interface between engine and stage, thus splitting the analysis into two parts: that for the engine and that for the stage. Accordingly, coordinate systems were defined for both the engine and stage, and coordinate transformations were derived to express the contribution of a given engine to the resultant thrust and moment vectors of the stage. The advantage of this approach is that a given engine type such as the J-2 need be analyzed only once. The resulting statistical model for the engine may then be used in the analysis of any stage employing that particular type of engine. The disadvantage is that the engine thrust and moment vector components used as inputs to the stage analysis are in general statistically dependent and are

described by probability distributions of up to six dimensions. The multivariate probability distributions are difficult (though not impossible) to manipulate in the classical solution and require more computer time in the Monte Carlo simulation.

#### 2.4.1 Coordinate System and Transformations

The coordinate system chosen for the engine has its origin at the ideal gimbal center, with one axis ( $u$ ) along the engine centerline and the other two axes ( $v$  and  $w$ ) in the engine gimbal plane. Total thrust applied to the stage by the engine is expressed as three force components and three moment components ( $F_u, F_v, F_w, M_u, M_v, M_w$ ) applied at the ideal gimbal center. All tolerances within the engine are taken into account by using dynamic test data (load cell measurements) from aligned engines as a basis for determining the distribution of the six engine vector components.

The cluster coordinate system was chosen such that one axis ( $x$ ) coincides with the cluster centerline and the other two axes ( $y$  and  $z$ ) lie in the ideal gimbal plane. The engine is considered as a rigid body and its position within the cluster is completely determined if the gimbal center location and the engine orientation are known. The gimbal center location is expressed in polar coordinates ( $R, \theta, x$ ) and the engine orientation is given as three small-angle errors ( $\psi, \delta, \gamma$ ) relative to the ideal orientation.

#### 2.4.2 Classical Solution

A classical solution of the engine cluster problem was obtained by applying the expected value operator to the coordinate transformation equations.

resulting in an expression for the variances of the  $i^{\text{th}}$  engine contributions to the resultant thrust and moment vectors of the cluster. A summation was then performed over all engines in the cluster to obtain the variances of the resultant thrust and moment vectors. A similar derivation was used to derive covariances between the cluster components. The end results were algebraic expressions for the variances and covariances of the resultant vector components as functions of engine performance and mounting variances.

#### 2.4.3 Monte Carlo Simulation

A Monte Carlo simulation of the engine cluster problem was programmed for the purpose of corroborating the classical solution. The procedure consists of programming a mechanism whereby random sample values of performance and mounting errors for each engine within a given cluster can be generated and the resultant thrust and moment vectors calculated. Repetition of the process a large number of times yields a sample population of the resultant vectors, from which the desired variances and covariances may be calculated empirically. The Monte Carlo program was designed to accommodate the multivariate distributions arising at the engine-to-stage interface. It covers a more general class of cluster configurations and with fewer assumptions than does the classical solution.

#### 2.4.4 Data Acquisition

A sizable portion of the study effort was devoted to collecting sufficient hardware data to permit a statistical analysis of some engine cluster configurations used in the Saturn stages. The primary data needed for such an analysis were: (1) engine static test firing data with sufficient instrumentation to allow determination of dynamic forces and moments generated by the engine;

(2) nominal stage geometry; and (3) engine-to-stage final alignment measured values. In addition, it was necessary to gather secondary information such as (1) specified tolerances on each input variable, (2) engine alignment and static test firing procedures, and (3) stage alignment procedures.

The engines from which to select those to be analyzed were the H-1, J-2, F-1, RL-10, and M-1. Of these, the RL-10 engine was discarded first due to lack of the necessary dynamic test data and second due to its obsolescence in the Saturn program. The M-1 engine was eliminated due to lack of time under the contract. An analysis was performed on each of the remaining three engines.

Some data were gathered on each of the Saturn stages in which the H-1, J-2, or F-1 engines are used; viz., the S-I, S-IB, S-IC, S-II, and S-IVB stages. Of these only the S-I stage had sufficient preserved alignment data on which to base a statistical analysis.

#### 2.4.5 Statistical Analysis of Hardware

A statistical analysis was performed on each of the engines H-1, J-2, and F-1, to determine the covariance matrix of the thrust and moment components ( $F_u, F_v, F_w, M_u, M_v, M_w$ ). The results of the H-1 and F-1 engine analyses were then used as input data in the analysis of the S-I and S-IC stages, respectively. The S-I stage was analyzed using mounting error distributions based on actual alignment measurement data from two test and ten flight models. In the absence of sufficient alignment experience, hypothetical distributions for the S-IC stage mounting errors were developed based on specified engine-to-stage alignment tolerances. Both the classical and Monte Carlo techniques were applied to each of the stages, and reasonable correspondence was obtained for each case.

## 2.5 INTERNATIONAL SYSTEM OF UNITS

The contract under which this study was performed contained the requirement that all dimensional numerics be expressed in the International System of Units [G2]. In compliance with this requirement, all derived numerical quantities appearing in this report are stated in the International System followed by the equivalent value in the English System. Since all field data gathered on the various engines and stages were in English units, conversion to International was necessary. The conversion factors used in the study are shown in Table 2-1.

Table 2-1. CONVERSION FACTORS USED IN THIS STUDY,  
ENGLISH UNITS TO INTERNATIONAL UNITS

QUANTITY	TO CONVERT		MULTIPLY BY
	FROM	TO	
Length	inches (in.)	centimeters (cm)	2.54*
Force or Thrust	pounds (lb)	newtons (N)	4.4482216152605* (approx. 4.44822)
Moment	pound-inches (lb-in.)	newton-meters (Nm)	.1129848290276167* (approx. .112985)

\*These conversion factors are exact.



### SECTION III

#### COORDINATE SYSTEM AND TRANSFORMATIONS

This section describes the coordinate axis system chosen for the engine cluster study and lists the coordinate transformations necessary to express engine thrust and moment vectors in terms of cluster coordinates. The general coordinate system for a cluster of  $n$  engines is shown in Figure 3-1. The delivered thrust and moment vectors of each individual engine are expressed in terms of the  $uvw$ -axis frame embedded in the engine. The resultant thrust and moment vectors for the cluster are obtained in terms of the  $xyz$ -axis frame embedded in the cluster. There are six degrees of freedom in mounting an engine in the cluster: three coordinates locating the origin of the  $uvw$ -axis within the cluster frame and three angles establishing the orientation of the  $uvw$ -axis frame within the cluster frame. The following paragraphs discuss each axis system in more detail.

#### 3.1 ENGINE COORDINATE SYSTEM

The engine coordinate system ( $uvw$ -axes of Figure 3-1) is a righthanded frame, the  $u$ -axis of which coincides with the nominal thrust vector. The  $u$ -axis is positive in the direction of delivered thrust and the origin is taken to be the nominal gimbal point (or an equivalent point for an ungimbaled engine). The  $vw$ -plane is perpendicular to the  $u$ -axis and contains the nominal gimbal point and thrust vector pierce point. The positive  $v$ -axis passes through a specified reference point on the engine and, for the engines investigated in this study, was chosen to bisect the right angle formed by the actuator attach points and the gimbal point. The positive  $w$ -axis is chosen to complete the righthanded  $uvw$  frame.

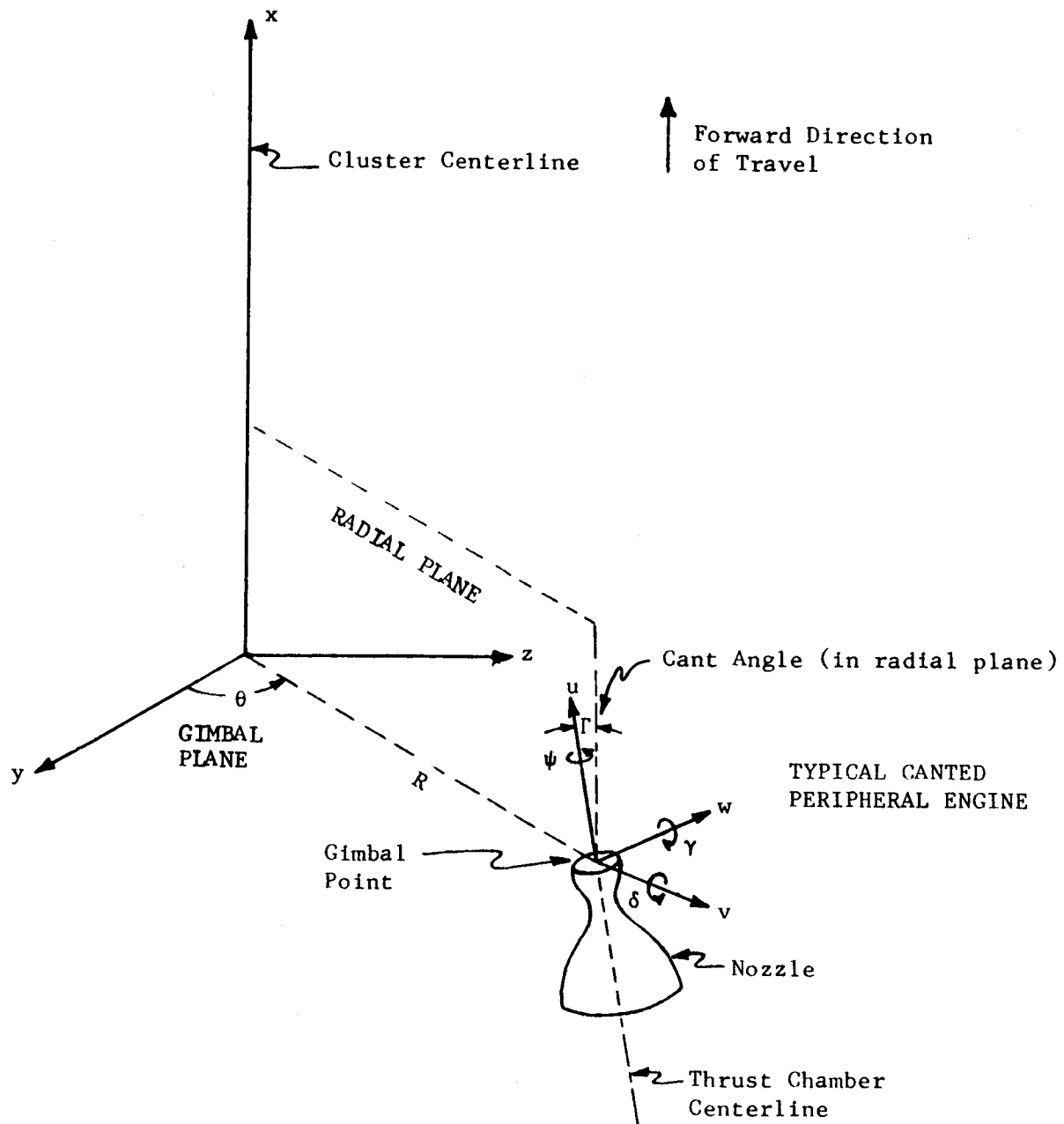


Figure 3-1. ENGINE CLUSTER COORDINATE SYSTEM

The overall thrust vector characteristics of any given engine are described by three perpendicular components of thrust vector and three components of moment vector. Once the statistical properties of these six components are obtained for a particular type of engine, any cluster configuration employing that engine type may be analyzed. The choice of engine axes is not rigid and should be made to simplify the probability distributions of the thrust and moment vector components. The classical and Monte Carlo solutions given in Sections IV and VI are independent of the engine axes chosen, provided the nominal  $v$ -axis coincides with the radial line joining origins of the  $xyz$  and  $uvw$  frames. (In the case of a canted engine the  $v$ -axis will intersect the radial line at the nominal gimbal point but will be rotated in a vertical plane by the amount of the cant angle.)

### 3.2 CLUSTER COORDINATE SYSTEM

The cluster coordinate system is the righthanded  $xyz$  frame shown in Figure 3-1. The  $x$ -axis is the longitudinal centerline of the vehicle, positive in the forward direction of travel. The  $yz$ -plane is perpendicular to the  $x$ -axis and contains the ideal gimbal point of each engine in the cluster. (This is in accord with the stated ground rule that the engine cluster is assumed to have all gimbal points in the same plane.) The positive  $z$ -axis is oriented such that it points vertically downward when the vehicle is in normal horizontal flight, and the  $y$ -axis is chosen to complete a righthanded  $xyz$  frame.

The gimbal point location of each engine is expressed in cylindrical coordinates  $(R, \theta, x)$ , due to the radial symmetry of engine cluster geometry.  $R$  is the length of the radial line to the gimbal point,  $\theta$  is the angle from the

positive y-axis to the radial line, and  $x$  is the displacement of the gimbal point above the  $yz$ -plane ( ideally zero). In the case of a center engine the gimbal point is expressed in rectangular coordinates  $(x, y, z)$  and is nominally located at  $(0, 0, 0)$ .

An uncanted engine is oriented in the cluster such that the nominal  $u$ -axis of the engine is parallel to the cluster  $x$ -axis, and the nominal  $v$ -axis is coincident with the radial line  $R$ . The positive  $v$ -axis may be directed either inward or outward. Errors in engine orientation are represented by three small angles  $\psi$ ,  $\delta$ , and  $\gamma$ . These are positive rotations about the actual  $u$ ,  $v$ , and  $w$  axes, respectively, which would have to be performed in order to bring the engine to its nominal orientation. Small angle approximations are used in the analysis, making the order of rotations immaterial.

The orientation of a canted engine is treated exactly as an uncanted one with the exception that the engine is rotated through the nominal cant angle about the  $w$ -axis. This results in the rotation of the nominal  $u$ -axis of the engine toward the cluster  $x$ -axis. The angle  $\Gamma$  is treated as a deterministic quantity with angle  $\gamma$  as the statistical component.

For the case of a center engine the same small angles are used to describe engine orientation errors. The center engine has  $R_N = 0$  and the angle  $\theta$  takes on a special meaning: it is the deterministic angle from the positive  $y$ -axis to the positive  $v$ -axis of the center engine. By choosing variables in this manner, the center engine becomes a special case of a peripheral engine with a radial displacement of  $R = 0$ .

### 3.3 COORDINATE TRANSFORMATIONS

Both the Monte Carlo and classical solutions of the engine cluster problem require coordinate transformations which express the contribution of each engine to the resultant thrust and moment vectors of a cluster. These transformations are listed in this paragraph and their derivations are given in Appendix A of this report. Transformations are given for each of the following cases:

- (1) canted peripheral engine, v-axis outward
- (2) canted peripheral engine, v-axis inward
- (3) uncanted peripheral engine, v-axis outward
- (4) uncanted peripheral engine, v-axis inward
- (5) center engine.

In each case there are two transformations of the following forms:

$$\text{force vector, } \vec{F}_{xyz} = [A] \vec{F}_{uvw}$$

$$\text{and moment vector, } \vec{M}_{xyz} = [A] \vec{M}_{uvw} + [B] \vec{F}_{uvw} ;$$

where

$$\vec{F}_{uvw} = \begin{bmatrix} F_u \\ F_v \\ F_w \end{bmatrix} \quad \text{is the delivered engine thrust vector,}$$

$$\vec{M}_{uvw} = \begin{bmatrix} M_u \\ M_v \\ M_w \end{bmatrix} \quad \text{is the delivered engine moment vector,}$$

$\vec{F}_{xyz} = \begin{bmatrix} F_x \\ F_y \\ F_z \end{bmatrix}$  is the equivalent engine thrust vector in cluster coordinates,

and  $\vec{M}_{xyz} = \begin{bmatrix} M_x \\ M_y \\ M_z \end{bmatrix}$  is the equivalent engine moment vector about the cluster origin.

Mathematically, the transformations replace the thrust and moment vectors in engine coordinates by an equivalent thrust and moment vector pair acting at the cluster origin, taking into account the engine mounting within the cluster as described by the A and B matrices. Once the contribution of each engine has been transformed, vector components may be summed to find the resultant vectors for the cluster.

CASE 1: Canted Peripheral Engine, v-axis Outward.

$$[A] = \begin{bmatrix} c\Gamma - \gamma s\Gamma & \gamma c\Gamma + s\Gamma & \psi s\Gamma - \delta c\Gamma \\ -c\theta(\gamma c\Gamma + s\Gamma) - \delta s\theta & c\theta(c\Gamma - \gamma s\Gamma) + \psi s\theta & c\theta(\delta s\Gamma + \psi c\Gamma) - s\theta \\ -s\theta(\gamma c\Gamma + s\Gamma) + \delta c\theta & s\theta(c\Gamma - \gamma s\Gamma) - \psi c\theta & s\theta(\delta s\Gamma + \psi c\Gamma) + c\theta \end{bmatrix}$$

$$[B] = \begin{bmatrix} \delta R & -\psi R & R \\ \hline R s\theta(c\Gamma - \gamma s\Gamma) + x[s\theta(s\Gamma + \gamma c\Gamma) - \delta c\theta] & R s\theta(\gamma c\Gamma + s\Gamma) + x[s\theta(\gamma s\Gamma - c\Gamma) + \psi c\theta] & R s\theta(\psi s\Gamma - \delta c\Gamma) - x[s\theta(\psi c\Gamma + \delta s\Gamma) + c\theta] \\ \hline R c\theta(\gamma s\Gamma - c\Gamma) - x[c\theta(\gamma c\Gamma + s\Gamma) + \delta s\theta] & -R c\theta(s\Gamma + \gamma c\Gamma) + x[c\theta(c\Gamma - \gamma s\Gamma) + \psi s\theta] & R c\theta(\delta c\Gamma - \psi s\Gamma) + x[c\theta(\delta s\Gamma + \psi c\Gamma) - s\theta] \end{bmatrix}$$

NOTE:  $s\Gamma = \sin\Gamma$

$c\Gamma = \cos\Gamma$

CASE 2: Canted Peripheral Engine, v-axis Inward.

$$[A] = \begin{bmatrix} c\Gamma + \gamma s\Gamma & \gamma c\Gamma - s\Gamma & -\psi s\Gamma - \delta c\Gamma \\ c\theta(\gamma c\Gamma - s\Gamma) + \delta s\theta & -c\theta(c\Gamma + \gamma s\Gamma) - \psi s\theta & c\theta(\delta s\Gamma - \psi c\Gamma) + s\theta \\ s\theta(\gamma c\Gamma - s\Gamma) - \delta c\theta & -s\theta(c\Gamma + \gamma s\Gamma) + \psi c\theta & s\theta(\delta s\Gamma - \psi c\Gamma) - c\theta \end{bmatrix}$$

$$[B] = \begin{bmatrix} -\delta R & \psi R & -R \\ \begin{matrix} R s\theta (c\Gamma + \gamma s\Gamma) \\ + x [s\theta (s\Gamma - \gamma c\Gamma) + \delta c\theta] \end{matrix} & \begin{matrix} R s\theta (\gamma c\Gamma - s\Gamma) \\ + x [s\theta (\gamma s\Gamma - c\Gamma) - \psi c\theta] \end{matrix} & \begin{matrix} -R s\theta (\psi s\Gamma + \delta c\Gamma) \\ + x [s\theta (\psi c\Gamma - \delta s\Gamma) + c\theta] \end{matrix} \\ \begin{matrix} -R c\theta (\gamma s\Gamma + c\Gamma) \\ + x [c\theta (\gamma c\Gamma - s\Gamma) + \delta s\theta] \end{matrix} & \begin{matrix} R c\theta (s\Gamma - \gamma c\Gamma) \\ - x [c\theta (c\Gamma + \gamma s\Gamma) + \psi s\theta] \end{matrix} & \begin{matrix} R c\theta (\delta c\Gamma + \psi s\Gamma) \\ + x [c\theta (\delta s\Gamma - \psi c\Gamma) + s\theta] \end{matrix} \end{bmatrix}$$

CASE 3: Uncanted Peripheral Engine, v-axis Outward.

$$[A] = \begin{bmatrix} 1 & \gamma & -\delta \\ -\delta s\theta - \gamma c\theta & c\theta + \psi s\theta & \psi c\theta - s\theta \\ \delta c\theta - \gamma s\theta & s\theta - \psi c\theta & \psi s\theta + c\theta \end{bmatrix}$$

$$[B] = \begin{bmatrix} \delta R & -\psi R & R \\ R s\theta + x(\gamma s\theta - \delta c\theta) & \gamma R s\theta + x(\psi c\theta - s\theta) & -\delta R s\theta - x(\psi s\theta + c\theta) \\ -R c\theta - x(\gamma c\theta + \delta s\theta) & -\gamma R c\theta + x(c\theta + \psi s\theta) & \delta R c\theta + x(\psi c\theta - s\theta) \end{bmatrix}$$

September 1966

CASE 4: Uncanted Peripheral Engine, v-axis Inward.

$$[A] = \begin{bmatrix} 1 & \gamma & -\delta \\ \delta s\theta + \gamma c\theta & -c\theta - \psi s\theta & -\psi c\theta + s\theta \\ -\delta c\theta + \gamma s\theta & -s\theta + \psi c\theta & -\psi s\theta - c\theta \end{bmatrix}$$

$$[B] = \begin{bmatrix} -\delta R & \psi R & -R \\ R s\theta - x(\gamma s\theta - \delta c\theta) & \gamma R s\theta - x(\psi c\theta - s\theta) & -\delta R s\theta + x(\psi s\theta + c\theta) \\ -R c\theta + x(\gamma c\theta + \delta s\theta) & -\gamma R c\theta - x(c\theta + \psi s\theta) & \delta R c\theta - x(\psi c\theta - s\theta) \end{bmatrix}$$

CASE 5: Center Engine.

$$[A] = \begin{bmatrix} 1 & \gamma & -\delta \\ -\delta s\theta - \gamma c\theta & c\theta + \psi s\theta & \psi c\theta - s\theta \\ \delta c\theta - \gamma s\theta & s\theta - \psi c\theta & \psi s\theta + c\theta \end{bmatrix}$$

$$[B] = \begin{bmatrix} z(\gamma c\theta + \delta s\theta) + y(\delta c\theta - \gamma s\theta) & -z(c\theta + \psi s\theta) + y(s\theta - \psi c\theta) & z(s\theta - \psi c\theta) + y(c\theta + \psi s\theta) \\ z + x(\gamma s\theta - \delta c\theta) & \gamma z - x(s\theta - \psi c\theta) & -\delta z - x(c\theta + \psi s\theta) \\ -y - x(\gamma c\theta + \delta s\theta) & -\gamma y + x(c\theta + \psi s\theta) & \delta y + x(-s\theta + \psi c\theta) \end{bmatrix}$$



## SECTION IV

### CLASSICAL PROBABILITY SOLUTION OF AN ENGINE CLUSTER

#### 4.1 GENERAL

This section presents the classical probability solution of the resultant thrust and moment vectors of a rocket engine cluster. The solutions are algebraic equations expressing the six variances and  $\binom{6}{2} = 15$  covariances of the resultant vector components as functions of the engine performance and alignment errors. Solutions are given for the cases of (1) a single engine located at the cluster center, and (2) a ring of two or more engines equally spaced in a circle about the cluster center. A method is given for combining the contributions of each ring in a multi-ring cluster, thus extending the applicability of the classical solution to complex cluster geometries. All equations are written for  $v_N$ -axis outward on peripheral engines. Equations for the  $v_N$ -axis inward may be obtained by substituting the circled signs  $\oplus$  and  $\ominus$  as indicated directly above each equation.

#### 4.2 ASSUMPTIONS AND APPROXIMATIONS

This subsection itemizes the assumptions and approximations employed in deriving the classical solution. Some of these were necessary to permit a closed solution at all and others were made to shorten the resulting equations to a usable length. The simplifying assumptions were chosen as those thought to be most reasonable.

##### 4.2.1 Geometrical Assumptions

(1) Nominal engine centers within a ring are equally spaced on a circle about the cluster center.

(2) Nominal gimbal points of all engines lie in the same plane.



(3) Engines within a ring are assumed to be statistically independent both in alignment and performance.

(4) Engines within a ring are assumed to be identical both in performance and alignment characteristics. For example, all engines making up a ring are assumed to produce thrust and moment vectors which obey the same distribution functions.

(5) Individual rings within a cluster are assumed to be statistically independent.

The following approximations involving the angle  $\theta$  are made. In these approximations  $\theta = \theta_o + \Delta\theta$ , where  $\theta_o$  is the nominal and  $\Delta\theta$  is the statistical small angle portion.

a.  $\sin \theta \approx \sin \theta_o + \Delta\theta \cos \theta_o$

b.  $E[\sin \theta] \approx \sin \theta_o$

c.  $\text{Var} [\sin \theta] \approx \sigma_{\theta}^2 \cos^2 \theta_o$

d.  $\cos \theta \approx \cos \theta_o - \Delta\theta \sin \theta_o$

e.  $E[\cos \theta] \approx \cos \theta_o$

f.  $\text{Var}[\cos \theta] \approx \sigma_{\theta}^2 \sin^2 \theta_o$

g.  $\sin \theta \cos \theta \approx (1 - 2\Delta\theta^2) \sin \theta_o \cos \theta_o + \Delta\theta(\cos^2 \theta_o - \sin^2 \theta_o)$

h.  $E[\sin \theta \cos \theta] \approx (1 - 2\sigma_{\theta}^2) \sin \theta_o \cos \theta_o$ .

In addition to the small angle approximation of  $\theta$ , the approximations used in the coordinate transformations described in Section III also apply here.

September 1966

## 4.3 SOLUTION FOR A RING CONSISTING OF ONE CENTER ENGINE

4.3.1 Expected Values

$$E[F_x] = \mu_{Fu}$$

$$E[F_y] = E[F_z] = E[M_x] = E[M_y] = E[M_z] = 0.$$

4.3.2 Variances

$$\text{Var}[F_x] = \sigma_{Fu}^2 + \sigma_\gamma^2 \sigma_{Fv}^2 + \sigma_\delta^2 \sigma_{Fw}^2$$

$$\begin{aligned} \text{Var}[F_y] = & (\sigma_{Fu}^2 + \mu_{Fu}^2)(\sigma_\gamma^2 c_{\theta_o}^2 + 2\sigma_\gamma \delta s_{\theta_o} c_{\theta_o} + \sigma_\delta^2 s_{\theta_o}^2) + \sigma_{Fv}^2 (c_{\theta_o}^2 + \sigma_\psi^2 s_{\theta_o}^2) \\ & + \sigma_{Fw}^2 (\sigma_\psi^2 c_{\theta_o}^2 + s_{\theta_o}^2) \end{aligned}$$

$$\begin{aligned} \text{Var}[F_z] = & (\sigma_{Fu}^2 + \mu_{Fu}^2)(\sigma_\gamma^2 s_{\theta_o}^2 - 2\sigma_\gamma \delta s_{\theta_o} c_{\theta_o} + \sigma_\delta^2 c_{\theta_o}^2) + \sigma_{Fv}^2 (s_{\theta_o}^2 + \sigma_\psi^2 c_{\theta_o}^2) \\ & + \sigma_{Fw}^2 (\sigma_\psi^2 s_{\theta_o}^2 + c_{\theta_o}^2) \end{aligned}$$

$$\begin{aligned} \text{Var}[M_x] = & \sigma_{Mu}^2 + \sigma_\gamma^2 \sigma_{Mv}^2 + \sigma_\delta^2 \sigma_{Mw}^2 + (\sigma_{Fu}^2 + \mu_{Fu}^2) \{ \sigma_z^2 (\sigma_\gamma^2 c_{\theta_o}^2 \\ & + 2\sigma_\gamma \delta s_{\theta_o} c_{\theta_o} + \sigma_\delta^2 s_{\theta_o}^2) + \sigma_y^2 (\sigma_\gamma^2 s_{\theta_o}^2 - 2\sigma_\gamma \delta s_{\theta_o} c_{\theta_o} + \sigma_\delta^2 c_{\theta_o}^2) \} \\ & + \sigma_{Fv}^2 \{ \sigma_z^2 (c_{\theta_o}^2 + \sigma_\psi^2 s_{\theta_o}^2) + \sigma_y^2 (s_{\theta_o}^2 + \sigma_\psi^2 c_{\theta_o}^2) \} \\ & + \sigma_{Fw}^2 \{ \sigma_z^2 (\sigma_\psi^2 c_{\theta_o}^2 + s_{\theta_o}^2) + \sigma_y^2 (\sigma_\psi^2 s_{\theta_o}^2 + c_{\theta_o}^2) \} - \sigma_{MvMw} \sigma_\gamma \delta \end{aligned}$$

$$\begin{aligned} \text{Var}[M_y] = & \sigma_{Mu}^2 (\sigma_\gamma^2 c_{\theta_o}^2 + 2\sigma_\gamma \delta s_{\theta_o} c_{\theta_o} + \sigma_\delta^2 s_{\theta_o}^2) + \sigma_{Mv}^2 (c_{\theta_o}^2 + \sigma_\psi^2 s_{\theta_o}^2) \\ & + \sigma_{Mw}^2 (\sigma_\psi^2 c_{\theta_o}^2 + s_{\theta_o}^2) + (\sigma_{Fu}^2 + \mu_{Fu}^2) \{ \sigma_z^2 + \sigma_x^2 (\sigma_\gamma^2 s_{\theta_o}^2 \\ & - 2\sigma_\gamma \delta s_{\theta_o} c_{\theta_o} + \sigma_\delta^2 c_{\theta_o}^2) + \sigma_{Fv}^2 \{ \sigma_\gamma^2 \sigma_z^2 + \sigma_x^2 (s_{\theta_o}^2 + \sigma_\psi^2 c_{\theta_o}^2) \} \\ & + \sigma_{Fw}^2 \{ \sigma_\delta^2 \sigma_z^2 + \sigma_x^2 (\sigma_\psi^2 s_{\theta_o}^2 + c_{\theta_o}^2) \} + \sigma_{MuMv} (-\sigma_\gamma \psi s_{\theta_o} c_{\theta_o} - \sigma_\delta \psi s_{\theta_o}^2) \end{aligned}$$

$$\begin{aligned}
& + \sigma_{MuMw}(-\sigma_{\gamma\psi}c^2\theta_o - \sigma_{\delta\psi}s\theta_o c\theta_o) + \sigma_{MvMw}(\sigma_{\psi}^2 - 1)s\theta_o c\theta_o \\
\text{Var}[M_z] = & \sigma_{Mu}^2(\sigma_{\gamma}^2 s^2\theta_o - 2\sigma_{\gamma\delta} s\theta_o c\theta_o + \sigma_{\delta}^2 c^2\theta_o) + \sigma_{Mv}^2(s^2\theta_o + \sigma_{\psi}^2 c^2\theta_o) \\
& + \sigma_{Mw}^2(\sigma_{\psi}^2 s^2\theta_o + c^2\theta_o) + (\sigma_{Fu}^2 + \mu_{Fu}^2)\{\sigma_y^2 + \sigma_x^2(\sigma_{\gamma}^2 c^2\theta_o \\
& + 2\sigma_{\gamma\delta} s\theta_o c\theta_o + \sigma_{\delta}^2 s^2\theta_o)\} + \sigma_{Fv}^2\{\sigma_{\gamma}^2 \sigma_y^2 + \sigma_x^2(c^2\theta_o + \sigma_{\psi}^2 s^2\theta_o)\} \\
& + \sigma_{Fw}^2\{\sigma_{\delta}^2 \sigma_y^2 + \sigma_x^2(\sigma_{\psi}^2 c^2\theta_o + s^2\theta_o)\} + \sigma_{MuMv}(\sigma_{\delta\psi} s\theta_o c\theta_o - \sigma_{\delta\psi} c^2\theta_o) \\
& + \sigma_{MuMw}(-\sigma_{\gamma\psi} s^2\theta_o + \sigma_{\delta\psi} s\theta_o c\theta_o) + \sigma_{MvMw} s\theta_o c\theta_o (1 - \sigma_{\psi}^2).
\end{aligned}$$

#### 4.3.3 Covariances

$$\text{Cov}[F_x, F_y] = \sigma_{Fv}^2 \sigma_{\gamma\psi} s\theta_o - \sigma_{Fw}^2 \sigma_{\delta\psi} c\theta_o$$

$$\text{Cov}[F_x, F_z] = -\sigma_{Fv}^2 \sigma_{\gamma\psi} c\theta_o - \sigma_{Fw}^2 \sigma_{\delta\psi} s\theta_o$$

$$\begin{aligned}
\text{Cov}[F_y, F_z] = & (\sigma_{Fu}^2 + \mu_{Fu}^2)\{\sigma_{\gamma}^2 s\theta_o c\theta_o - \sigma_{\gamma\delta} c^2\theta_o + \sigma_{\gamma\delta} s^2\theta_o - \sigma_{\delta}^2 s\theta_o c\theta_o\} \\
& + \sigma_{Fv}^2(1 - \sigma_{\psi}^2)s\theta_o c\theta_o + \sigma_{Fw}^2(\sigma_{\psi}^2 - 1)s\theta_o c\theta_o
\end{aligned}$$

$$\text{Cov}[F_x, M_x] = \sigma_{FuMu} + \sigma_{\gamma}^2 \sigma_{FvMv} - \sigma_{FvMw} \sigma_{\gamma\delta} - \sigma_{FwMv} \sigma_{\gamma\delta} + \sigma_{FwMw} \sigma_{\delta}^2$$

$$\begin{aligned}
\text{Cov}[F_x, M_y] = & \sigma_{FuMv} c\theta_o - \sigma_{FuMw} s\theta_o + \sigma_{FvMu}(-\sigma_{\gamma}^2 c\theta_o - \sigma_{\gamma\delta} s\theta_o) \\
& + \sigma_{FvMv} \sigma_{\gamma\psi} s\theta_o + \sigma_{FvMw} \sigma_{\gamma\psi} c\theta_o + \sigma_{FwMu}(\sigma_{\delta\gamma} c\theta_o + \sigma_{\delta}^2 s\theta_o) \\
& - \sigma_{FwMv} \sigma_{\delta\psi} s\theta_o - \sigma_{FwMw} \sigma_{\delta\psi} c\theta_o
\end{aligned}$$

$$\begin{aligned} \text{Cov}[F_x, M_z] &= \sigma_{FuMv} s\theta_o + \sigma_{FuMw} c\theta_o + \sigma_{FvMu} (-\sigma_\gamma^2 c\theta_o - \sigma_{\gamma\delta} s\theta_o) \\ &+ \sigma_{FvMv} \sigma_\gamma \psi s\theta_o + \sigma_{FvMw} \sigma_\gamma \psi c\theta_o + \sigma_{FwMu} (\sigma_{\gamma\delta} c\theta_o + \sigma_\delta^2 s\theta_o) \\ &- \sigma_{FwMv} \sigma_\delta \psi s\theta_o - \sigma_{FwMw} \sigma_\delta \psi c\theta_o \end{aligned}$$

$$\begin{aligned} \text{Cov}[F_y, M_x] &= \sigma_{FuMv} (-\sigma_\gamma^2 c\theta_o - \sigma_{\gamma\delta} s\theta_o) + \sigma_{FuMw} (\sigma_{\gamma\delta} c\theta_o + \sigma_\delta^2 s\theta_o) \\ &+ \sigma_{FvMu} c\theta_o + \sigma_{FvMv} \sigma_\gamma \psi s\theta_o - \sigma_{FvMw} \sigma_\delta \psi s\theta_o - \sigma_{FwMu} s\theta_o \\ &+ \sigma_{FwMv} \sigma_\gamma \psi c\theta_o - \sigma_{FwMw} \sigma_\delta \psi c\theta_o \end{aligned}$$

$$\begin{aligned} \text{Cov}[F_y, M_y] &= \sigma_{FuMu} (\sigma_\gamma^2 c^2\theta_o + 2\sigma_{\gamma\delta} s\theta_o c\theta_o + \sigma_\delta^2 s^2\theta_o) + \sigma_{FuMv} (-\sigma_\gamma \psi s\theta_o c\theta_o \\ &- \sigma_\delta \psi s^2\theta_o) + \sigma_{FuMw} (-\sigma_\gamma \psi c^2\theta_o - \sigma_\delta \psi s\theta_o c\theta_o) \\ &+ \sigma_{FvMu} (-\sigma_\gamma \psi s\theta_o c\theta_o - \sigma_\delta \psi s^2\theta_o) + \sigma_{FvMv} (c^2\theta_o + \sigma_\psi^2 s^2\theta_o) \\ &+ \sigma_{FvMw} (\sigma_\psi^2 - 1) s\theta_o c\theta_o + \sigma_{FwMu} (-\sigma_\gamma \psi c^2\theta_o - \sigma_\delta \psi s\theta_o c\theta_o) \\ &+ \sigma_{FwMv} (\sigma_\psi^2 - 1) s\theta_o c\theta_o + \sigma_{FwMw} (\sigma_\psi^2 c^2\theta_o + s^2\theta_o) \end{aligned}$$

$$\begin{aligned} \text{Cov}[F_y, M_z] &= \sigma_{FuMu} \{(\sigma_\gamma^2 - \sigma_\delta^2) s\theta_o c\theta_o + \sigma_{\gamma\delta} (s^2\theta_o - c^2\theta_o)\} \\ &+ \sigma_{FuMv} (\sigma_\gamma \psi c^2\theta_o + \sigma_\delta \psi s\theta_o c\theta_o) + \sigma_{FuMw} (-\sigma_\gamma \psi s\theta_o c\theta_o - \sigma_\delta \psi s^2\theta_o) \\ &+ \sigma_{FvMu} (-\sigma_\gamma \psi s^2\theta_o + \sigma_\delta \psi s\theta_o c\theta_o) + \sigma_{FvMv} s\theta_o c\theta_o (1 - \sigma_\psi^2) \\ &+ \sigma_{FvMw} (c^2\theta_o + \sigma_\psi^2 s^2\theta_o) + \sigma_{FwMu} (-\sigma_\gamma \psi s\theta_o c\theta_o + \sigma_\delta \psi c^2\theta_o) \\ &+ \sigma_{FwMv} (-\sigma_\psi^2 c^2\theta_o - s^2\theta_o) + \sigma_{FwMw} (\sigma_\psi^2 - 1) s\theta_o c\theta_o \end{aligned}$$

$$\text{Cov}[F_z, M_x] = \sigma_{FuMv}(-\sigma_\gamma^2 s_{\theta_o}^2 + \sigma_{\gamma\delta} c_{\theta_o}) + \sigma_{FuMw}(\sigma_{\gamma\delta} s_{\theta_o} - \sigma_\delta^2 c_{\theta_o}^2)$$

$$+ \sigma_{FvMu} s_{\theta_o} - \sigma_{FvMv} \sigma_{\gamma\psi} c_{\theta_o} + \sigma_{FvMw} \sigma_{\delta\psi} c_{\theta_o}$$

$$+ \sigma_{FwMu} c_{\theta_o} + \sigma_{FwMv} \sigma_{\gamma\psi} s_{\theta_o} - \sigma_{FwMw} \sigma_{\delta\psi} s_{\theta_o}$$

$$\begin{aligned} \text{Cov}[F_z, M_y] = & \sigma_{FuMu} \{(\sigma_\gamma^2 - \sigma_\delta^2) s_{\theta_o} c_{\theta_o} - \sigma_{\gamma\delta} (s_{\theta_o}^2 - c_{\theta_o}^2)\} \\ & + \sigma_{FuMv} (\sigma_{\delta\psi} s_{\theta_o} c_{\theta_o} - \sigma_{\gamma\psi} s_{\theta_o}^2) + \sigma_{FuMw} (\sigma_{\delta\psi} c_{\theta_o}^2 - \sigma_{\gamma\psi} s_{\theta_o} c_{\theta_o}) \\ & + \sigma_{FvMu} (\sigma_{\gamma\psi} c_{\theta_o}^2 + \sigma_{\delta\psi} s_{\theta_o} c_{\theta_o}) + \sigma_{FvMv} s_{\theta_o} c_{\theta_o} (1 - \sigma_\psi^2) \\ & + \sigma_{FvMw} (-\sigma_\psi^2 c_{\theta_o}^2 - s_{\theta_o}^2) + \sigma_{FwMu} (-\sigma_{\gamma\psi} s_{\theta_o} c_{\theta_o} - \sigma_{\delta\psi} s_{\theta_o}^2) \\ & + \sigma_{FwMv} (\sigma_\psi^2 s_{\theta_o}^2 + c_{\theta_o}^2) + \sigma_{FwMw} (\sigma_\psi^2 - 1) s_{\theta_o} c_{\theta_o} \end{aligned}$$

$$\begin{aligned} \text{Cov}[F_z, M_z] = & \sigma_{FuMu} (\sigma_\gamma^2 s_{\theta_o}^2 - 2\sigma_{\gamma\delta} s_{\theta_o} c_{\theta_o} + \sigma_\delta^2 c_{\theta_o}^2) \\ & + \sigma_{FuMv} (\sigma_{\gamma\psi} s_{\theta_o} c_{\theta_o} - \sigma_{\delta\psi} c_{\theta_o}^2) + \sigma_{FuMw} (-\sigma_{\gamma\psi} s_{\theta_o}^2 + \sigma_{\delta\psi} s_{\theta_o} c_{\theta_o}) \\ & + \sigma_{FvMu} (\sigma_{\gamma\psi} s_{\theta_o} c_{\theta_o} - \sigma_{\delta\psi} c_{\theta_o}^2) + \sigma_{FvMv} (s_{\theta_o}^2 - \sigma_\psi^2 c_{\theta_o}^2) \\ & + \sigma_{FvMw} (1 - \sigma_\psi^2) s_{\theta_o} c_{\theta_o} + \sigma_{FwMu} (-\sigma_{\gamma\psi} s_{\theta_o}^2 + \sigma_{\delta\psi} s_{\theta_o} c_{\theta_o}) \\ & + \sigma_{FwMv} (1 - \sigma_\psi^2) s_{\theta_o} c_{\theta_o} + \sigma_{FwMw} (\sigma_\psi^2 s_{\theta_o}^2 + c_{\theta_o}^2) \end{aligned}$$

$$\begin{aligned} \text{Cov}[M_x, M_y] = & \sigma_{MuMv} \{(1 - \sigma_\gamma^2) c_{\theta_o} - \sigma_{\gamma\delta} s_{\theta_o}\} + \sigma_{MuMw} \{(\sigma_\delta^2 - 1) s_{\theta_o} + \sigma_{\gamma\delta} c_{\theta_o}\} \\ & + \sigma_{Mv}^2 \sigma_{\gamma\psi} s_{\theta_o} + \sigma_{MvMw} (\sigma_{\gamma\psi} c_{\theta_o} - \sigma_{\delta\psi} s_{\theta_o}) - \sigma_{Mw}^2 \sigma_{\delta\psi} c_{\theta_o} \\ & + \sigma_{FuFv} \sigma_z^2 \{(\sigma_\gamma^2 c_{\theta_o} + \sigma_{\gamma\delta} s_{\theta_o}) - c_{\theta_o}\} + \sigma_{FuFw} \sigma_z^2 \{(1 - \sigma_\delta^2) s_{\theta_o} - \sigma_{\gamma\delta} c_{\theta_o}\} \\ & + \sigma_{Fv}^2 \sigma_z^2 \sigma_{\gamma} s_{\theta_o} + \sigma_{Fw}^2 \sigma_z^2 \sigma_{\delta\psi} c_{\theta_o} + \sigma_{FvFw} \sigma_z^2 (\sigma_{\delta\psi} s_{\theta_o} - \sigma_{\gamma\psi} c_{\theta_o}) \end{aligned}$$

$$\begin{aligned} \text{Cov}[M_x, M_z] &= \sigma_{MuMv} \{ (1 - \sigma_\gamma^2) s_{\theta_o} + \sigma_{\gamma\delta} c_{\theta_o} \} + \sigma_{MuMw} \{ (1 - \sigma_\delta^2) c_{\theta_o} + \sigma_{\gamma\delta} s_{\theta_o} \} \\ &\quad - \sigma_{Mv}^2 \sigma_{\gamma\psi} c_{\theta_o} - \sigma_{Mw}^2 \sigma_{\delta\psi} s_{\theta_o} + \sigma_{MvMw} \{ \sigma_{\gamma\psi} s_{\theta_o} + \sigma_{\delta\psi} c_{\theta_o} \} \\ &\quad + \sigma_{FuFv} \sigma_y^2 \{ (\sigma_\gamma^2 - 1) s_{\theta_o} - \sigma_{\gamma\delta} c_{\theta_o} \} + \sigma_{FuFw} \sigma_y^2 \{ -\sigma_{\gamma\delta} s_{\theta_o} + (\sigma_\delta^2 - 1) c_{\theta_o} \} \\ &\quad - \sigma_{FvFw} \sigma_y^2 (\sigma_{\delta\psi} c_{\theta_o} + \sigma_{\gamma\psi} s_{\theta_o}) + \sigma_{Fv}^2 \sigma_y^2 \sigma_{\gamma\psi} c_{\theta_o} + \sigma_{Fw}^2 \sigma_y^2 \sigma_{\delta\psi} s_{\theta_o} \end{aligned}$$

$$\begin{aligned} \text{Cov}[M_y, M_z] &= \sigma_{Mu}^2 \{ (\sigma_\gamma^2 - \sigma_\delta^2) s_{\theta_o} c_{\theta_o} + \sigma_{\gamma\delta} (s_{\theta_o}^2 - c_{\theta_o}^2) \} \\ &\quad + \sigma_{MuMv} \{ \sigma_{\gamma\psi} c_{\theta_o}^2 - s_{\theta_o}^2 \} + 2\sigma_{\delta\psi} s_{\theta_o} c_{\theta_o} + \sigma_{MuMw} \{ -2\sigma_{\gamma\psi} s_{\theta_o} c_{\theta_o} \\ &\quad + \sigma_{\delta\psi} (c_{\theta_o}^2 - s_{\theta_o}^2) \} + \sigma_{MvMw} (\sigma_\psi^2 + 1) (c_{\theta_o}^2 - s_{\theta_o}^2) \\ &\quad + \sigma_{Mv}^2 (1 - \sigma_\psi^2) s_{\theta_o} c_{\theta_o} + \sigma_{Mw}^2 (\sigma_\psi^2 - 1) s_{\theta_o} c_{\theta_o} \\ &\quad - (\sigma_{Fu}^2 + \mu_{Fu}^2) \sigma_x^2 \{ (\sigma_\gamma^2 - \sigma_\delta^2) s_{\theta_o} c_{\theta_o} + \sigma_{\gamma\delta} (s_{\theta_o}^2 - c_{\theta_o}^2) \} \\ &\quad + \sigma_{FuFv} \sigma_x^2 \{ \sigma_{\gamma\psi} (s_{\theta_o}^2 - c_{\theta_o}^2) - 2\sigma_{\delta\psi} s_{\theta_o} c_{\theta_o} \} + \sigma_{FuFw} \sigma_x^2 (2\sigma_{\gamma\psi} s_{\theta_o} c_{\theta_o} \\ &\quad + \sigma_{\delta\psi}) - \sigma_{Fw}^2 \sigma_x^2 (\sigma_\psi^2 - 1) s_{\theta_o} c_{\theta_o} \\ &\quad + \sigma_{FvFw} \sigma_x^2 (\sigma_\psi^2 - 1) \end{aligned}$$



#### 4.4 SOLUTION FOR A RING OF TWO ENGINES

##### 4.4.1 Expected Values

$$E[F_x] = 2\mu_{Fu}c\Gamma$$

$$E[F_y] = E[F_z] = E[M_x] = E[M_y] = E[M_z] = 0$$

##### 4.4.2 Variances\*

$$\begin{aligned} \text{Var}[F_x] = & 2\{\sigma_\gamma^2(\sigma_{Fu}^2 + \mu_{Fu}^2)s_\Gamma^2 + \sigma_{Fu}^2c_\Gamma^2 + \sigma_{Fv}^2(\sigma_\gamma^2c_\Gamma^2 + s_\Gamma^2) \\ & + \sigma_{Fw}^2(\sigma_\delta^2c_\Gamma^2 + \sigma_\psi^2s_\Gamma^2 \oplus - 2\sigma_\delta\psi s_\Gamma c_\Gamma)\} \end{aligned}$$

$$\begin{aligned} \text{Var}[F_y] = & 2\left\{(\sigma_{Fu}^2 + \mu_{Fu}^2)\{(\sigma_\gamma^2c_\Gamma^2 + s_\Gamma^2(1 - \sigma_\theta^2) + \sigma_\delta^2\sigma_\theta^2)\right. \\ & + \sigma_{Fv}^2\{(\sigma_\gamma^2s_\Gamma^2 + c_\Gamma^2)(1 - \sigma_\theta^2) + \sigma_\psi^2\sigma_\theta^2\} \\ & + \sigma_{Fw}^2\{(\sigma_\delta^2s_\Gamma^2 + \sigma_\psi^2c_\Gamma^2 \ominus + 2\sigma_\delta\psi s_\Gamma c_\Gamma)(1 - \sigma_\theta^2) + \sigma_\theta^2\} \\ & \left. - \mu_{Fu}^2s_\Gamma^2\right\} \end{aligned}$$

$$\begin{aligned} \text{Var}[F_z] = & 2\left\{(\sigma_{Fu}^2 + \mu_{Fu}^2)\{\sigma_\theta^2(\sigma_\gamma^2c_\Gamma^2 + s_\Gamma^2) + \sigma_\delta^2(1 - \sigma_\theta^2)\}\right. \\ & + \sigma_{Fv}^2\{\sigma_\theta^2(\sigma_\gamma^2s_\Gamma^2 + c_\Gamma^2) + \sigma_\psi^2(1 - \sigma_\theta^2)\} \\ & \left. + \sigma_{Fw}^2\{\sigma_\theta^2(\sigma_\delta^2s_\Gamma^2 + \sigma_\psi^2c_\Gamma^2 \ominus + 2\sigma_\delta\psi s_\Gamma c_\Gamma) + 1 - \sigma_\theta^2\}\right\} \end{aligned}$$

\*Variances and covariances for the two-engine case are valid only if the y-axis passes through the nominal gimbal point of each engine.

$$\begin{aligned} \text{Var}[M_x] = & 2 \left\{ \sigma_{Mu}^2 (c^2 \Gamma + \sigma_\gamma^2 s^2 \Gamma) + \sigma_{Mv}^2 (\sigma_\gamma^2 c^2 \Gamma + s^2 \Gamma) \right. \\ & + \sigma_{Mw}^2 (\sigma_\delta^2 c^2 \Gamma + \sigma_\psi^2 s^2 \Gamma - 2\sigma_\delta \sigma_\psi s \Gamma c \Gamma) \\ & + (\sigma_R^2 + R_o^2) \{ \sigma_\delta^2 (\sigma_{Fu}^2 + \mu_{Fu}^2) + \sigma_{Fv}^2 \sigma_\psi^2 + \sigma_{Fw}^2 \} \\ & + R_o \{ -\sigma_{MuFu} \sigma_{\gamma\delta} s \Gamma + \sigma_{MuFv} \sigma_{\gamma\psi} s \Gamma + \sigma_{MuFw} c \Gamma \\ & + \sigma_{MvFu} \sigma_{\gamma\delta} c \Gamma - \sigma_{MvFv} \sigma_{\gamma\psi} c \Gamma + \sigma_{MvFw} s \Gamma \\ & + \sigma_{MwFu} (-\sigma_\delta^2 c \Gamma + \sigma_\psi^2 s \Gamma) - \sigma_{MwFv} (\sigma_\psi^2 s \Gamma - \sigma_\delta \sigma_\psi c \Gamma) \} \\ & + \sigma_{MuMv} (1 - \sigma_\gamma^2) s \Gamma c \Gamma + \sigma_{MuMw} (\sigma_{\gamma\delta} s \Gamma c \Gamma - \sigma_{\gamma\psi} s^2 \Gamma) \\ & \left. + \sigma_{MvMw} (\sigma_{\gamma\psi} c \Gamma s \Gamma - \sigma_{\gamma\delta} c^2 \Gamma) \right\} \end{aligned}$$

$$\begin{aligned} \text{Var}[M_y] = & 2 \left\{ \sigma_{Mu}^2 \{ (\sigma_\gamma^2 c^2 \Gamma + s^2 \Gamma) (1 - \sigma_\theta^2) + \sigma_\delta^2 \sigma_\theta^2 \} + \sigma_{Mv}^2 \{ (\sigma_\gamma^2 s^2 \Gamma + c^2 \Gamma) (1 - \sigma_\theta^2) \right. \\ & + \sigma_\psi^2 \sigma_\theta^2 \} + \sigma_{Mw}^2 \{ (\sigma_\delta^2 s^2 \Gamma + \sigma_\psi^2 c^2 \Gamma + 2\sigma_\delta \sigma_\psi s \Gamma c \Gamma) (1 - \sigma_\theta^2) + \sigma_\theta^2 \} \\ & + (\sigma_{Fu}^2 + \mu_{Fu}^2) \{ \sigma_\theta^2 (\sigma_R^2 + R_o^2) (c^2 \Gamma + \sigma_\gamma^2 s^2 \Gamma) + \sigma_x^2 \sigma_\theta^2 (\sigma_\gamma^2 c^2 \Gamma + s^2 \Gamma) \\ & + \sigma_x^2 \sigma_\delta^2 (1 - \sigma_\theta^2) \} + \sigma_{Fv}^2 \{ \sigma_\theta^2 (\sigma_R^2 + R_o^2) (\sigma_\gamma^2 c^2 \Gamma + s^2 \Gamma) \\ & + \sigma_x^2 \sigma_\theta^2 (\sigma_\gamma^2 s^2 \Gamma + c^2 \Gamma) + \sigma_x^2 \sigma_\psi^2 (1 - \sigma_\theta^2) \} + \sigma_{Fw}^2 \{ \sigma_\theta^2 (\sigma_R^2 + R_o^2) (\sigma_\delta^2 c^2 \Gamma \\ & + \sigma_\psi^2 s^2 \Gamma - 2\sigma_\delta \sigma_\psi c \Gamma s \Gamma) + \sigma_x^2 \sigma_\theta^2 (\sigma_\delta^2 s^2 \Gamma + \sigma_\psi^2 c^2 \Gamma + 2\sigma_\delta \sigma_\psi s \Gamma c \Gamma) + \sigma_x^2 (1 - \sigma_\theta^2) \} \\ & + R_o \sigma_\theta^2 \{ \sigma_{MuFu} \sigma_{\gamma\delta} s \Gamma - \sigma_{MuFv} \sigma_{\gamma\psi} c \Gamma + \sigma_{MuFw} (\sigma_\delta^2 c \Gamma - \sigma_\delta \sigma_\psi s \Gamma) - \sigma_{MvFu} \sigma_{\gamma\psi} s \Gamma \\ & + \sigma_{MvFv} \sigma_{\gamma\psi} c \Gamma - \sigma_{MvFw} (\sigma_\psi^2 c \Gamma - \sigma_\psi^2 s \Gamma) - \sigma_{MwFu} c \Gamma - \sigma_{MwFv} s \Gamma \} \\ & + \sigma_{MuMv} \{ (1 - \sigma_\theta^2) (\sigma_\gamma^2 - 1) s \Gamma c \Gamma - \sigma_\theta^2 \sigma_\delta \sigma_\psi \} - \sigma_{MuMw} (1 - \sigma_\theta^2) (\sigma_{\gamma\psi} c^2 \Gamma + \sigma_{\gamma\delta} c \Gamma s \Gamma) \\ & \left. - \sigma_{MvMw} (1 - \sigma_\theta^2) (\sigma_{\gamma\delta} s^2 \Gamma + \sigma_{\gamma\psi} s \Gamma c \Gamma) \right\} \end{aligned}$$

September 1966

$$\begin{aligned}
\text{Var}[M_z] = & 2 \left\{ \sigma_{Mu}^2 \{ \sigma_\theta^2 (\sigma_\gamma^2 c^2 \Gamma + s^2 \Gamma) + \sigma_\delta^2 (1 - \sigma_\theta^2) \} + \sigma_{Mv}^2 \{ \sigma_\theta^2 (\sigma_\gamma^2 s^2 \Gamma + c^2 \Gamma) \right. \\
& + \sigma_\psi^2 (1 - \sigma_\theta^2) \} + \sigma_{Mw}^2 \{ \sigma_\theta^2 (\sigma_\delta^2 s^2 \Gamma + \sigma_\psi^2 c^2 \Gamma + 2\sigma_\delta \psi s \Gamma c \Gamma) + (1 - \sigma_\theta^2) \} \\
& + (\sigma_{Fu}^2 + \mu_{Fu}^2) \{ (\sigma_R^2 + R_o^2) (\sigma_\gamma^2 s^2 \Gamma + c^2 \Gamma) (1 - \sigma_\theta^2) + \sigma_x^2 (\sigma_\gamma^2 c^2 \Gamma \\
& + s^2 \Gamma) (1 - \sigma_\theta^2) + \sigma_\delta^2 \sigma_\theta^2 \} + \sigma_{Fv}^2 \{ (\sigma_R^2 + R_o^2) (\sigma_\gamma^2 c^2 \Gamma + s^2 \Gamma) (1 - \sigma_\theta^2) \\
& + \sigma_x^2 \{ (\sigma_\gamma^2 s^2 \Gamma + c^2 \Gamma) (1 - \sigma_\theta^2) + \sigma_\psi^2 \sigma_\theta^2 \} + \sigma_{Fw}^2 (\sigma_R^2 + R_o^2) (\sigma_\delta^2 c^2 \Gamma \\
& + \sigma_\psi^2 s^2 \Gamma - 2\sigma_\delta \psi c \Gamma s \Gamma) (1 - \sigma_\theta^2) + \sigma_x^2 (\sigma_\delta^2 s^2 \Gamma + \sigma_\psi^2 c^2 \Gamma + 2\sigma_\delta \psi s \Gamma c \Gamma) (1 - \sigma_\theta^2) \\
& + \sigma_x^2 \sigma_\theta^2 \} + R_o (1 - \sigma_\theta^2) \{ \sigma_{MuFu} \sigma_\gamma \sigma_\delta s \Gamma - \sigma_{MuFv} \sigma_\gamma \sigma_\delta c \Gamma + \sigma_{MuFw} (\sigma_\delta^2 c \Gamma - \sigma_\delta \psi s \Gamma) \\
& - \sigma_{MvFu} \sigma_\gamma \psi s \Gamma + \sigma_{MvFv} \sigma_\gamma \psi c \Gamma + \sigma_{MvFw} (-\sigma_\delta \psi c \Gamma + \sigma_\psi^2 s \Gamma) - \sigma_{MwFu} c \Gamma - \sigma_{MwFv} s \Gamma \} \\
& - \sigma_{MwMv} \{ \sigma_\theta^2 (\sigma_\gamma^2 - 1) s \Gamma c \Gamma - \sigma_\delta \psi (1 - \sigma_\theta^2) \} - \sigma_{MuMw} \sigma_\theta^2 (\sigma_\gamma \sigma_\delta s \Gamma c \Gamma + \sigma_\gamma \psi c^2 \Gamma) \\
& \left. - \sigma_{MvMw} \sigma_\theta^2 (\sigma_\delta \gamma s^2 \Gamma + \sigma_\gamma \psi s \Gamma c \Gamma) - R_o^2 \mu_{Fu}^2 c^2 \Gamma \right\}
\end{aligned}$$

#### 4.4.3 Covariances

$$\text{Cov}[F_x, F_y] = 0$$

$$\text{Cov}[F_x, F_z] = 0$$

$$\text{Cov}[F_y, F_z] = 2 \{ (\sigma_{Fu}^2 + \mu_{Fu}^2) (-\sigma_\gamma \sigma_\delta c \Gamma) + \sigma_{Fv}^2 (1 - 2\sigma_\theta^2) \sigma_\gamma \psi s \Gamma \}$$

$$\begin{aligned}
\text{Cov}[F_x, M_x] = & 2 \left\{ -R_o \{ \sigma_\gamma \sigma_\delta (\sigma_{Fu}^2 + \mu_{Fu}^2) s \Gamma + \sigma_\gamma \psi \sigma_{Fv}^2 c \Gamma \} \right. \\
& + \sigma_{FuMu} (c^2 \Gamma + \sigma_\gamma^2 s^2 \Gamma) + \sigma_{FuMv} (1 - \sigma_\gamma^2) s \Gamma c \Gamma \\
& + \sigma_{FuMw} (\sigma_\gamma \sigma_\delta s \Gamma c \Gamma - \sigma_\gamma \psi s^2 \Gamma) + \sigma_{FvMu} (1 - \sigma_\gamma^2) s \Gamma c \Gamma \\
& + \sigma_{FvMv} (\sigma_\gamma^2 c^2 \Gamma + s^2 \Gamma) + \sigma_{FvMw} (\sigma_\gamma \psi s \Gamma c \Gamma - \sigma_\gamma \sigma_\delta c^2 \Gamma) \\
& + \sigma_{FwMu} (\sigma_\gamma \sigma_\delta s \Gamma c \Gamma - \sigma_\gamma \psi s^2 \Gamma) + \sigma_{FwMv} (\sigma_\delta \psi s \Gamma c \Gamma - \sigma_\gamma \sigma_\delta c^2 \Gamma) \\
& \left. + \sigma_{FwMw} (\sigma_\delta^2 c^2 \Gamma + \sigma_\psi^2 s^2 \Gamma - 2\sigma_\delta \psi s \Gamma c \Gamma) \right\}
\end{aligned}$$

$$\text{Cov}[F_x, M_y] = 0$$

$$\text{Cov}[F_x, M_z] = 0$$

$$\text{Cov}[F_y, M_x] = 0$$

$$\begin{aligned} \text{Cov}[F_y, M_y] = & 2 \left\{ R_o \sigma_\theta^2 \{ \sigma_{\gamma\delta} (\sigma_{Fu}^2 + \mu_{Fu}^2) s\Gamma + \sigma_{\gamma\psi} \sigma_{Fv}^2 c\Gamma \} \right. \\ & + \sigma_{FuMu} \{ (\sigma_\gamma^2 c^2\Gamma + s^2\Gamma)(1 - \sigma_\theta^2) + \sigma_\delta^2 \sigma_\theta^2 \} + \sigma_{FuMv} \{ (\sigma_\gamma^2 - 1)(1 - \sigma_\theta^2) s\Gamma c\Gamma \\ & - \sigma_\delta \psi \sigma_\theta^2 \} - \sigma_{FuMw} (\sigma_{\gamma\psi} c^2\Gamma + \sigma_{\gamma\delta} s\Gamma c\Gamma)(1 - \sigma_\theta^2) + \sigma_{FvMu} \{ (\sigma_\gamma^2 - 1)(1 - \sigma_\theta^2) s\Gamma c\Gamma \\ & - \sigma_\delta \psi \sigma_\theta^2 \} + \sigma_{FvMv} \{ (\sigma_\gamma^2 s^2\Gamma + c^2\Gamma)(1 - \sigma_\theta^2) + \sigma_\psi^2 \sigma_\theta^2 \} - \sigma_{FvMw} (\sigma_{\gamma\delta} s^2\Gamma \\ & + \sigma_{\gamma\psi} s\Gamma c\Gamma)(1 - \sigma_\theta^2) + \sigma_{FwMu} (-\sigma_{\gamma\delta} s\Gamma c\Gamma - \sigma_{\gamma\psi} c^2\Gamma)(1 - \sigma_\theta^2) \\ & - \sigma_{FwMv} (\sigma_{\gamma\delta} s^2\Gamma + \sigma_{\gamma\psi} s\Gamma c\Gamma)(1 - \sigma_\theta^2) + \sigma_{FwMw} \{ (\sigma_\delta^2 s^2\Gamma + \sigma_\psi^2 c^2\Gamma \\ & \left. + 2\sigma_\delta \psi s\Gamma c\Gamma)(1 - \sigma_\theta^2) + \sigma_\theta^2 \} \right\} \end{aligned}$$

$$\begin{aligned} \text{Cov}[F_y, M_z] = & 2 \left\{ R_o (1 - \sigma_\theta^2) \{ (\sigma_{Fu}^2 + \mu_{Fu}^2)(1 - \sigma_\gamma^2) s\Gamma c\Gamma + \sigma_{Fv}^2 (\sigma_\gamma^2 - 1) s\Gamma c\Gamma \right. \\ & + \sigma_{Fw}^2 \{ \sigma_\delta^2 s\Gamma c\Gamma + \sigma_\delta \psi (c^2\Gamma - s^2\Gamma) - \sigma_\psi^2 s\Gamma c\Gamma \} - \sigma_{FuMu} \sigma_{\gamma\delta} (1 - 2\sigma_\theta^2) c\Gamma \\ & + \sigma_{FuMv} (\sigma_{\gamma\psi} c\Gamma (1 - \sigma_\theta^2) + \sigma_{\gamma\delta} \sigma_\theta^2 s\Gamma) - \sigma_{FuMw} \{ s\Gamma (1 - \sigma_\theta^2) + \sigma_\theta^2 (\sigma_\delta \psi c\Gamma \\ & + \sigma_\delta^2 s\Gamma) \} - \sigma_{FvMu} \{ \sigma_{\gamma\psi} \sigma_\theta^2 c\Gamma + \sigma_{\gamma\delta} s\Gamma (1 - \sigma_\theta^2) \} + \sigma_{FvMv} \sigma_{\gamma\psi} (1 - 2\sigma_\theta^2) s\Gamma \\ & + \sigma_{FvMw} \{ c\Gamma (1 - \sigma_\theta^2) + \sigma_\theta^2 (\sigma_\psi^2 c\Gamma + \sigma_\delta \psi s\Gamma) \} + \sigma_{FwMu} \{ \sigma_\theta^2 s\Gamma + (\sigma_\delta^2 s\Gamma \\ & + \sigma_\delta \psi c\Gamma)(1 - \sigma_\theta^2) \} - \sigma_{FwMv} \{ \sigma_\theta^2 c\Gamma + (\sigma_\delta \psi s\Gamma + \sigma_\psi^2 c\Gamma)(1 - \sigma_\theta^2) \} \\ & \left. - R_o \mu_{Fu}^2 s\Gamma c\Gamma \right\} \end{aligned}$$

$$\text{Cov}[F_z, M_x] = 0$$

$$\begin{aligned} \text{Cov}[F_z, M_y] = 2 \left\{ R_o \{ (\sigma_{Fu}^2 + \mu_{Fu}^2)(\sigma_\gamma^2 - 1)\sigma_\theta^2 s\Gamma c\Gamma + \sigma_{Fv}^2 \sigma_\theta^2 (1 - \sigma_\gamma^2) s\Gamma c\Gamma \right. \\ + \sigma_{Fw}^2 \sigma_\theta^2 \{ (\sigma_\psi^2 - \sigma_\delta^2) s\Gamma c\Gamma + \sigma_\delta \psi (s^2\Gamma - c^2\Gamma) \} \} - \sigma_{FuMu} \sigma_\gamma \delta c\Gamma \\ - \sigma_{FuMv} \{ \sigma_\gamma \psi \sigma_\theta^2 c\Gamma + \sigma_\gamma \delta s\Gamma (1 - \sigma_\theta^2) \} + \sigma_{FuMw} \{ \sigma_\theta^2 s\Gamma + (\sigma_\delta^2 s\Gamma + \sigma_\delta \psi c\Gamma)(1 - \sigma_\theta^2) \} \\ + \sigma_{FvMu} \{ \sigma_\gamma \delta \sigma_\theta^2 s\Gamma + \sigma_\gamma \psi c\Gamma (1 - \sigma_\theta^2) \} + \sigma_{FvMv} \sigma_\gamma \psi s\Gamma \\ - \sigma_{FvMw} \{ \sigma_\theta^2 c\Gamma + (\sigma_\psi^2 c\Gamma + \sigma_\delta \psi s\Gamma)(1 - \sigma_\theta^2) \} - \sigma_{FwMu} \{ s\Gamma (1 - \sigma_\theta^2) \\ + \sigma_\theta^2 (\sigma_\delta \psi c\Gamma + \sigma_\delta^2 s\Gamma) \} + \sigma_{FwMv} \{ c\Gamma (1 - \sigma_\theta^2) + \sigma_\theta^2 (\sigma_\psi^2 c\Gamma + \sigma_\delta \psi s\Gamma) \} \} \end{aligned}$$

$$\begin{aligned} \text{Cov}[F_z, M_z] = 2 \left\{ R_o (1 - \sigma_\theta^2) \{ (\sigma_{Fu}^2 + \mu_{Fu}^2) \sigma_\gamma \delta s\Gamma + \sigma_{Fv}^2 \sigma_\gamma \psi c\Gamma \} \right. \\ + \sigma_{FuMu} \{ \sigma_\theta^2 (\sigma_\gamma^2 c^2\Gamma + s^2\Gamma) + \sigma_\delta^2 (1 - \sigma_\theta^2) \} + \sigma_{FuMv} \{ \sigma_\theta^2 (\sigma_\gamma^2 - 1) s\Gamma c\Gamma \\ - \sigma_\delta \psi (1 - \sigma_\theta^2) \} - \sigma_{FuMw} \sigma_\theta^2 (\sigma_\gamma \psi c^2\Gamma + \sigma_\delta \gamma s\Gamma c\Gamma) + \sigma_{FvMu} \{ \sigma_\theta^2 (\sigma_\gamma^2 - 1) s\Gamma c\Gamma \\ - \sigma_\delta \psi (1 - \sigma_\theta^2) \} + \sigma_{FvMv} \{ \sigma_\theta^2 (\sigma_\gamma^2 s^2\Gamma + c^2\Gamma) + \sigma_\psi^2 (1 - \sigma_\theta^2) \} \\ - \sigma_{FvMw} \sigma_\theta^2 (\sigma_\gamma \delta s^2\Gamma + \sigma_\gamma \psi s\Gamma c\Gamma) - \sigma_{FwMu} \sigma_\theta^2 (\sigma_\gamma \psi c^2\Gamma + \sigma_\gamma \delta s\Gamma c\Gamma) \\ - \sigma_{FwMv} \sigma_\theta^2 (\sigma_\gamma \delta s^2\Gamma + \sigma_\gamma \psi s\Gamma c\Gamma) + \sigma_{FwMw} \{ \sigma_\theta^2 (\sigma_\delta^2 s^2\Gamma + \sigma_\psi^2 c^2\Gamma \\ + 2\sigma_\delta \psi s\Gamma c\Gamma) + 1 - \sigma_\theta^2 \} \} \end{aligned}$$

$$\text{Cov}[M_x, M_y] = 0$$

$$\text{Cov}[M_x, M_z] = 0$$

$$\begin{aligned}
 \text{Cov}[M_y, M_z] = & 2 \left\{ -\sigma_{Mu}^2 \sigma_{\gamma\delta} c\Gamma + \sigma_{Mv}^2 \sigma_{\gamma\psi} s\Gamma (1 - 2\sigma_\theta^2) - (\sigma_{Fu}^2 + \mu_{Fu}^2) \sigma_{\gamma\delta} c\Gamma + \sigma_{Fv}^2 \sigma_{\gamma\psi} s\Gamma \right. \\
 & + \sigma_{MuMv} (1 - 2\sigma_\theta^2) (\sigma_{\gamma\psi} c\Gamma + \sigma_{\gamma\psi} s\Gamma) - \sigma_{MuMw} (1 - 2\sigma_\theta^2) \{ \sigma_{\delta\psi} c\Gamma + (\sigma_\delta^2 - 1) s\Gamma \} \\
 & - \sigma_{MvMw} (1 - 2\sigma_\theta^2) \{ (\sigma_\psi^2 - 1) c\Gamma + \sigma_{\delta\psi} s\Gamma \} \left. \right\} + 2R_o (1 - 2\sigma_\theta^2) \left\{ \sigma_{MuFu} (1 - \sigma_\gamma^2) s\Gamma c\Gamma \right. \\
 & + \sigma_{MuFv} (\sigma_\gamma^2 c^2\Gamma + s^2\Gamma) + \sigma_{MuFw} (\sigma_{\gamma\psi} s\Gamma c\Gamma + \sigma_{\gamma\delta} c^2\Gamma) - \sigma_{MvFu} (\sigma_\gamma^2 s^2\Gamma + c^2\Gamma) \\
 & - \sigma_{MvFv} (1 - \sigma_\gamma^2) s\Gamma c\Gamma - \sigma_{MvFw} (\sigma_{\gamma\delta} s\Gamma c\Gamma + \sigma_{\gamma\psi} s^2\Gamma) + \sigma_{MwFu} (\sigma_{\gamma\psi} s\Gamma c\Gamma + \sigma_{\gamma\delta} s^2\Gamma) \\
 & \left. - \sigma_{MwFv} (\sigma_{\gamma\delta} s\Gamma c\Gamma + \sigma_{\gamma\psi} c^2\Gamma) - \sigma_{MwFw} \{ (\sigma_\psi^2 - \sigma_\delta^2) s\Gamma c\Gamma + \sigma_{\delta\psi} (c^2\Gamma - s^2\Gamma) \} \right\}
 \end{aligned}$$

#### 4.5 SOLUTION FOR A RING OF N ENGINES (N > 2)

##### 4.5.1 Expected Value

$$E[F_x] = N \mu_{Fu} c \Gamma$$

$$E[F_y] = E[F_z] = E[M_x] = E[M_y] = E[M_z] = 0$$

##### 4.5.2 Variances

$$\begin{aligned} \text{Var}[F_x] = N \{ & \sigma_{\gamma}^2 (\sigma_{Fu}^2 + \mu_{Fu}^2) s^2 \Gamma + \sigma_{Fu}^2 c^2 \Gamma + \sigma_{Fv}^2 (\sigma_{\gamma}^2 c^2 \Gamma + s^2 \Gamma) \\ & + \sigma_{Fw}^2 (\sigma_{\delta}^2 c^2 \Gamma + \sigma_{\psi}^2 s^2 \Gamma - 2\sigma_{\delta\psi} s \Gamma c \Gamma) \} \end{aligned}$$

$$\text{Var}[F_y] =$$

$$\begin{aligned} \text{Var}[F_z] = \frac{N}{2} (1 + \sigma_{\theta}^2) \{ & (\sigma_{Fu}^2 + \mu_{Fu}^2) (\sigma_{\gamma}^2 c^2 \Gamma + s^2 \Gamma + \sigma_{\delta}^2) \\ & + \sigma_{Fv}^2 (\sigma_{\gamma}^2 s^2 \Gamma + c^2 \Gamma + \sigma_{\psi}^2) \\ & + \sigma_{Fw}^2 (\sigma_{\delta}^2 s^2 \Gamma + \sigma_{\psi}^2 c^2 \Gamma + 2\sigma_{\delta\psi} s \Gamma c \Gamma + 1) \} - \frac{N}{2} \mu_{Fu}^2 s^2 \Gamma \end{aligned}$$

$$\begin{aligned} \text{Var}[M_x] = N \{ & \sigma_{Mu}^2 (c^2 \Gamma + \sigma_{\gamma}^2 s^2 \Gamma) + \sigma_{Mv}^2 (\sigma_{\gamma}^2 c^2 \Gamma + s^2 \Gamma) \\ & + \sigma_{Mw}^2 (\sigma_{\delta}^2 c^2 \Gamma + \sigma_{\psi}^2 s^2 \Gamma - 2\sigma_{\delta\psi} s \Gamma c \Gamma) \\ & + (\sigma_R^2 + R_o^2) \{ (\sigma_{Fu}^2 + \mu_{Fu}^2) \sigma_{\delta}^2 + \sigma_{Fv}^2 \sigma_{\psi}^2 + \sigma_{Fw}^2 \} \\ & + R_o \{ -\sigma_{MuFu} \sigma_{\gamma\delta} s \Gamma + \sigma_{MuFv} \sigma_{\gamma\psi} s \Gamma + \sigma_{MuFw} c \Gamma \} \end{aligned}$$

$$\begin{aligned}
 & \ominus + \sigma_{MvFu} \sigma_{\gamma\delta} c\Gamma - \sigma_{MvFv} \sigma_{\gamma\psi} c\Gamma + \sigma_{MvFw} s\Gamma \\
 & + \sigma_{MwFu} (\ominus \sigma_{\delta}^2 c\Gamma + \sigma_{\delta\psi} s\Gamma) + \sigma_{MwFv} (\sigma_{\delta\psi} c\Gamma - \sigma_{\psi}^2 s\Gamma) \\
 & \ominus + \sigma_{MuMv} (1 - \sigma_{\gamma}^2) s\Gamma c\Gamma + \sigma_{MuMw} (\sigma_{\gamma\delta} s\Gamma c\Gamma - \sigma_{\gamma\psi} s^2\Gamma) \\
 & + \sigma_{MvMw} (\sigma_{\gamma\psi} c\Gamma s\Gamma - \sigma_{\gamma\delta} c^2\Gamma) \}
 \end{aligned}$$

$$\text{Var}[M_y] =$$

$$\begin{aligned}
 \text{Var}[M_z] &= \frac{N}{2} (1 + \sigma_{\theta}^2) \{ \sigma_{Mu}^2 (\sigma_{\gamma}^2 c^2\Gamma + s^2\Gamma + \sigma_{\delta}^2) \\
 & + \sigma_{Mv}^2 (\sigma_{\gamma}^2 s^2\Gamma + c^2\Gamma + \sigma_{\psi}^2) \\
 & + \sigma_{Mw}^2 (\sigma_{\delta}^2 s^2\Gamma + \sigma_{\psi}^2 c^2\Gamma + 2\sigma_{\delta\psi} s\Gamma c\Gamma + 1) \\
 & + (\sigma_{Fu}^2 + \mu_{Fu}^2) \{ (\sigma_R^2 + R_o^2) (c^2\Gamma + \sigma_{\gamma}^2 s^2\Gamma) + \sigma_x^2 (\sigma_{\gamma}^2 c^2\Gamma + s^2\Gamma + \sigma_{\delta}^2) \} \\
 & + \sigma_{Fv}^2 \{ (\sigma_R^2 + R_o^2) (\sigma_{\gamma}^2 c^2\Gamma + s^2\Gamma) + \sigma_x^2 (\sigma_{\gamma}^2 s^2\Gamma + c^2\Gamma + \sigma_{\psi}^2) \} \\
 & + \sigma_{Fw}^2 \{ (\sigma_R^2 + R_o^2) (\sigma_{\delta}^2 c^2\Gamma + \sigma_{\psi}^2 s^2\Gamma - 2\sigma_{\delta\psi} s\Gamma c\Gamma) \\
 & + \sigma_x^2 (\sigma_{\delta}^2 s^2\Gamma + \sigma_{\psi}^2 c^2\Gamma + 2\sigma_{\delta\psi} s\Gamma c\Gamma + 1) \} \\
 & + R_o \{ \sigma_{MuFu} \sigma_{\delta\gamma} s\Gamma - \sigma_{MuFv} \sigma_{\delta\gamma} c\Gamma + \sigma_{MuFw} (\sigma_{\delta}^2 c\Gamma - \sigma_{\delta\psi} s\Gamma) \\
 & - \sigma_{MvFu} \sigma_{\psi\gamma} s\Gamma - \sigma_{MvFv} \sigma_{\psi\gamma} c\Gamma + \sigma_{MvFw} (\sigma_{\psi}^2 s\Gamma - \sigma_{\psi\delta} c\Gamma) \\
 & \ominus - \sigma_{MwFu} c\Gamma - \sigma_{MwFv} s\Gamma \} + \sigma_{MuMv} \{ (\sigma_{\gamma}^2 - 1) s\Gamma c\Gamma - \sigma_{\delta\psi} \} \\
 & - \sigma_{MuMw} (\sigma_{\gamma\psi} c^2\Gamma + \sigma_{\gamma\delta} s\Gamma c\Gamma) - \sigma_{MvMw} (\sigma_{\gamma\delta} s^2\Gamma + \sigma_{\gamma\psi} s\Gamma c\Gamma) \} - \frac{N}{2} R_o^2 \mu_{Fu}^2 c^2\Gamma
 \end{aligned}$$



#### 4.5.3 Covariances

$$\text{Cov}[F_x, F_y] = 0$$

$$\text{Cov}[F_x, F_z] = 0$$

$$\text{Cov}[F_y, F_z] = 0$$

$$\begin{aligned} \text{Cov}[F_x, M_x] = N \{ & -R_o \sigma_{\gamma\delta} (\sigma_{Fw}^2 + \mu_{Fu}^2) s\Gamma + R_o \sigma_{\gamma\psi} \sigma_{Fv}^2 c\Gamma \\ & + \sigma_{FuMu} (c^2\Gamma + \sigma_{\gamma s}^2 \Gamma) + \sigma_{FuMv} (1 - \sigma_{\gamma}^2) s\Gamma c\Gamma \\ & + \sigma_{FuMw} (\sigma_{\gamma\psi} s\Gamma c\Gamma - \sigma_{\gamma\psi} s^2\Gamma) + \sigma_{FvMu} (1 - \sigma_{\gamma}^2) s\Gamma c\Gamma \\ & + \sigma_{FvMv} (\sigma_{\gamma}^2 c^2\Gamma + s^2\Gamma) + \sigma_{FvMw} (\sigma_{\gamma\psi} s\Gamma c\Gamma - \sigma_{\gamma\delta} c^2\Gamma) \\ & + \sigma_{FwMu} (\sigma_{\gamma\delta} s\Gamma c\Gamma - \sigma_{\gamma\psi} s^2\Gamma) + \sigma_{FwMv} (\sigma_{\gamma\psi} s\Gamma c\Gamma - \sigma_{\gamma\delta} c^2\Gamma) \\ & + \sigma_{FwMw} (\sigma_{\delta}^2 c^2\Gamma + \sigma_x^2 s^2\Gamma - 2\sigma_{\delta\psi} s\Gamma c\Gamma) \} \end{aligned}$$

$$\text{Cov}[F_x, M_y] = 0$$

$$\text{Cov}[F_x, M_z] = 0$$

$$\text{Cov}[F_y, M_x] = 0$$

$$\text{Cov}[F_y, M_y] =$$

$$\begin{aligned} \text{Cov}[F_z, M_z] = & \frac{N}{2} (1 + \sigma_{\theta}^2) \{ R_o \sigma_{\gamma\delta} (\sigma_{Fu}^2 + \mu_{Fu}^2) s\Gamma + R_o \sigma_{Fv}^2 \sigma_{\gamma\psi} c\Gamma \\ & + \sigma_{FuMu} (\sigma_{\gamma}^2 c^2\Gamma + s^2\Gamma + \sigma_{\delta}^2) + \sigma_{FuMv} \{ (\sigma_{\gamma}^2 - 1) s\Gamma c\Gamma - \sigma_{\delta\psi} \} \} \end{aligned}$$

$$\begin{aligned}
 & - \sigma_{FuMw}(\sigma_Y \psi^2 \Gamma + \sigma_{Y\delta} s \Gamma c \Gamma) + \sigma_{FvMu} \{ (\sigma_Y^2 - 1) s \Gamma c \Gamma - \sigma_{\delta\psi} \} \\
 & + \sigma_{FvMv}(\sigma_Y^2 s^2 \Gamma + c^2 \Gamma + \sigma_{\psi}^2) - \sigma_{FvMw}(\sigma_{Y\delta}^2 \Gamma + \sigma_{Y\psi} s \Gamma c \Gamma) \\
 & - \sigma_{FwMu}(\sigma_Y \psi^2 \Gamma + \sigma_{Y\delta} s \Gamma c \Gamma) - \sigma_{FwMv}(\sigma_{Y\delta} s^2 \Gamma + \sigma_{Y\psi} s \Gamma c \Gamma) \\
 & + \sigma_{FwMw}(\sigma_{\delta}^2 s^2 \Gamma + \sigma_{\psi}^2 c^2 \Gamma + 2\sigma_{\delta\psi} s \Gamma c \Gamma + 1) \}
 \end{aligned}$$

$$\text{Cov}[F_y, M_z] =$$

$$\begin{aligned}
 - \text{Cov}[F_z, M_y] &= \frac{N}{2}(1 + \sigma_{\theta}^2) \{ R_o(\sigma_{Fu}^2 + \mu_{Fu}^2)(1 - \sigma_Y^2) s \Gamma c \Gamma + R_o \sigma_{Fv}^2(\sigma_Y^2 - 1) s \Gamma c \Gamma \\
 & + R_o \sigma_{Fw}^2(\sigma_{\delta}^2 - \sigma_{\psi}^2) s \Gamma c \Gamma + \sigma_{\delta\psi}(c^2 \Gamma - s^2 \Gamma) \} \\
 & + \sigma_{FuMv}(\sigma_Y \psi c \Gamma + \sigma_{Y\delta} s \Gamma) \\
 & - \sigma_{FuMw}(\sigma_Y s \Gamma + \sigma_{\delta}^2 s \Gamma + \sigma_{\delta\psi} c \Gamma) - \sigma_{FvMu}(\sigma_{Y\delta} s \Gamma + \sigma_{Y\psi} c \Gamma) \\
 & + \sigma_{FvMw}(c \Gamma + \sigma_{\psi}^2 c \Gamma + \sigma_{\delta\psi} s \Gamma) + \sigma_{FwMu}(\sigma_Y s \Gamma + \sigma_{\delta}^2 s \Gamma + \sigma_{\delta\psi} c \Gamma) \\
 & - \sigma_{FwMv}(c \Gamma + \sigma_{\delta\psi} s \Gamma - \sigma_{\psi}^2 c \Gamma) \} - \frac{N}{2} R_o \mu_{Fu}^2 s \Gamma c \Gamma
 \end{aligned}$$

$$\text{Cov}[F_z, M_x] = 0$$

$$\text{Cov}[M_x, M_y] = 0$$

$$\text{Cov}[M_x, M_z] = 0$$

$$\text{Cov}[M_y, M_z] = 0$$

#### 4.6 ANALYSIS OF MULTI-RING CLUSTERS

With the exception of the S-IV and S-IVB stages all cluster configurations used in the Saturn program would be classed as multi-ring, since each consists of an outer ring of four engines plus either an inner ring (S-IB stage), or a center engine (S-IC and S-II stages). The classical solutions just presented may be extended to cover such multi-ring configurations provided the rings can be assumed statistically independent.

Each ring in the cluster is analyzed in a common cluster coordinate system and solved using the equations in the previous paragraphs. The means, variances, and covariances are then summed over the rings to obtain the total:

$$\begin{aligned}
 E[F_x] &= \sum_{i=1}^{NR} F_{x_i} \\
 \text{Var}[F_x] &= \sum_{i=1}^{NR} \text{Var}[F_{x_i}] \\
 &\vdots \\
 \text{Cov}[M_y, M_z] &= \sum_{i=1}^{NR} \text{Cov}[M_{y_i}, M_{z_i}],
 \end{aligned}$$

where  $i = i^{\text{th}}$  ring

NR = number of rings.

#### 4.7 SOLUTION FOR MOMENT ABOUT VEHICULAR C.G.

The classical solution may be extended to obtain the statistical properties of the moment induced about an arbitrary vehicular c.g. by an engine cluster. Let the coordinates of the c.g. be random variables  $(x_g, y_g, z_g)$  as shown in Figure 4-1, with covariance matrix

$$\begin{bmatrix} \sigma_{x_g}^2 & \sigma_{x_g y_g} & \sigma_{x_g z_g} \\ \sigma_{x_g y_g} & \sigma_{y_g}^2 & \sigma_{y_g z_g} \\ \sigma_{x_g z_g} & \sigma_{y_g z_g} & \sigma_{z_g}^2 \end{bmatrix}$$

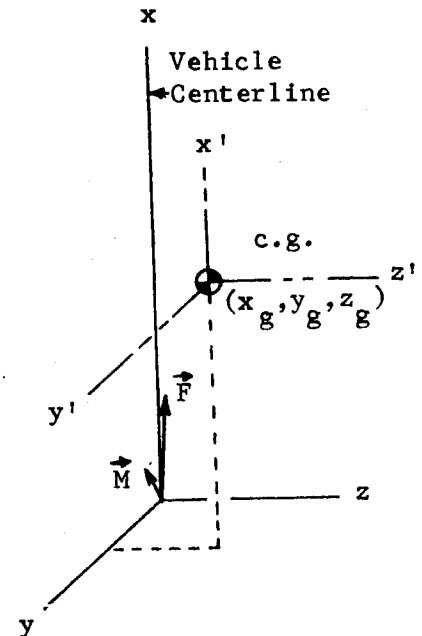


Figure 4-1.

COORDINATE SYSTEM USED FOR  
DERIVATION OF MOMENT  
ABOUT VEHICULAR C.G.

and mean vector  $\vec{\mu}_g^T = (\mu_{x_g}, \mu_{y_g}, \mu_{z_g})$ . The moment\* about the c.g. in terms of the  $x'y'z'$ -frame ( $||$  to the  $xyz$ -frame) may be written as

$$\begin{bmatrix} M_{x_g} \\ M_{y_g} \\ M_{z_g} \end{bmatrix} = \begin{bmatrix} M_x \\ M_y \\ M_z \end{bmatrix} + \begin{bmatrix} 0 & z_g & -y_g \\ -z_g & 0 & x_g \\ y_g & -x_g & 0 \end{bmatrix} \begin{bmatrix} F_x \\ F_y \\ F_z \end{bmatrix}.$$

The following solution may be derived assuming the resultant thrust vector at the cluster center is statistically independent of the vehicular c.g. location.

\*NOTE. The thrust at the c.g. is identical to that at the cluster center. Thus the solutions for variance of force components are applicable to the c.g.

#### 4.7.1 Expected Values

$$E[M_{x_g}] = 0$$

$$E[M_{y_g}] = -\mu_{z_g} E[F_x]$$

$$E[M_{z_g}] = \mu_{y_g} E[F_x].$$

#### 4.7.2 Variances

$$\begin{aligned} \text{Var}[M_{x_g}] &= \text{Var}[M_x] + 2\mu_{z_g} \text{Cov}[F_y, M_x] - 2\mu_{y_g} \text{Cov}[F_z, M_x] \\ &\quad + (\sigma_{z_g}^2 + \sigma_{z_g}^2) \text{Var}[F_y] - 2(\sigma_{y_g z_g} + \mu_{y_g} \mu_{z_g}) \text{Cov}[F_y, F_z] \\ &\quad + (\sigma_{y_g}^2 + \sigma_{y_g}^2) \text{Var}[F_z] \end{aligned}$$

$$\begin{aligned} \text{Var}[M_{y_g}] &= \text{Var}[M_y] - 2\mu_{z_g} \text{Cov}[F_x, M_y] + 2\mu_{x_g} \text{Cov}[F_z, M_y] \\ &\quad + (\sigma_{z_g}^2 + \sigma_{z_g}^2) \text{Var}[F_x] + \sigma_{z_g}^2 E^2[F_x] - 2(\sigma_{x_g z_g} + \mu_{x_g} \mu_{z_g}) \text{Cov}[F_x, F_y] \\ &\quad + (\sigma_{x_g}^2 + \sigma_{x_g}^2) \text{Var}[F_z] \end{aligned}$$

$$\begin{aligned} \text{Var}[M_{z_g}] &= \text{Var}[M_z] + 2\mu_{y_g} \text{Cov}[F_x, M_z] - 2\mu_{x_g} \text{Cov}[F_z, M_z] \\ &\quad + (\sigma_{y_g}^2 + \mu_{y_g}^2) \text{Var}[F_x] + \sigma_{y_g}^2 E^2[F_x] \\ &\quad - 2(\sigma_{x_g y_g} + \mu_{x_g} \mu_{y_g}) \text{Cov}[F_x, F_y] + (\sigma_{x_g}^2 + \mu_{x_g}^2) \text{Var}[F_y]. \end{aligned}$$

#### 4.7.3 Covariances

$$\text{Cov}[F_{x_g}, F_{y_g}] = \text{Cov}[F_x, F_y]$$

$$\text{Cov}[F_{x_g}, F_{z_g}] = \text{Cov}[F_x, F_z]$$

$$\text{Cov}[F_{y_g}, F_{z_g}] = \text{Cov}[F_y, F_z]$$

$$\text{Cov}[F_{x_g}, M_{x_g}] = \text{Cov}[F_x, M_x] + \mu_{z_g} \text{Cov}[F_x, F_y] - \mu_{y_g} \text{Cov}[F_x, F_z]$$

$$\text{Cov}[F_{x_g}, M_{y_g}] = \text{Cov}[F_x, M_y] - \mu_{z_g} \text{Var}[F_x] + \mu_{x_g} \text{Cov}[F_x, F_z]$$

$$\text{Cov}[F_{x_g}, M_{z_g}] = \text{Cov}[F_x, M_z] + \mu_{y_g} \text{Var}[F_x] - \mu_{x_g} \text{Cov}[F_x, F_y]$$

$$\text{Cov}[F_{y_g}, M_{x_g}] = \text{Cov}[F_y, M_x] + \mu_{z_g} \text{Var}[F_y] - \mu_{y_g} \text{Cov}[F_y, F_z]$$

$$\text{Cov}[F_{y_g}, M_{y_g}] = \text{Cov}[F_y, M_y] - \mu_{z_g} \text{Cov}[F_x, F_y] + \mu_{x_g} \text{Cov}[F_y, F_z]$$

$$\text{Cov}[F_{y_g}, M_{z_g}] = \text{Cov}[F_y, M_z] + \mu_{y_g} \text{Cov}[F_x, F_y] - \mu_{x_g} \text{Var}[F_y]$$

$$\text{Cov}[F_{z_g}, M_{x_g}] = \text{Cov}[F_z, M_x] + \mu_{z_g} \text{Cov}[F_z, F_y] - \mu_{y_g} \text{Var}[F_z]$$

$$\text{Cov}[F_{z_g}, M_{y_g}] = \text{Cov}[F_z, M_y] - \mu_{z_g} \text{Cov}[F_x, F_z] + \mu_{x_g} \text{Var}[F_z]$$

$$\text{Cov}[F_{z_g}, M_{z_g}] = \text{Cov}[F_z, M_z] + \mu_{y_g} \text{Cov}[F_x, F_z] - \mu_{x_g} \text{Cov}[F_y, F_z].$$

$$\begin{aligned} \text{Cov}[M_{x_g}, M_{y_g}] &= \text{Cov}[M_x, M_y] - \mu_{z_g} \text{Cov}[F_x, M_x] + \mu_{x_g} \text{Cov}[F_z, M_x] \\ &\quad + \mu_{z_g} \text{Cov}[F_y, M_y] + (\sigma_{z_g}^2 + \mu_{z_g}^2) \text{Cov}[F_x, F_y] \\ &\quad + (\text{Cov}[x_g, z_g] + \mu_{x_g} \mu_{z_g}) \text{Cov}[F_y, F_z] - \mu_{y_g} \text{Cov}[F_z, M_y] \\ &\quad - (\text{Cov}[x_g, y_g] + \mu_{x_g} \mu_{y_g}) \text{Var}[F_z] + (\text{Cov}[y_g, z_g] \\ &\quad + \mu_{y_g} \mu_{z_g}) \text{Cov}[F_z, F_x] \end{aligned}$$

$$\begin{aligned} \text{Cov}[M_{x_g}, M_{z_g}] &= \text{Cov}[M_x, M_z] + \mu_{y_g} \text{Cov}[F_x, M_x] - \mu_{x_g} \text{Cov}[F_y, M_x] \\ &\quad + \mu_{z_g} \text{Cov}[F_y, M_z] + (\text{Cov}[y_g, z_g] + \mu_{y_g} \mu_{z_g}) \text{Cov}[F_x, F_y] \\ &\quad - (\text{Cov}[x_g, z_g] + \mu_{x_g} \mu_{z_g}) \text{Var}[F_y] \\ &\quad - \mu_{y_g} \text{Cov}[F_z, M_z] - (\sigma_{y_g}^2 + \mu_{y_g}^2) \text{Cov}[F_x, F_z] \\ &\quad + (\text{Cov}[x_g, y_g] + \mu_{x_g} \mu_{y_g}) \text{Cov}[F_y, F_z] \end{aligned}$$

$$\begin{aligned} \text{Cov}[M_{y_g}, M_{z_g}] &= \text{Cov}[M_y, M_z] + \mu_{y_g} \text{Cov}[F_x, M_y] - \mu_{x_g} \text{Cov}[F_y, M_y] \\ &\quad - \mu_{z_g} \text{Cov}[F_x, M_z] - (\text{Cov}[y_g, z_g] + \mu_{y_g} \mu_{z_g}) \text{Var}[F_x] \\ &\quad - \text{Cov}[y_g, z_g] E^2[F_x] + (\text{Cov}[x_g, z_g] + \mu_{x_g} \mu_{z_g}) \text{Cov}[F_x, F_y] \\ &\quad + \mu_{x_g} \text{Cov}[F_z, M_z] + (\text{Cov}[x_g, y_g] + \mu_{x_g} \mu_{y_g}) \text{Cov}[F_x, F_z] \\ &\quad - (\sigma_{x_g}^2 + \mu_{x_g}^2) \text{Cov}[F_y, F_z] \end{aligned}$$

## SECTION V

### STATISTICAL OPTIMIZATION OF AN ENGINE CLUSTER

The classical solution presented in subsections 4.3 through 4.7 can be used as an analytical tool for optimizing the design and manufacture of engine clusters. Optimization here means choosing the cluster parameters in such a way that the statistical spreads of the resultant thrust and moment vectors are minimized. Two types of optimization immediately come to mind:

- (1) Geometrical Optimization - Judiciously choose the geometry of the initial cluster layout so as to minimize thrust and moment uncertainties while satisfying other physical constraints.
- (2) Tolerance Optimization - Given a cluster geometry, choose the most liberal set of manufacturing and performance tolerances which meet the required resultant accuracy.

The following paragraphs illustrate each of these optimizations.

#### 5.1 GEOMETRICAL OPTIMIZATION

Optimization of cluster geometry consists of laying out an engine complement within the physical constraints of the problem, such that the statistical uncertainty of the resultant thrust and moment vectors is minimized. Basically, such an optimization necessitates answering one or more of the following questions:

- (1) Should peripheral engines be canted, and if so, how much?
- (2) At what radius from the cluster center should a ring of engines be placed?



- (3) Which is better, a ring of N engines or a center engine plus a ring of N-1 engines?
- (4) Which is better, one engine of thrust F or N small engines each of thrust F/N?

#### 5.1.1 Optimization of Cant Angle $\Gamma$

Consider a ring of N equally spaced peripheral engines, each with the same cant angle  $\Gamma$ . The optimization problem consists of choosing  $\Gamma$  in the interval  $0 \leq \Gamma \leq \Gamma_{\max}$  such that some combination of output variances is minimized. The interval 0 to  $\Gamma_{\max}$  is established by other physical constraints, in particular the amount of forward thrust one is willing to sacrifice toward improving thrust vector alignment. The equations given in subsections 4.5 and 4.7 express the variances of the resultant thrust and moment vector components of a ring of engines as functions of cant angle. The following example will illustrate how these equations may be employed to optimize the cant angle.

Suppose it is desired to choose the cant angle such that the pitch and yaw moments about the vehicular c.g. are minimized. In order to simplify the algebra it is assumed that all inputs are deterministic with the exception of the engine thrust,  $F_u$ , which is statistical with known variance  $\sigma_{Fu}^2$ . When a small angle approximation is made for the cant angle (reasonable for cant angles up to 10 degrees), the following general solution results.

$$\text{Var}[F_x] \approx N \sigma_{Fu}^2$$

$$\text{Var}[F_y] = \text{Var}[F_z] \approx \frac{N}{2} \sigma_{Fu}^2 \Gamma^2$$

$$\text{Var}[M_x] = 0$$

$$\text{Var}[M_y] = \text{Var}[M_z] \approx \frac{N}{2} R_o^2 \sigma_{Fu}^2$$

The variances of the moments about the c.g. may be written, given that the c.g. is located at  $(x_g, y_g, z_g) = (\mu_{x_g}, 0, 0)$ ,

$$\text{Var}[M_{x_g}] = 0 \quad (\text{deterministic})$$

$$\text{Var}[M_{y_g}] = \text{Var}[M_y] + 2\mu_{x_g} \text{Cov}[F_z, M_y] + \mu_{x_g}^2 \text{Var}[F_z]$$

$$\text{Var}[M_{z_g}] = \text{Var}[M_z] - 2\mu_{x_g} \text{Cov}[F_y, M_z] + \mu_{x_g}^2 \text{Var}[F_y].$$

Since, for a ring of engines,

$$\text{Cov}[F_y, M_z] = -\text{Cov}[F_z, M_y],$$

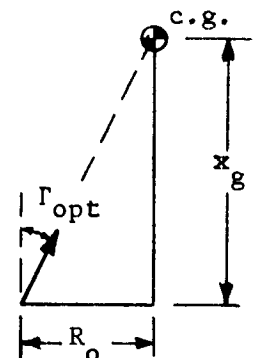
$$\text{Var}[M_y] = \text{Var}[M_z],$$

and  $\text{Var}[F_y] = \text{Var}[F_z],$

$$\begin{aligned} \text{Var}[M_{y_g}] &= \text{Var}[M_{z_g}] \\ &= \frac{N}{2} R_o^2 \sigma_{Fu}^2 - 2\mu_{x_g} \left( \frac{N}{2} R_o \sigma_{Fu}^2 \Gamma \right) + \mu_{x_g}^2 \frac{N}{2} \sigma_{Fu}^2 \Gamma^2 \\ &= \frac{N}{2} \sigma_{Fu}^2 (\mu_{x_g}^2 \Gamma^2 - 2\mu_{x_g} R_o \Gamma + R_o^2). \end{aligned}$$

The optimum  $\Gamma$  is obtained as follows.

$$\begin{aligned} \frac{\partial \text{Var}[M_{y_g}]}{\partial \Gamma} &= 2\mu_{x_g}^2 \Gamma - 2\mu_{x_g} R_o = 0 \\ \Gamma_{\text{opt}} &= \frac{2\mu_{x_g} R_o}{2\mu_{x_g}^2} = \frac{R_o}{\mu_{x_g}}. \end{aligned}$$



September 1966

The physical interpretation of this result is that the engines should be canted to the angle which causes the extended engine centerline to pass through the vehicle c.g. The reduction in variance to be had by canting the engines is as follows:

$$\text{No canting: } \text{Var}[M_{y_g}] = \text{Var}[M_{z_g}] = \frac{N}{2} R_o^2 \sigma_{Fu}^2$$

$$\begin{aligned} \text{Optimum canting: } \text{Var}[M_{y_g}] = \text{Var}[M_{z_g}] &= \frac{N}{2} \sigma_{Fu}^2 \left\{ \mu_{x_g}^2 \left( \frac{R_o}{\mu_{x_g}} \right) - 2\mu_{x_g} R_o \left( \frac{R_o}{\mu_{x_g}} \right) + R_o^2 \right\} \\ &= 0 . \end{aligned}$$

Therefore, the pitch and yaw moments about the c.g. due to engine thrust variation can be completely eliminated by canting the engine centerlines to intersect the c.g. (Such canting is not practical in actual designs since the locations of the c.g. varies with flight times.)

Although canting reduces pitch and yaw moments about the c.g., it introduces statistical variations in side thrust as evidenced by the following:

$$\text{No canting: } \text{Var}[F_y] = \text{Var}[F_z] = 0$$

$$\text{Optimum canting: } \text{Var}[F_y] = \text{Var}[F_z] \approx \frac{N}{2} \sigma_{Fu}^2 \frac{R_o^2}{\mu_{x_g}^2} .$$

Since canting improves some parameters while degrading others, it might be desirable to adjust the cant angle such that a weighted sum of all the affected parameters is minimized.

Examination of the general solution for a ring of  $N > 2$  engines will show that inclusion of more statistical input variables in the equations does not change the quadratic form of each of the variances:

$$\text{Var}[ ] = A\Gamma^2 + B\Gamma + C.$$

The optimum cant angle can always be found which minimizes a given variance or combination of variances, although in general no small angle exists which will completely zero the variance of interest. As an example of a slightly more complicated case let both thrust magnitude  $F_u$  and c.g. longitudinal location  $x_g$  be random variables with known variances  $\sigma_{F_u}^2$  and  $\sigma_{x_g}^2$ , respectively. The optimum cant angle becomes

$$\Gamma_{\text{opt}} \approx \frac{R_o}{\mu_{x_g} + \left( \frac{\sigma_{x_g}^2}{\mu_{x_g}} \right)},$$

a somewhat smaller cant than before.

### 5.1.2 Optimization of Radius $R_o$

The nominal radius  $R_o$  of a ring of  $N > 2$  engines may be optimized in a manner similar to the cant angle. To simplify the problem to reasonable proportions, assume that all covariances between engine thrust and moment components and between small angle orientation errors are zero (a much less severe set of assumptions than those used in cant angle optimization). Assume a deterministic c.g. at  $(\mu_{x_g}, 0, 0)$ . Examination of the general solution reveals that the variances of the resultant force components for the cluster are not functions of  $R_o$ , and that each of the resultant moment components about the vehicular c.g. is of the form

$$\text{Var}[M] = A + B R_o^2,$$

where A and B are positive. This form shows that the variance of each moment component about the c.g. increases as the square of the ring radius. Therefore, the radius  $R_o$  should be made small; in other words a ring of engines should be bunched together as close to the cluster center as is physically possible.

A side benefit derived from making  $R_o$  small is the fact that the optimum cant angle  $\Gamma_{\text{opt}} = R_o / \mu_{xg}$  derived in the previous paragraph is made correspondingly smaller, thus reducing the amount of forward thrust lost in canting.

Inclusion of the terms omitted in the initial assumption will result in moment variances which are quadratic functions of  $R_o$ , making possible nonzero optimum radii.

### 5.1.3 Inclusion of a Center Engine

In laying out a cluster of N identical engines, the question naturally arises: Which is better, a ring of N engines or one center engine plus N-1 peripheral engines? Again the classical solution may be employed to answer this question from the standpoint of thrust vector misalignment. The following assumptions are made to form an illustrative example:

- (1) All engines are uncanted.
- (2) Each engine produces random thrust and moment components with  $\sigma_{Fv}^2 = \sigma_{Fw}^2$  and  $\sigma_{Mv}^2 = \sigma_{Mw}^2$ .

- (3) All input covariances are zero.
- (4) There are no mounting errors.
- (5) Vehicle c.g. is deterministic at  $(\mu_{x_g}, 0, 0)$ .
- (6)  $\theta_o = 0$  for the center engine.

These assumptions yield resultant variances as follows:

Center engine:  $\text{Var}[F_x] = \sigma_{Fu}^2$

$$\text{Var}[F_y] = \text{Var}[F_z] = \sigma_{Fv}^2$$

$$\text{Var}[M_x] = \sigma_{Mu}^2$$

$$\text{Var}[M_y] = \text{Var}[M_z] = \sigma_{Mv}^2$$

$$\text{Var}[M_{x_g}] = \sigma_{Mu}^2$$

$$\text{Var}[M_{y_g}] = \text{Var}[M_{z_g}] = \sigma_{Mv}^2 + \mu_{x_g}^2 \sigma_{Fv}^2$$

Ring of  $N > 2$  engines:

$$\text{Var}[F_x] = N \sigma_{Fu}^2$$

$$\text{Var}[F_y] = \text{Var}[F_z] = \frac{N}{2} (\sigma_{Fv}^2 + \sigma_{Fw}^2) = N \sigma_{Fv}^2$$

$$\text{Var}[M_x] = N (\sigma_{Mu}^2 + R_o^2 \sigma_{Fv}^2)$$

$$\begin{aligned} \text{Var}[M_y] = \text{Var}[M_z] &= \frac{N}{2} \{ (\sigma_{Mv}^2 + \sigma_{Mw}^2) + R_o^2 (\sigma_{Fu}^2 + \mu_{Fu}^2) \} \\ &= N \{ \sigma_{Mv}^2 + \frac{1}{2} R_o^2 (\sigma_{Fu}^2 + \mu_{Fu}^2) \} \end{aligned}$$

$$\text{Var}[M_{x_g}] = N (\sigma_{Mu}^2 + R_o^2 \sigma_{Fv}^2)$$

$$\text{Var}[M_{y_g}] = \text{Var}[M_{z_g}] = N \{ \sigma_{Mv}^2 + \mu_{x_g}^2 \sigma_{Fv}^2 + \frac{1}{2} R_o^2 (\sigma_{Fu}^2 + \mu_{Fu}^2) \} .$$

These equations show that the resultant force components are identical for either configuration. However, the moment about the c.g. is different for the two configurations. The moment variances are of the forms

$$\text{Center engine: } \begin{cases} \text{Var}[M_{x_g}] = A \\ \text{Var}[M_{y_g}] = \text{Var}[M_{z_g}] = B \end{cases}$$

$$\text{N-engine ring: } \begin{cases} \text{Var}[M_{x_g}] = N(A + C R_o^2) \\ \text{Var}[M_{y_g}] = \text{Var}[M_{z_g}] = N(B + D R_o^2) \end{cases}$$

$$\text{(N-1)-engine ring plus center engine : } \begin{cases} \text{Var}[M_{x_g}] = NA + (N-1) C R_o^2 \\ \text{Var}[M_{y_g}] = \text{Var}[M_{z_g}] = NB + (N-1) D R_o^2 \end{cases}$$

From these results it would appear that the center engine configuration is always superior in that it yields lower moment variances, and this is indeed true provided the radius of the ring does not have to be enlarged to allow room for the center engine.

September 1966

If it is assumed that each engine requires a circular area of diameter  $d$  in the gimbal plane, then the effect of a center engine on ring radius may be determined geometrically as illustrated in Table 5-1. For clusters of six or more engines it is advantageous to have a center engine, since the ring radius either stays constant or decreases. However, for clusters of five engines or less the ring radius is increased by inclusion of a center engine, thereby partially offsetting the benefits derived from the center engine. Consequently, numerical calculation of the variances is necessary to determine which configuration is best for clusters of five or less engines.

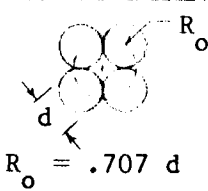
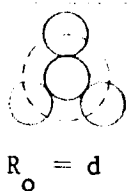
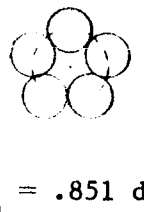
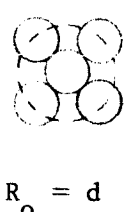
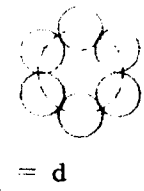

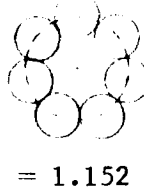
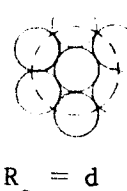
It should be borne in mind that other factors such as thrust vector control system design may override thrust vector alignment considerations in determining the positions of peripheral engines.

#### 5.1.4 Choice of Number of Engines Comprising a Cluster

As a final topic under geometrical optimization the problem of selecting the number of engines in a cluster will be considered. This problem will arise when several sizes of engines are available from which to select a complement yielding the total thrust required of the stage being designed. The classical solution can be employed to determine which engine yields the best resultant thrust vector characteristics by allowing numerical evaluation of the resultant variances of each cluster configuration under consideration. A simple example will illustrate the application and will permit some general observations.



Table 5-1. A COMPARISON OF RING RADIUS FOR RING AND CENTER ENGINE CONFIGURATIONS

NUMBER OF ENGINES	CLUSTER CONFIGURATION		EFFECT ON RING RADIUS OF ADDING A CENTER ENGINE
	RING	CENTER ENGINE	
4	 $R_o = .707 d$	 $R_o = d$	$R_o$ INCREASED BY 2.93 d
5	 $R_o = .851 d$	 $R_o = d$	$R_o$ INCREASED BY .149 d
6	 $R_o = d$	 $R_o = d$	NO CHANGE IN $R_o$
7	 $R_o = 1.152 d$	 $R_o = d$	$R_o$ DECREASED BY .152 d
$n > 7$	$R_o = \frac{d}{2} \csc \frac{\pi}{n}$	$R_o = \frac{d}{2} \csc \frac{\pi}{n-1}$	$R_o$ DECREASED

Suppose a cluster design is required to develop a total thrust of  $F_c$ , and that two types of engines are available:

Type 1 (small engine): Thrust  $F_1 = \frac{F_c}{n}$ ;  $n$  engines required

Type 2 (large engine): Thrust  $F_2 = \frac{F_c}{m} = \frac{n}{m} F_1$ ;  $m$  engines required

where  $n > m > 2$  ( $n, m$  integers).

The following assumptions and ground rules are made to simplify the problem.

- (1) The configuration choice is limited to an uncanted ring of either  $n$  type 1 or  $m$  type 2 engines.
- (2) Each engine produces random thrust and moment components with known force and moment components

$$\sigma_{Fu_{1,2}} = \sigma_{Fv_{1,2}} = \sigma_{Fw_{1,2}} = k_F F_{1,2}$$

$$\sigma_{Mu_{1,2}} = \sigma_{Mv_{1,2}} = \sigma_{Mw_{1,2}} = k_M F_{1,2} \quad ,$$

(types 1 and 2, respectively) where  $k_F$  and  $k_M$  are proportionality constants. This is a fair assumption in that the standard deviation is the same fractional part of the rated thrust for both the small and large engines.

- (3) All input covariances are zero.
- (4) There are no mounting errors.
- (5) The gimbal plane mounting area required for each engine is proportional to its rated thrust:  $A_1 = k_A F_1$ ,  $A_2 = k_A F_2$

$A_2 = k_A \frac{n}{m} F_1 = \frac{n}{m} A_1$ . Therefore, the diameters of the mounting area circles are related as  $d_2 = \sqrt{\frac{n}{m}} d_1$ . (This assumption is reasonable if both engines have the same exit velocity.)

(6) The vehicular c.g. is deterministic at  $(\mu_{x_g}, 0, 0)$ .

Based on these assumptions, the cluster variances are as follows:

Cluster of  $n$  small engines:

$$\text{Var}[F_{x_1}] = \text{Var}[F_{y_1}] = \text{Var}[F_{z_1}] = n\sigma_{F_1}^2$$

$$\text{Var}[M_{x_{g_1}}] = n(\sigma_{M_1}^2 + R_{o_1}^2 \sigma_{F_1}^2)$$

$$\text{Var}[M_{y_{g_1}}] = \text{Var}[M_{z_{g_1}}] = n \{ \sigma_{M_1}^2 + \mu_{x_g}^2 \sigma_{F_1}^2 + \frac{1}{2} R_{o_1}^2 (\sigma_{F_1}^2 + \mu_{F_1}^2) \}.$$

Cluster of  $m$  large engines:

$$\text{Var}[F_{x_2}] = \text{Var}[F_{y_2}] = \text{Var}[F_{z_2}] = m\sigma_{F_2}^2$$

$$\text{Var}[M_{x_{g_2}}] = m(\sigma_{M_2}^2 + R_{o_2}^2 \sigma_{F_2}^2)$$

$$\text{Var}[M_{y_{g_2}}] = \text{Var}[M_{z_{g_2}}] = m \{ \sigma_{M_2}^2 + \mu_{x_g}^2 \sigma_{F_2}^2 + \frac{1}{2} R_{o_2}^2 (\sigma_{F_2}^2 + \mu_{F_2}^2) \}.$$

But  $\mu_{F_2} = \frac{n}{m} \mu_{F_1}$

$$\sigma_{F_2} = \frac{n}{m} \sigma_{F_1}$$

$$\sigma_{M_2} = \frac{n}{m} \sigma_{M_1}$$

$$R_{o1} = \frac{d_1}{2 s \frac{\pi}{n}}$$

$$R_{o2} = \frac{d_2}{2 s \frac{\pi}{m}} = \frac{\sqrt{\frac{n}{m}} d_1}{2 s \frac{\pi}{m}} = \sqrt{\frac{n}{m}} \frac{s \frac{\pi}{n}}{s \frac{\pi}{m}} R_{o1}.$$

Substitution into the expressions for the second cluster yields

$$\text{Var}[F_{x_2}] = \text{Var}[F_{y_2}] = \text{Var}[F_{z_2}] = n \cdot \frac{n}{m} \sigma_{F_1}^2$$

$$\text{Var}[M_{x_{g_2}}] = n \cdot \frac{n}{m} (\sigma_{F_1}^2 + \frac{n}{m} \frac{s^2 \frac{\pi}{n}}{s^2 \frac{\pi}{m}} R_{o1}^2 \sigma_{F_1}^2)$$

$$\text{Var}[M_{y_{g_2}}] = \text{Var}[M_{z_{g_2}}]$$

$$= n \cdot \frac{n}{m} \{ \sigma_{M_1}^2 + \mu_{x_g}^2 \sigma_{F_1}^2 + \frac{n}{2m} \frac{s^2 \frac{\pi}{n}}{s^2 \frac{\pi}{m}} R_{o1}^2 (\sigma_{F_1}^2 + \mu_{F_1}^2) \}.$$

These results show that a ring of  $n$  small engines provides lower resultant thrust variances (by a factor of  $\frac{n}{m}$ ) than does an equivalent ring of  $m$  large engines. Going to a larger number of engines also tends to reduce the resultant moment variances about the vehicular c.g. However, the increased ring radius at which the larger number of engines must be placed tends to cancel this benefit and a numerical calculation is necessary in each case to determine the preferred geometry.

## 5.2 TOLERANCE OPTIMIZATION

Tolerance optimization is the problem of choosing the most liberal set of manufacturing and performance tolerances (variances) for a given stage configuration, without exceeding the prespecified limits on resultant thrust and moment vector uncertainty. One method of optimizing tolerances is

proposed in the following example, wherein the Lagrange multiplier technique is applied to the classical probability solution equations presented in Section IV.

Consider the problem of optimizing the input variances on a cluster consisting of a ring of  $n > 2$  engines obeying the classical solution given in subsection 4.5. For notational convenience the following symbology is introduced.

Input variances:

$$x_1 = \sigma_{Fu}^2$$

$$x_2 = \sigma_{Fv}^2$$

$$x_3 = \sigma_{Fw}^2$$

$$x_4 = \sigma_{Mu}^2$$

$$x_5 = \sigma_{Mv}^2$$

$$x_6 = \sigma_{Mw}^2$$

$$x_7 = \sigma_{\psi}^2$$

$$x_8 = \sigma_{\delta}^2$$

$$x_9 = \sigma_{\gamma}^2$$

$$x_{10} = \sigma_x^2$$

$$x_{11} = \sigma_R^2$$

Output variances:

$$y_1 = \text{Var } [F_x]$$

$$y_2 = \text{Var } [F_y]$$

$$y_3 = \text{Var } [F_z]$$

$$y_4 = \text{Var } [M_x]$$

$$y_5 = \text{Var } [M_y]$$

$$y_6 = \text{Var } [M_z]$$

$C_i$  are constants within the variance equations

(All covariances are assumed to be zero.)

The problem is formulated as that of maximizing a given cost function

$$w = a_1 x_1 + a_2 x_2 + \dots + a_{11} x_{11},$$

subject to the constraint that none of the tolerances on the output variances is exceeded:

$$y_1 \leq y_{1\max}$$

$$y_2 \leq y_{2\max}$$

$$\vdots$$

$$y_6 \leq y_{6\max}$$

In the cost function  $w$ , the constants  $a_i$  are weighting factors chosen to normalize the various units of  $x_i$  and to reflect the relative difficulty (or expense) of controlling each input variance.

The "Lagrange multiplier" method [G3] may be used to solve for the  $x_i$  if it can be assumed that the most liberal set of input variances will drive the output variances to their limits. The constraints may then be stated as:

$$\phi_1 = y_1 - y_{1\max} = 0$$

$$\phi_2 = y_2 - y_{2\max} = 0$$

$$\vdots$$

$$\phi_6 = y_6 - y_{6\max} = 0.$$

A typical constraint would be of the form

$$\begin{aligned} \phi_1 = c_1 x_1 + c_2 x_2 + c_3 x_9 + c_4 x_1 x_9 + c_5 x_2 x_9 + c_6 x_3 x_9 + c_7 x_3 x_8 \\ - y_{1\max} = 0. \end{aligned}$$

The desired solution may be obtained by solving the following set of nonlinear simultaneous algebraic equations:

$$\frac{\partial w}{\partial x_1} + \lambda_1 \frac{\partial \phi_1}{\partial x_1} + \lambda_2 \frac{\partial \phi_2}{\partial x_1} + \dots + \lambda_6 \frac{\partial \phi_6}{\partial x_1} = 0$$

$$\frac{\partial w}{\partial x_2} + \lambda_1 \frac{\partial \phi_1}{\partial x_2} + \lambda_2 \frac{\partial \phi_2}{\partial x_2} + \dots + \lambda_6 \frac{\partial \phi_6}{\partial x_2} = 0$$

⋮

$$\frac{\partial w}{\partial x_{11}} + \lambda_1 \frac{\partial \phi_1}{\partial x_{11}} + \lambda_2 \frac{\partial \phi_2}{\partial x_{11}} + \dots + \lambda_6 \frac{\partial \phi_6}{\partial x_{11}} = 0$$

$$\phi_1 = 0$$

$$\phi_2 = 0$$

⋮

$$\phi_6 = 0.$$

The above set consists of 17 equations in 17 unknowns:  $x_1, x_2, \dots, x_{11}, \lambda_1, \lambda_2, \dots, \lambda_6$ . Since the equations are in general nonlinear, some numerical iteration techniques would be necessary to obtain a solution. The result would be the most liberal set of input variances  $x_i$  which drive all output variances to their specified limits.

## SECTION VI

### MONTE CARLO SIMULATION

#### 6.1 GENERAL

A digital computer program was written for the Monte Carlo simulation of thrust misalignment in engine clusters. The program is fully documented in a companion report NSL/Huntsville TR-292-6-081, "Monte Carlo Simulation of the Resultant Thrust of Rocket Engine Clusters," and is only summarized here [G4].

#### 6.2 PROGRAM SUMMARY

The Monte Carlo program was written to provide an empirical method of checking the results of the classical solutions. As such, it was written for the same coordinate system and coordinate transformations as described herein for the classical solutions.

The principle of operation is as follows: The program generates a random sample value for each random variable input to the cluster model, using a pseudo-random-number generating subroutine. These input random samples can be made to obey any legitimate probability density function of up to six dimensions. When input samples have been generated for each engine in the cluster, they are inserted in the coordinate transformation and the resultant thrust and moment vectors calculated. Repetition of this process a large number of times generates a sample population of the six components of cluster thrust and moment. The program performs a statistical analysis of this population to determine the means, variances, covariances, and linear correlation coefficients of the six output components. In addition, histograms are plotted for each of the components.

The results of applying the program to the S-I and S-IC Saturn stages are presented in Section VIII.



SECTION VII  
CURRENT ALIGNMENT REQUIREMENTS AND TECHNIQUES FOR  
SATURN VEHICLE STAGES

7.1 BACKGROUND

One of the major requirements under this study was to determine the probability distributions on random variations affecting the resultant thrust and moment vectors of actual engine clusters. This requirement was fulfilled by collecting information from engine manufacturers, engine and stage alignment personnel, etc. Information secured included engine model specifications, alignment procedures, engine and stage dimensions and tolerances, optical alignment results, and static test firing data. (No flight test data was used.) The necessary data were then gleaned from the documentation, analyzed and processed to obtain best estimates of the probability distributions.

The engines to be investigated were chosen at the outset of the study as follows:

- (1) H-1 engine; cluster of 8 used on S-I, S-IB stages,
- (2) F-1 engine; cluster of 5 used on S-IC stage,
- (3) J-2 engine; cluster of 5 used on S-II stage, one center engine used on S-IVB stage.

This section presents the specified thrust vector alignment requirements for each configuration and summarizes the alignment theory and practices used in producing the stages. The results of the statistical analyses performed on the various engines and stages are given in Section VIII.

The sources from which the information was obtained are referenced by number at the end of this report. All numerical data obtained from the referenced documents were in the English system of units (pound-inch-second) and were converted to the International System of Units (Newton-meter-second) [2] for presentation herein, as required by the contract.

## 7.2 ENGINE MODEL SPECIFICATIONS AND ENGINE-TO-STAGE ALIGNMENT REQUIREMENTS

The following subsections contain those portions of the engine model specifications and stage alignment specifications which pertain to thrust vector alignment. Special terms used therein are defined in the ABBREVIATIONS AND DEFINITIONS.

### 7.2.1 Model Specification, H-1 Engine [1,2,3,4] (See Figure 7-1.)

1. Thrust magnitude: To date, four classes of H-1 engines have been specified; rated sea level thrust and tolerances are 734 kN (165 kip)  $\pm$  3 percent, 836 kN (188 kip)  $\pm$  3 percent, 900 kN (200 kip)  $\pm$  3 percent, 912  $\pm$  9 kN (205  $\pm$  2 kip). (The 912 kN engine was not analyzed in this study.)
2. Dynamic thrust vector position: (Identical for all four classes).  
The dynamic thrust vector (DTV) shall not deviate from the geometric thrust vector by more than 6.350 mm (0.250 in.) lateral displacement, measured in the gimbal plane and 30 min angularity.
3. Geometric thrust vector position: (Identical for all four classes).  
The geometric thrust vector (GTV) shall be adjusted to intersect the gimbal plane at an angle of not more than 5 min from the normal to that plane.

September 1966

4. Gimbal slide adjustment: (Identical for all four classes). The engine shall be provided with a gimbal bearing assembly which shall be capable of an adjustment for lateral displacements of the GTV of 6.350 mm (0.250 in.) in any direction.
5. Gimbal center position: (Identical for all four classes). The gimbal center shall be adjusted to be within 1.626 mm (0.064 in.) TIR of the pierce point of the GTV in the gimbal plane and shall lie within 3.175 mm (0.125 in.) TIR of the engine centerline.
6. Waiver of dynamic thrust vector alignment: (Identical for all four classes). Verification of item 2 is not required to be demonstrated.

H-1 ENGINE

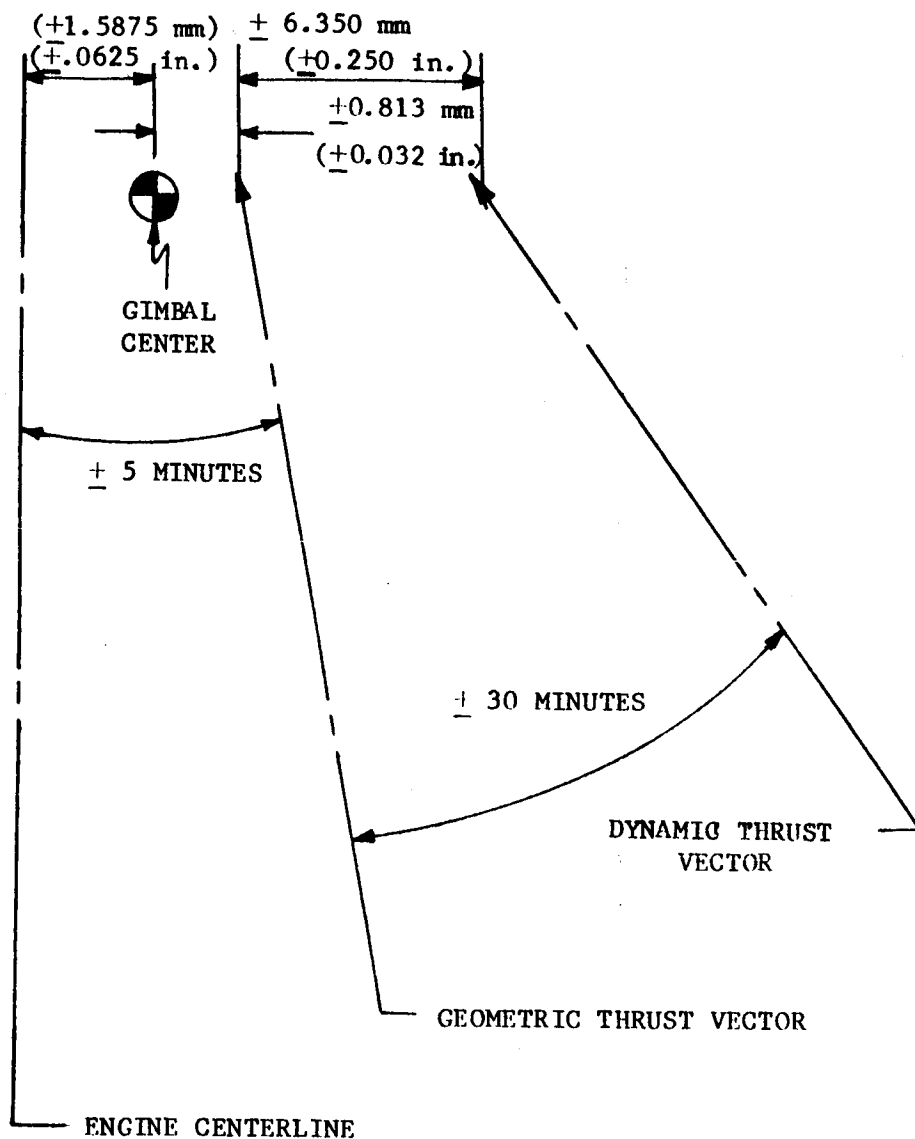


Figure 7-1. MODEL SPECIFICATION REQUIREMENTS

### 7.2.2 H-1 Engine to S-I and S-IB Stage Alignment Requirements. [5,6,7,8,9]

The GTV is to be aligned to a 3-deg nominal cant angle and a 6-deg nominal cant angle for the inboard and outboard H-1 engines, respectively. The basic angles lie in respective position planes. The tolerance of the GTV to the basic cant angle is 0 deg 30 min conical half-angle. (See Figure 7-2 for illustration.) No tolerance is specified for angular mounting error about the engine centerline, nor is any attempt made to measure this parameter.

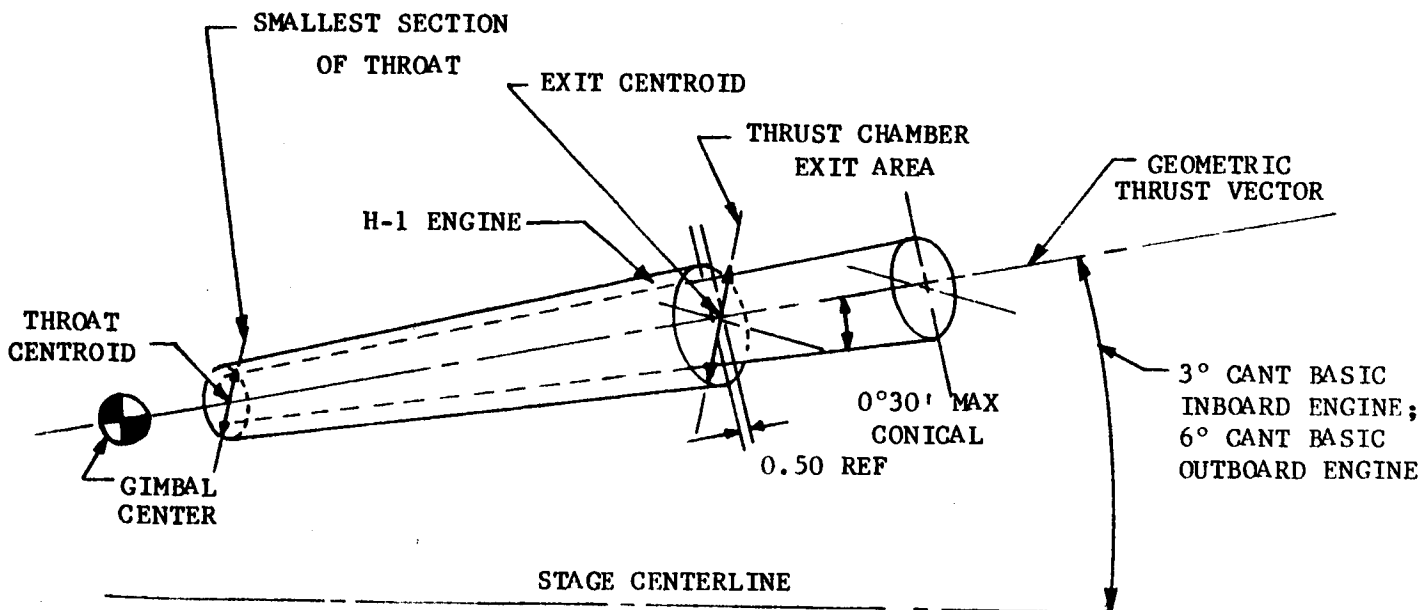


Figure 7-2. ALIGNED ENGINE FOR S-I AND S-IB STAGES IN A VERTICAL STATIC CONDITION

7.2.3 Model Specification, F-1 Engine [10,11,12,13] (See Figure 7-3.)

1. Thrust magnitude: The F-1 engine is required to have a rated sea level thrust of 6,700 kN (1,500 kip)  $\pm$  3 percent.
2. Actual thrust vector position: The actual thrust vector (ATV) shall lie within 30 min of the engine centerline and pass within 15.2 mm (0.6 in.) of the gimbal center.
3. Thrust chamber centerline position: The thrust chamber centerline (TCCL) shall lie within 30 min of the engine centerline and shall pass within 6.35 mm (0.250 in.) of the gimbal center.
4. Gimbal center: The gimbal center shall lie within 0.254 mm (0.010 in.) of the engine centerline.

F-1 ENGINE

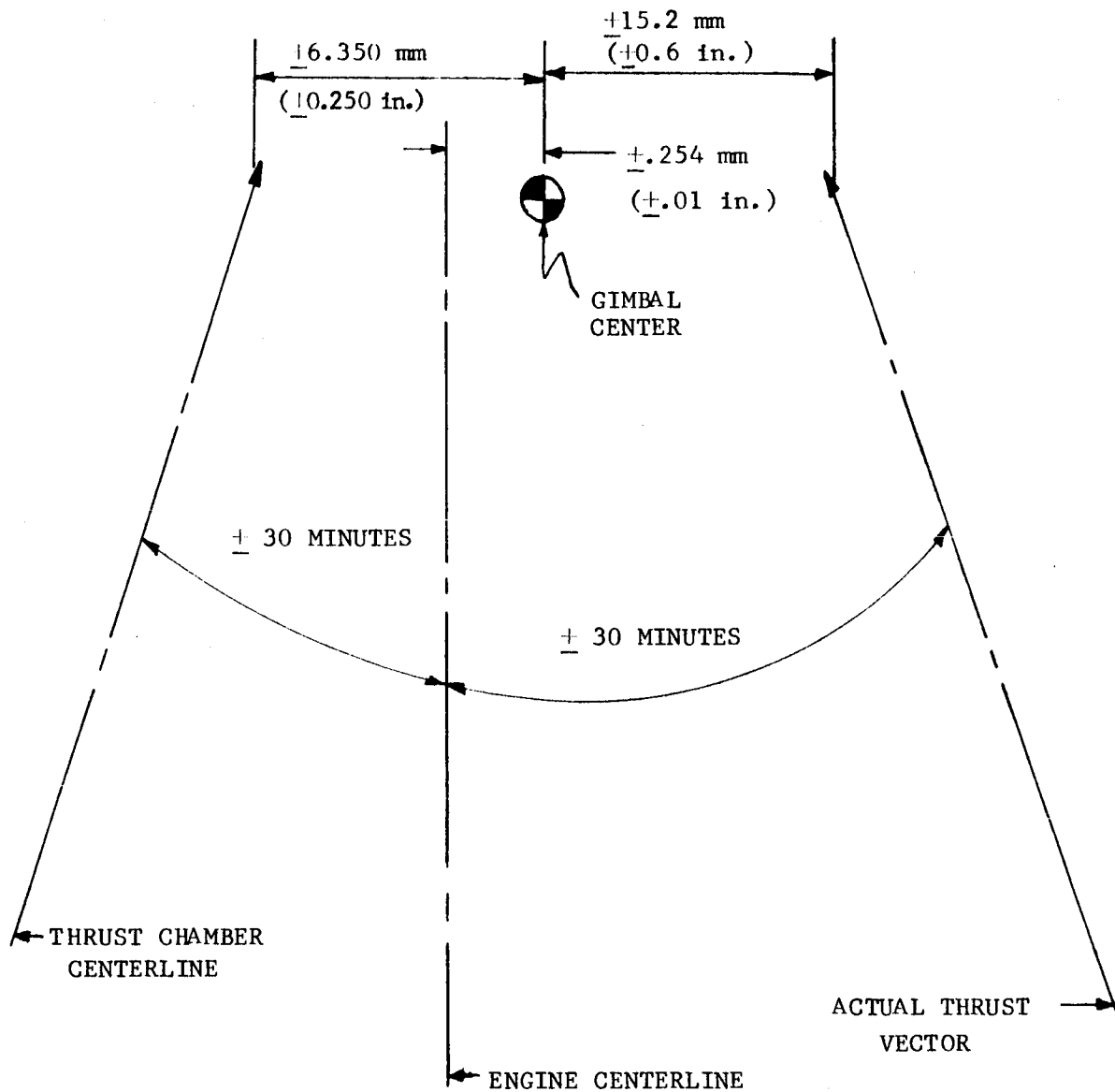


Figure 7-3. MODEL SPECIFICATION REQUIREMENTS

#### 7.2.4 F-1 Engine to S-IC Stage Alignment Requirements [14,15]

The thrust chamber centerline (TCCL) of each outboard engine is required to be aligned to a basic cant angle of 29 min, within a conical half-angle tolerance of 42 min. (See Figure 7-4.) The small cant angle is required in order to compensate for stage deflection under full thrust and is accomplished by inducing a 20.5 min cant angle in the  $-x_g$  and  $-z_g$  axes of each outboard engine. The TCCL of the center engine is required to be aligned parallel to the stage centerline within 10 min.

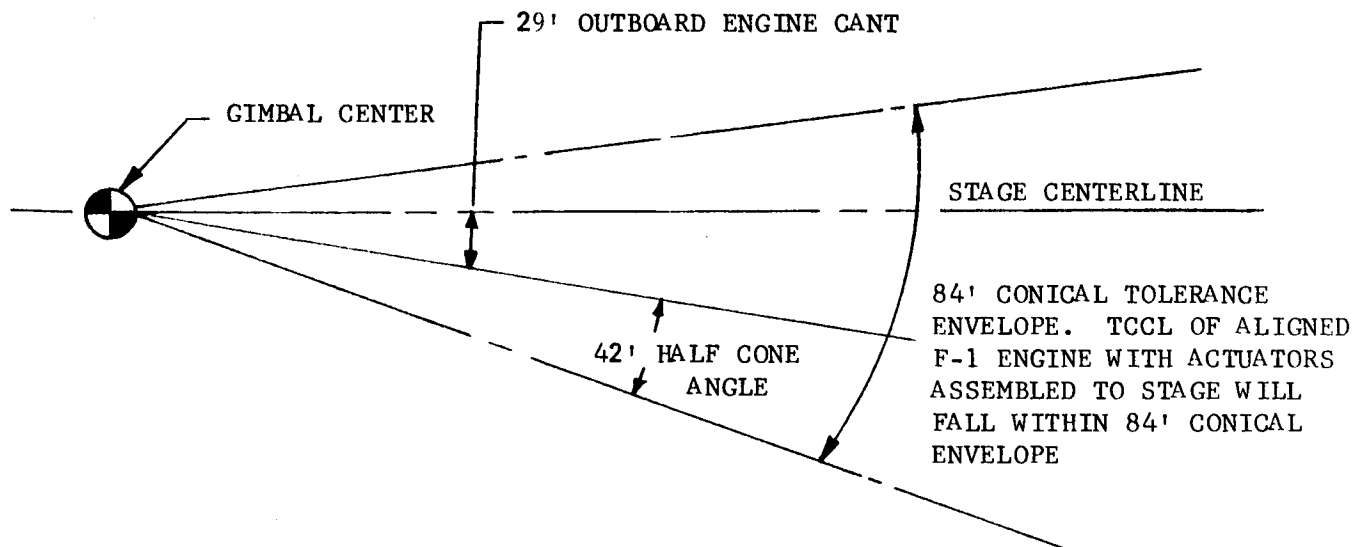


Figure 7-4. ALIGNED ENGINE TO S-IC STAGE ORIENTATION IN VERTICAL STATIC CONDITION



7.2.5 Model Specification, J-2 Engine [16,17,18] (See Figure 7-5.)

1. The J-2 engine is designed to operate at a nominal vacuum thrust level of 890 kN (200 kip)  $\pm$  3 percent. (Thrust alignment tests were calibrated at 1000 kN (225 kip)  $\pm$  3 percent.)
2. The actual thrust vector (ATV) shall be within 40 min of the engine centerline and pass within 10.16 mm (0.400 in.) of the gimbal center.
3. The ATV shall be measured with an accuracy of 10 min angularity and 3.81 mm (0.15 in.) lateral displacement.
4. The geometric thrust vector (GTV) shall be within 5 min of the engine centerline and pass within 0.762 mm (0.030 in.) of the gimbal center.
5. The gimbal center shall be within 0.250 mm (0.010 in.) of the engine centerline.

7.2.6 J-2 Engine to S-II Stage Alignment Requirements [19,20]

The nominal GTV of each control engine (outboard) shall be positioned at 1 deg from the vertical stage datum system in direction (outboard) toward the midpoint of a line between the actuators. The variation of the GTV from its nominal position shall not exceed 22 min in any direction. See Figure 7-6 for illustration.

7.2.7 J-2 Engine to S-IVB Stage Alignment Requirements [21,22]

The GTV of the single control engine shall be aligned within 22 min of the stage datum system. See Figure 7-7 for illustration.

J-2 ENGINE

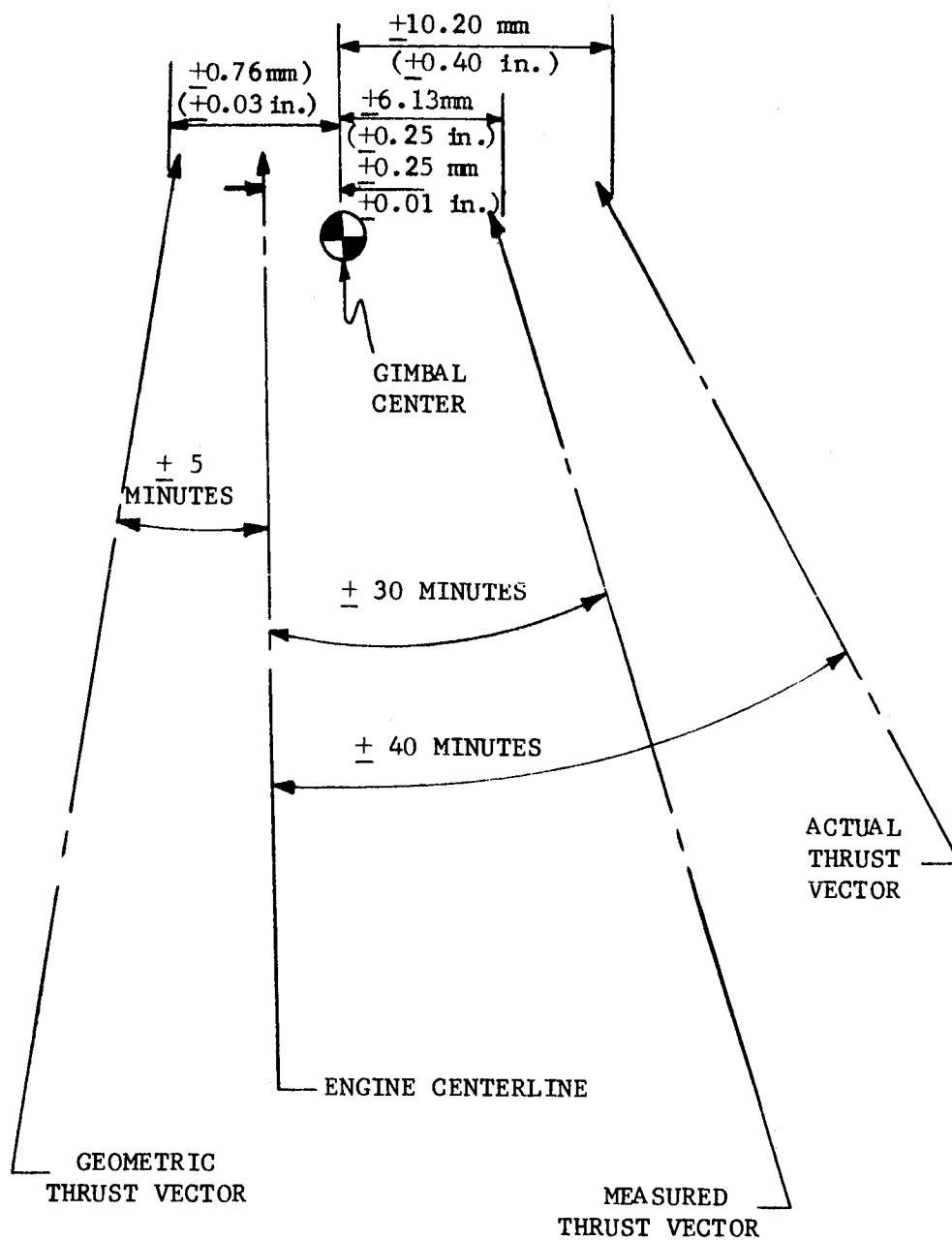


Figure 7-5. MODEL SPECIFICATION REQUIREMENTS

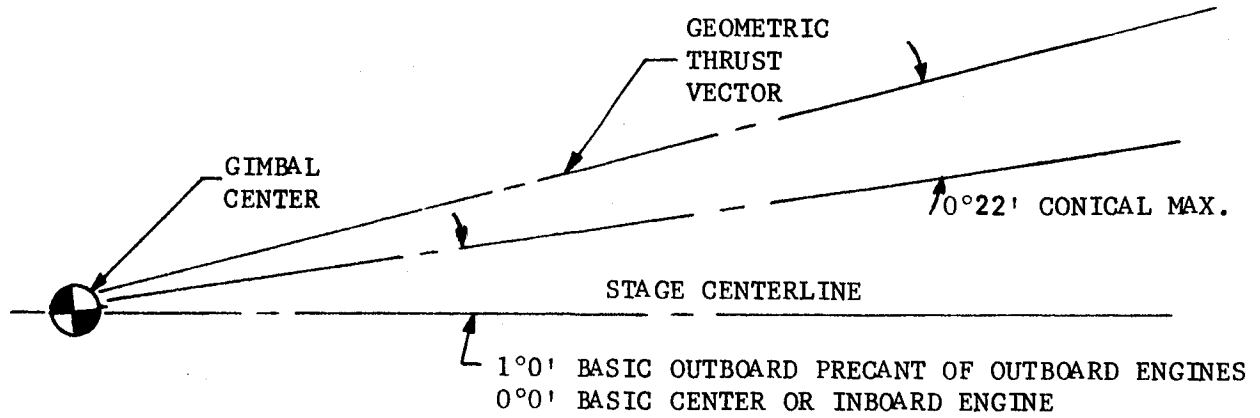


Figure 7-6. ALIGNED ENGINE FOR S-II STAGE ORIENTATION IN VERTICAL STATIC CONDITION

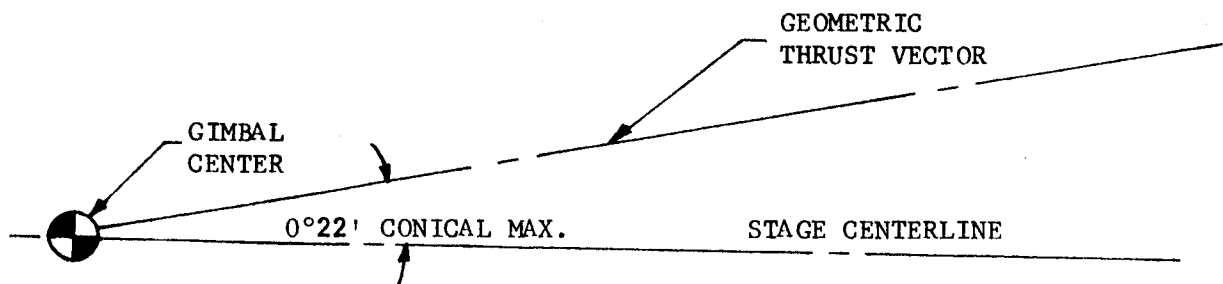


Figure 7-7. ALIGNED ENGINE FOR S-IVB STAGE ORIENTATION IN VERTICAL STATIC CONDITION

### 7.3 THEORY OF ENGINE ALIGNMENT [2,12,17,23,24,25]

Each rocket engine undergoes alignment tests, and if required, adjustments to ensure that the provisions of the corresponding model specifications are satisfied. This subsection briefly describes the theory of alignment and the techniques used on the H-1, J-2, and F-1 engines. References are cited in which the reader can find a more detailed treatment of these topics.

#### 7.3.1 Engine Operation

Understanding engine alignment requires a familiarity with the basic concepts of engine construction and operation. In simple terms a liquid-fueled rocket engine consists of a thrust chamber in which combustion of the propellants occurs, and a nozzle through which the combustion products escape. (See Figure 7-8.) Thrust is generated as a reaction force proportional to the momentum gained by the escaping gases, and is in a direction opposite to that of the flow. The shape of the nozzle and its expansion ratio (ratio of exit area to throat area) are chosen within physical constraints to maximize the engine efficiency over the design range of ambient pressure. Fuel and oxidizer are introduced into the chamber by means of the "injectors", and are pumped to the chamber with a gas turbine dual-section pump. Propellants must be brought to the chamber via flexible couplings to allow gimbaling of the engine.

#### 7.3.2 Thrust Vector Control

All three engine types (H-1, J-2, and F-1) are designed to be gimbaled for thrust vector control of the stages on which they are used. (See Figure 7-9.) The injector end of the thrust chamber is attached to the stage by means

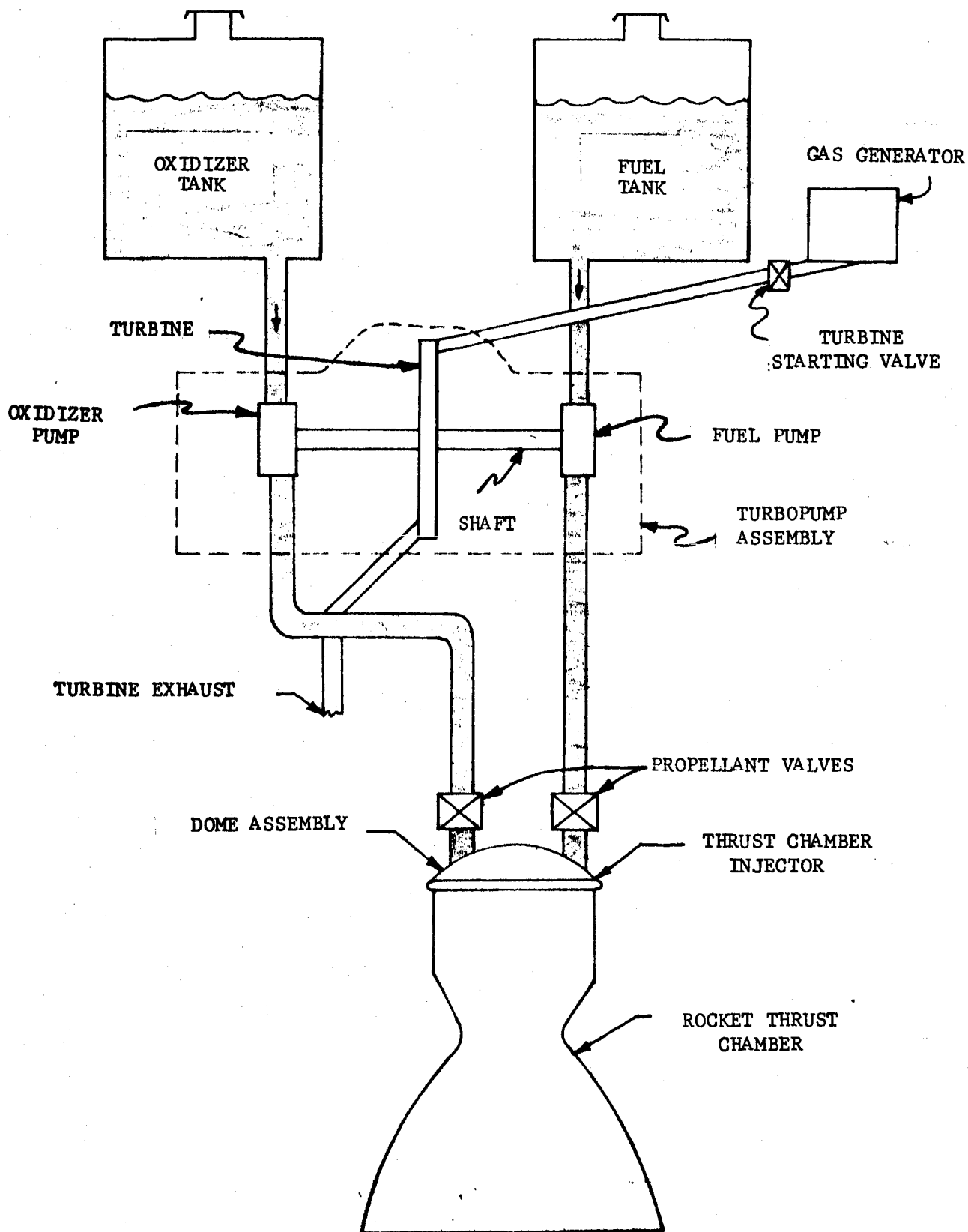


Figure 7-8. BI-PROPELLANT LIQUID-FUEL ROCKET ENGINE

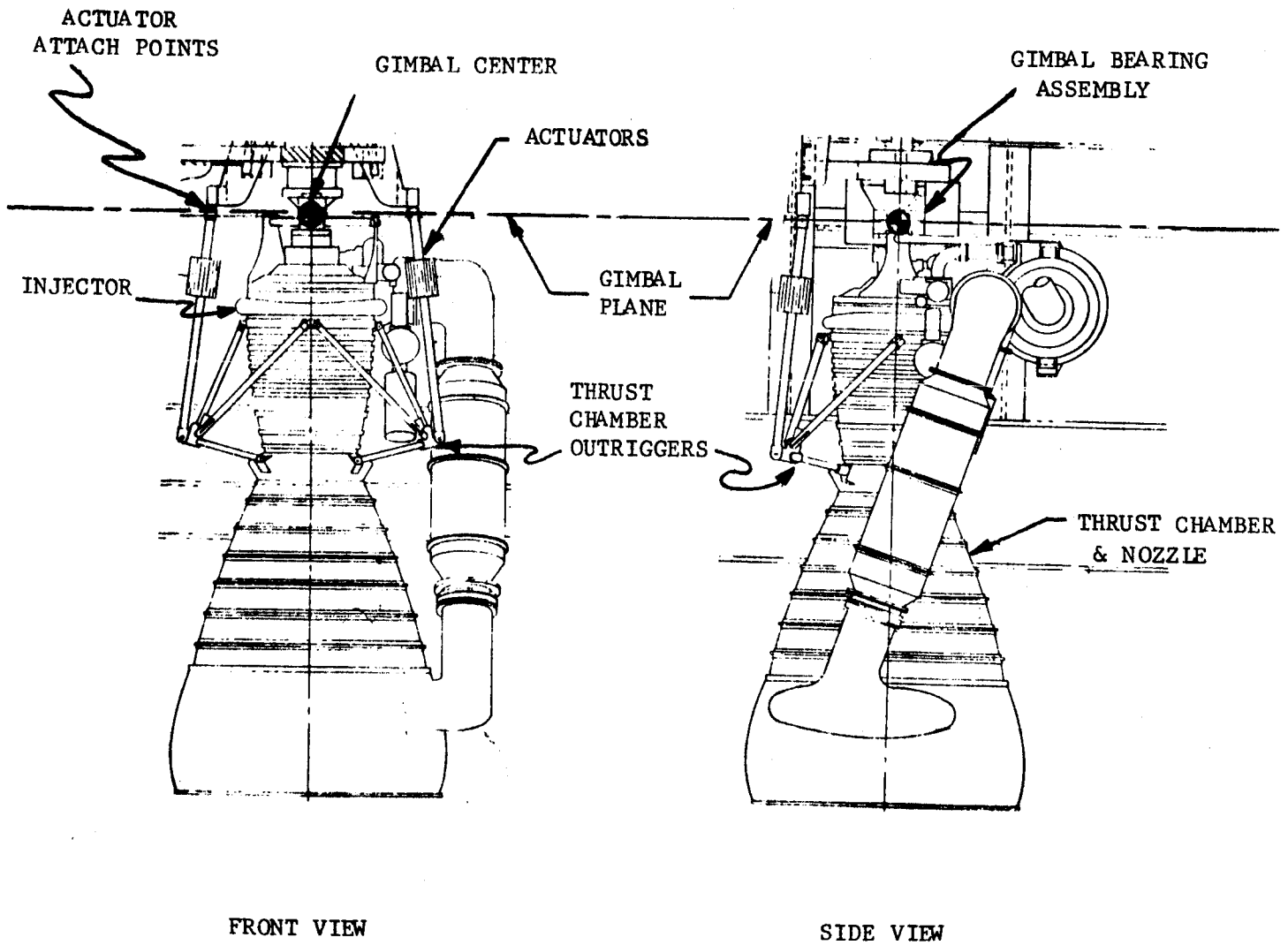


Figure 7-9. H-1 THRUST CHAMBER AND GIMBAL

of a gimbal bearing assembly, essentially a universal joint which allows the thrust chamber two degrees (pitch and yaw) of rotational freedom with respect to the stage. Thus, the thrust chamber centerline is free to rotate approximately 7 deg in any direction from its center position, tracing out a conical volume whose apex is at the gimbal center.

The position of the engine with respect to the stage is controlled by two hydraulic actuators. Extending and retracting the actuators produces angular motion of the thrust chamber in each of two orthogonal planes. The actuators are pinned to the thrust chamber outriggers and to the "actuator attach points" on the stage, and are controlled by electrical signals from the attitude control system. Fixed engines (those not used for thrust vector control) are also manufactured with the gimbal bearing assembly, but are held rigidly to the stage by means of "stiff arms" in place of actuators.

### 7.3.3 Engine Thrust Vector Characteristics

A rocket engine in steady-state operation delivers a complex force and moment vector which are resultants of the distributed forces applied by escaping exhaust gases, propellant flow, exterior pressures, and other sources. The assumption is usually made, however, that engine performance can be adequately characterized by a single concentrated force vector called the "actual thrust vector". Ideally this actual thrust vector lies along the engine centerline, acts through the gimbal center, and possesses a magnitude equal to the rated thrust of the engine.

The actual thrust vector of any realistic engine is, of course, corrupted by both magnitude and alignment errors. The actual thrust vector does not coincide with the thrust chamber centerline, nor does the thrust chamber centerline coincide with the ideal engine mounting axis, the so-called "engine centerline".

Magnitude errors are corrected by reorificing the thrust chamber injectors, and alignment errors are corrected by mechanical adjustment of the thrust chamber position relative to the engine centerline. Ideal engine alignment exists when the actual thrust vector and the engine centerline coincide. This implies that the thrust chamber centerline of a perfectly aligned engine will not in general lie on the engine centerline.

Two types of alignment errors are possible:

- (1) Pierce point displacement error - The actual thrust vector intersects the gimbal plane at a point other than the gimbal center.
- (2) Angularity error - The actual thrust vector is displaced from the engine centerline by some nonzero angle.

Pierce point error causes a static moment about the gimbal center equal to the product of the pierce point displacement times the thrust magnitude. This moment must be overcome by the actuators in order to hold the engine at a fixed gimbal angle. The second type of alignment error, angularity error, causes no actuator loads but creates side forces which are applied to the stage via the gimbal bearing assembly.

#### 7.3.4 Engine Alignment Adjustments

Two types of alignment adjustments may be made on an engine: (1) lateral adjustment of the thrust chamber with respect to the gimbal center, and (2) angular adjustment of the thrust chamber with respect to the engine centerline. Lateral adjustment is accomplished by means of two mutually perpendicular "gimbal slides" located between the thrust chamber and the gimbal bearing



assembly. (See Figure 7-10.) After adjustment the gimbal slides are clamped, making the thrust chamber and lower gimbal pillow block a single rigid assembly. Angular adjustment of the thrust chamber centerline is accomplished by adjusting the lengths of the actuators in their center (or zero deflection command) positions.

### 7.3.5 Alignment Techniques

Two alignment techniques have been used with the H-1, J-2, and F-1 engines: optical alignment and dynamic alignment. Optical alignment is performed by placing the engine in a jig simulating the engine connect points on the stage. The pierce point and angularity of the thrust chamber centerline are then derived. Gimbal slide adjustments and actuator lengths are calculated which yield a perfectly aligned thrust chamber centerline within measurement accuracy. Optical alignment can be accomplished with relatively little expenditure of time and money and allows the thrust chamber centerline to be positioned with extreme accuracy. The disadvantage is that optimal alignment does not account for the position of the actual thrust vector, the alignment of which is the end objective of engine alignment.

Dynamic alignment is performed by static test firing the engine in a test stand sufficiently instrumented to measure not only the magnitude but also the position of the dynamic thrust vector. Calculations are then made to determine the gimbal slide adjustments and actuator lengths which will zero the pierce point and angularity errors of the dynamic thrust vector assuming perfect measurements. Thus, dynamic alignment overcomes, within the measurement accuracy, the fundamental deficiency of optical alignment by allowing direct alignment

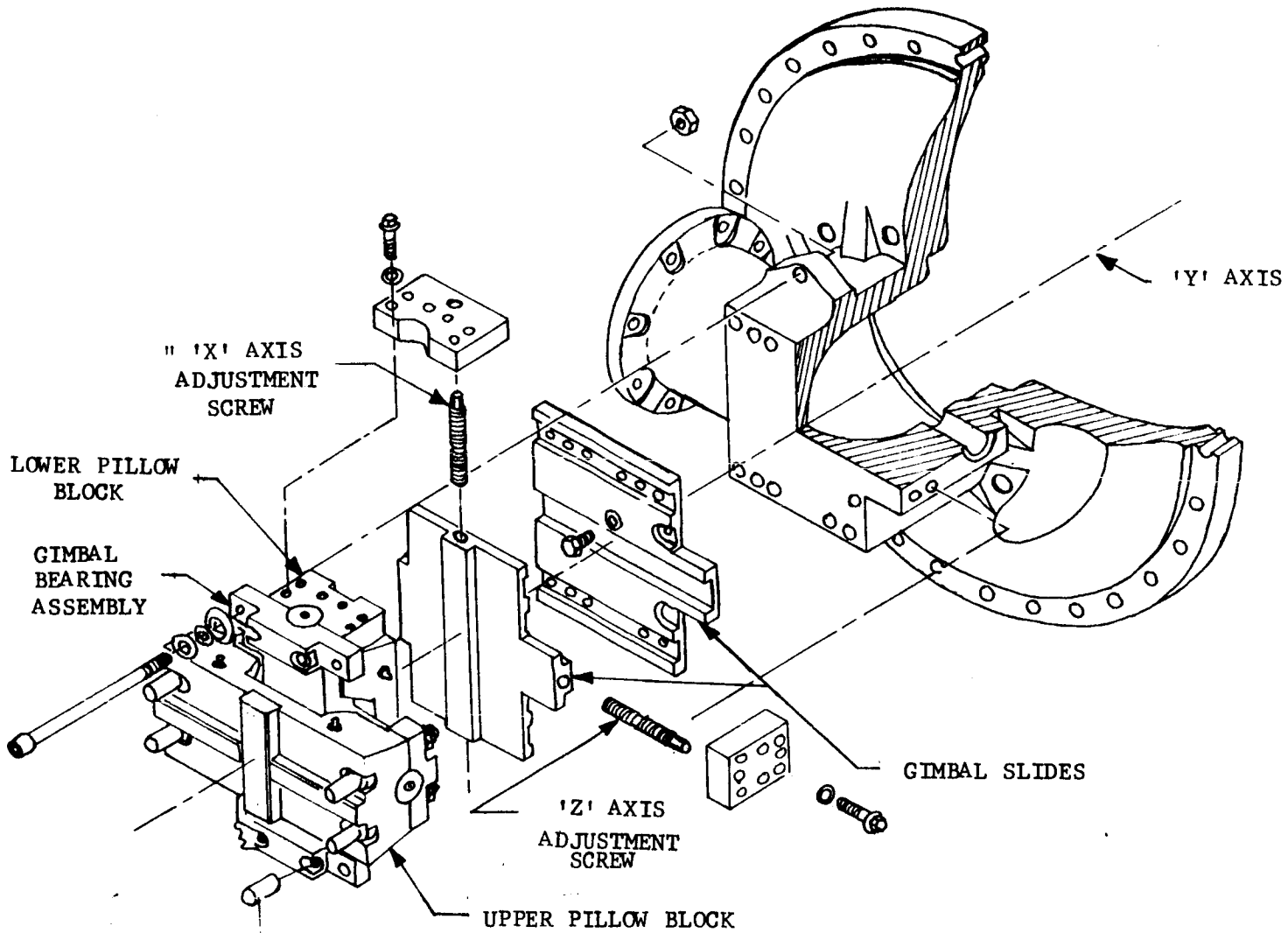


Figure 7-10. DOME-BEARING ASSEMBLY

of the measured thrust vector itself. Dynamic alignment, however, is not without shortcomings: (1) it is time consuming and expensive, and (2) it suffers from considerable uncertainty due both to measurement inaccuracy and nonrepeatability of engine performance.

In summary, optical alignment makes possible the alignment of the thrust chamber centerline with extreme accuracy while dynamic alignment makes possible the alignment of the actual thrust vector with somewhat less accuracy.

Aside from economical considerations, the question of which method is better is synonymous with the question: "Which would have the smaller variation from perfect alignment of the actual thrust vector, a group of engines having undergone the optical alignment procedure or an identical group having undergone dynamic alignment?" The success of the optical method is dependent upon the thrust chamber centerline and the actual thrust vector lying in close proximity to each other, while the success of the dynamic method is dependent upon the actual thrust vector lying in close proximity to the measured thrust vector. Consequently, a comparison of these two uncertainties is necessary to intelligently select the better method for any given type of engine. As an example, the dynamic method would appear more appropriate for engines designed to operate in the atmosphere than for high altitude engines, since the latter tend to exhibit marked variations in operating characteristics when test fired on the ground.

#### 7.4 ENGINE ALIGNMENT PROCEDURES [11,12,17,25,26,27,28,29,30,31]

The procedures used to align the production H-1, J-2, and F-1 engines were investigated and are summarized in this subsection. Further details on the alignment procedures can be found in the cited references.

September 1966

An optical alignment procedure is used to align the H-1 and J-2 engines. Although the alignment stands and associated equipment vary somewhat for the two engines, the basic procedure is the same and is discussed in subsection 7.4.1. The production H-1 engine relies wholly upon the optical method for thrust alignment, with no attempt being made to measure the position of the dynamic thrust vector during static test firing. (Dynamic alignment tests were performed on several R&D H-1 engines at MSFC. [29]) The J-2 engine is aligned optically and then static test fired once, at which time the position of the dynamic thrust vector is determined and recorded. No further adjustment is made unless the dynamic thrust vector position is outside the allowable tolerances. (Of the forty-six J-2 engines for which test data were gathered during this study, none was adjusted as a result of the dynamic test.)

Unlike the H-1 and J-2 engines, the F-1 is dynamically aligned. A crude optical alignment is performed with the engine mounted in the static test stand. The engine is then static test fired from two to four times and the position of the dynamic thrust vector determined each time. The average position of the dynamic thrust vector is derived from these test results, and the corresponding alignment adjustments are calculated. The dynamic test stand and procedure used are similar to those for the J-2 and R&D H-1 engines, and are described in subsection 7.4.2.

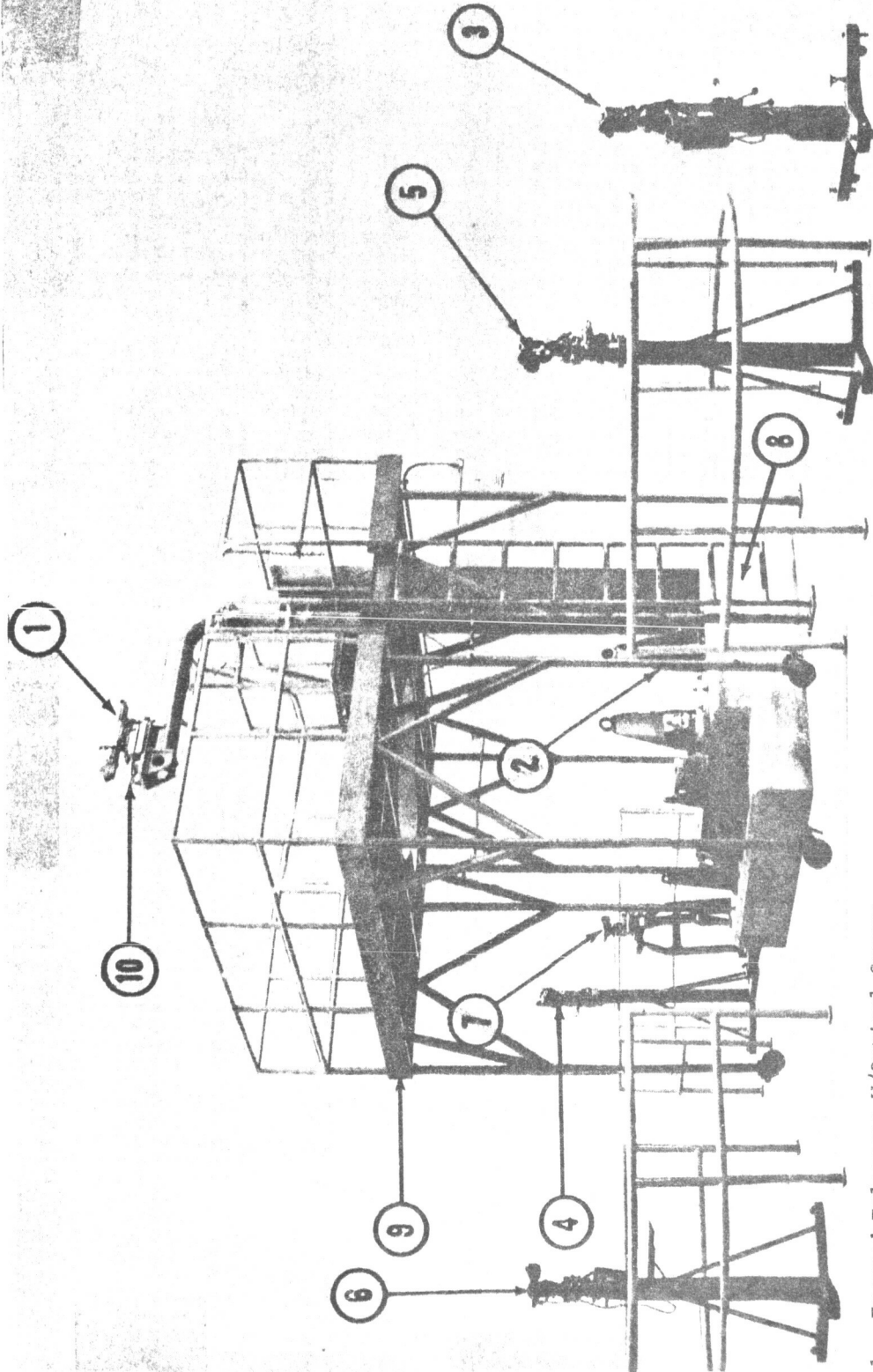
#### 7.4.1 Optical Alignment [25,26,27,30]

Optical alignment procedures, test stands, and related equipment exist for all three engines investigated in this study (H-1, J-2, and F-1), although detailed optical alignment as described in this subsection is not performed on the production F-1 engine. The procedures and equipment used for each engine are similar, and only that for the H-1 engine will be discussed here.

The test stand and related equipment used in the optical alignment of the H-1 engine are shown in Figure 7-11. The stand consists of a pedestal with engine attach points duplicating the geometry of an ideal stage, as illustrated in Figure 7-12. The basic reference is the engine centerline, defined as a line passing through the center of the intersection of the upper pillow block tongue and groove, and being perpendicular to the mounting surface of the upper pillow block. This line is established by an optical instrument suspended above the engine mount block of the alignment stand prior to placement of the engine in the stand. The mounting surface of the engine mount block is set level and the simulated stage actuator attach point centers are set to the basic stage dimension within plus or minus 0.001 in. The dimensions are set so that the engine may be aligned on the vertical (i.e., the simulated stage actuator attach points on the engine alignment stand are set to provide the correct cant angle when the engine is installed on the stage).

Two basic vertical reference planes are established with optical instruments the 0 - 180 deg and the 90 - 270 deg planes. These planes are within 30 sec of perpendicularity and intersect at the engine centerline.

A thrust chamber calibration tool or "spider" (Figure 7-13) is used to locate the position of the geometric thrust vector. The spider is an optical tube with legs at each end, designed to fit inside the thrust chamber as shown in Figure 7-14. When the spider is mounted in the thrust chamber, the radii of the throat and exit planes are measured at 15 deg intervals with the radius indicator at each end of the spider. The area centroids of the throat and exit areas are then calculated and the spider tube is adjusted until its centerline passes



1. Farrand Telescope W/Optical Square
2. Taylor Hobson Telescope W/Optical Square & Adapter
3. Wild T-2 Theodolite
4. Wild T-2 Theodolite
5. Wild T-2 Theodolite
6. Wild T-2 Theodolite
7. Wild N-3 Level
8. Alignment Stand
9. Working Platform
10. Mirror Mount

Figure 7-11. H-1 ENGINE ALIGNMENT STAND WITH INSTRUMENTS IN POSITION

September 1966

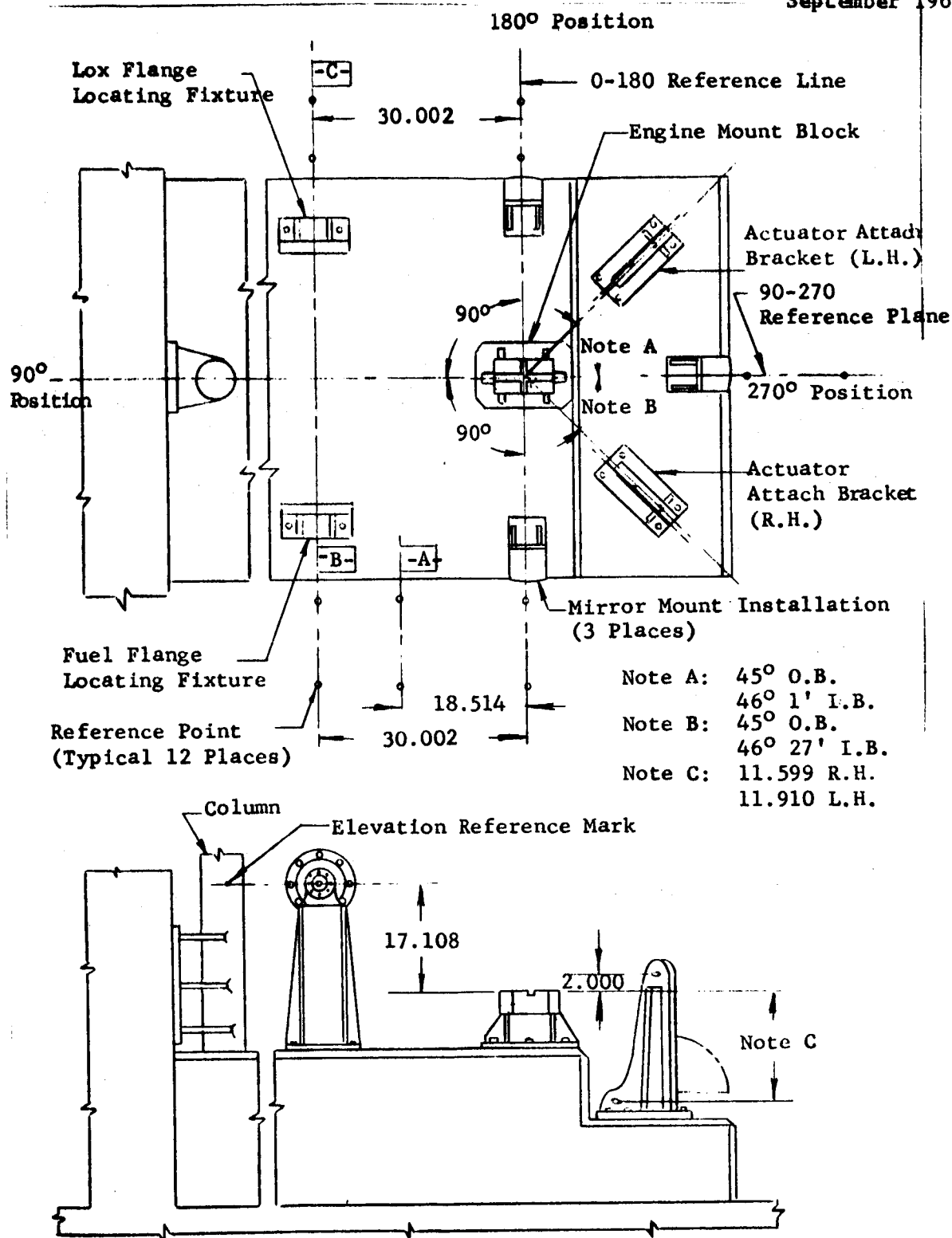


Figure 7-12. H-1 ENGINE ALIGNMENT STAND, BASIC GEOMETRY

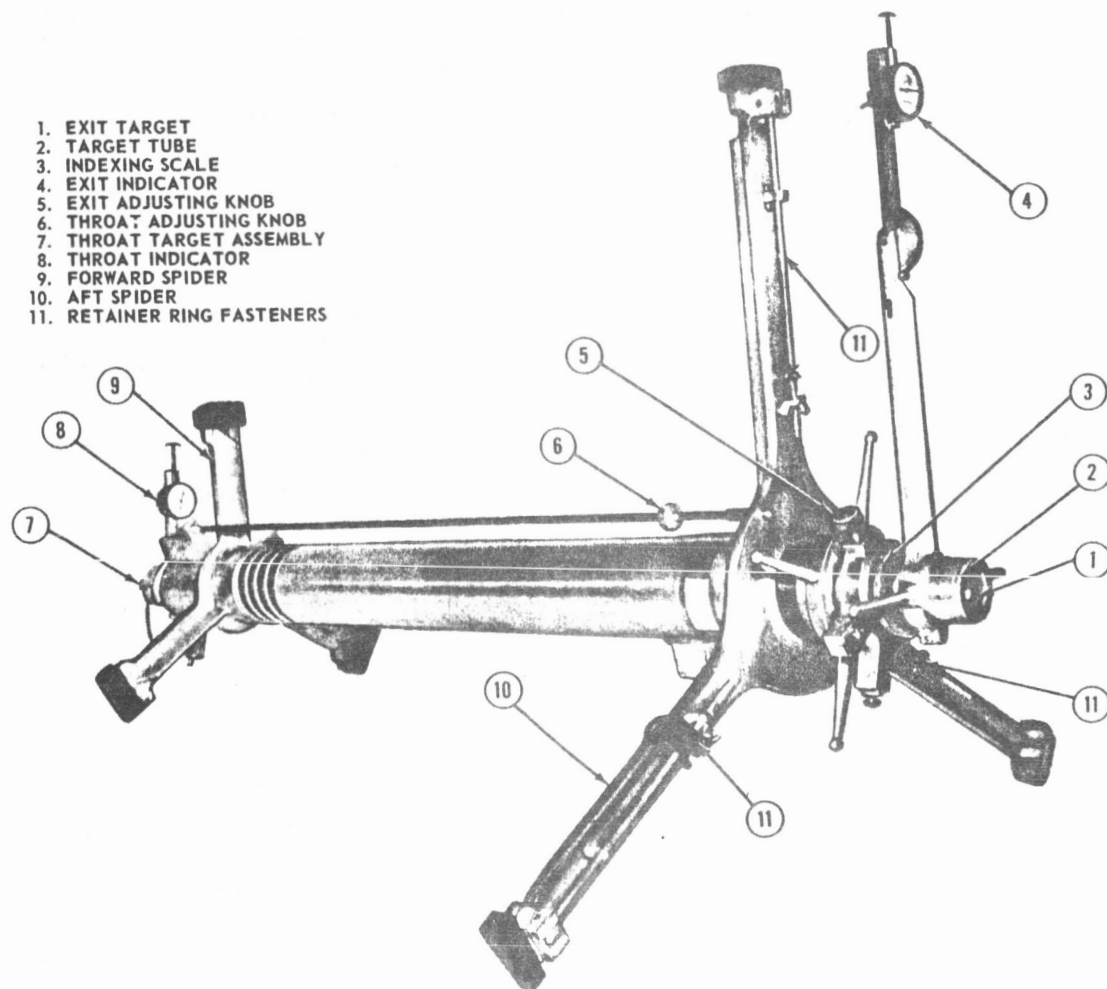
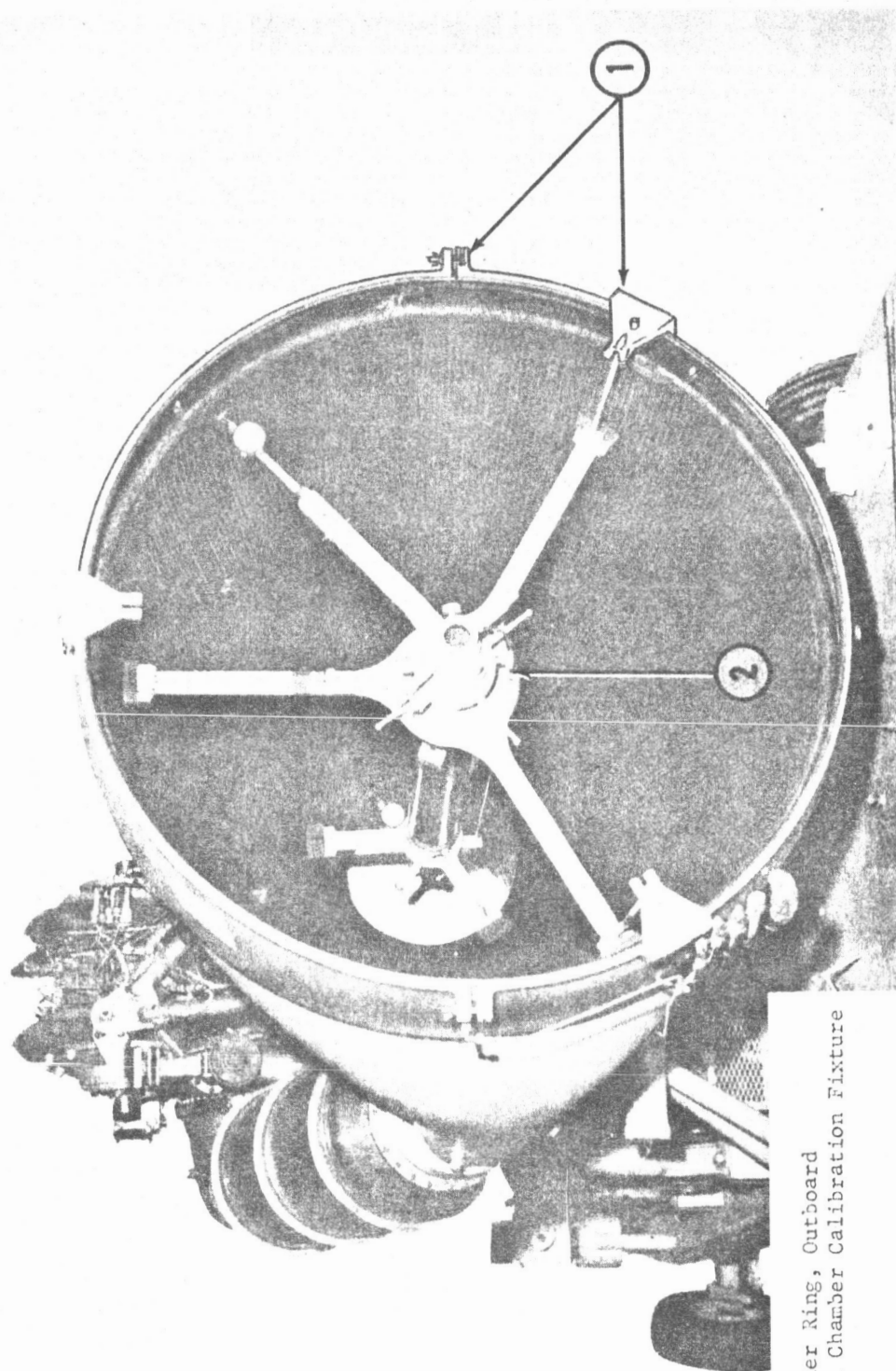


Figure 7-13. THRUST CHAMBER CALIBRATION FIXTURE





1. Retainer Ring, Outboard
2. Thrust Chamber Calibration Fixture

Figure 7-14. PLACEMENT OF THRUST CHAMBER CALIBRATION FIXTURE, H-1 OUTBOARD ENGINE

through the two centroids. The centerline of the spider tube then coincides with the engine geometric thrust vector and defines the position of this vector for the remainder of the optical tests.

The engine is mounted gimbal-down in the alignment stand and is retained in a vertical position by two adjustable length dummy actuator links (essentially turnbuckles), as shown in Figure 7-15. The dummy actuator links are adjusted until the geometric thrust vector (spider centerline) is parallel to the engine centerline, as determined by sighting down from above the engine. The displacement between the engine centerline and the geometric thrust vector is recorded.

The position of the gimbal center is determined by optically measuring the positions of the gimbal axes relative to the vertical reference planes and calculating the point of intersection of the two axes. The pierce point displacement of the geometric thrust vector relative to the gimbal center is calculated. If the pierce point displacement of the geometric thrust vector is found to exceed the allowable tolerance, the gimbal slides are adjusted as required, and the dummy actuator links are readjusted to maintain the parallelism of the geometric thrust vector and the engine centerline.

Optical alignment is achieved when the pierce point displacement is within tolerance and the geometric thrust vector is parallel to the engine centerline. The length of each dummy actuator is measured with vernier calipers and the engine is removed from the alignment stand. The actuator lengths and geometric pierce point displacement are recorded in the accompanying engine logbook.

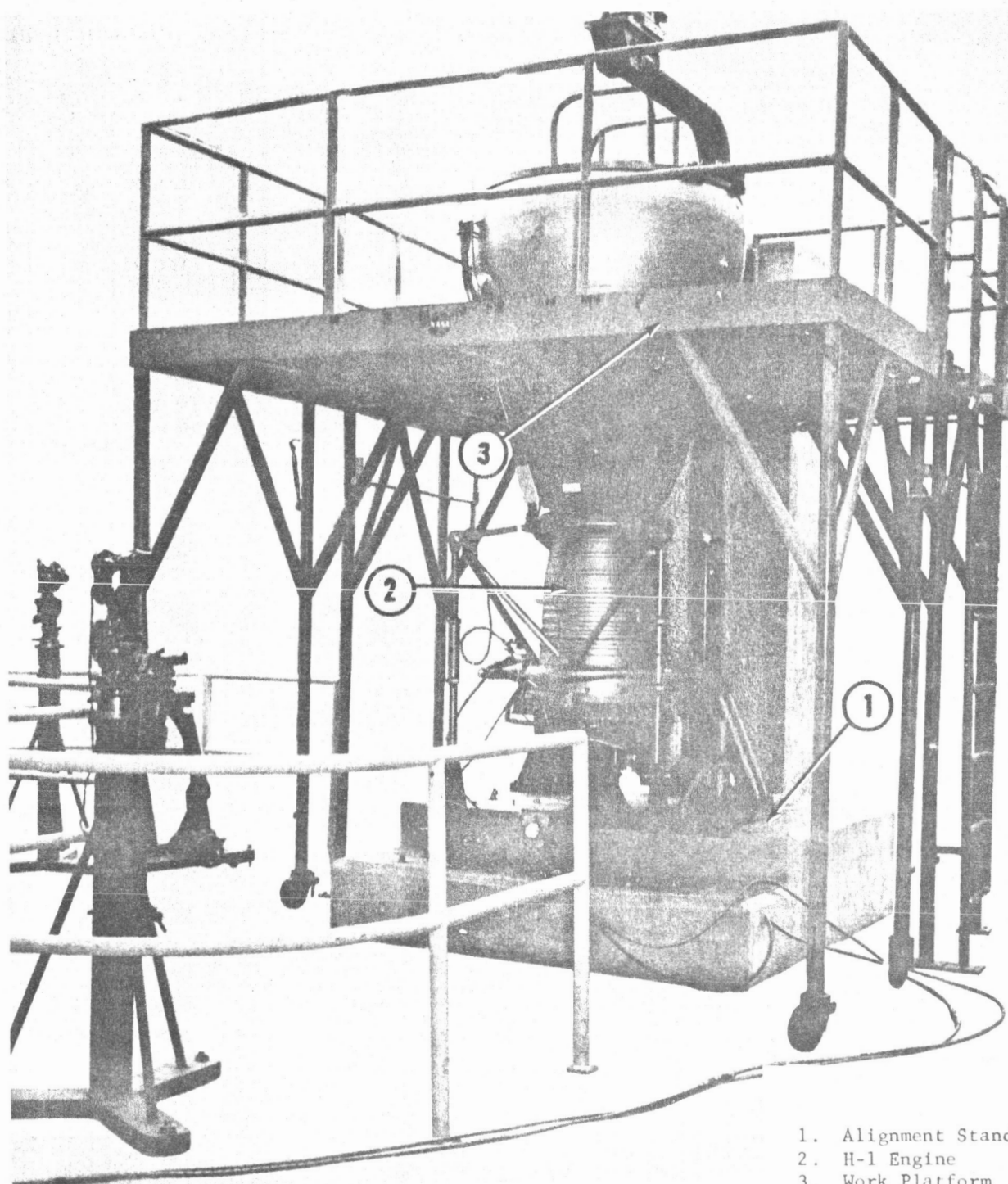


Figure 7-15. ALIGNMENT STAND AND WORK PLATFORM

#### 7.4.2 Dynamic Alignment Procedure [12,13,17,28,29,32,33,34,35]

The dynamic alignment procedure for the F-1 engine will be outlined in this subsection. The procedure is essentially the same as that for the J-2 [28] and R&D H-1 [29] engines, with the exception that the F-1 is given an abbreviated optical alignment rather than the detailed optical alignment performed on the J-2 and H-1.

The optical alignment of the F-1 engine is performed with the engine mounted in a nozzle-down position in the dynamic test stand. A series of ten wires are stretched between diametrically opposite points equally spaced around the exit ring. A plumb bob is suspended inside the thrust chamber from the center of the injection plate. The dummy actuators are adjusted until the plumb bob hangs directly over the center of the exit plane area, as determined by the intersection of the wires. This, in effect, makes the thrust chamber centerline parallel to the vertical reference (engine centerline) established by the dynamic test stand. No adjustment to the engine gimbal slides is made.

The dynamic test stand is equipped with a complement of six load cells which measure the forces generated by the engine during static firing, as shown in Figures 7-16 and 7-17. The main load cell (V) measures the thrust magnitude along the engine centerline, the horizontal load cells ( $L_{11}$ ,  $L_{12}$ , and  $L_2$ ) measure thrust components due to angularity misalignment, and the dummy actuator load cells ( $L_x$  and  $L_z$ ) measure actuator loads due to pierce point displacement errors. The main load cell is attached to the thrust frame by flexure rods so that the spring rates in the horizontal directions are negligible compared to those of the horizontal load cells. Two load cells are used in parallel along axis 1 (-) to restrain rotation of the engine about its centerline.

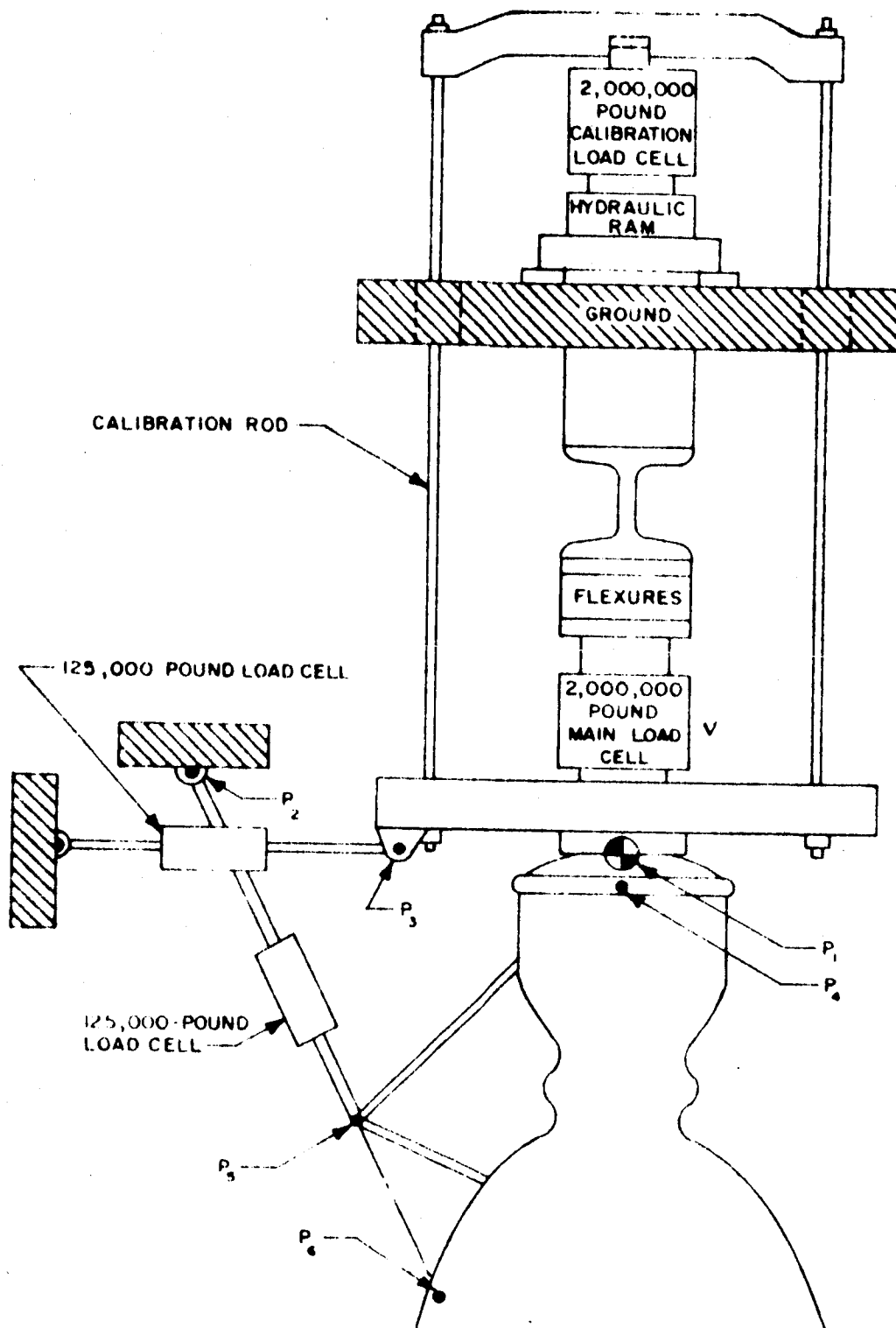


Figure 7-16. ENGINE ACCEPTANCE THRUST MEASURING SYSTEM SCHEMATIC

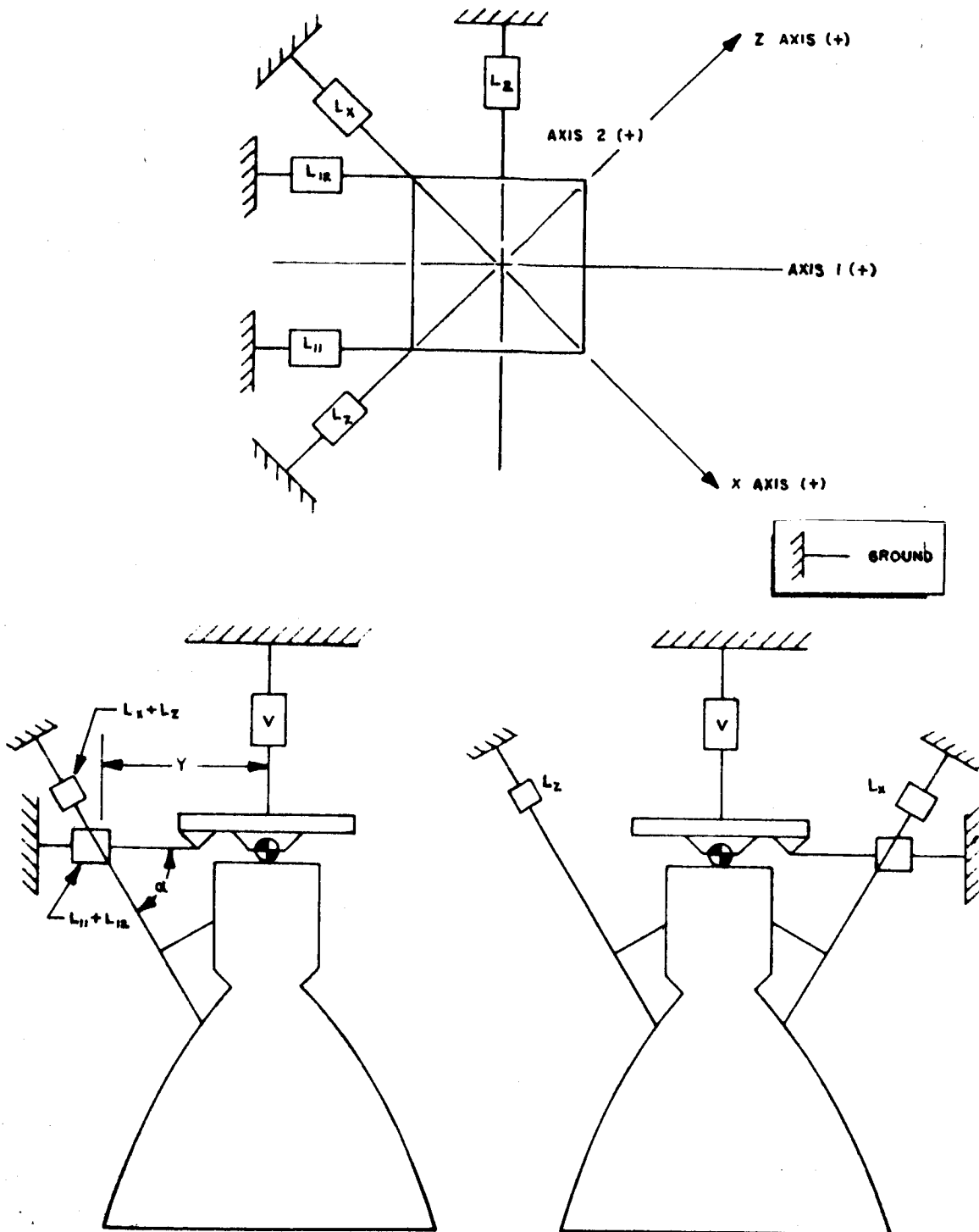


Figure 7-17. F-1 ENGINE ACCEPTANCE TEST STAND SCHEMATIC

September 1966

The load cells are calibrated in preload tests at which time some types of measurement errors can be accounted for. The automatic sequencer used to control the test energizes the recording system prior to engine ignition, and the analog outputs of all load cells are recorded throughout the static firing. The recorded load cell readings at a particular one-second slice time (usually 35 seconds after ignition) are taken as representative of steady-state performance, and are submitted to the digital computer [12] for calculation of dynamic thrust vector misalignment and the adjustments required to correct it. In the case of the F-1 engine, the results of two or more dynamic tests are averaged to obtain the necessary alignment adjustments, whereas for the J-2 engine no adjustment is made unless the position of the dynamic thrust vector is outside the specified tolerance.

The load cell configuration just described makes possible the calculation of main thrust, two side thrust components, and the pitch and yaw moments about the gimbal center, the latter four of which are used to determine the necessary alignment adjustments. In addition it appears that the same load cell configuration, perhaps with some minor modification, could be used to measure the roll moment (moment about the thrust chamber centerline) generated by the engine. (No mention of roll moment was found in any NASA or contractor documents reviewed under this contract.) While there is no way to adjust roll moment to zero, the size of steady-state roll moment to be expected from a particular engine is valuable knowledge. This is especially true in single engine stages such as the S-IVB, where the roll moment generated by the engine is applied directly to the stage and must be cancelled by the auxiliary roll control system.

## 7.5 STAGE ALIGNMENT TECHNIQUES [12,15,19,36,37,38,39,40,41,42,43,44,45]

Stage alignment may be defined as the dimensional quality of the assembled stage structure compared with the ideal geometry set forth by the control drawing package. The alignment of any structure must be kept sufficiently accurate to permit assembly of mating parts. However, additional accuracy requirements are placed on airframes since structural misalignment will cause c.g. offset and thrust misalignment in flight. This study was limited to consideration of thrust misalignment with respect to the stage centerline, and no analysis was conducted on c.g. offset or stage-to-stage misalignment.

### 7.5.1 Stage Structure Alignment

In simple terms, stage alignment consists of aligning the various stage sections such as the thrust structure, propellant tanks, intertank skirts (if applicable), and forward skirt (Figure 7-18). Each of the stage sections is optically indexed after assembly with tooling marks that form two planes, 90 deg apart, and intersect on the centerline of the section (a line connecting the centers of the upper and lower rings of the section). For the purposes of explanation, only the thrust structure section of the S-IC stage will be discussed in more detail.

The thrust structure is designed and manufactured within specified tolerance using plane (E) as the control surface (Figure 7-19). The thrust structure centerline and the longitudinal reference plane are controlled with respect to reference plane (E). The actuator attach points for the stage are located using the longitudinal reference plane and the engine centerline as controlled references. This procedure allows fabrication of a thrust structure assembly having control dimensions with respect to reference plane (E).



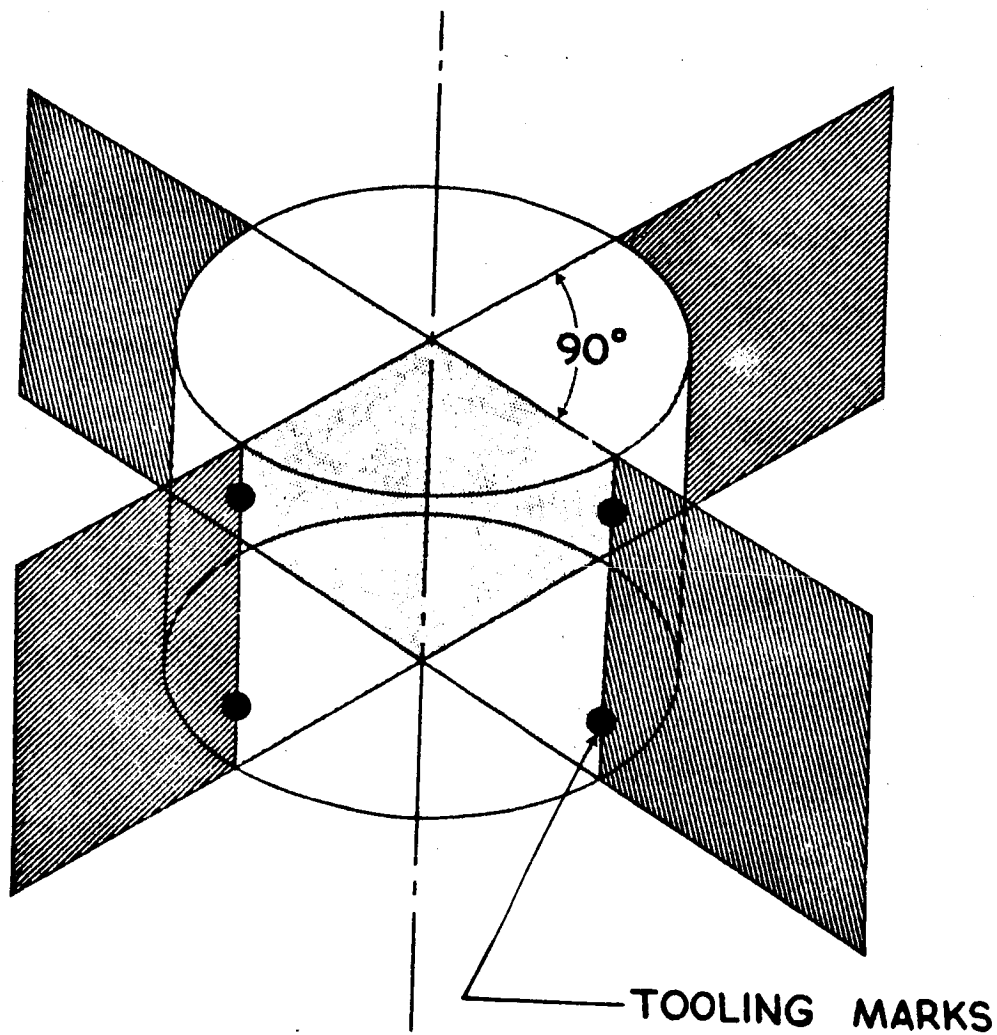


Figure 7-18. TYPICAL STAGE SECTION

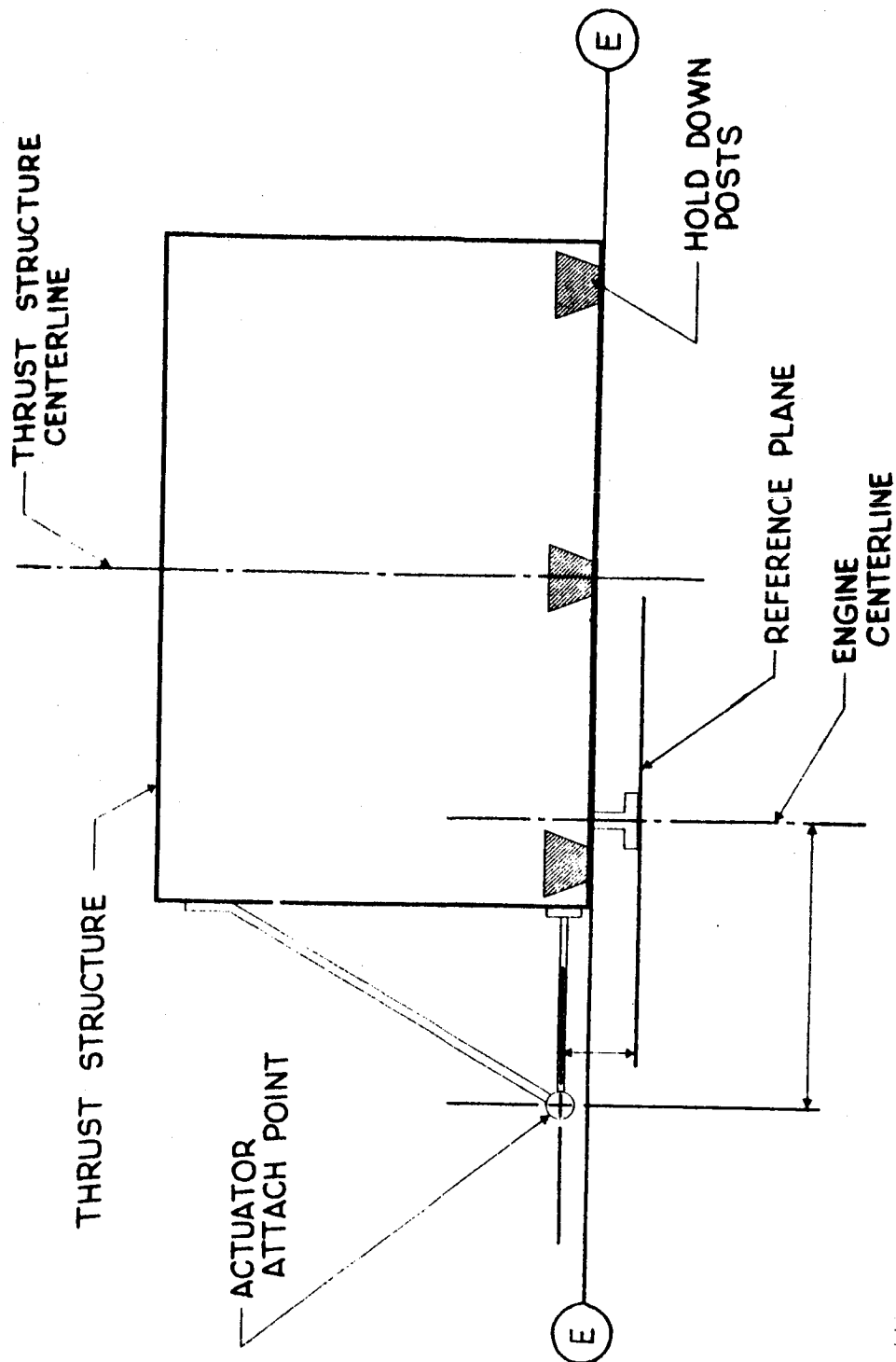


Figure 7-19. THRUST STRUCTURE ASSEMBLY

An assembly tool (Figure 7-20) is used during vertical stage assembly to define a horizontal plane, reference plane (E), and has provisions for supporting the thrust structure hold-down posts. The optical tools located 90 deg apart will define four planes perpendicular to the horizontal reference plane (E), which are used to control stage assembly. The centerline formed by these four planes establishes a vertical reference line. The thrust structure is positioned on the assembly tool so that the reference plane (E) of the thrust structure and horizontal tool planes are coincident, and the index marks on the thrust structure line up with the optical tools. The other stage sections and subassemblies, such as the propellant tanks, outriggers, and intertank and forward skirts are positioned so that the index marks lie on the planes defined by the optical tools. The above operations produce a stage assembly (Figures 7-21 and 7-22) which has the centerline of each individual section aligned to a vertical reference line.

#### 7.5.2 Engine-to-Stage Alignment

Engines are supplied to the stage contractor along with the prescribed actuator lengths determined from optical or dynamic engine alignment tests. Prior to assembly on the stage, each engine is checked in an optical alignment stand to verify that the pierce point and angularity errors of the geometric thrust vector are within the specified tolerance. The engines are then mounted on the stage, and the actuator lengths for each engine are adjusted to the values set forth in the engine logbook.

When the stage is fully assembled, the geometric thrust vector angularity with respect to the stage centerline is measured and recorded for each engine. This test is for historical data purposes only. The measurement is made by

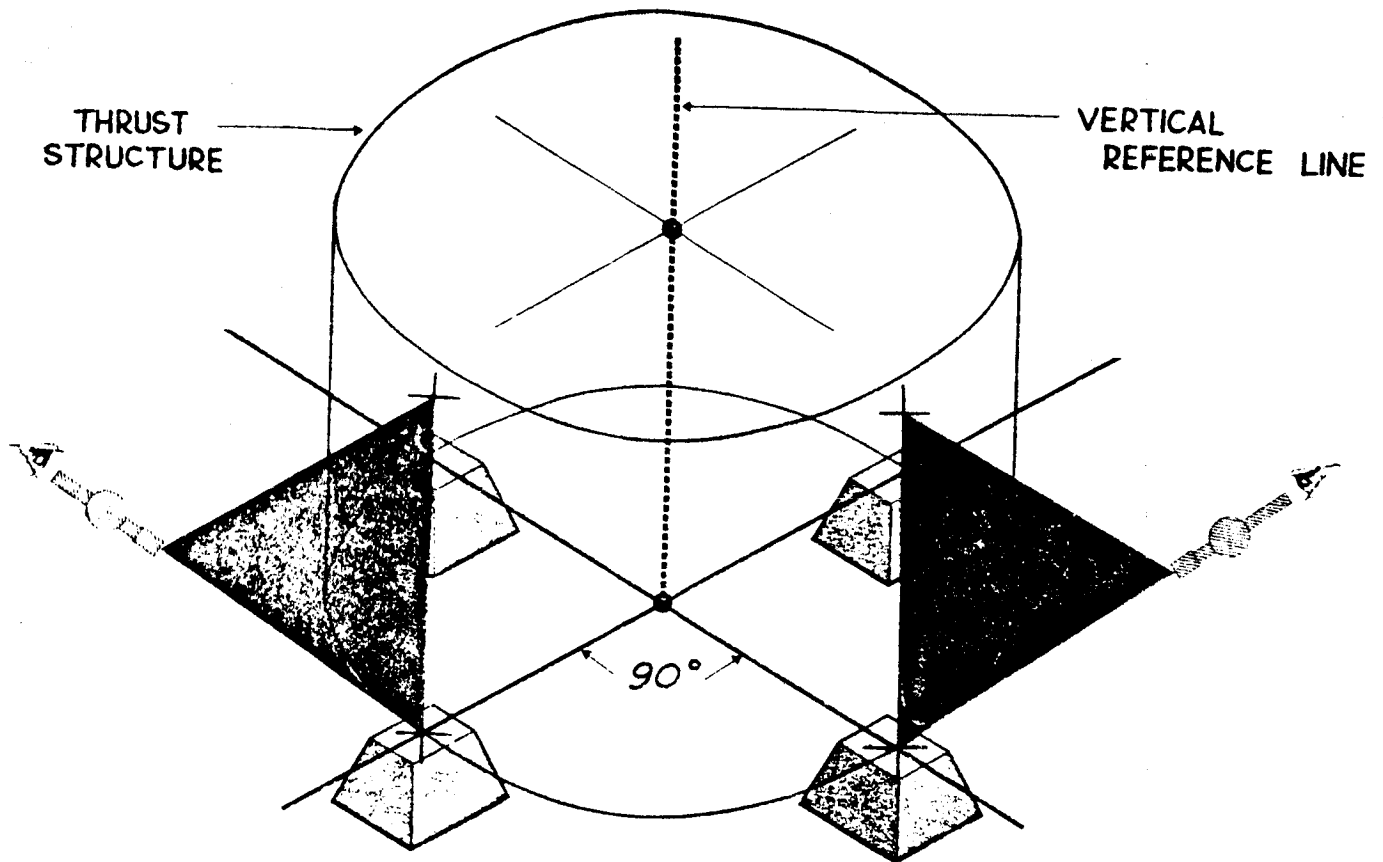


Figure 7-20. S-IC STAGE VERTICAL ASSEMBLY TOOL

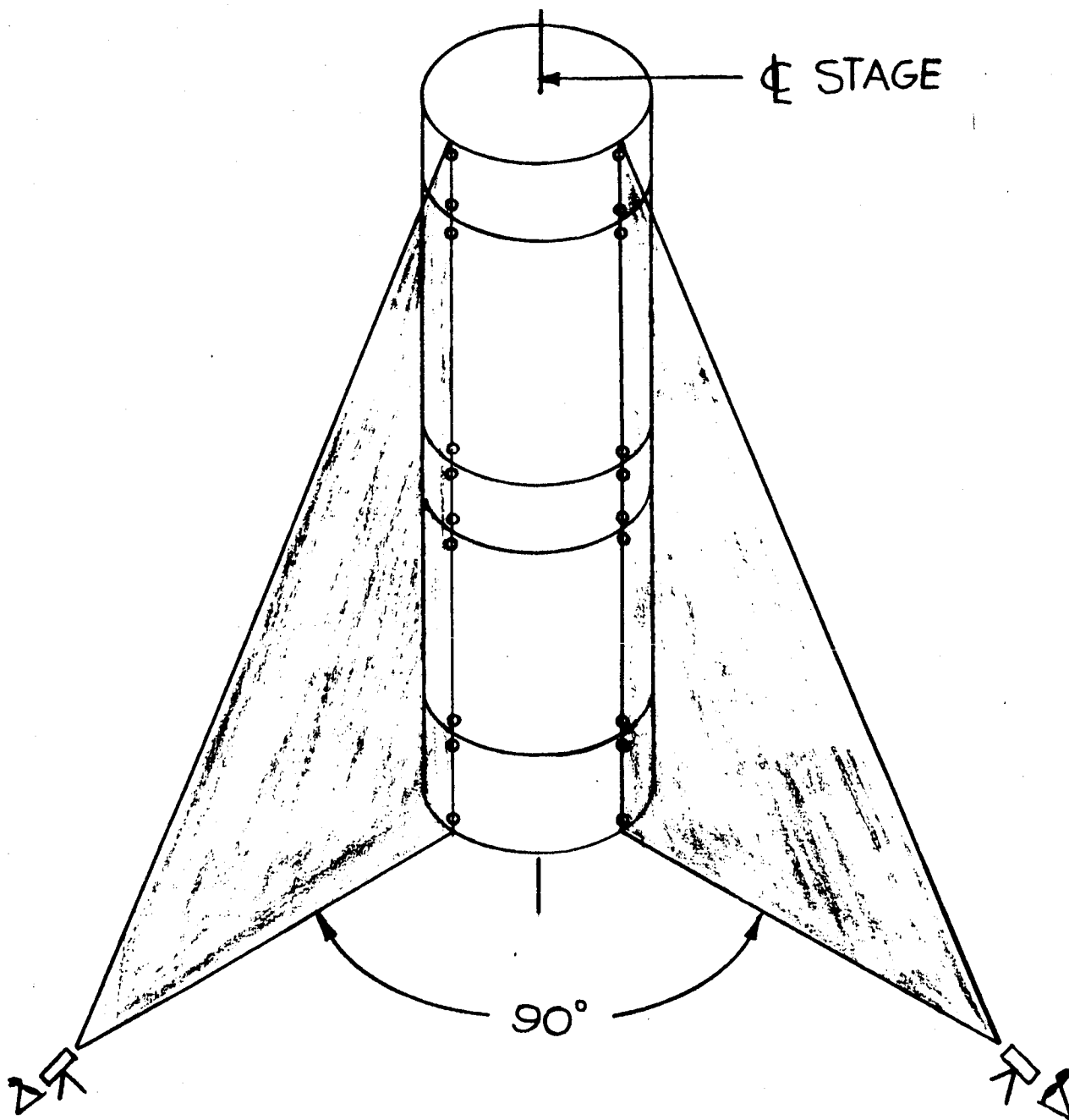


Figure 7-21. STAGE TOOLING MARKS

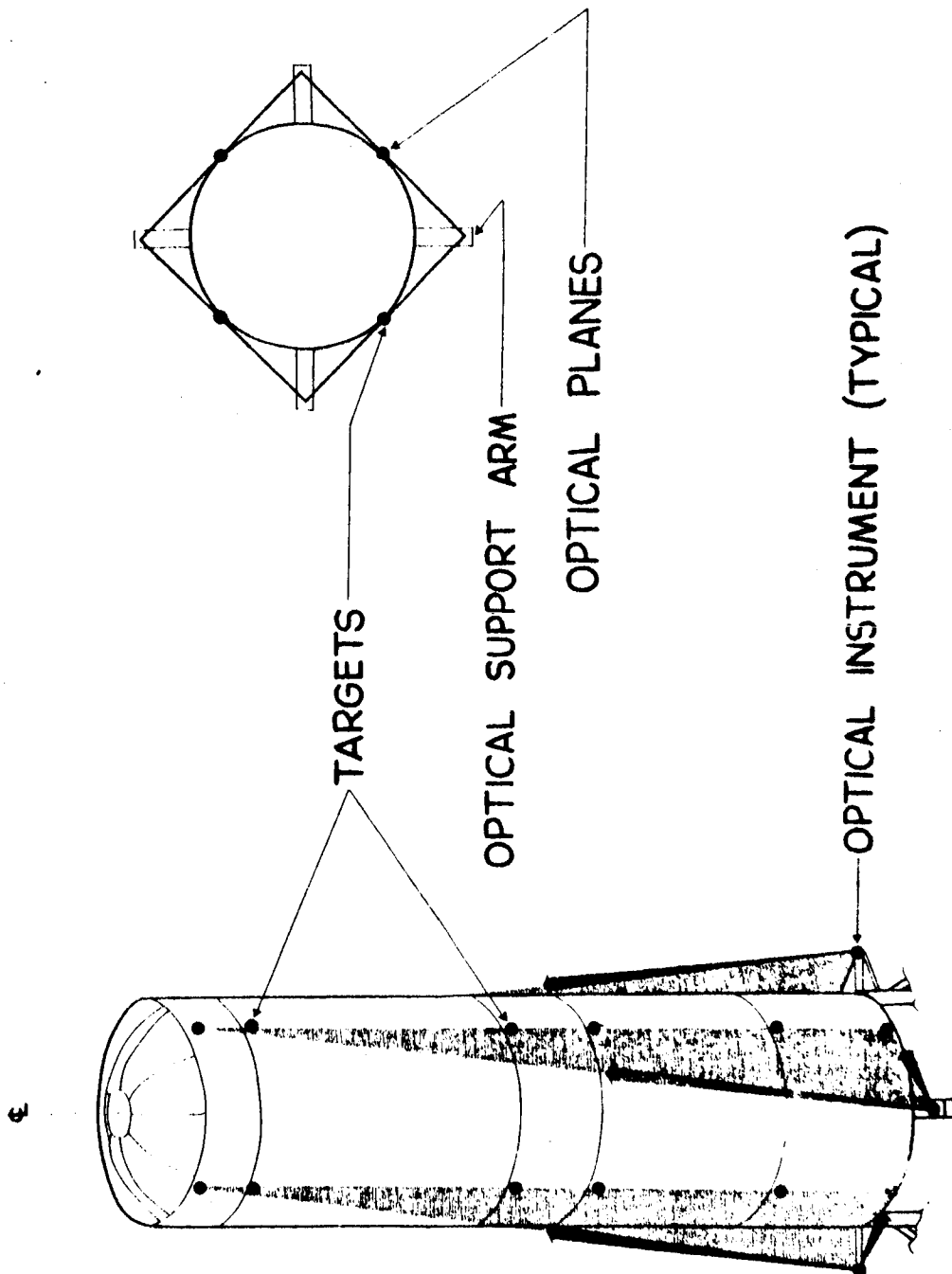
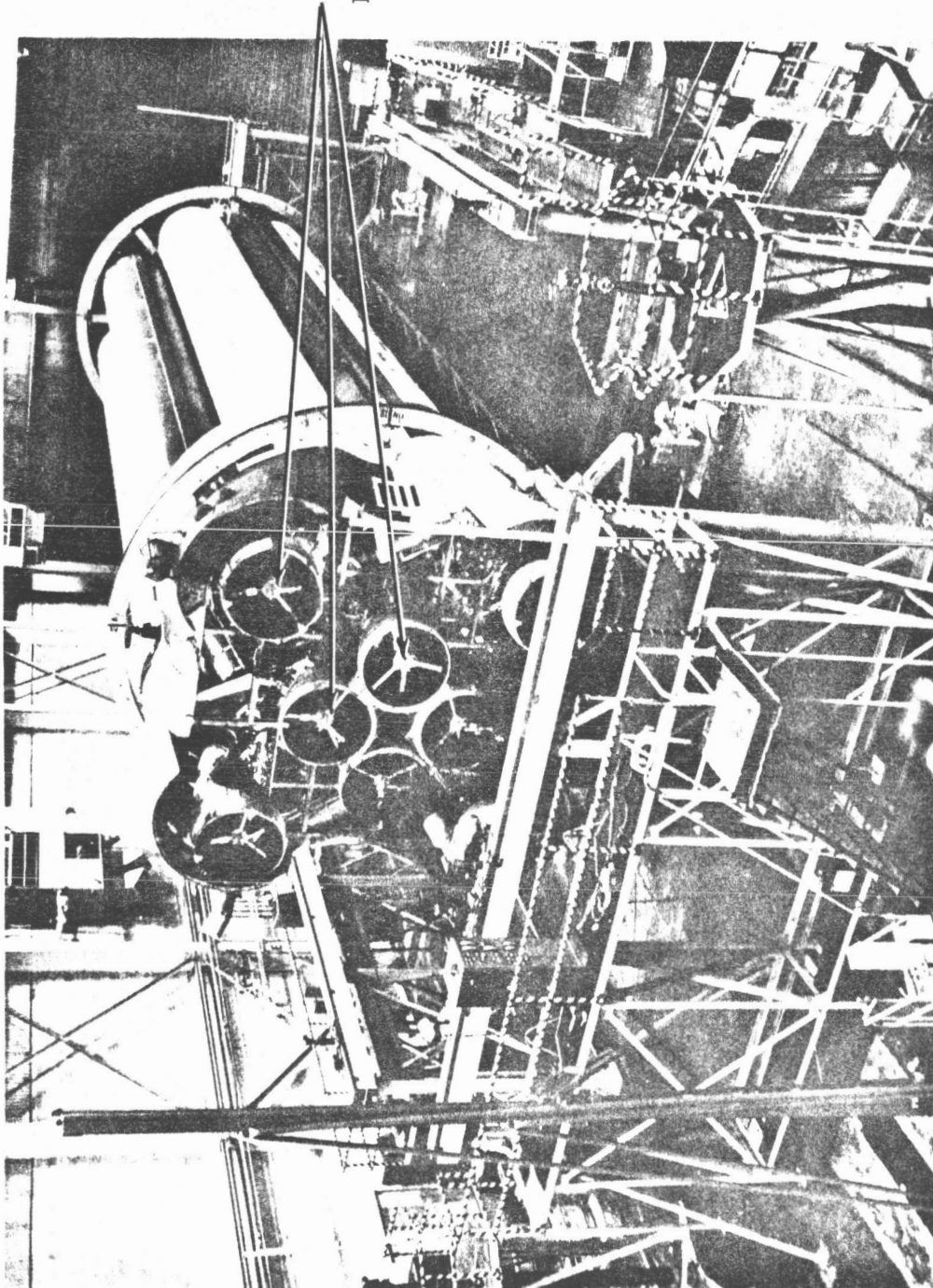


Figure 7-22. STAGE ALIGNMENT

temporarily installing the thrust chamber calibration fixture in the thrust chamber of each clustered engine (Figure 7-23) and optically determining the actual cant angle and the angle perpendicular to the cant plane.

In summary the engine-to-stage alignment consists of mounting each engine on the stage with the actuator lengths specified by the engine manufacturer . Both components of the geometrical engine cant angle are measured but no attempt is made to correct errors in these angles due to stage imperfection. The gimbal center locations of the installed engines were measured in terms of the stage coordinate system on the early S-I stages, but this test has been deleted on all current stages.



Thrust Chamber  
Calibration  
Fixtures (8 Total)

Figure 7-23. ENGINE-TO-STAGE ALIGNMENT, S-I STAGE



## SECTION VIII

### STATISTICAL ANALYSIS OF SATURN ENGINES AND STAGES

#### 8.1 GENERAL

This section presents the results obtained by applying the classical (Section IV) and Monte Carlo (Section VI) solutions to the S-I/S-IB and S-IC stages. Statistical models for each of the Saturn program engines (H-1, J-2, and F-1) are presented, based on dynamic test data, for use in stage analysis. Probability distributions for the engine-to-stage mounting errors are based on alignment measurement data in the analysis of the S-I/S-IB stage and on stated tolerances in the analysis of the S-IC stage. Little alignment measurement data could be found for the S-IC, S-II, or S-IVB stages. No information of any kind could be found on roll moment ( $M_u$ ) generated by any of the engines or on roll axis engine-to-stage mounting errors ( $\psi$ ). Consequently, these parameters were made deterministic in the investigation.

Coordinate systems for the engines and stages were chosen in accordance with the general coordinate system defined in Section III.

Engine coordinates: u-axis: engine centerline

v-axis: bisecting angle between actuator operating  
planes

Stage coordinates: x-axis: stage centerline

z-axis: pointing vertically downward in normal  
horizontal flight.

Geometry and tolerance data were obtained for the S-II and S-IVB stages and are summarized in subsection 8.6.

September 1966

## 8.2 H-1 ENGINE MODEL

### 8.2.1 Available Data [29]

A statistical model of the H-1 engine was formulated based on the results of dynamic tests of the R&D version H-1 performed at MSFC [29]. As was mentioned in the previous section, the production H-1 engine is optically aligned and demonstration of dynamic thrust vector alignment is not required. Consequently, no dynamic alignment data was available from the manufacturer, although a large amount of optical alignment data was obtained. It was decided to base the statistical model on the R&D dynamic tests in spite of the small sample size, since only dynamic alignment tests contain information of the dynamic thrust vector position.

The dynamic alignment data available on the H-1 engine were load cell measurements resulting from twenty-nine static test firings conducted by the Test Laboratory of MSFC. The tests were performed on two R&D engines, an 836 kN (188 kip) inboard engine and a 900 kN (200 kip) outboard engine, neither of which was optically aligned. The load cell placement and test stand configuration were identical for the two engines except for the actuator positions and is illustrated in Figure 8-1 for the outboard engine. Load cell readings obtained from the tests were in the form of strip-chart recordings. Load cell outputs were taken from the strip charts at a three-second slice time, beginning thirty-two seconds after ignition. Loads due to engine thrust were obtained by adding algebraically the prefiring values to the slice time values, and the results are listed in Table 8-1. Compressive forces are positive and tensile forces are negative.

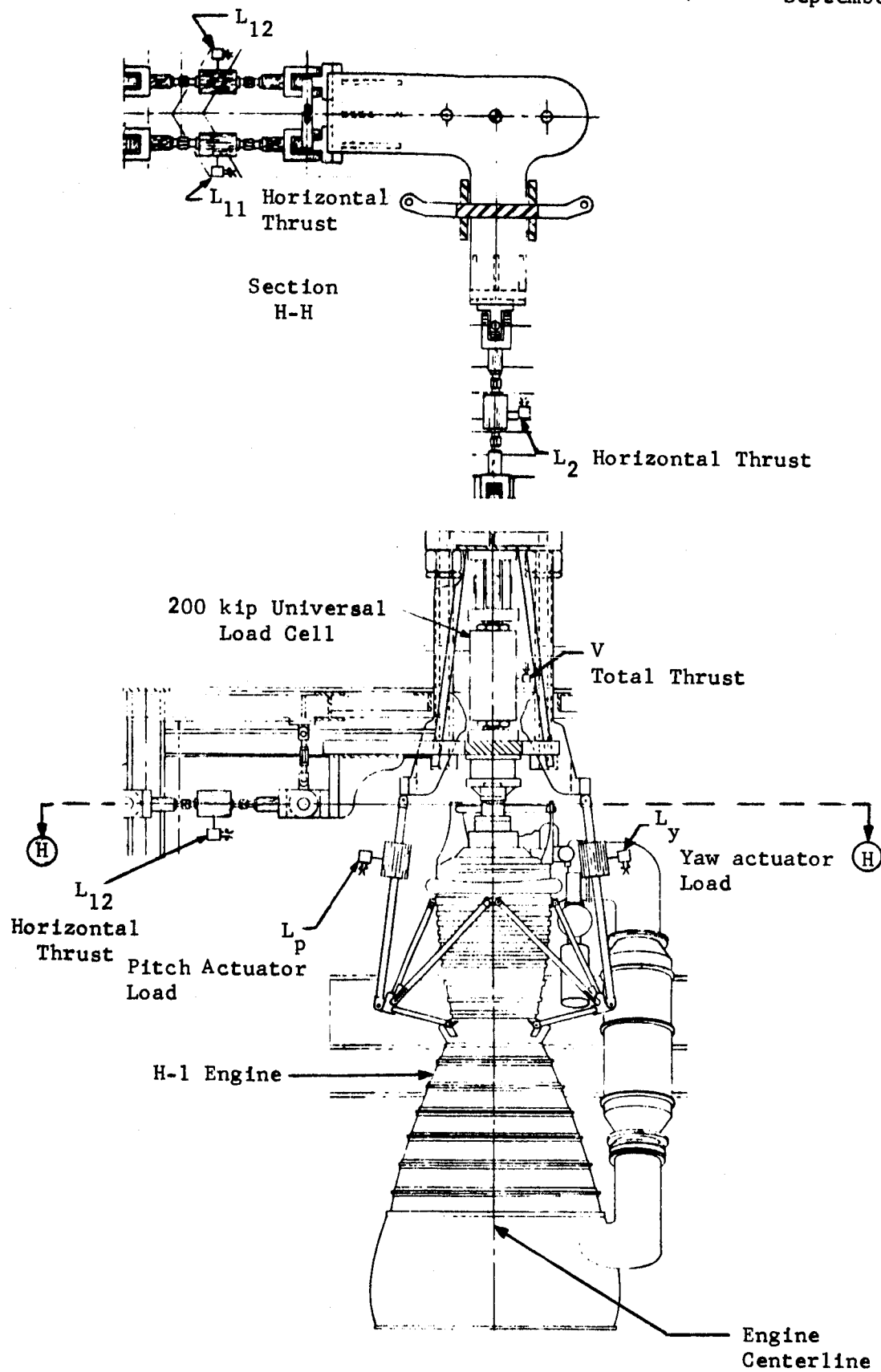


Figure 8-1. LOAD CELL ARRANGEMENT, DYNAMIC TEST STAND, OUTBOARD H-1 ENGINE

Table 8-1. LOAD CELL READINGS DUE TO ENGINE THRUST, R&D H-1 ENGINE

TEST NO.	V kip	L <sub>11</sub> kip	L <sub>12</sub> kip	L <sub>2</sub> kip	L <sub>y</sub> kip	L <sub>p</sub> kip
(a) 836 kN (188 kip) Inboard Engine						
1	194.2	0.672	1.480	-3.900	0.390	-1.200
2	181.9	0.875	1.440	-3.400	0.425	-1.100
3	185.1	0.796	1.160	-3.400	0.402	-1.103
4	184.9	0.835	1.400	-3.300	0.361	-1.100
5	182.3	0.954	1.360	-3.200	0.407	-1.000
6	190.9	1.676	1.360	-3.700	0.443	-1.200
7	183.6	0.875	1.360	-3.300	0.501	-1.000
8	195.4	0.756	1.240	-3.700	0.529	-1.140
9	190.7	1.074	0.960	-3.500	0.377	-0.900
10	181.8	0.914	1.160	-3.300	0.431	-0.900
11	184.4	0.840	1.320	-3.500	0.483	-1.000
12	181.0	0.958	1.200	-3.500	0.418	-1.000
13	181.3	1.20	0.880	-3.600	0.463	-1.000
14	178.7	1.20	0.880	-2.800	0.500	-1.100
(b) 900 kN (200 kip) Outboard Engine						
1	195.0	0.482	0.620	-0.200	1.071	-0.100
2	197.3	0.800	1.800	-0.200	1.011	-0.100
3	196.5	0.804	1.860	0	0.778	-0.100
4	199.0	0.900	2.300	-0.400	0.600	1.900
5	193.9	0.909	0.955	0	0.339	1.800
6	197.6	0.080	0.497	-0.300	0.230	1.400
7	197.5	0.100	0.600	-0.400	0.300	1.500
8	200.7	0.160	0.478	-0.200	0.100	1.500
9	200.5	0.100	0.600	-1.000	0.149	1.217
10	199.6	0.300	0.500	-0.300	0.065	1.259
11	198.6	0.140	0.320	-0.200	0.081	1.212
12	202.2	0.357	0.396	-0.200	0.029	1.362
13	195.6	0.440	0.122	-0.169	0.048	1.401
14	197.7	0.319	0.278	-0.160	0.108	1.374
15	200.7	0.400	-0.100	+0.200	0.165	1.403

### 8.2.2 Parameter Derivation

The load cell readings for each test listed in Table 8-1 were processed to obtain the equivalent forces and moments ( $F_u$ ,  $F_v$ ,  $F_w$ ,  $M_v$ ,  $M_w$ ) in the  $uvw$  coordinate system. The following conversion equations were used to obtain the necessary parameters, and are readily derived from the geometry shown in Figure 8-2.

Inboard: (Actuators set  $32^\circ$  off perpendicular to gimbal plane)

$$F_u \doteq V \quad (8-1)$$

$$F_v = L_2 + \frac{\sqrt{2}}{2} (L_y + L_p) \sin 32^\circ \quad (8-2)$$

$$F_w = -(L_{11} + L_{12}) + \frac{\sqrt{2}}{2} (L_y - L_p) \sin 32^\circ \quad (8-3)$$

$$M_v = d_A (L_y - L_p) \cos 32^\circ \quad (8-4)$$

$$M_w = -d_A (L_y + L_p) \cos 32^\circ \quad (8-5)$$

Outboard: (Actuators approximated as parallel to engine centerline)

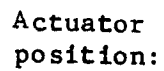
$$F_u \doteq V \quad (8-6)$$

$$F_v \doteq L_2 \quad (8-7)$$

$$F_w \doteq -(L_{11} + L_{12}) \quad (8-8)$$

$$M_v \doteq d_A (L_y - L_p) \quad (8-9)$$

$$M_w \doteq -d_A (L_y + L_p) \quad (8-10)$$



**Figure 8-2. COORDINATE SYSTEM AND ACTUATOR POSITIONS, H-1 ENGINE**

When these equations are applied to the test data, the force and moment components listed in Table 8-2 result.

### 8.2.3 Statistical Analysis

Sample means, variances, covariances, and linear correlation coefficients were calculated for the force and moment components, using the following standard formulae:

$$E[x] = \frac{1}{n} \sum_{i=1}^n x_i \quad (8-11)$$

$$\text{Var}[x] = \frac{\sum_{i=1}^n x_i^2 - \left( \sum_{i=1}^n x_i \right)^2}{n(n-1)} \quad (8-12)$$

$$\text{Cov}[x,y] = \frac{\sum_{i=1}^n x_i y_i - \frac{\sum_{i=1}^n x_i \sum_{i=1}^n y_i}{n}}{n-1} \quad (8-13)$$

$$\rho [x,y] = \frac{\text{Cov}[x,y]}{\sqrt{\text{Var}[x] \text{Var}[y]}} \quad (8-14)$$

where  $x$  and  $y$  are any two components and  $n$  = no. of samples. The resulting statistical parameters for each engine are listed in Table 8-3 and histograms are shown in Figures 8-3 and 8-4. The deviation of sample mean from ideal mean was subtracted from each sample value in order to remove the effect of bias present in the test engines. This is justified for two reasons:

- (1) The test engines were not optically aligned before the tests and (2) the bias of the two engines gives practically no information as to the bias of the total population of engines. Forcing the means to their ideal values does not affect the variances but does change the covariances and correlation coefficients.

September 1966

Table 8-2(a). DERIVED DYNAMIC FORCE AND MOMENT COMPONENTS,  
INBOARD R&D H-1 ENGINE (836 kN)

TEST #	Fu		Fv*		Fw*	
	kN	kip	N	lb	N	lb
1	836.845	194.2	-2370.902	-533	360.306	81
2	809.132	181.9	80.068	18	- 475.960	-107
3	823.366	185.1	13.345	3	1116.504	251
4	822.476	184.9	391.444	88	- 191.274	- 43
5	810.911	182.3	1076.470	242	- 631.647	-142
6	849.166	190.9	-1427.879	-321	-3447.372	-775
7	816.693	183.6	787.335	177	- 124.550	- 28
8	869.183	195.4	-1178.779	-265	1214.364	273
9	848.276	190.7	- 146.791	- 33	395.892	89
10	808.687	181.8	- 836.266	-188	311.375	70
11	820.252	184.4	- 44.482	- 10	177.928	40
12	805.128	181.0	- 244.652	- 55	75.620	17
13	806.463	181.3	- 609.406	-137	502.649	113
14	794.897	178.7	2842.414	639	725.060	163
SAMPLE MEAN	824.89	185.43	-16298.3	-3664	-7401.8	-1644

TEST #	Mv*		Mw*	
	Nm	lb-in.	Nm	lb-in.
1	-164.817	-1458.75	384.573	3403.75
2	- 59.334	- 525.15	103.285	914.15
3	- 76.915	- 680.75	208.768	1847.75
4	59.334	525.15	221.953	1964.45
5	160.422	1419.85	- 50.544	- 447.35
6	-285.683	-2528.50	263.707	2334.00
7	- 15.383	- 136.15	-226.348	-2003.35
8	327.436	-2898.05	- 15.383	- 136.15
9	399.956	3539.90	-180.200	-1594.90
10	312.053	2761.90	-268.102	-2372.90
11	21.976	194.50	-188.990	-1672.90
12	140.644	1244.80	- 70.322	- 622.40
13	57.136	505.70	-153.829	-1361.50
14	-197.780	-1750.50	- 35.161	- 311.20
SAMPLE MEAN	-2780.	-24600.	-1150.	-10200.

\* Sample mean has been subtracted from each entry in this column.



September 1966

Table 8-2(b). DERIVED DYNAMIC FORCE AND MOMENT COMPONENTS, OUTBOARD  
R&D H-1 ENGINE (900 kN)

TEST NO.	Fu		Fv*		Fw*	
	kN	kip	N	lb	N	lb
1	867.403	195.000	155.688	35	351.409	79
2	877.634	197.300	155.688	35	-6312.026	-1419
3	874.076	196.500	1045.332	235	-6596.713	-1483
4	885.196	199.000	- 733.957	-165	-8980.960	-2019
5	862.510	193.900	1045.332	235	-3038.135	- 683
6	878.969	197.600	- 289.134	- 65	2686.726	604
7	878.524	197.500	- 733.957	-165	2139.595	481
8	892.758	200.700	155.688	35	2415.384	543
9	891.868	200.500	-3402.899	-765	2139.595	481
10	887.865	199.600	- 289.134	- 65	1694.772	381
11	883.417	198.600	155.688	35	3207.168	721
12	899.430	202.200	155.688	35	1903.839	428
13	870.072	195.600	293.583	66	2753.449	619
14	879.413	197.700	333.617	75	2597.761	584
15	892.758	200.700	1934.976	435	3029.239	681
SAMPLE MEAN	881.46	198.16	-1045.3	-235	-5253.4	-1181

TEST NO.	Mv*		Mw*	
	Nm	lb-in.	Nm	lb-in.
1	-4364.351	-38627.70	1063.618	9413.80
2	-4232.497	-37460.70	1195.472	10580.80
3	-3720.466	-32928.85	1707.503	15112.65
4	1065.816	9433.25	-2296.448	-20325.25
5	1419.623	12564.70	-1503.130	-13303.80
6	802.109	7099.25	- 362.597	- 3209.25
7	1439.401	12739.75	- 164.817	- 1458.75
8	1285.572	11378.25	- 318.646	- 2820.25
9	555.982	4920.85	195.583	1731.05
10	832.875	7371.55	287.880	2547.95
11	694.428	6146.20	356.004	3150.90
12	1172.231	10375.10	140.644	1244.80
13	1182.286	10464.10	13.185	116.70
14	991.099	8771.95	- 59.334	- 525.15
15	929.567	8227.35	- 248.324	- 2197.85
SAMPLE MEAN	1790.	15850.	-3200.	-28300.

\* Sample mean has been subtracted from each entry in this column.

September 1966

Table 8-3(a). STATISTICAL PARAMETERS, 836 kN  
(188 kip) R&D H-1 ENGINE.

FORCE COMPONENT	MEAN N (1b)	STD. DEVIATION N (1b)	VARIANCE N <sup>2</sup> (1b <sup>2</sup> )
Fu	824.89x10 <sup>3</sup> (185.44x10 <sup>3</sup> )	23285. (5234.6)	121.89x10 <sup>6</sup> (27.401x10 <sup>6</sup> )
Fv	0 (0)	1247.2 (280.38)	15554x10 <sup>6</sup> (.07861x10 <sup>6</sup> )
Fw	0 (0)	1126.0 (253.14)	1.2679x10 <sup>6</sup> (.06408x10 <sup>6</sup> )
MOMENT COMPONENT	Nm (1b-in.)	Nm (1b-in.)	N <sup>2</sup> <sub>m</sub> (1b <sup>2</sup> -in <sup>2</sup> )
Mv	0 (0)	210.39 (1861.2)	.04422x10 <sup>6</sup> (3.464x10 <sup>6</sup> )
Mw	0 (0)	204.73 (1812.0)	.04191x10 <sup>6</sup> (3.283x10 <sup>6</sup> )

COMPONENT PAIR	COVARIANCE				LINEAR CORRELATION COEFFICIENT (DIMENSIONLESS)
	METRIC UNIT		ENGLISH UNIT		
Fu,Fv Fu,Fw Fv,Fw	-22.224 - 2.2207 .28394	N <sup>2</sup> x10 <sup>6</sup>	-1.1232 = .11223 .01435	1b <sup>2</sup> x10 <sup>6</sup>	-.765 -.085 .202
Fu,Mv Fu,Mw Fv,Mv Fv,Mw Fw,Mv Fw,Mw	- 1.7516 2.0821 .07173 = .12179 .03960 = .06801	N <sup>2</sup> <sub>m</sub> x10 <sup>6</sup>	-3.4852 4.1427 .14273 = .24232 .07879 = .13533	1b <sup>2</sup> in. x10 <sup>6</sup>	-.358 .437 .274 -.477 .167 -.295
Mv,Mw	= .02453	N <sup>2</sup> <sub>m</sub> <sup>2</sup> x10 <sup>6</sup>	-1.9218	(1b-in) <sup>2</sup> x10 <sup>6</sup>	-.570

Table 8-3(b). STATISTICAL PARAMETERS, 900 KN (200 kip)  
R&D H-1 ENGINE

FORCE COMPONENT	MEAN N (lb)	STD. DEVIATION N (lb)	VARIANCE N <sup>2</sup> (lb <sup>2</sup> )
Fu	881.46x10 <sup>3</sup> (198.16x10 <sup>3</sup> )	10420. (2342.4)	108.58x10 <sup>6</sup> (5.4869x10 <sup>6</sup> )
Fv	0 (0)	1167.2 (262.39)	1.3623x 10 <sup>6</sup> (.06885x10 <sup>6</sup> )
Fw	0 (0)	4162.9 (935.85)	17.329x10 <sup>6</sup> (.87581x10 <sup>6</sup> )
MOMENT COMPONENT	Nm (lb-in.)	Nm (lb-in.)	Nm <sup>2</sup> (lb <sup>2</sup> -in. <sup>2</sup> )
Mv	0 (0)	2145.2 (18986.)	.04602x10 <sup>8</sup> (3.6049x10 <sup>8</sup> )
Mw	0 (0)	985.69 (8724.1)	.00972x10 <sup>8</sup> (.76110x10 <sup>8</sup> )

COMPONENT PAIR	COVARIANCE				LINEAR CORRELATION COEFFICIENT (DIMENSIONLESS)
	METRIC UNIT		ENGLISH UNIT		
Fu,Fv	- 5.32321	N <sup>2</sup>	- .26903	lb <sup>2</sup>	- .438
Fu,Fw	14.38570	x10 <sup>6</sup>	.72704	x10 <sup>6</sup>	.332
Fv,Fw	- 1.79841		- .09089		- .370
Fu,Mv	8.49666	N <sup>2</sup> m <sup>6</sup> x10 <sup>6</sup>	16.906	lb <sup>2</sup> -in. x10 <sup>6</sup>	.380
Fu,Mw	- 3.20984		- 6.3867		.313
Fv,Mv	- .93395		- 1.8583		- .373
Fv,Mw	.24052		.47857		.209
Fw,Mv	4.38895		8.7328		.491
Fw,Mw	- 1.92047		- 3.8212		- .468
Mv,Mw	- 1.50494	N <sup>2</sup> m <sup>2</sup> x10 <sup>6</sup>	-117.89	(lb-in) <sup>2</sup> x10 <sup>6</sup>	- .712

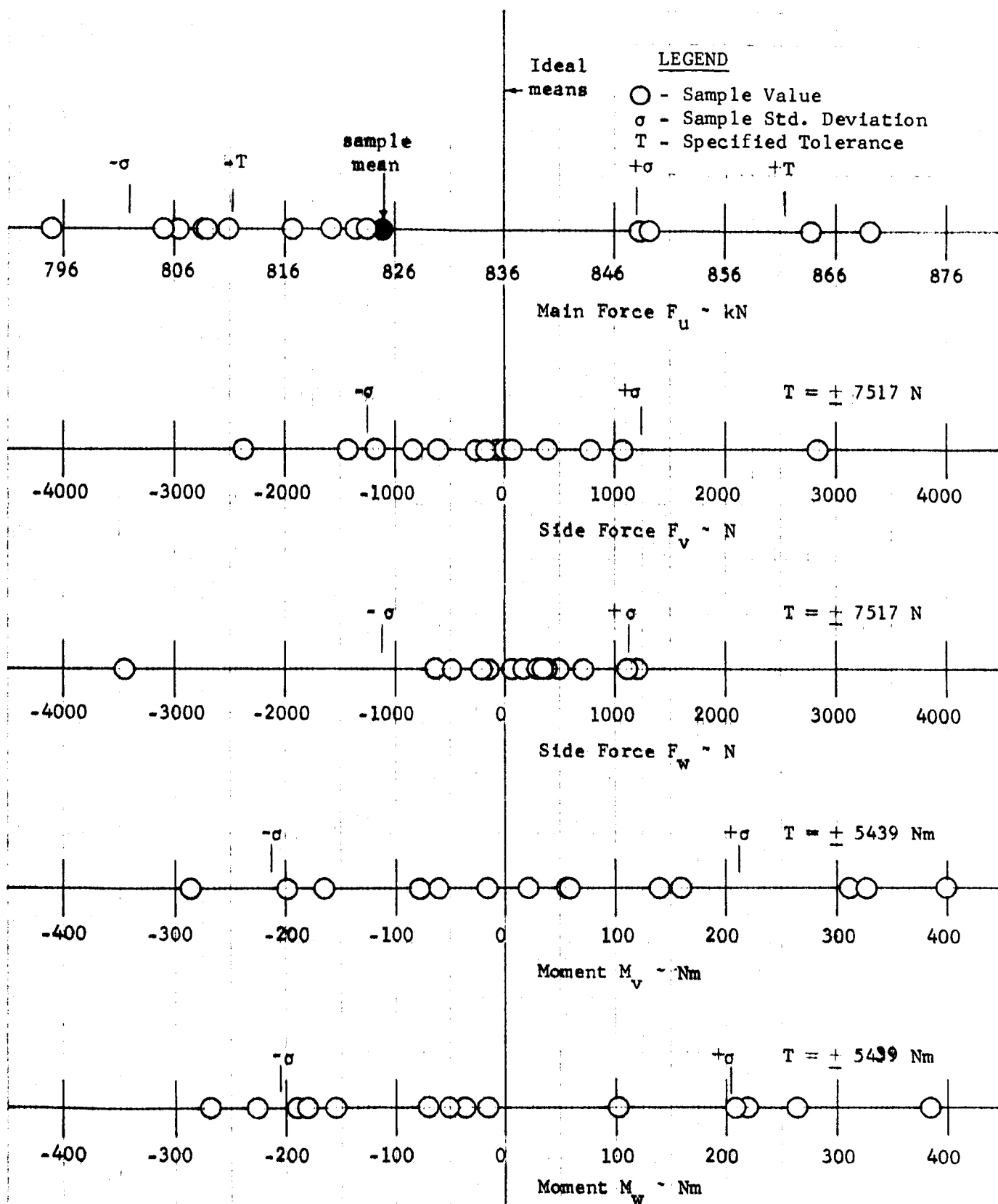


Figure 8-3. SAMPLE PATTERN OF DYNAMIC THRUST AND MOMENT COMPONENTS, 836 kN (188 KIP) H-1 R&D ENGINE

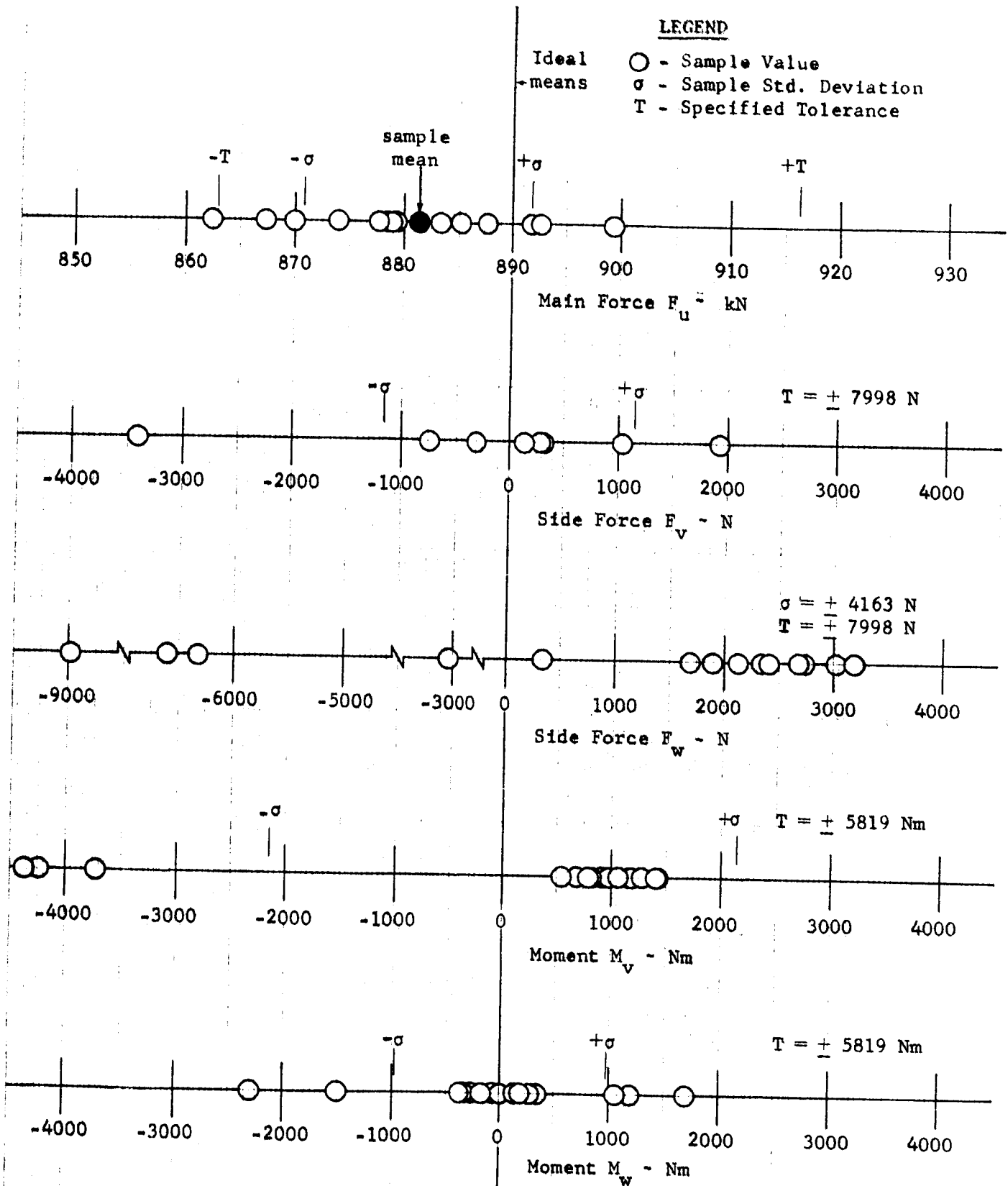


Figure 8-4. SAMPLE PATTERN OF DYNAMIC THRUST AND MOMENT COMPONENTS, 900 kN (200 KIP) H-1 R&D ENGINE

### 8.3 J-2 ENGINE MODEL

#### 8.3.1 Available Data [46]

The production J-2 engine is optically aligned and then static test fired once to determine the position and magnitude of the dynamic thrust vector. If the dynamic thrust vector is within tolerance, no further alignment adjustments are made. A data reduction computer program is used by the manufacturer to calculate from the slice time load cell readings the equivalent magnitude, pierce point displacement and angularity of the dynamic thrust vector which would exist in a vacuum environment. Single test data of this type were gathered on forty-six J-2 engines and are listed in Table 8-4. These data are in terms of the engine manufacturer's coordinate system shown in Figure 8-5.

#### 8.3.2 Parameter Derivation

Parameter derivation in this case consisted of transforming the given magnitude, pierce point and angularity data into force and moment components in terms of the standard uvw axes. The conversion formulae used can be written from inspection of Figure 8-5.

Pierce point displacement:

$$\begin{aligned} v_p &= Z_p \\ w_p &= -X_p \end{aligned}$$

Angularity:

$$\alpha_v = \frac{\sqrt{2}}{2}(\alpha_1 + \alpha_2)$$

$$\alpha_w = \frac{\sqrt{2}}{2}(\alpha_1 - \alpha_2)$$

Table 8-4. MANUFACTURER'S DYNAMIC TEST DATA, J-2 ENGINE.

F  lb	X <sub>p</sub> in.	Z <sub>p</sub> in.	α <sub>1</sub> min	α <sub>2</sub> min
0.22583E 06	-0.58140E 00	0.36430E 00	0.27800E 01	0.10100E 01
0.22601E 06	0.17930E 00	0.34990E 00	-0.22730E 02	0.29880E 02
0.22383E 06	-0.67000E-02	0.82000E-02	-0.16510E 02	0.58300E 01
0.22912E 06	0.28240E 00	0.16780E 00	-0.12880E 02	0.13030E 02
0.22994E 06	-0.40730E 00	-0.36400E-01	-0.59600E 01	0.33300E 01
0.22517E 06	-0.35610E 00	0.36640E 00	-0.76000E 00	0.23000E 01
0.22659E 06	-0.39310E 00	0.63790E 00	-0.38700E 01	0.20210E 02
0.22387E 06	-0.36100E-01	-0.10590E 00	-0.12070E 02	-0.12600E 01
0.22271E 06	-0.16200E-01	0.22890E 00	-0.95300E 01	0.54700E 01
0.22643E 06	-0.29610E 00	0.27770E 00	0.38000E 01	0.15950E 02
0.22453E 06	0.43100E-01	-0.19380E 00	-0.60000E 01	0.91000E 00
0.22813E 06	0.24980E 00	0.26460E 00	-0.15860E 02	-0.16700E 01
0.22608E 06	0.46870E 00	-0.82500E-01	-0.23010E 02	0.62400E 01
0.22661E 06	0.31600E-01	0.67600E-01	0.12900E 02	-0.36900E 01
0.22857E 06	-0.52000E-01	0.20860E 00	-0.10900E 02	-0.14700E 01
0.22651E 06	-0.29000E-01	0.12730E 00	-0.95300E 01	-0.13780E 02
0.22700E 06	-0.33700E-01	0.20530E 00	-0.11460E 02	0.41000E 01
0.22493E 06	0.27890E 00	0.70300E-01	-0.94300E 01	0.14200E 01
0.22697E 06	-0.98200E-01	-0.90800E-01	0.13790E 02	0.10280E 02
0.22925E 06	-0.61000E-01	0.48700E-01	0.28300E 01	0.73800E 01
0.22630E 06	-0.10790E 00	0.61100E-01	0.99700E 01	0.16730E 02
0.22696E 06	-0.98000E-02	0.17810E 00	0.88200E 01	0.50400E 01
0.22132E 06	-0.41200E-01	-0.11300E-01	0.87100E 01	0.14480E 02
0.22569E 06	0.33240E 00	0.35130E 00	-0.41900E 01	0.92600E 01
0.22380E 06	-0.94200E-01	0.22970E 00	-0.10500E 01	0.59500E 01
0.22635E 06	0.17170E 00	0.83800E-01	-0.23200E 01	0.18420E 02
0.22663E 06	-0.11100E 00	0.20420E 00	-0.26900E 01	0.83200E 01
0.23126E 06	-0.22340E 00	0.87800E-01	-0.20600E 01	0.50800E 01
0.22667E 06	0.91500E-01	-0.43400E-01	-0.16320E 02	0.20220E 02
0.22273E 06	-0.19120E 00	0.27480E 00	0.48500E 01	-0.25900E 01
0.22279E 06	-0.19920E 00	-0.51500E-01	0.11670E 02	0.12000E 02
0.22549E 06	-0.18230E 00	0.54000E-02	0.10510E 02	0.10250E 02
0.22763E 06	-0.14940E 00	0.57340E 00	0.14300E 01	0.50400E 01
0.22370E 06	-0.26020E 00	0.26130E 00	0.68800E 01	0.84200E 01
0.22370E 06	-0.52100E-01	-0.33920E 00	0.74300E 01	0.12640E 02
0.22362E 06	-0.12440E 00	-0.10430E 00	-0.10300E 01	0.12330E 02
0.22315E 06	-0.17020E 00	-0.31630E 00	0.87500E 01	0.60300E 01
0.23036E 06	-0.23290E 00	0.58400E-01	0.58700E 01	0.13100E 01
0.23370E 06	-0.17690E 00	-0.45700E-01	0.13100E 01	0.13400E 02
0.23149E 06	-0.89500E-01	0.14330E 00	0.14000E 01	0.57100E 01
0.22687E 06	-0.19220E 00	0.18730E 00	-0.42500E 01	0.28300E 01
0.22586E 06	-0.10100E 00	0.26520E 00	0.36200E 01	0.13840E 02
0.23202E 06	-0.27830E 00	0.27070E 00	0.12740E 02	0.15170E 02
0.22927E 06	0.19900E-01	0.25910E 00	0.57600E 01	0.73800E 01
0.22840E 06	0.25700E-01	-0.10370E 00	0.45700E 01	0.12130E 02
0.22923E 06	0.54700E-01	0.87800E-01	0.11230E 02	0.68700E 01





Transformation equations:

$$F_u = |F| \cos \alpha_R \quad (8-15)$$

$$F_v = |F| \sin \alpha_v \quad (8-16)$$

$$F_w = |F| \sin \alpha_w \quad (8-17)$$

$$M_v = w_p \cdot F_u \quad (8-19)$$

$$M_w = -v_p \cdot F_u \quad (8-19)$$

where  $(x_p, z_p)$  = given pierce point coordinates,

$(\alpha_1, \alpha_2)$  = given angularity about #2 and #1 respectively,

$$\alpha_R = \sqrt{\alpha_1^2 + \alpha_2^2},$$

$|F|$  = dynamic thrust magnitude,

$(v_p, w_p)$  = pierce point displacement in uvw axis,

and  $(\alpha_v, \alpha_w)$  = angularity in uvw axis.

Application of equations (8-15) through (8-19) to the data in Table 8-4 results in the force and moment components shown in Table 8-5.

### 8.3.3 Statistical Analysis

A statistical analysis was performed on the test data in Table 8-5 using equations (8-11) through (8-14). The resulting statistical parameters obtained for the J-2 engine are listed in Table 8-6. Histograms, tolerances, and sample means and sigmas are shown for each of the components in Figure 8-6.

Table 8-5a. ENGINE THRUST AND MOMENT COMPONENTS IN METRIC UNITS, J-2 ENGINE.

Fu N	Fv N	Fw N	Mv Nm	Mw Nm
0.10045E 07	0.78310E 03	0.36572E 03	0.14834E 05	-0.92952E 04
0.10052E 07	0.14785E 04	-0.10878E 05	-0.45782E 04	-0.89342E 04
0.99566E 06	-0.21872E 04	-0.45752E 04	0.16944E 03	-0.20737E 03
0.10191E 07	0.31445E 02	-0.54316E 04	-0.73104E 04	-0.43438E 04
0.10228E 07	-0.55332E 03	-0.19545E 04	0.10581E 05	0.94567E 03
0.10016E 07	0.31728E 03	-0.63044E 03	0.90598E 04	-0.93218E 04
0.10079E 07	0.33875E 04	-0.49922E 04	0.10063E 05	-0.16330E 05
0.99581E 06	-0.27303E 04	-0.22142E 04	0.91310E 03	0.26786E 04
0.99069E 06	-0.82733E 03	-0.30566E 04	0.40765E 03	-0.57599E 04
0.10072E 07	0.40917E 04	-0.25171E 04	0.75752E 04	-0.71044E 04
0.99879E 06	-0.10456E 04	-0.14196E 04	-0.10934E 04	0.49165E 04
0.10147E 07	-0.36590E 04	-0.29618E 04	-0.64385E 04	-0.68200E 04
0.10056E 07	-0.34690E 04	-0.60506E 04	-0.11972E 05	0.21073E 04
0.10080E 07	0.19096E 04	0.34398E 04	-0.80908E 03	-0.17308E 04
0.10167E 07	-0.25870E 04	-0.19721E 04	0.13429E 04	-0.53872E 04
0.10075E 07	-0.48309E 04	0.88080E 03	0.74217E 03	-0.32578E 04
0.10097E 07	-0.15286E 04	-0.32318E 04	0.86435E 03	-0.52656E 04
0.10005E 07	-0.16485E 04	-0.22329E 04	-0.70880E 04	-0.17866E 04
0.10096E 07	0.49986E 04	0.72893E 03	0.25182E 04	0.23285E 04
0.10197E 07	0.21416E 04	-0.95439E 03	0.15800E 04	-0.12614E 04
0.10066E 07	0.55283E 04	-0.13996E 04	0.27588E 04	-0.15622E 04
0.10095E 07	0.28781E 04	0.78495E 03	0.25130E 03	-0.45670E 04
0.98446E 06	0.46959E 04	-0.11684E 04	0.10302E 04	0.28256E 03
0.10039E 07	0.10469E 04	-0.27774E 04	-0.84761E 04	-0.89581E 04
0.99554E 06	0.10033E 04	-0.14334E 04	0.23820E 04	-0.58084E 04
0.10068E 07	0.33344E 04	-0.42953E 04	-0.43911E 04	-0.21431E 04
0.10080E 07	0.11674E 04	-0.22829E 04	0.28422E 04	-0.52286E 04
0.10287E 07	0.63903E 03	-0.15108E 04	0.58374E 04	-0.22942E 04
0.10082E 07	0.80884E 03	-0.75782E 04	-0.23433E 04	0.11114E 04
0.99078E 06	0.46057E 03	0.15162E 04	0.48117E 04	-0.69156E 04
0.99101E 06	0.48249E 04	-0.67268E 02	0.50142E 04	0.12963E 04
0.10030E 07	0.42831E 04	0.53643E 02	0.46445E 04	-0.13757E 03
0.10125E 07	0.13475E 04	-0.75187E 03	0.38424E 04	-0.14747E 05
0.99506E 06	0.31315E 04	-0.31520E 03	0.65764E 04	-0.66042E 04
0.99508E 06	0.41079E 04	-0.10663E 04	0.13168E 04	0.85733E 04
0.99471E 06	0.23120E 04	-0.27335E 04	0.31430E 04	0.26352E 04
0.99263E 06	0.30177E 04	0.55535E 03	0.42912E 04	0.79748E 04
0.10247E 07	0.15133E 04	0.96113E 03	0.60618E 04	-0.15200E 04
0.10395E 07	0.31453E 04	-0.25851E 04	0.46709E 04	0.12066E 04
0.10297E 07	0.15059E 04	-0.91287E 03	0.23408E 04	-0.37480E 04
0.10091E 07	-0.29476E 03	-0.14696E 04	0.49266E 04	-0.48010E 04
0.10046E 07	0.36082E 04	-0.21120E 04	0.25774E 04	-0.67677E 04
0.10320E 07	0.59251E 04	-0.51587E 03	0.72957E 04	-0.70964E 04
0.10198E 07	0.27564E 04	-0.33984E 03	-0.51550E 03	-0.67119E 04
0.10159E 07	0.34899E 04	-0.15799E 04	-0.66322E 03	0.26761E 04
0.10196E 07	0.37963E 04	0.91447E 03	-0.14167E 04	-0.22740E 04

Table 8-5b. ENGINE THRUST AND MOMENT COMPONENTS IN ENGLISH UNITS, J-2 ENGINE

Fu lb	Fv lb	Fw lb	Mv lb-in.	Mw lb-in.
0.22583E 06	0.17604E 03	0.82218E 02	0.13129E 06	-0.82270E 05
0.22599E 06	0.33238E 03	-0.24456E 04	-0.40520E 05	-0.79074E 05
0.22383E 06	-0.49171E 03	-0.10285E 04	0.14996E 04	-0.18354E 04
0.22911E 06	0.70691E 01	-0.12210E 04	-0.64702E 05	-0.38445E 05
0.22994E 06	-0.12439E 03	-0.43939E 03	0.93656E 05	0.83699E 04
0.22517E 06	0.71327E 02	-0.14172E 03	0.80185E 05	-0.82505E 05
0.22658E 06	0.76156E 03	-0.11222E 04	0.89070E 05	-0.14453E 06
0.22386E 06	-0.61381E 03	-0.49777E 03	0.80816E 04	0.23707E 05
0.22271E 06	-0.18599E 03	-0.68716E 03	0.36080E 04	-0.50980E 05
0.22643E 06	0.91985E 03	-0.56588E 03	0.67046E 05	-0.62880E 05
0.22453E 06	-0.23508E 03	-0.31913E 03	-0.96775E 04	0.43515E 05
0.22812E 06	-0.82257E 03	-0.66585E 03	-0.56986E 05	-0.60362E 05
0.22608E 06	-0.77987E 03	-0.13602E 04	-0.10596E 06	0.18651E 05
0.22661E 06	0.42930E 03	0.77329E 03	-0.71609E 04	-0.15319E 05
0.22857E 06	-0.58159E 03	-0.44336E 03	0.11886E 05	-0.47681E 05
0.22650E 06	-0.10860E 04	0.19801E 03	0.65687E 04	-0.28834E 05
0.22700E 06	-0.34366E 03	-0.72654E 03	0.76501E 04	-0.46604E 05
0.22493E 06	-0.37059E 03	-0.50199E 03	-0.62734E 05	-0.15812E 05
0.22697E 06	0.11237E 04	0.16387E 03	0.22288E 05	0.20609E 05
0.22925E 06	0.48145E 03	-0.21455E 03	0.13984E 05	-0.11164E 05
0.22629E 06	0.12428E 04	-0.31466E 03	0.24417E 05	-0.13826E 05
0.22696E 06	0.64703E 03	0.17646E 03	0.22242E 04	-0.40421E 05
0.22131E 06	0.10556E 04	-0.26266E 03	0.91182E 04	0.25008E 04
0.22569E 06	0.23536E 03	-0.62438E 03	-0.75020E 05	-0.79285E 05
0.22380E 06	0.22557E 03	-0.32224E 03	0.21082E 05	-0.51408E 05
0.22635E 06	0.74960E 03	-0.96563E 03	-0.38864E 05	-0.18968E 05
0.22662E 06	0.26244E 03	-0.51323E 03	0.25155E 05	-0.46277E 05
0.23126E 06	0.14366E 03	-0.33964E 03	0.51665E 05	-0.20305E 05
0.22666E 06	0.18183E 03	-0.17036E 04	-0.20740E 05	0.98374E 04
0.22273E 06	0.10354E 03	0.34086E 03	0.42587E 05	-0.61208E 05
0.22278E 06	0.10846E 04	-0.15122E 02	0.44379E 05	0.11473E 05
0.22549E 06	0.96289E 03	0.12059E 02	0.41107E 05	-0.12176E 04
0.22763E 06	0.30293E 03	-0.16902E 03	0.34008E 05	-0.13052E 06
0.22369E 06	0.70399E 03	-0.70860E 02	0.58206E 05	-0.58452E 05
0.22370E 06	0.92349E 03	-0.23973E 03	0.11654E 05	0.75880E 05
0.22362E 06	0.51976E 03	-0.61451E 03	0.27818E 05	0.23323E 05
0.22315E 06	0.67840E 03	0.12484E 03	0.37980E 05	0.70583E 05
0.23036E 06	0.34021E 03	0.21607E 03	0.53652E 05	-0.13453E 05
0.23369E 06	0.70710E 03	-0.58116E 03	0.41341E 05	0.10680E 05
0.23149E 06	0.33854E 03	-0.20522E 03	0.20718E 05	-0.33172E 05
0.22687E 06	-0.66264E 02	-0.33039E 03	0.43604E 05	-0.42493E 05
0.22586E 06	0.81116E 03	-0.47480E 03	0.22812E 05	-0.59899E 05
0.23202E 06	0.13320E 04	-0.11597E 03	0.64572E 05	-0.62809E 05
0.22927E 06	0.61968E 03	-0.76399E 02	-0.45626E 04	-0.59405E 05
0.22840E 06	0.78458E 03	-0.35517E 03	-0.58700E 04	0.23685E 05
0.22923E 06	0.85344E 03	0.20558E 03	-0.12539E 05	-0.20126E 05

Table 8-6. STATISTICAL PARAMETERS, J-2 ENGINE.

FORCE COMPONENT	MEAN N (1b)	STD. DEVIATION N (1b)	VARIANCE N <sup>2</sup> (1b <sup>2</sup> )
Fu	1007.9 x10 <sup>3</sup> (226.591x10 <sup>3</sup> )	12144. (2730.2)	147.49x10 <sup>6</sup> (7.4538x10 <sup>6</sup> )
Fv	1393.6 (313.3)	2616.3 (588.16)	6.8448x10 <sup>6</sup> (.34593x10 <sup>6</sup> )
Fw	-1777.6 (-399.62)	2502.5 (562.58)	6.2623x10 <sup>6</sup> (.31649 x10 <sup>6</sup> )
MOMENT COMPONENT	Nm (1b-in.)	Nm (1b-in.)	Nm <sup>2</sup> (1b <sup>2</sup> -in. <sup>2</sup> )
Mv	1742.9 (15425.)	5205.3 (46071.)	2.7095x10 <sup>7</sup> 2.1225x10 <sup>9</sup>
Mw	-3042.6 (-26929.)	5132.0 (45422.)	2.6337x10 <sup>7</sup> (2.0631x10 <sup>9</sup> )

COMPONENT PAIR	COVARIANCE				LINEAR CORRELATION COEFFICIENT (dimensionless)
	METRIC UNIT		ENGLISH UNIT		
Fu,Fv	1.5808	N <sup>2</sup>  x10 <sup>6</sup>	.07989	1b <sup>2</sup>  x10 <sup>6</sup>	.050
Fu,Fw	.34488		.01743		.011
Fv,Fw	1.5576		.07872		.240
Fu,Mv	4.5523	N <sup>2</sup> <sub>m</sub>  x10 <sup>6</sup>	9.0579	1b <sup>2</sup> in.  x10 <sup>6</sup>	.072
Fu,Mw	-9.1148		-18.136		-.146
Fv,Mw	4.6146		9.1817		.339
Fv,Mw	.75764		1.5075		.056
Fw,Mv	5.4591		10.862		.419
Fw,Mw	1.5333		3.0509		.119
Mv,Mw	-5.2305	N <sup>2</sup> M <sup>2</sup> x10 <sup>6</sup>	-409.73	(1b-in.) <sup>2</sup> x10 <sup>6</sup>	-.196

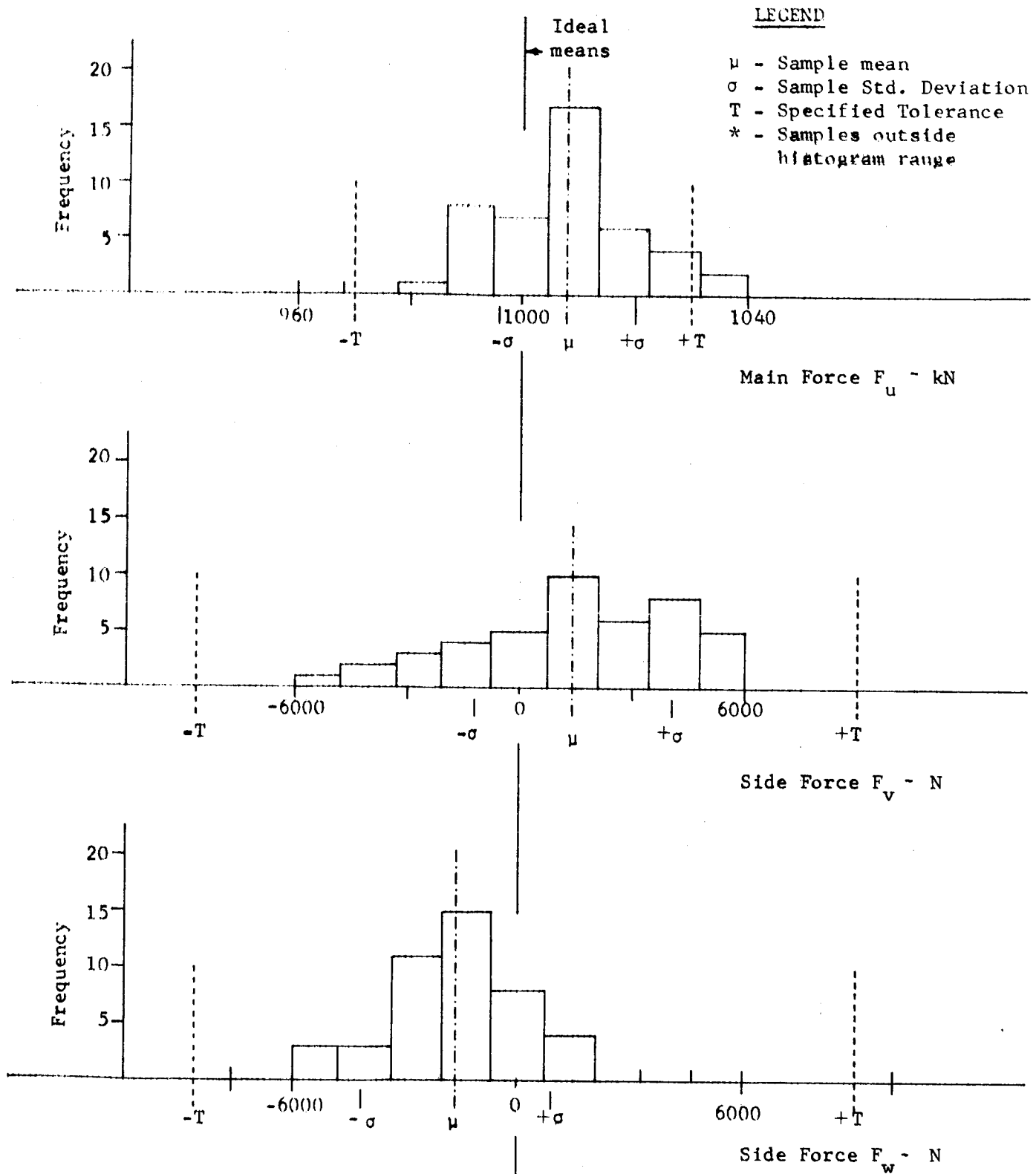


Figure 8-6a. HISTOGRAMS OF DYNAMIC THRUST COMPONENTS, J-2 ENGINE

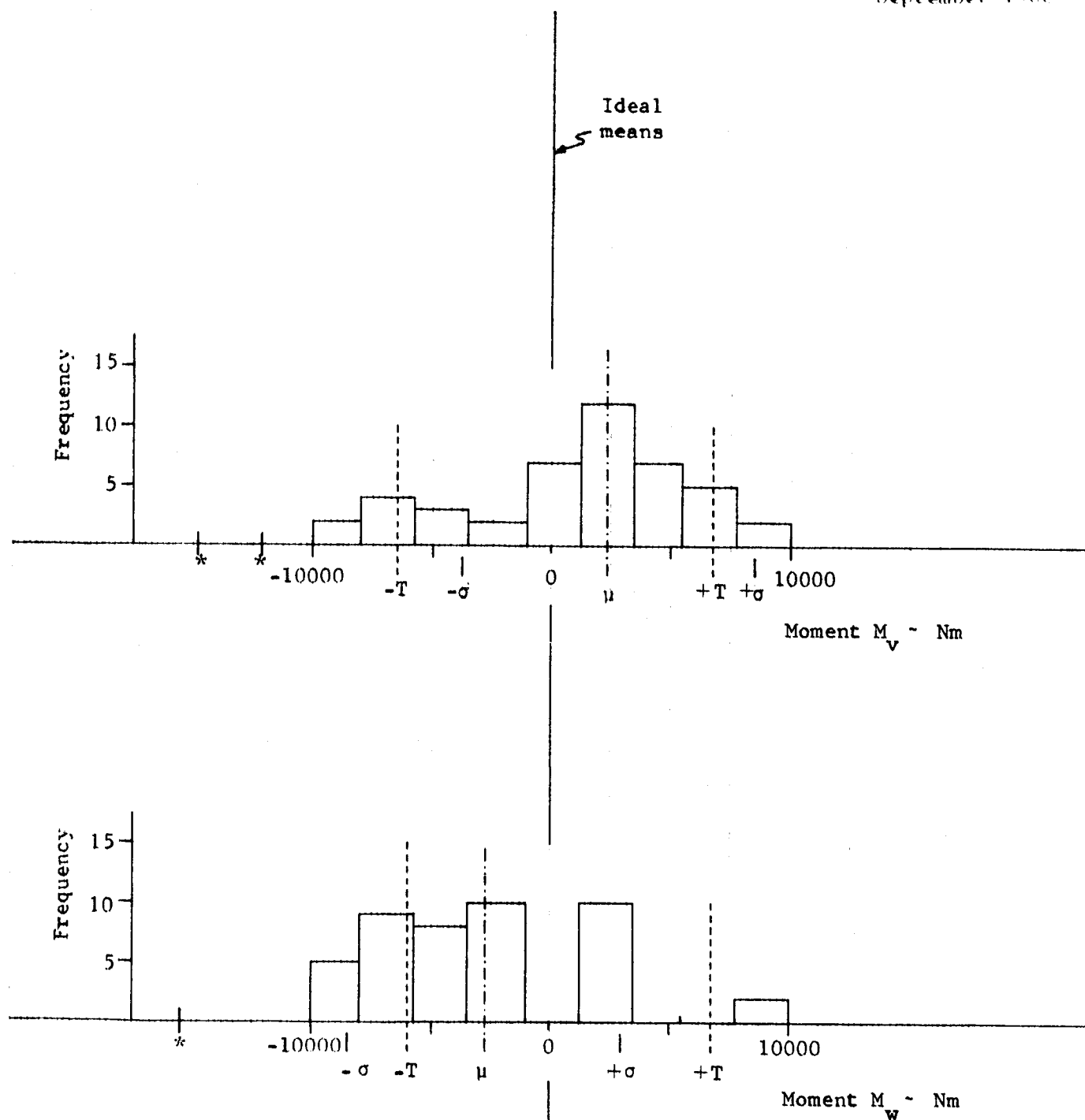


Figure 8-6b. HISTOGRAMS OF DYNAMIC MOMENT COMPONENTS, J-2 ENGINE

## 8.4 F-1 ENGINE MODEL

### 8.4.1 Available Data [47]

Each production F-1 engine is static fired on the dynamic alignment stand from two to four times, and the magnitude and position of the dynamic thrust vector is determined each time. These test results are then averaged together and the F-1 engine is adjusted to null out the average alignment error. In view of this procedure the pierce point and angularity data were altered to the values which would have occurred had the engine received the final alignment prior to dynamic testing. Each test was then treated as a separate sample, which resulted in a total of thirty-nine tests on ten engines. The magnitude, pierce point displacement, and angularity errors after adjustment of the means are tabulated in Table 8-7 and are in terms of the manufacturer's coordinate system (Figure 8-7).

### 8.4.2 Parameter Derivation

The magnitude, pierce point, and angularity data were transformed into force and moment components in the standard uvw axes. The conversion formulae are similar to those for the J-2 and can be written from inspection of Figure 8-7.

Pierce point displacement:

$$v_p = -\frac{\sqrt{2}}{2} (x_p + z_p)$$

$$w_p = \frac{\sqrt{2}}{2} (x_p - z_p)$$

Table 8-7. MANUFACTURER'S DYNAMIC TEST DATA, F-1 ENGINE

(F) lb	X <sub>p</sub> in.	Z <sub>p</sub> in.	α <sub>x</sub> min	α <sub>z</sub> min
0.15168E 07	0.30614E-01	0.31242E-01	0.18314E 01	0.25314E 01
0.15168E 07	0.23914E-01	0.17342E-01	0.10014E 01	0.16014E 01
0.15168E 07	0.22114E-01	-0.23157E-01	0.14914E 01	-0.41857E 00
0.15168E 07	0.14714E-01	0.12642E-01	0.73142E 00	0.51142E 00
0.15168E 07	-0.35685E-01	-0.72571E-02	-0.17785E 01	-0.78571E-01
0.15168E 07	-0.19385E-01	-0.10357E-01	-0.92857E 00	-0.20785E 01
0.15168E 07	-0.36285E-01	-0.20457E-01	-0.23485E 01	-0.20685E 01
0.15321E 07	-0.63666E-02	0.29700E-01	-0.38666E 00	-0.27066E 01
0.15321E 07	0.24333E-02	0.28500E-01	0.53333E 00	-0.38066E 01
0.15321E 07	0.10033E-01	0.34600E-01	0.57333E 00	-0.33266E 01
0.15321E 07	0.48333E-02	-0.22300E-01	0.29333E 00	-0.45766E 01
0.15321E 07	-0.32666E-02	-0.30700E-01	-0.10566E 01	0.68933E 01
0.15321E 07	-0.76666E-02	-0.39800E-01	0.43333E-01	0.75233E 01
0.15278E 07	0.27460E-01	0.13920E-01	0.50800E 00	0.27400E 00
0.15278E 07	0.85600E-02	0.14020E-01	0.14480E 01	0.75400E 00
0.15278E 07	-0.38400E-02	0.16520E-01	-0.21200E 00	-0.56600E 00
0.15278E 07	-0.11340E-01	-0.11080E-01	-0.88200E 00	-0.15600E 00
0.15278E 07	-0.20840E-01	-0.33380E-01	-0.86200E 00	-0.30600E 00
0.15168E 07	-0.65500E-02	-0.95000E-03	-0.54500E 00	0.38000E 00
0.15168E 07	0.65500E-02	0.95000E-03	0.54500E 00	-0.38000E 00
0.15276E 07	-0.18400E-01	-0.15066E-01	-0.28000E 00	-0.70333E 00
0.15276E 07	0.27000E-01	0.10233E-01	0.14000E 00	-0.11033E 01
0.15276E 07	-0.86000E-02	0.48333E-02	0.14000E 00	0.18066E 01
0.15001E 07	-0.13350E-01	-0.68250E-01	0.72000E 00	0.29750E 00
0.15001E 07	0.10250E-01	0.27950E-01	-0.62000E 00	-0.94250E 00
0.15001E 07	0.25150E-01	0.41150E-01	0.24000E 00	0.75750E 00
0.15001E 07	-0.22050E-01	-0.85000E-03	-0.34000E 00	-0.11250E 00
0.15077E 07	-0.11000E-01	0.29033E-01	0.20433E 01	0.25866E 01
0.15077E 07	0.85000E-02	-0.30866E-01	-0.68666E 00	-0.13933E 01
0.15077E 07	0.25000E-02	0.18333E-02	-0.13566E 01	-0.11933E 01
0.15176E 07	-0.26333E-02	-0.11766E-01	0.30000E-01	0.82000E 00
0.15176E 07	0.19666E-02	0.23533E-01	0.20000E-01	0.78000E 00
0.15176E 07	0.66666E-03	-0.11766E-01	-0.50000E-01	-0.16000E 01
0.15425E 07	-0.30000E-02	0.40300E-01	-0.17066E 01	0.10266E 01
0.15425E 07	0.10700E-01	-0.24500E-01	0.13033E 01	-0.67333E 00
0.15425E 07	-0.77000E-02	-0.15800E-01	0.40333E 00	-0.35333E 00
0.15311E 07	-0.47000E-02	0.17166E-01	0.81333E 00	0.63000E 00
0.15311E 07	0.70000E-03	-0.15333E-02	-0.50666E 00	0.21000E 00
0.15311E 07	0.40000E-02	-0.15633E-01	-0.30666E 00	-0.84000E 00



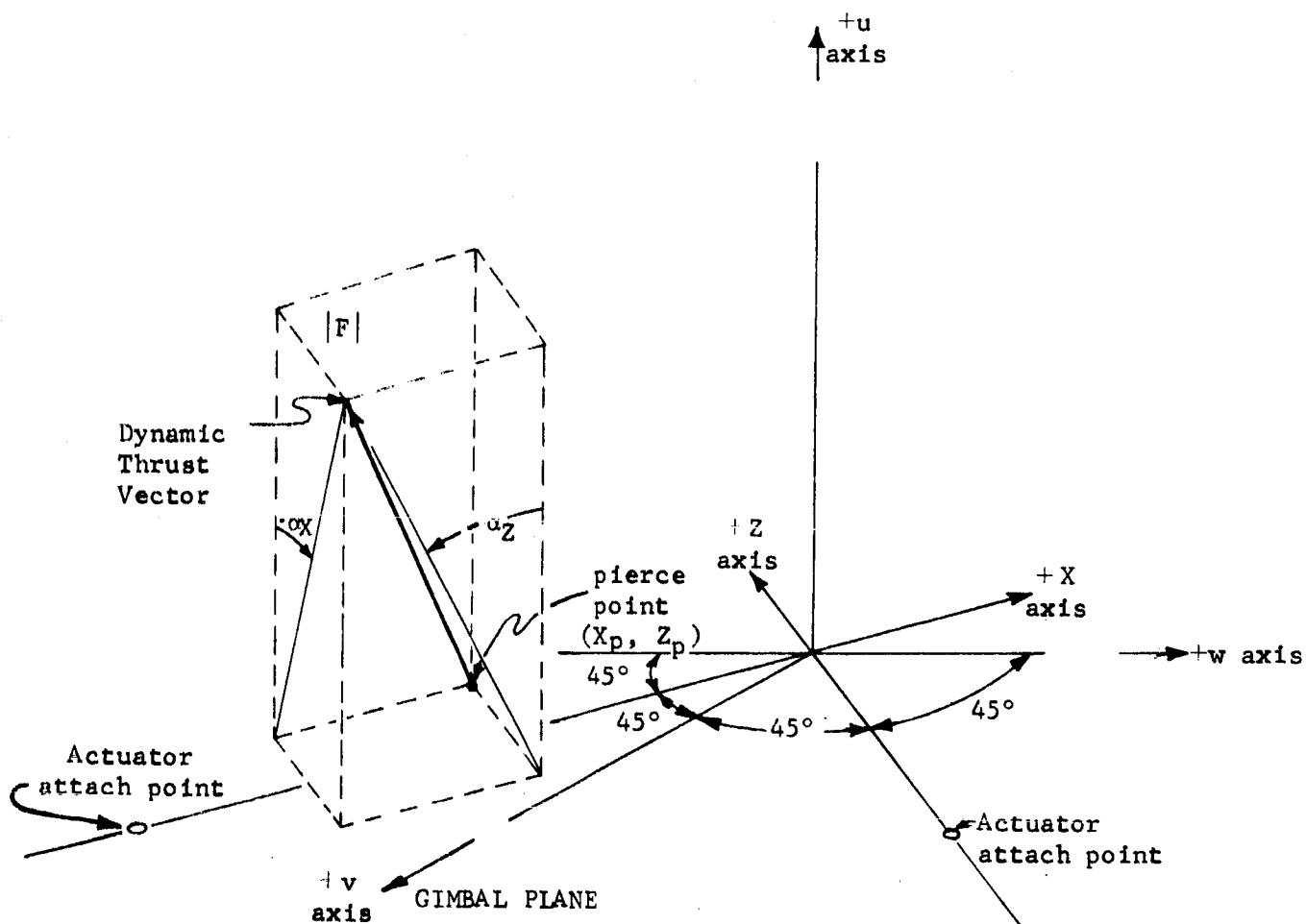


Figure 8-7. COORDINATE SYSTEM, F-1 ENGINE

Angularity:

$$\alpha_v = -\frac{\sqrt{2}}{2} (\alpha_z + \alpha_x)$$

$$\alpha_w = \frac{\sqrt{2}}{2} (\alpha_z - \alpha_x)$$

Transformation equations:

$$F_u = |F| \cos \alpha_R \quad (8-20)$$

$$F_v = |F| \sin \alpha_v \quad (8-21)$$

$$F_w = |F| \sin \alpha_w \quad (8-22)$$

$$M_v = w_p \cdot F_u \quad (8-23)$$

$$M_w = -v_p \cdot F_u \quad (8-24)$$

where  $(x_p, z_p)$  given pierce point coordinates,

$(\alpha_x, \alpha_z)$  given angularity about x and z axes, respectively,

$$\alpha_R = \sqrt{\alpha_x^2 + \alpha_z^2},$$

$|F|$  dynamic thrust magnitude,

$(v_p, w_p)$  = pierce point displacement in terms of uvw frame,

and  $(\alpha_v, \alpha_w)$  angularity in terms of uvw frame.

Application of equations (8-20) through (8-24) to the data in Table 8-7 results in the force and moment components shown in Table 8-8.

#### 8.4.3 Statistical Analysis

A statistical analysis was performed on the test data in Table 8-8 using equations (8-11) through (8-14). The resulting statistical parameters obtained for the F-1 engine are given in Table 8-9. Histograms and equivalent normal distributions are shown in Figure 8-8.

### 8.5 S-I/S-IB STAGE ANALYSIS

#### 8.5.1 Stage Description and Tolerances

The S-I stage is the first stage of the now obsolete Saturn I vehicle, and the S-IB is the first stage of the uprated Saturn I vehicle. The two stages have identical engine cluster geometry and the analytical results obtained for the S-I stage should be indicative of the S-IB.

The S-I stage consists of eight H-1 engines arranged as shown in Figure 8-9. The four inboard engines are equally spaced on a circle of radius 81.28 cm (32 in.) about the stage centerline and each engine is canted 3 deg with respect to the stage centerline. The inboard engines are not used for control and stiff arms replace the actuators. Each inboard engine is oriented such that the actuator attach points are toward the stage center (v-axis inward), except that each is rotated 10 deg 30 min clockwise about its centerline (looking forward) to avoid interference between stiff arms securing adjacent engines.

Table 8-8a. ENGINE THRUST AND MOMENT COMPONENTS  
IN METRIC UNITS, F-1 ENGINE

$F_u$ N	$F_v$ N	$F_w$ N	$M_v$ Nm	$M_w$ Nm
0.67473E 07	-0.60550E 04	-0.97150E 03	-0.76174E 02	0.74962E 04
0.67473E 07	-0.36124E 04	-0.83272E 03	0.79637E 03	0.49998E 04
0.67473E 07	-0.14889E 04	0.26508E 04	0.54863E 04	-0.12638E 03
0.67473E 07	-0.17249E 04	0.30533E 03	0.25102E 03	0.33153E 04
0.67473E 07	0.25774E 04	-0.23593E 04	-0.34451E 04	-0.52041E 04
0.67473E 07	0.41735E 04	0.15960E 04	-0.10941E 04	-0.36044E 04
0.67473E 07	0.61304E 04	-0.38860E 03	-0.19182E 04	-0.68764E 04
0.68154E 07	0.43364E 04	0.32523E 04	-0.44148E 04	0.28562E 04
0.68154E 07	0.45887E 04	0.60840E 04	-0.31907E 04	0.37865E 04
0.68154E 07	0.38598E 04	0.54672E 04	-0.30071E 04	0.54635E 04
0.68154E 07	0.60046E 04	0.68270E 04	0.33213E 04	-0.21380E 04
0.68154E 07	-0.81822E 04	-0.11144E 05	0.33580E 04	-0.41578E 04
0.68154E 07	-0.10607E 05	-0.10485E 05	0.39334E 04	-0.58103E 04
0.67962E 07	-0.10931E 04	0.32711E 03	0.16527E 04	0.50510E 04
0.67962E 07	-0.30782E 04	0.97016E 03	-0.66647E 03	0.27562E 04
0.67962E 07	0.10875E 04	0.49486E 03	-0.24852E 04	0.15477E 04
0.67962E 07	0.14510E 04	-0.10148E 04	-0.31737E 02	-0.27367E 04
0.67962E 07	0.16327E 04	-0.77724E 03	0.15307E 04	-0.66183E 04
0.67473E 07	0.22899E 03	-0.12837E 04	-0.67864E 03	-0.90889E 03
0.67473E 07	-0.22899E 03	0.12837E 04	0.67864E 03	0.90889E 03
0.67951E 07	0.13744E 04	0.59169E 03	-0.40681E 03	-0.40844E 04
0.67951E 07	0.13464E 04	0.17378E 04	0.20462E 04	0.45441E 04
0.67951E 07	-0.27208E 04	-0.23295E 04	-0.16394E 04	-0.45970E 03
0.66731E 07	-0.13966E 04	0.57992E 03	0.65799E 04	-0.97800E 04
0.66731E 07	0.21446E 04	0.44266E 03	-0.21214E 04	0.45784E 04
0.66731E 07	-0.13691E 04	-0.71031E 03	-0.19176E 04	0.79462E 04
0.66731E 07	0.62109E 03	-0.31226E 03	-0.25408E 04	-0.27446E 04
0.67069E 07	-0.63873E 04	-0.74955E 03	-0.48224E 04	0.21723E 04
0.67069E 07	0.28694E 04	0.97488E 03	0.47421E 04	-0.26943E 04
0.67069E 07	0.35178E 04	-0.22532E 03	0.80307E 02	0.52199E 03
0.67509E 07	-0.11803E 04	-0.10969E 04	0.11074E 04	-0.17460E 04
0.67509E 07	-0.11108E 04	-0.10553E 04	-0.26149E 04	0.30918E 04
0.67509E 07	0.22911E 04	0.21523E 04	0.15075E 04	-0.13458E 04
0.68613E 07	0.95969E 03	-0.38576E 04	-0.53360E 04	0.45966E 04
0.68613E 07	-0.88913E 03	0.27897E 04	0.43378E 04	-0.17006E 04
0.68613E 07	-0.70565E 02	0.10678E 04	0.99820E 03	-0.28960E 04
0.68109E 07	-0.20220E 04	0.25684E 03	-0.26749E 04	0.15250E 04
0.68109E 07	0.41561E 03	-0.10040E 04	0.27320E 03	-0.10194E 03
0.68109E 07	0.16064E 04	0.74717E 03	0.24017E 04	-0.14230E 04

Table 8-8b. ENGINE THRUST AND MOMENT COMPONENTS IN ENGLISH UNITS, F-1 ENGINE

F <sub>u</sub> lb	F <sub>v</sub> lb	F <sub>w</sub> lb	M <sub>v</sub> in.-lb	M <sub>w</sub> in.-lb
0.15168E 07	-0.13612E 04	-0.21840E 03	-0.67420E 03	0.66347E 05
0.15168E 07	-0.81210E 03	-0.18720E 03	0.70484E 04	0.44252E 05
0.15168E 07	-0.33473E 03	0.59592E 03	0.48557E 05	-0.11185E 04
0.15168E 07	-0.38777E 03	0.68641E 02	0.22217E 04	0.29343E 05
0.15168E 07	0.57943E 03	-0.53040E 03	-0.30492E 05	-0.46060E 05
0.15168E 07	0.93824E 03	0.35880E 03	-0.96839E 04	-0.31901E 05
0.15168E 07	0.13781E 04	-0.87361E 02	-0.16977E 05	-0.60861E 05
0.15321E 07	0.97487E 03	0.73115E 03	-0.39074E 05	0.25279E 05
0.15321E 07	0.10315E 04	0.13677E 04	-0.28240E 05	0.33513E 05
0.15321E 07	0.86771E 03	0.12290E 04	-0.26615E 05	0.48356E 05
0.15321E 07	0.13499E 04	0.15347E 04	0.29396E 05	-0.18923E 05
0.15321E 07	-0.18394E 04	-0.25054E 04	0.29721E 05	-0.36799E 05
0.15321E 07	-0.23846E 04	-0.23573E 04	0.34813E 05	-0.51425E 05
0.15278E 07	-0.24575E 03	0.73538E 02	0.14628E 05	0.44705E 05
0.15278E 07	-0.69201E 03	0.21810E 03	-0.58988E 04	0.24394E 05
0.15278E 07	0.24450E 03	0.11125E 03	-0.21996E 05	0.13699E 05
0.15278E 07	0.32620E 03	-0.22815E 03	-0.28089E 03	-0.24221E 05
0.15278E 07	0.36706E 03	-0.17473E 03	0.13547E 05	-0.58577E 05
0.15168E 07	0.51480E 02	-0.28860E 03	-0.60064E 04	-0.80443E 04
0.15168E 07	-0.51480E 02	0.28860E 03	0.60064E 04	0.80443E 04
0.15276E 07	0.30897E 03	0.13301E 03	-0.36006E 04	-0.36150E 05
0.15276E 07	0.30269E 03	0.39067E 03	0.18111E 05	0.40219E 05
0.15276E 07	-0.61167E 03	-0.52369E 03	-0.14510E 05	-0.40687E 04
0.15001E 07	-0.31397E 03	0.13037E 03	0.58237E 05	-0.86560E 05
0.15001E 07	0.48214E 03	0.99514E 02	-0.18776E 05	0.40522E 05
0.15001E 07	-0.30780E 03	-0.15968E 03	-0.16972E 05	0.70330E 05
0.15001E 07	0.13962E 03	-0.70200E 02	-0.22488E 05	-0.24292E 05
0.15077E 07	-0.14359E 04	-0.16850E 03	-0.42682E 05	0.19226E 05
0.15077E 07	0.64508E 03	0.21916E 03	0.41971E 05	-0.23846E 05
0.15077E 07	0.79084E 03	-0.50655E 02	0.71077E 03	0.46200E 04
0.15176E 07	-0.26534E 03	-0.24661E 03	0.98015E 04	-0.15453E 05
0.15176E 07	-0.24973E 03	-0.23724E 03	-0.23144E 05	0.27365E 05
0.15176E 07	0.51507E 03	0.48386E 03	0.13342E 05	-0.11912E 05
0.15424E 07	0.21574E 03	-0.86722E 03	-0.47228E 05	0.40683E 05
0.15425E 07	-0.19988E 03	0.62715E 03	0.38393E 05	-0.15051E 05
0.15424E 07	-0.15863E 02	0.24007E 03	0.88348E 04	-0.25631E 05
0.15311E 07	-0.45457E 03	0.57740E 02	-0.23675E 05	0.13497E 05
0.15311E 07	0.93434E 02	-0.22571E 03	0.24180E 04	-0.90225E 03
0.15311E 07	0.36113E 03	0.16797E 03	0.21257E 05	-0.12595E 05

Table 8-9. STATISTICAL PARAMETERS, F-1 ENGINE

FORCE COMPONENT	MEAN N (lb)	STD. DEVIATION N (lb)	VARIANCE N <sup>2</sup> (lb <sup>2</sup> )
Fu	6.7711x10 <sup>6</sup> (1.5222x10 <sup>6</sup> )	52,053. (11,702.)	2709.4x10 <sup>6</sup> (136.93x10 <sup>6</sup> )
Fv	$\approx 0$	3632.2 (816.54)	13.193x10 <sup>6</sup> (.66674x10 <sup>6</sup> )
Fw	$\approx 0$	3345.8 (752.16)	11.194x10 <sup>6</sup> (.56575x10 <sup>6</sup> )
MOMENT COMPONENT	Nm (lb-in.)	Nn (lb-in.)	Nm <sup>2</sup> (lb <sup>2</sup> -in. <sup>2</sup> )
Mv	$\approx 0$	2897.4 (25644.)	.839x10 <sup>7</sup> (.64761x10 <sup>9</sup> )
Mw	$\approx 0$	4180.9 (37004.)	.1748x10 <sup>8</sup> (1.3693x10 <sup>9</sup> )

COMPONENT PAIR	COVARIANCE				LINEAR CORRELATION COEFFICIENT (DIMENSIONLESS)
	METRIC UNIT		ENGLISH UNIT		
Fu, Fv Fu, Fw Fv, Fw	- 16.24723 - 12.781 8463.8	N <sup>2</sup> x10 <sup>3</sup>	- .82112 - .64592 427.75	lb <sup>2</sup> x10 <sup>3</sup>	-.00009 -.00007 .696
Fu, Mv Fu, Mw Fv, Mv Fv, Mw Fw, Mv Fw, Mw	.00394 .00128 -2.2934 -1.166 -.68527 3.4739	N <sup>2</sup> <sub>m</sub> x10 <sup>6</sup>	.00784 .00255 -4.5632 -2.3201 -1.3635 6.912	lb <sup>2</sup> -in. x10 <sup>6</sup>	.00003 .000006 -.218 -.077 -.071 .248
Mv, Mw	-.00528	N <sup>2</sup> <sub>m</sub> <sup>2</sup> x10 <sup>9</sup>	-.41387	(lb - in.) <sup>2</sup> x10 <sup>9</sup>	-.436

September 1966

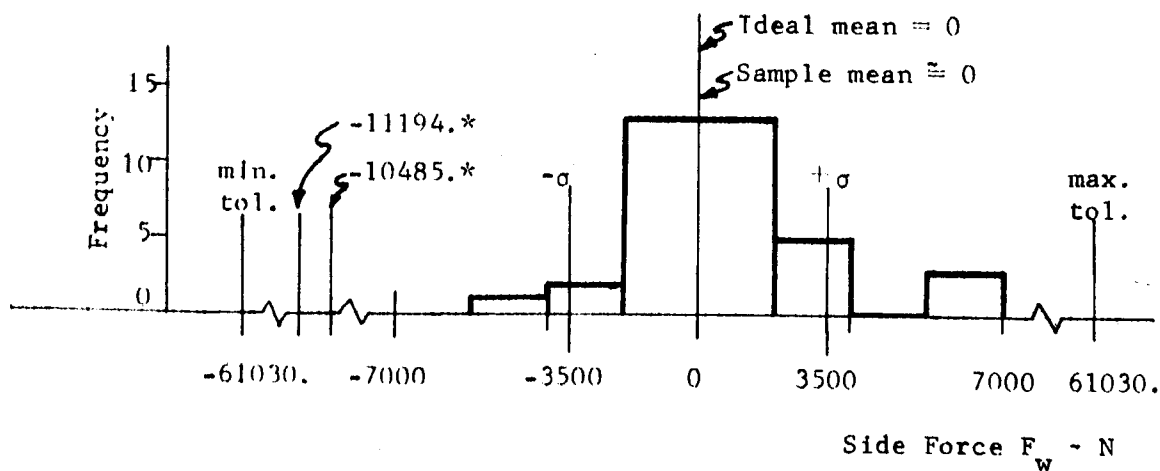
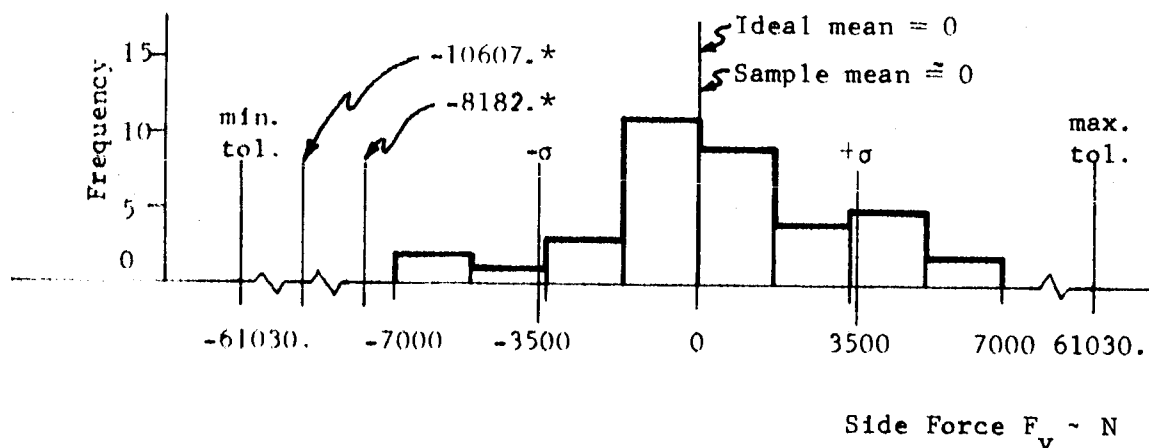
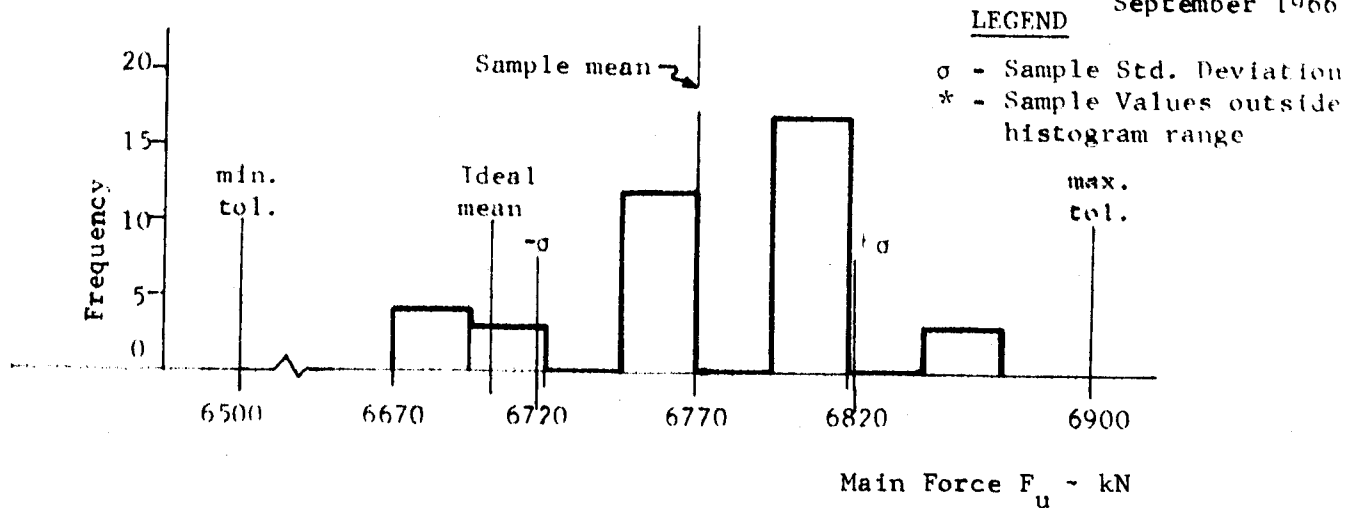


Figure 8-8a. HISTOGRAMS OF DYNAMIC THRUST COMPONENTS, F-1 ENGINE

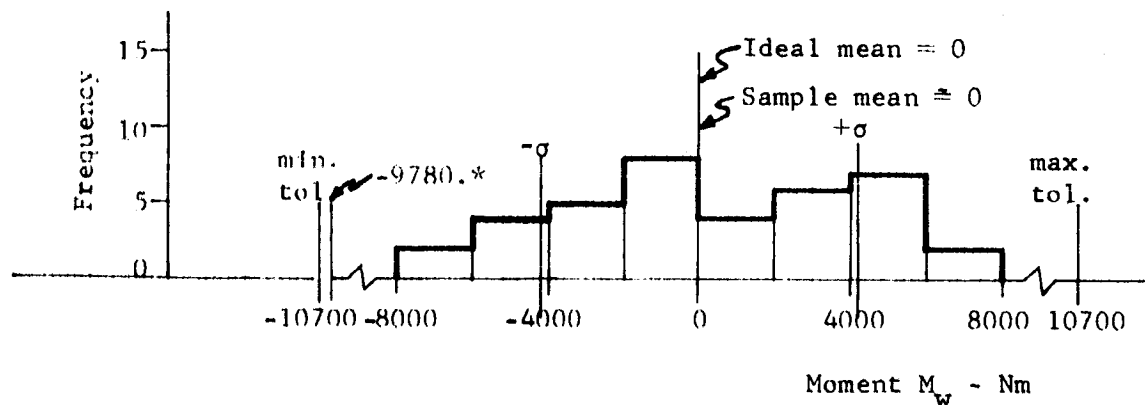
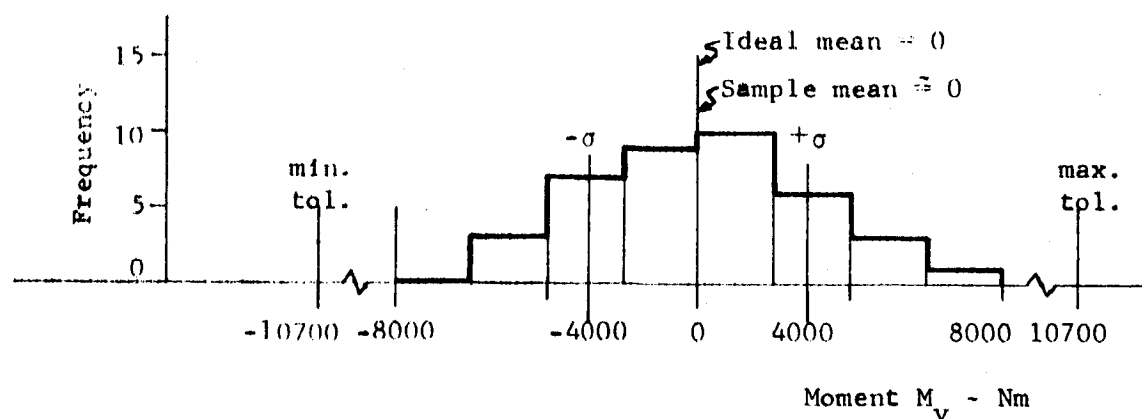
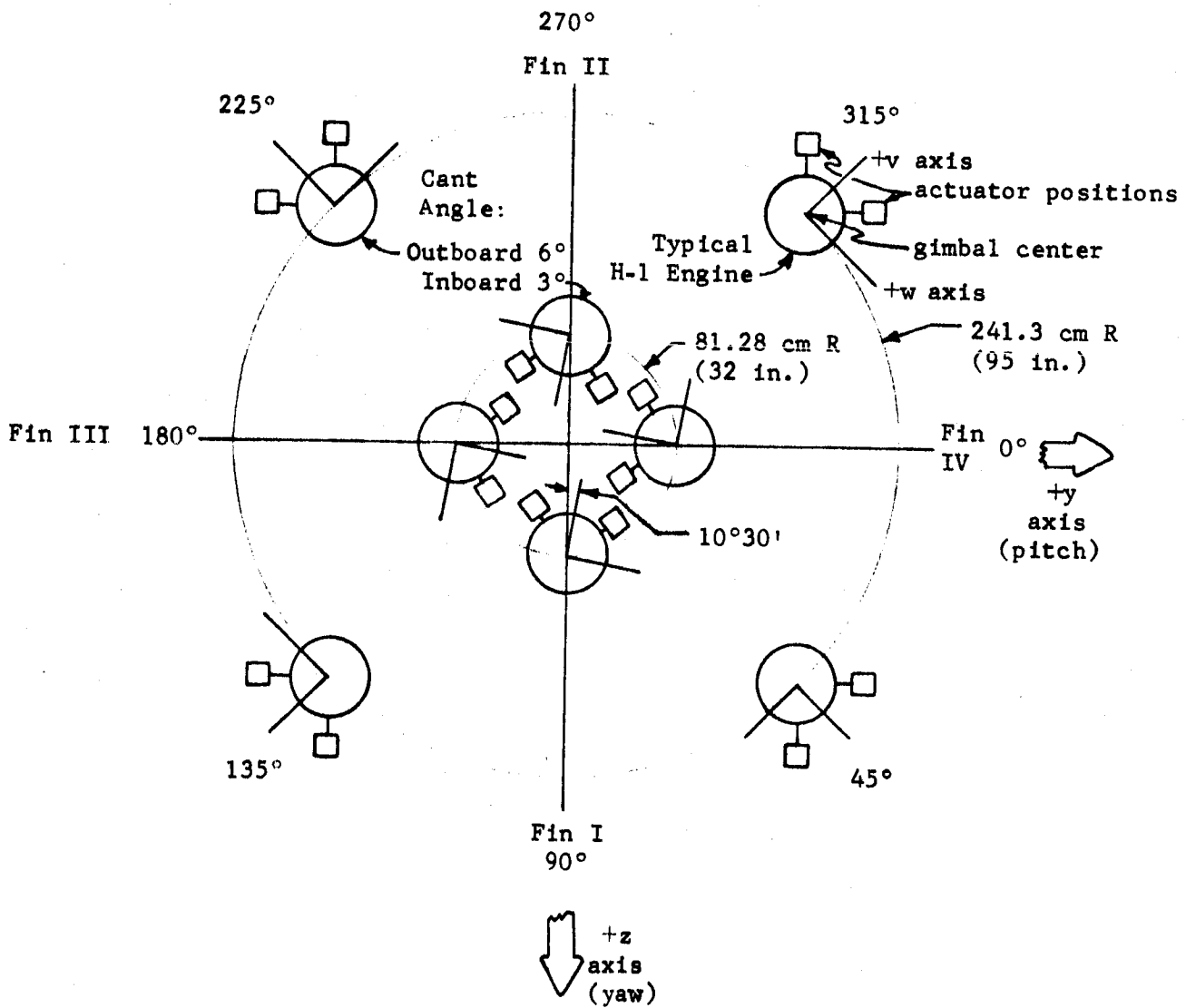


Figure 8-8b. HISTOGRAMS OF DYNAMIC MOMENT COMPONENTS, F-1 ENGINE





VIEW LOOKING FORWARD

Figure 8-9. THRUST FRAME GEOMETRY, S-I STAGE

The four outboard engines are equally spaced on a circle of radius 241.3 cm (95 in.) from the cluster, and each is canted 6 deg with respect to the stage centerline. The outboard engines are gimballed and are oriented such that the actuator attach points are away from the stage center (v-axis outward). Ideally, the gimbal points of all eight engines lie in the same plane. The nominal values and stated tolerances for the pertinent stage parameters are summarized in Table 8-10.

#### 8.5.2 Available Measurement Data [48 through 64]

The measurement data sought for use in the analysis consisted of post-static firing gimbal point locations ( $R$ ,  $\theta$ ,  $x$ ) and thrust chamber angularity ( $\phi$ ,  $\gamma$ ) for each stage manufactured. Field investigations revealed that, out of two test models and ten flight models of the S-I stage which were manufactured, complete data were available on four and partial data were available on the remaining eight. Although modifications were made to the structural design and alignment procedure of each succeeding stage, the measured alignment data were deemed sufficiently similar to justify lumping into one population for statistical purposes.

No data could be found on the seven S-IB stages which had been manufactured prior to completion of this contract, and no attempt was made to analyze this stage.

#### 8.5.3 Parameter Derivation

The available measurement data were processed to obtain the best estimates of the statistical properties of engine-to-stage mounting errors. The radius of each ring of engines and the displacement of the actual gimbal from the gimbal plane were treated as separate random variables, with the result that each

Table 8-10. NOMINAL VALUES AND TOLERANCES,  
ENGINE-TO-STAGE MOUNTING PARAMETERS, S-I STAGE

STAGE PARAMETER		NOMINAL	TOLERANCE
GIMBAL CENTER DISPLACEMENT	R (inboard)	81.28 cm (32 in.)	$\pm .0762$ cm ( $\pm .030$ in.)
	R (outboard)	241.3 cm (95 in.)	$\pm .0762$ cm ( $\pm .030$ in.)
	$\theta_1$	0°	$\pm 3'$ FOR each engine
	$\theta_2$	45°	
	$\theta_3$	90°	
	$\theta_4$	135°	
	$\theta_5$	180°	
	$\theta_6$	225°	
	$\theta_7$	270°	
	$\theta_8$	315°	
	x (inboard)	0	$\pm .0762$ cm ( $\pm .030$ in.)
	x (outboard)	0	$\pm .0381$ cm ( $\pm .015$ in.)
ENGINE ANGULARITY	$\Gamma$ (inboard)	3°	—
	$\Gamma$ (outboard)	6°	—
	$\psi$	10°30'	$\pm 10'$
	$\delta$	0	$\pm 30'$
	$\gamma$	0	$\pm 30'$

stage for which data was obtained yielded four samples of inboard R and x and four samples of outboard R and x. The angular position ( $\theta$ ) of each engine and the thrust chamber angularity ( $\delta$ ,  $\gamma$ ) were lumped together for both inboard and outboard engines, such that each documented stage yielded eight samples of each of these random variables. The resulting sample populations for all stages analyzed are listed in Table 8-11. These data were processed using equations (8-11) and (8-12) to determine the sample means and variances listed in Table 8-12. No attempt was made to calculate covariances since the sample sizes were different.

#### 8.5.4 Statistical Analysis

Both the classical solution described in Section IV and the Monte Carlo simulation program outlined in Section VI were employed to obtain the statistical characteristics of the resultant thrust and moment vectors of the S-I stage. The results of both solutions are presented in this subsection for comparison, and are in terms of the stage coordinate system shown in Figure 8-9.

The statistical models of engine performance and mounting errors used in the analysis are summarized in Table 8-13. As indicated in the table, the analysis was performed on a cluster of eight 900 kN (200 kip) H-1 engines, each with nominal thrust ( $F_u$ ) equal to the sample mean and nominal values of all other components ( $F_v$ ,  $F_w$ ,  $M_u$ ,  $M_v$ ,  $M_w$ ) equal to zero. Engine roll moment ( $M_u$ ) and rotational mounting error ( $\psi$ ) were assumed zero and deterministic for lack of data. All input random variables were assumed univariate normal with the exception of  $M_v$  and  $M_w$  which were assumed bivariate normal. (Input distribution shapes are necessary for the Monte Carlo simulation but are immaterial in the classical solution.) The 10 deg 30 min rotation of each of the inboard engines about its centerline violated the study groundrule stating that each peripheral engine

Table 8-11. ENGINE-TO-STAGE ALIGNMENT DATA, S-I STAGE

R(inboard) in.	R(outboard) in.	$\Delta\theta$ deg	$\delta$ min	$\gamma$ min
32.009	94.987	.003125	5.6	1.4
32.006	95.010	-.009375	5.4	-0.7
32.016	95.020	.019795	1.5	2.9
32.013	94.969	-.009375	-4.9	2.5
31.964	94.951	.003125	1.7	-1.5
32.009	94.983	-.001045	-1.0	5.3
31.993	94.979	-.009375	-1.7	4.5
31.989	94.953	.003125	4.4	0.9
x(inboard)	x(outboard)	-.005731	0.0	1.4
		.052599	4.8	-0.8
.004	-.013	.006769	0.3	2.6
.006	-.016	-.014061	-5.5	0.8
.006	-.003	-.009891	1.4	-0.3
-.005	-.012	-.014061	3.5	-7.0
-.004	.003	-.005731	1.8	-4.0
-.004	.009	-.009891	3.5	-4.6
-.004	-.002	-.002400	-3.8	1.4
-.015	-.001	.002330	-0.7	-4.2
0	.006	-.008790	4.3	2.2
.013	.001	-.000660	3.6	-0.9
.012	.012	-.010170	1.0	-0.5
.017	.001	.001770	0.8	-1.1
-.003	-.043	.007050	1.2	-2.9
.002	-.016	.007292	7.4	8.9
-.005	.009	-.006598	-4.9	-6.2
.002	-.001	-.004928	4.6	-1.1
-.030	-.050	-.004098	-4.5	-0.8
-.008	-.027	.014792	1.3	1.0
-.019	-.021	-.005208	-6.4	0.3
-.022	-.064	-.002988	6.1	5.3
.021		.001732	-2.2	-3.1
.017		.002189	4.2	-4.8
.014		.000239	10.1	-9.5
.020		-.001981	13.3	0.9
		-.000311	5.9	-3.3
		-.001701	-1.9	-0.2
		.000799	-3.5	-11.0
		.000799	2.0	-5.5
		-.000031	-5.8	-15.3
		.035592	1.4	-2.9
		.018922	-7.6	-4.9
		.016142	-8.1	-7.0
		-.008858	-5.6	-9.5
		.000872	5.5	-1.5
		-.044958	1.1	-6.5
		-.008858	-6.1	-5.3
		-.008858	-5.1	-2.9

Table 8-12. STATISTICAL PROPERTIES, ENGINE-TO-STAGE MOUNTING PARAMETERS, S-I STAGE

STAGE PARAMETER		MEAN	VARIANCE
Gimbal Center Displace- ment	R(inboard)	78.994 cm (31.999 in.)	$.19250 \times 10^{-2} \text{ cm}^2$ ( $.29841 \times 10^{-3} \text{ in.}^2$ )
	R(outboard)	241.25 cm (94.992 in.)	$.39004 \times 10^{-2} \text{ cm}^2$ ( $.60457 \times 10^{-3} \text{ in.}^2$ )
	$\theta$	*	$.19240 \times 10^{-3} \text{ deg}^2$
	x(inboard)	.03505 mm (.00138 in.)	$.42999 \times 10^{-2} \text{ mm}^2$ ( $.66650 \times 10^{-4} \text{ in.}^2$ )
	x(outboard)	.03175 cm (-.00125 in.)	$.49047 \times 10^{-2} \text{ mm}^2$ ( $.76023 \times 10^{-4} \text{ in.}^2$ )
Engine Angularity	$\delta$	0	$.00626 \text{ deg}^2$
	$\gamma$	0	$.00567 \text{ deg}^2$

Table 8-13. STATISTICAL INPUT MODEL, S-I STAGE

PARAMETER		MEAN	VARIANCE
Gimbal Center Displace- ment	R(inboard)	78.994 cm (31.999 in.)	$.19250 \times 10^{-2} \text{ cm}^2$ ( $.29841 \times 10^{-3} \text{ in.}^2$ )
	R(outboard)	241.25 cm (94.982 in.)	$.39004 \times 10^{-2} \text{ cm}^2$ ( $.60457 \times 10^{-3} \text{ in.}^2$ )
	$\theta$	*	$.19240 \times 10^{-3} \text{ deg}^2$
	x(inboard)	.03505 mm (.00138 in.)	$.42999 \times 10^{-2} \text{ mm}^2$ ( $.66650 \times 10^{-4} \text{ in.}^2$ )
	x(outboard)	.03175 mm (-.00125 in.)	$.49047 \times 10^{-2} \text{ mm}^2$ ( $.76023 \times 10^{-4} \text{ in.}^3$ )
Engine Angularity	$\delta$	0	$.00626 \text{ deg}^2$
	$\gamma$	0	$.00567 \text{ deg}^2$
900 kN (200 kip) H-1 Engine Forces and Moments	$F_u$	$188.46 \times 10^3 \text{ N}$ ( $198.16 \times 10^3 \text{ lb}$ )	$108.57 \times 10^6 \text{ N}^2$ ( $5.4869 \times 10^6 \text{ lb}^2$ )
	$F_v$	0	$1.3623 \times 10^6 \text{ N}^2$ ( $.06885 \times 10^6 \text{ lb}^2$ )
	$F_w$	0	$17.329 \times 10^6 \text{ N}^2$ ( $.87581 \times 10^6 \text{ lb}^2$ )
	$M_u$	0	0
	$M_v$	0	$.04602 \times 10^8 \text{ N}^2 \text{m}^2$ ( $3.6049 \times 10^8 \text{ lb}^2 \text{in.}^2$ )
	$M_w$	0	$.00972 \times 10^8 \text{ N}^2 \text{m}^2$ ( $.76110 \times 10^8 \text{ lb}^2 \text{in.}^2$ )

\*NOTE: The mean of angle  $\theta$  was taken to be the nominal (or ideal) value for each engine and  $\theta$  was distributed identically for all engines.

is mounted symmetrically about a radial plane from the cluster center. Consequently it was necessary to set this angle equal to zero in the analysis.

The variances of the resultant vector components as obtained from the classical solution are shown in Table 8-14. (Covariances were not calculated.) The results obtained from 500 Monte Carlo trials are summarized in Table 8-15 and the histograms shown in Figure 8-10. Comparison of the tables shows that the standard deviations calculated by the classical and Monte Carlo methods check within seven percent.

## 8.6 S-IC STAGE ANALYSIS

### 8.6.1 Stage Description and Tolerances [65,66]

The S-IC stage is the first stage of the Saturn V vehicle, consisting of five F-1 engines arranged as shown in Figure 8-11. The center engine is fixed (not gimballed) and the outer four engines are equally spaced on a circle of radius 462.3 cm (182 in.) from the stage center. Each outboard engine is canted at an angle of 29 min and is oriented such that the actuator attach points are away from the stage center (v-axis outward). The nominal values and stated tolerances for the pertinent stage parameters are summarized in Table 8-16.

### 8.6.2 Available Measurement Data [67]

At the time of this study only two flight models of the S-IC stage had been assembled. This was deemed too small a sample size to be of any significant value in a statistical analysis, and no attempt was made to utilize the alignment data. It was decided to analyze the stage using hypothetical probability distributions for the engine mounting errors, based upon the tolerance schedule, in lieu of actual alignment data.

Table 8-14. CLASSICAL SOLUTION FOR STATISTICAL PROPERTIES OF  
RESULTANT THRUST AND MOMENT VECTORS, S-I STAGE

FORCE COMPONENT	MEAN N (1b)	STD. DEVIATION N (1b)	VARIANCE N <sup>2</sup> (1b <sup>2</sup> )
F <sub>x</sub>	7051677. (1585280.)	29372.6 (6603.2)	86.2752 x 10 <sup>7</sup> (4.36027 x 10 <sup>7</sup> )
F <sub>y</sub>	0	9427.6 (2119.4)	8.88786 x 10 <sup>7</sup> (.449184 x 10 <sup>7</sup> )
F <sub>z</sub>	0	9427.6 (2119.4)	8.88786 x 10 <sup>7</sup> (.449184 x 10 <sup>7</sup> )
MOMENT COMPONENT	Nm (1b-in.)	Nm (1b-in.)	N <sup>2</sup> m <sup>2</sup> (1b <sup>2</sup> -in. <sup>2</sup> )
M <sub>x</sub>	0	22079.98 (195424.)	.487525 x 10 <sup>9</sup> (.381905 x 10 <sup>11</sup> )
M <sub>y</sub>	0	37635.72 (333103.6)	1.41645 x 10 <sup>9</sup> (1.10958 x 10 <sup>11</sup> )
M <sub>z</sub>	0	37635.72 (333103.6)	1.41645 x 10 <sup>9</sup> (1.10958 x 10 <sup>11</sup> )

Table 8-15. MONTE CARLO SOLUTION FOR STATISTICAL PROPERTIES OF  
RESULTANT THRUST AND MOMENT VECTORS, S-I STAGE

FORCE COMPONENT	MEAN N (1b)	STD. DEVIATION N (1b)	VARIANCE N <sup>2</sup> (1b <sup>2</sup> )
F <sub>x</sub>	7029213. (1580230.)	31247.4 (7024.7)	97.63986 x 10 <sup>7</sup> (4.934626 x 10 <sup>7</sup> )
F <sub>y</sub>	-633.4388 (-142.4027)	9520.5 (2140.3)	9.064282 x 10 <sup>7</sup> (.4581003 x 10 <sup>7</sup> )
F <sub>z</sub>	15.06592 (3.386953)	9224.7 (2073.8)	8.509386 x 10 <sup>7</sup> (.4300564 x 10 <sup>7</sup> )
MOMENT COMPONENT	Nm (1b-in.)	Nm (1b-in.)	N <sup>2</sup> m <sup>2</sup> (1b <sup>2</sup> -in. <sup>2</sup> )
M <sub>x</sub>	-711.0329 (-6293.162)	21453.90 (189882.7)	.4602701 x 10 <sup>9</sup> (.3605547 x 10 <sup>11</sup> )
M <sub>y</sub>	-2310.882 (-20452.47)	37499.11 (331894.6)	1.406183 x 10 <sup>9</sup> (1.101540 x 10 <sup>11</sup> )
M <sub>z</sub>	608.7936 (5388.269)	36669.87 (324555.2)	1.344679 x 10 <sup>9</sup> (1.053361 x 10 <sup>11</sup> )



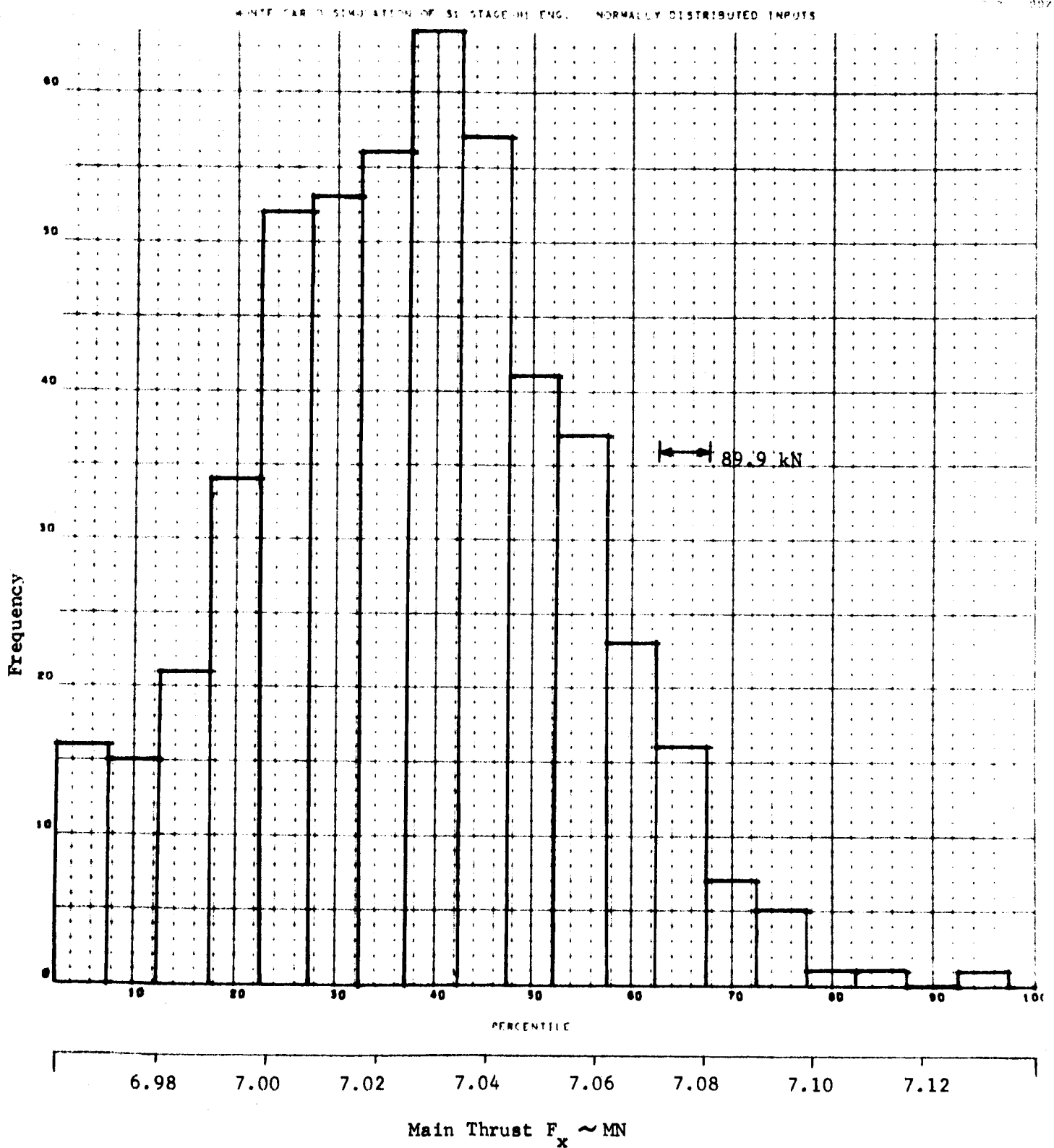


Figure 8-10. HISTOGRAMS FOR RESULTANT THRUST AND MOMENT VECTOR COMPONENTS, 500 MONTE CARLO TRIALS, NORMALLY DISTRIBUTED INPUTS, S-I STAGE. (a) MAIN THRUST COMPONENT

MONTE CARLO SIMULATION OF 31 STAGE-HI ENG. NORMALLY DISTRIBUTED INPUTS

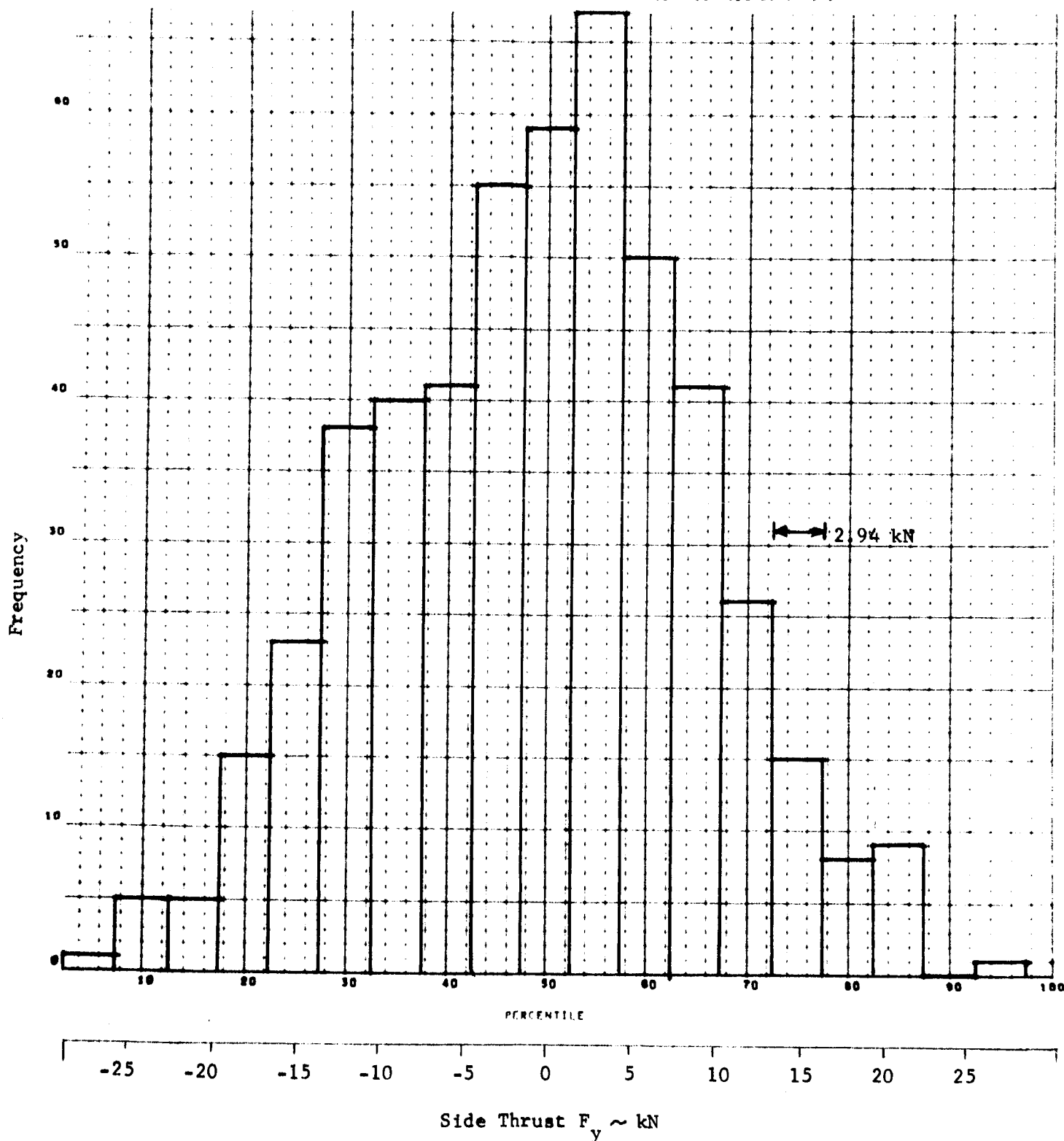


Figure 8-10(b). SIDE THRUST COMPONENT ALONG PITCH AXIS

442240  
006 006

MONTÉ CARLÉ SIMULATION OF S1 STAGE-HI ENG. NORMALLY DISTRIBUTED INPUTS

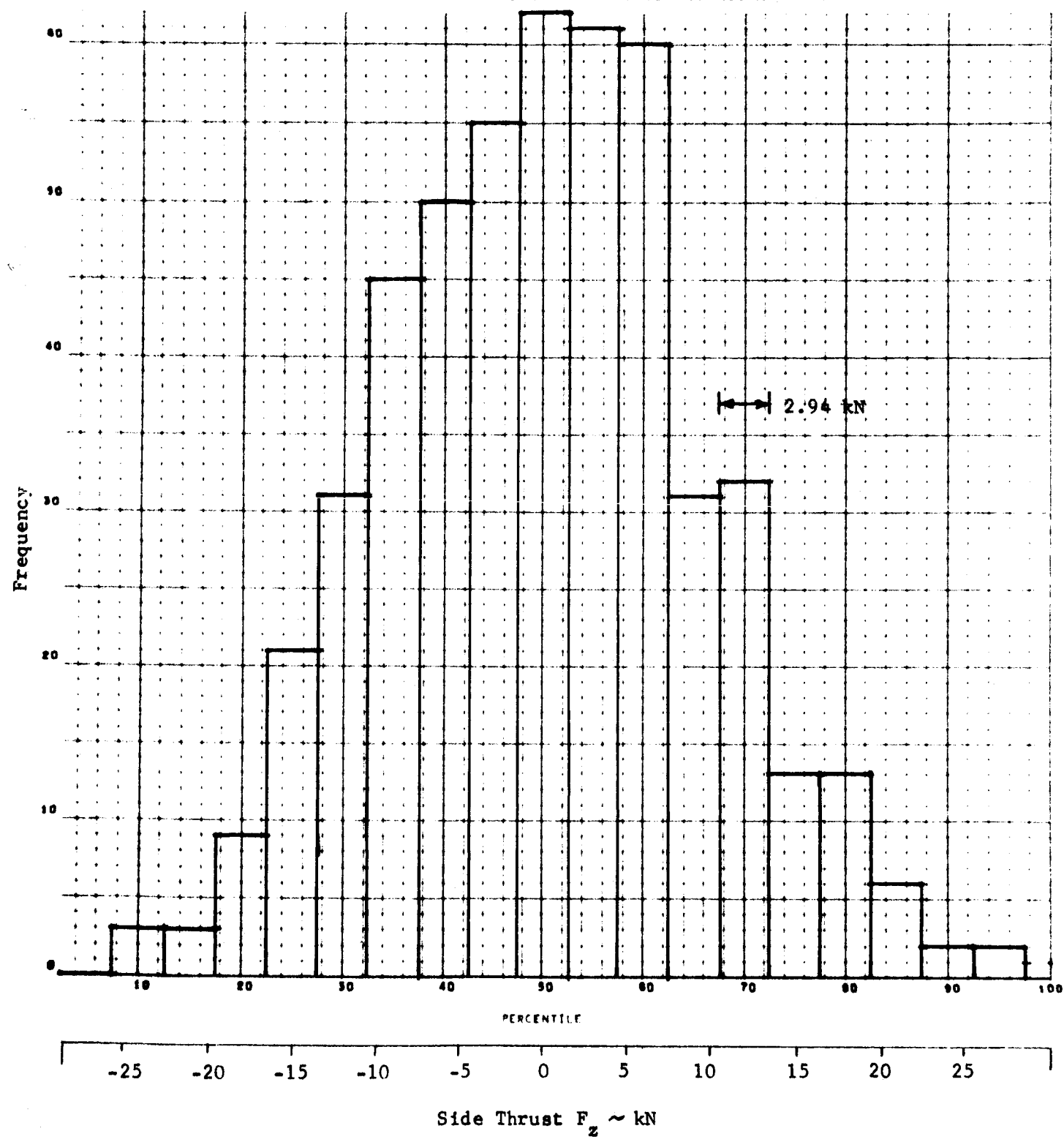


Figure 8-10(c). SIDE THRUST COMPONENT ALONG YAW AXIS

463260  
DDA

WHITE CARBO SIMULATION OF 51 STAGE HI ENG. NORMALLY DISTRIBUTED INPUTS

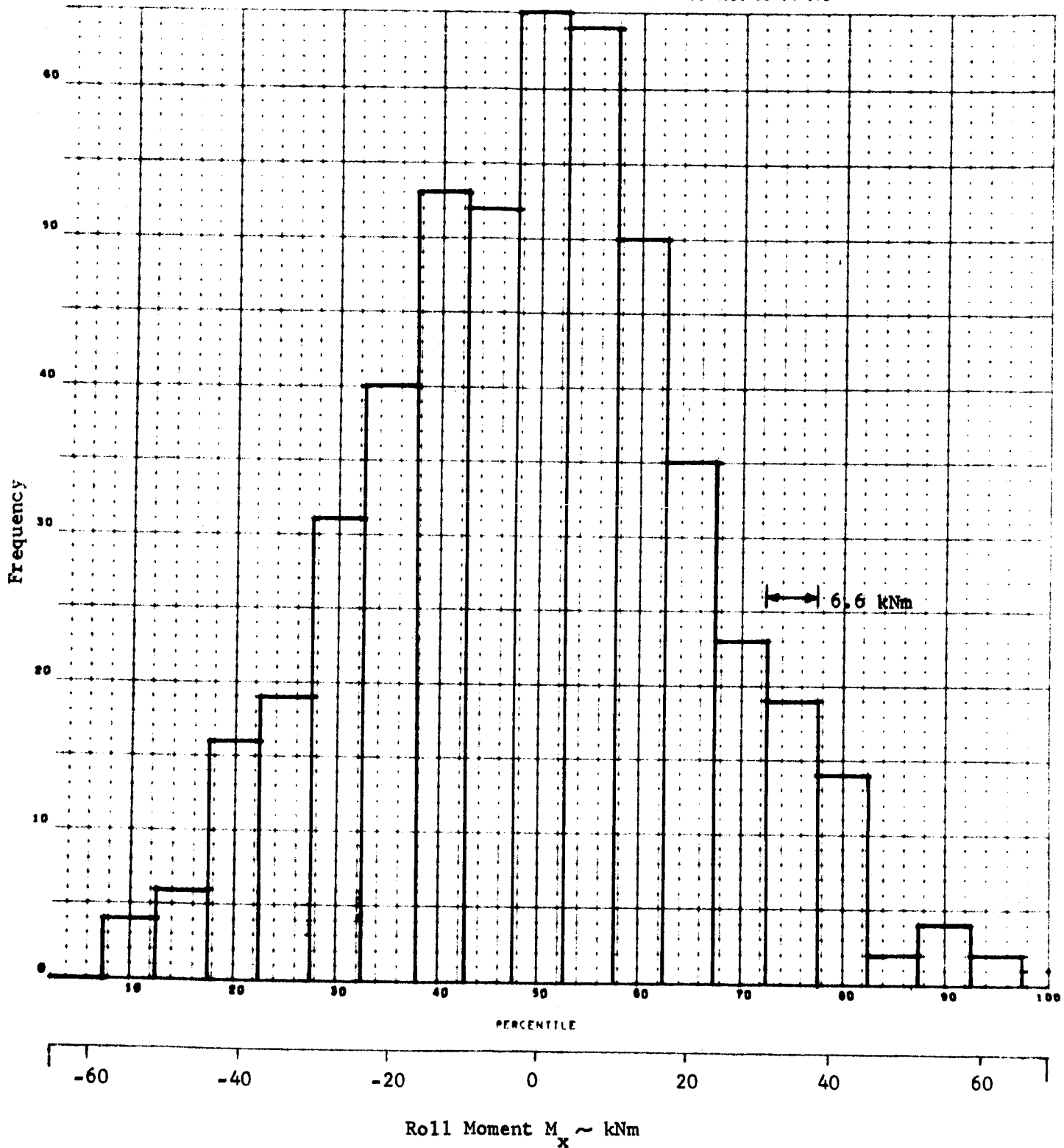


Figure 8-10(d). MOMENT ABOUT ROLL AXIS

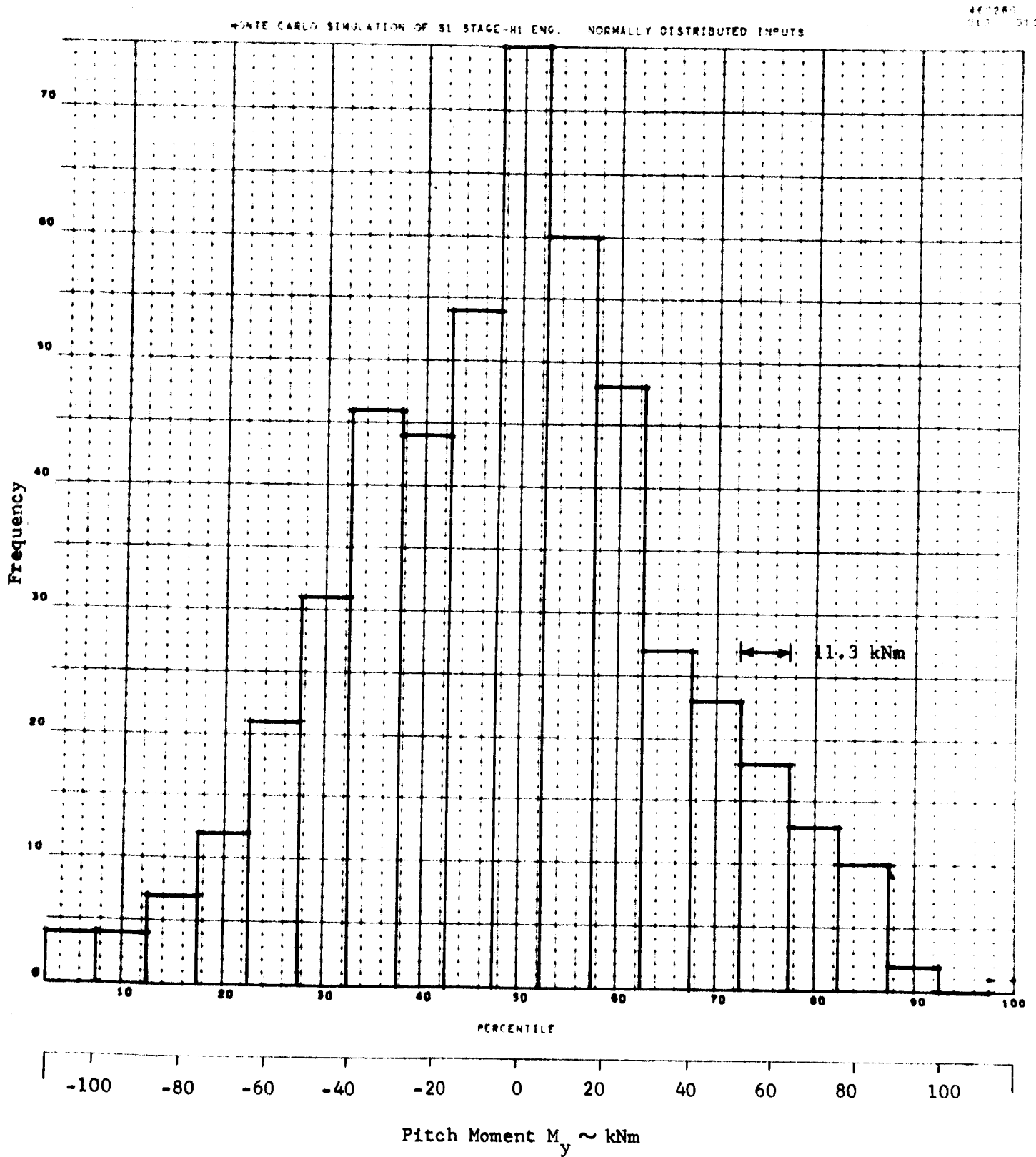


Figure 8-10(e). MOMENT ABOUT PITCH AXIS

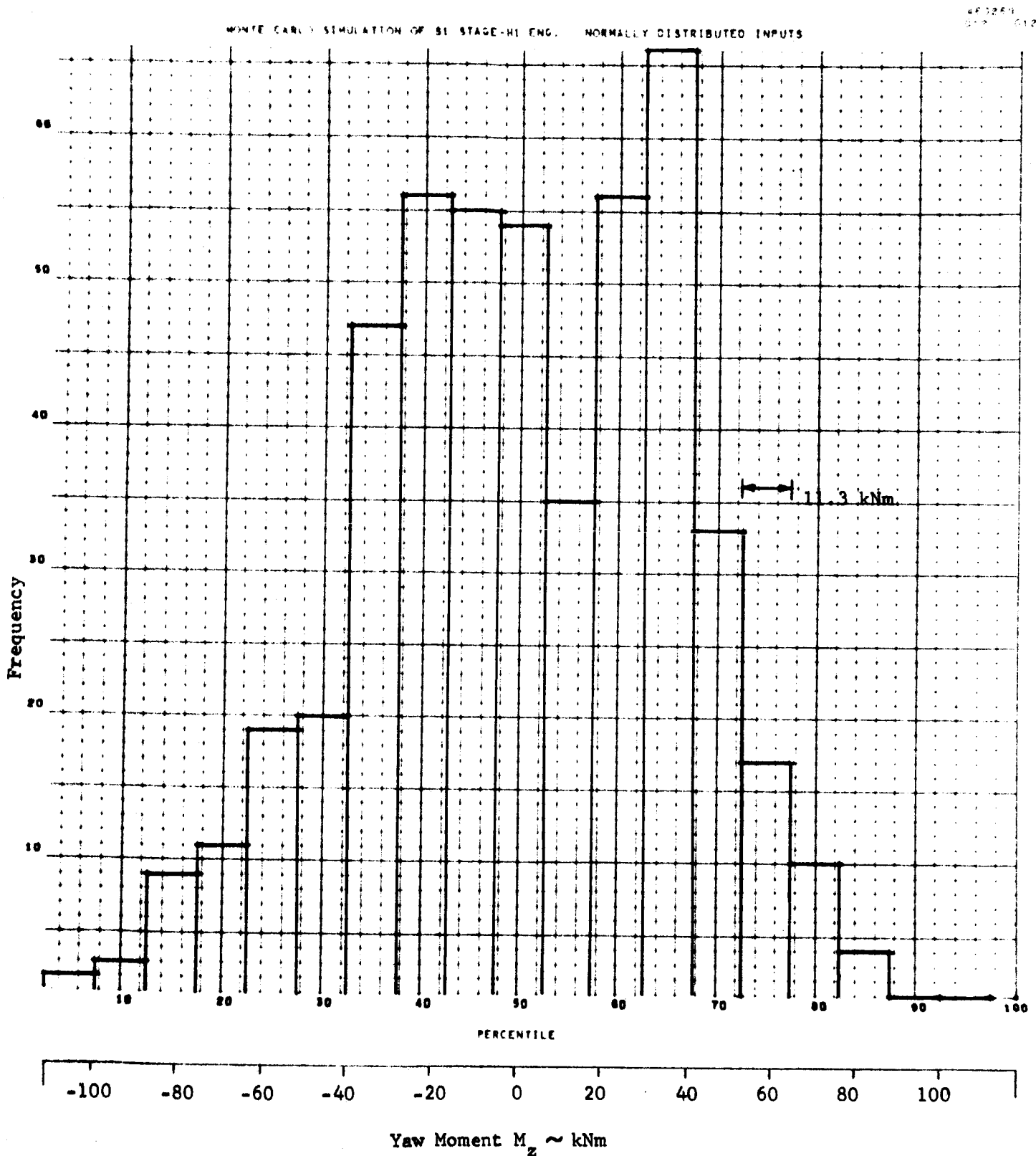
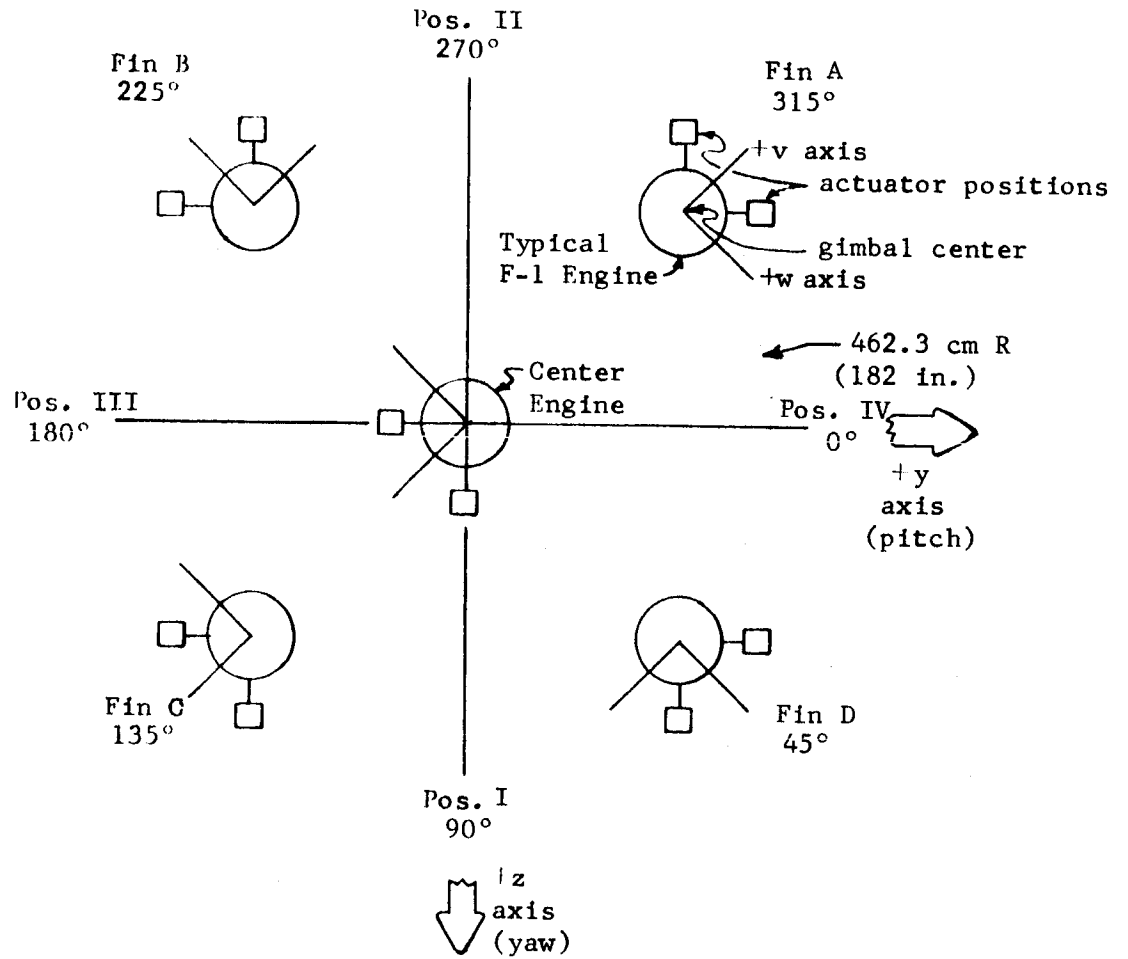


Figure 8-10(f). MOMENT ABOUT YAW AXIS



VIEW LOOKING FORWARD

Figure 8-11. THRUST FRAME GEOMETRY, S-IC STAGE

Table 8-16. NOMINAL VALUES AND TOLERANCES, ENGINE-TO-STAGE  
MOUNTING PARAMETERS, S-IC STAGE

STAGE PARAMETER		CENTER ENGINE		PERIPHERAL ENGINES		
		NOMINAL	TOLERANCE		NOMINAL	TOLERANCE
GIMBAL CENTER DISPLACEMENT	x	0	$\pm .0432$ cm ( $\pm .017$ in.)	x	0	$\pm .0432$ cm ( $\pm .017$ in.)
	y	0	$\pm 1.27$ cm ( $\pm .5$ in.)	R	462.3 cm (182 in.)	$\pm .0762$ cm ( $\pm .030$ in.)
	z	0	$\pm 1.27$ cm ( $\pm .5$ in.)	$\theta$	45°, 135°, 225°, 315°	$\pm 30''$
ENGINE ANGULARITY	$\theta$	135°	--	XX	XXXX	XXXX
	$\Gamma$	0	--	$\Gamma$	29'	--
	$\delta$	0	$\pm 10'$	$\delta$	0	$\pm 42'$
	$\gamma$	0	$\pm 10'$	$\gamma$	0	$\pm 42'$



### 8.6.3 Statistical Analysis

A statistical analysis using both the classical and Monte Carlo solutions was performed on the S-IC stage. The following three cases were investigated:

- Case 1: (Classical and Monte Carlo) All input random variables distributed as univariate normal with ideal means (except  $F_u$ , which had the sample mean);
- Case 2: (Classical and Monte Carlo) All input random variables uniformly distributed with ideal means (except  $F_u$ , which had sample mean);
- Case 3: (Monte Carlo only) Same as Case 1 except  $F_v$  and  $F_w$  distributed as bivariate normal.

The statistical models of engine performance and mounting errors used in each of the cases are summarized in Table 8-17. F-1 engine statistics were taken from Table 8-9. All covariances between engine components were neglected except in Case 3 where the covariance between  $F_v$  and  $F_w$  was considered.

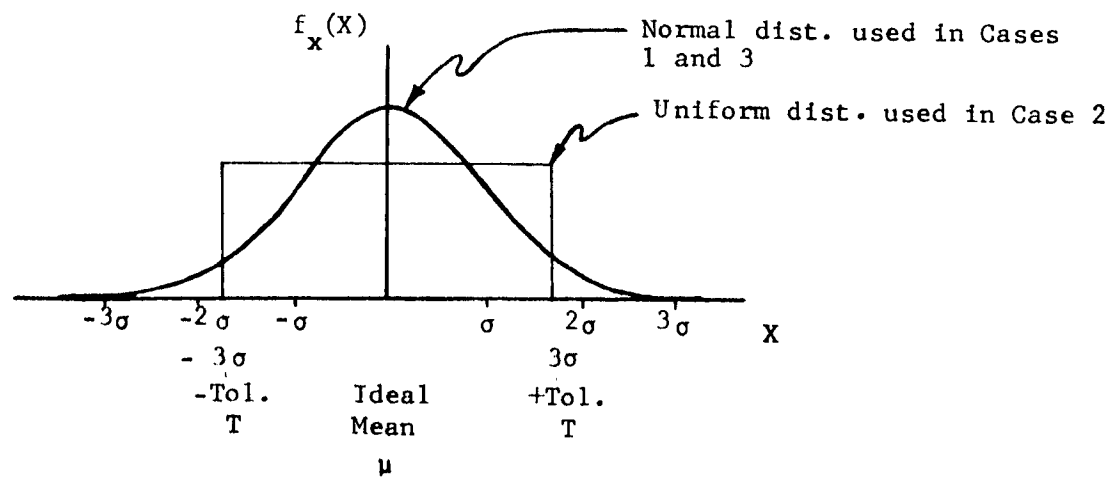


Figure 8-12. TYPICAL PROBABILITY DENSITY FUNCTIONS FOR MOUNTING ERRORS, S-IC STAGE

Table 8-17. STATISTICAL INPUT MODEL, S-IC STAGE

PARAMETER		MEAN	VARIANCE
GIMBAL CENTER DISPLACEMENT	R	462.3 cm (182 in.)	.0020097 cm <sup>2</sup> (.0003115 in. <sup>2</sup> )
	$\theta(\text{peripheral})$	*	2403 x 10 <sup>-6</sup> deg <sup>2</sup>
	x(center)	0	.000645 cm <sup>2</sup> (.0001 in. <sup>2</sup> )
	x(peripheral)	0	.000645 cm <sup>2</sup> (.0001 in. <sup>2</sup> )
	y(center)	0	.5581 cm <sup>2</sup> (.0865 in. <sup>2</sup> )
	z(center)	0	.5591 cm <sup>2</sup> (.0865 in. <sup>2</sup> )
ENGINE ANGULARITY	$\theta(\text{center})$	135°	—
	$\Gamma(\text{center})$	0	—
	$\Gamma(\text{peripheral})$	29'	—
	$\delta(\text{center})$	0	.009612 deg <sup>2</sup>
	$\delta(\text{peripheral})$	0	.016955 deg <sup>2</sup>
	$\gamma(\text{center})$	0	.009612 deg <sup>2</sup>
	$\gamma(\text{peripheral})$	0	.016955 deg <sup>2</sup>
F-1 ENGINE FORCES AND MOMENTS	F <sub>u</sub>	6.7711 x 10 <sup>6</sup> N (1.5222 x 10 <sup>6</sup> lb)	2709.4 x 10 <sup>6</sup> N <sup>2</sup> (136.93 x 10 <sup>6</sup> lb <sup>2</sup> )
	F <sub>v</sub> <sup>**</sup>	0	13.193 x 10 <sup>6</sup> N <sup>2</sup> (.66674 x 10 <sup>6</sup> lb <sup>2</sup> )
	F <sub>w</sub> <sup>**</sup>	0	11.194 x 10 <sup>6</sup> N <sup>2</sup> (.56575 x 10 <sup>6</sup> lb <sup>2</sup> )
	M <sub>u</sub>	0	0
	M <sub>v</sub>	0	.839 x 10 <sup>7</sup> N <sup>2</sup> m <sup>2</sup> (.64761 x 10 <sup>7</sup> lb <sup>2</sup> in. <sup>2</sup> )
	M <sub>w</sub>	0	.1748 x 10 <sup>7</sup> N <sup>2</sup> m <sup>2</sup> (1.3693 x 10 <sup>9</sup> lb <sup>2</sup> in. <sup>2</sup> )

\* NOTE 1. The mean of angle  $\theta$  was taken to be the nominal (or ideal) value for each engine and  $\theta$  was distributed identically for all engines.

\*\* NOTE 2. In case 3,  $\sigma_{F_v F_w} = 8463.8 \times 10^3 \text{ N}^2$  (427.75 x 10<sup>3</sup> lb<sup>2</sup>).

Engine mounting error distributions ( $R$ ,  $\theta$ ,  $x$ ,  $\delta$ ,  $Y$ ) were constructed from the corresponding tolerances as shown in Figure 8-12. For Case 2 each input error was assumed to be uniformly distributed over the tolerance interval. For the other cases each mounting error was assumed to be normally distributed with the same standard deviation as the corresponding uniform distribution. This choice causes the tolerance boundaries to coincide with the  $\sqrt{3}\sigma$  points for both the uniform and normal distributions as shown by the following derivation:

Consider a random variable  $X$  uniformly distributed over the interval  $(\mu - T) \leq X \leq (\mu + T)$ . The probability density function must be

$$f_x(X) = \begin{cases} 0 & , \quad X \leq (\mu - T) \\ \frac{1}{2T} & , \quad (\mu - T) < X \leq (\mu + T) \\ 0 & , \quad (\mu + T) < X \end{cases}$$

The variance is given by

$$\begin{aligned} \sigma_x^2 &= E[X^2] - E^2[X] \\ &= \int_{-\infty}^{\infty} X^2 f_x(X) dX - \mu^2 \\ &= \frac{T^2}{3} \end{aligned}$$

Therefore the standard deviation is

$$\sigma_x = \frac{T}{\sqrt{3}}$$

and a normal distribution having the same standard deviation will have its  $\sqrt{3}\sigma$

points at the tolerance boundaries. This choice of standard deviation for the normal distribution should be pessimistic compared to the real situation, since approximately four percent of the samples will fall outside the specified tolerance. (Of course, no out-of-tolerance samples are possible with the uniform distribution.)

The results of Case 1 classical and Monte Carlo solutions are shown in Tables 8-18 and 8-19 and Figure 8-13. Comparison of the two methods shows that the standard deviation calculated by each compare within three percent. The effect of the input distributions shapes on the resultant thrust and moment vectors can be seen by comparing the results of Case 2 (Tables 8-18 and 8-20 and Figure 8-14) with those of Case 1. Since the input variances are identical for the two cases, the output variances are also identical according to the classical solution, and this is strongly supported by the similarity of the Monte Carlo solutions for Cases 1 and 2.

Case 3 was investigated to determine the importance of the covariance between  $F_v$  and  $F_w$  in the F-1 engine. As shown in Table 8-9, this pair has the largest linear correlation coefficient of any of the F-1 parameters. The covariance between  $F_v$  and  $F_w$  was not included in the derivation of the classical solution (refer to subsection 4.2.2), and therefore can be taken into account only in the Monte Carlo solution. A comparison of the results of Cases 1 and 3 (Tables 8-19 and 8-21) shows that the dependence between  $F_v$  and  $F_w$  has a negligible effect on the resultant thrust and moment of the stage.

Table 8-18. CLASSICAL SOLUTION FOR STATISTICAL PROPERTIES OF RESULTANT THRUST AND MOMENT VECTORS, S-IC STAGE, CASES 1 AND 2

FORCE COMPONENT	MEAN N (1b)	STD. DEVIATION N (1b)	VARIANCE $N^2$ (1b <sup>2</sup> )
Fx	33854969.8 (7610900.)	116391.3 (26165.8)	$1.3547 \times 10^{10}$ ( $6.8465 \times 10^8$ )
Fy	0	96511.7 (21696.7)	$.93146 \times 10^{10}$ ( $4.7075 \times 10^8$ )
Fz	0	96511.7 (21696.7)	$.93146 \times 10^{10}$ ( $4.7075 \times 10^8$ )
MOMENT COMPONENT	Nm (1b-in.)	Nm (1b-in.)	$N^2 m^2$ (1b <sup>2</sup> -in. <sup>2</sup> )
Mx	0	442650.4 (3917779.9)	$1.9594 \times 10^{11}$ ( $1.5349 \times 10^{13}$ )
My	0	344011.0 (3044749.5)	$1.1834 \times 10^{11}$ ( $.92705 \times 10^{13}$ )
Mz	0	344011.0 (3044749.5)	$1.1834 \times 10^{11}$ ( $.92705 \times 10^{13}$ )

Table 8-19. MONTE CARLO SOLUTION FOR STATISTICAL PROPERTIES OF RESULTANT THRUST AND MOMENT VECTORS, S-IC STAGE, CASE 1

FORCE COMPONENT	MEAN N (1b)	STD. DEVIATION N (1b)	VARIANCE $N^2$ (1b <sup>2</sup> )
Fx	33851998. (7610232.)	116108. (26101.3)	$1.3481 \times 10^{10}$ ( $6.8133 \times 10^8$ )
Fy	-2264.6 (-509.11)	95653.2 (21503.7)	$.91496 \times 10^{10}$ ( $4.6241 \times 10^8$ )
Fz	-3341.5 (-751.21)	96822.2 (21766.5)	$.93745 \times 10^{10}$ ( $4.7378 \times 10^8$ )
MOMENT COMPONENT	Nm (1b-in.)	Nm (1b-in.)	$N^2 m^2$ (1b <sup>2</sup> -in. <sup>2</sup> )
Mx	-3059.3 (-27077.)	431331. (3817591.)	$1.8605 \times 10^{11}$ ( $1.4564 \times 10^{13}$ )
My	6774.4 (59958.)	344802. (3051754.)	$1.1889 \times 10^{11}$ ( $.93132 \times 10^{13}$ )
Mz	6677.5 (59101.)	344699. (3050836.)	$1.1882 \times 10^{11}$ ( $.93076 \times 10^{13}$ )

460260  
002 002

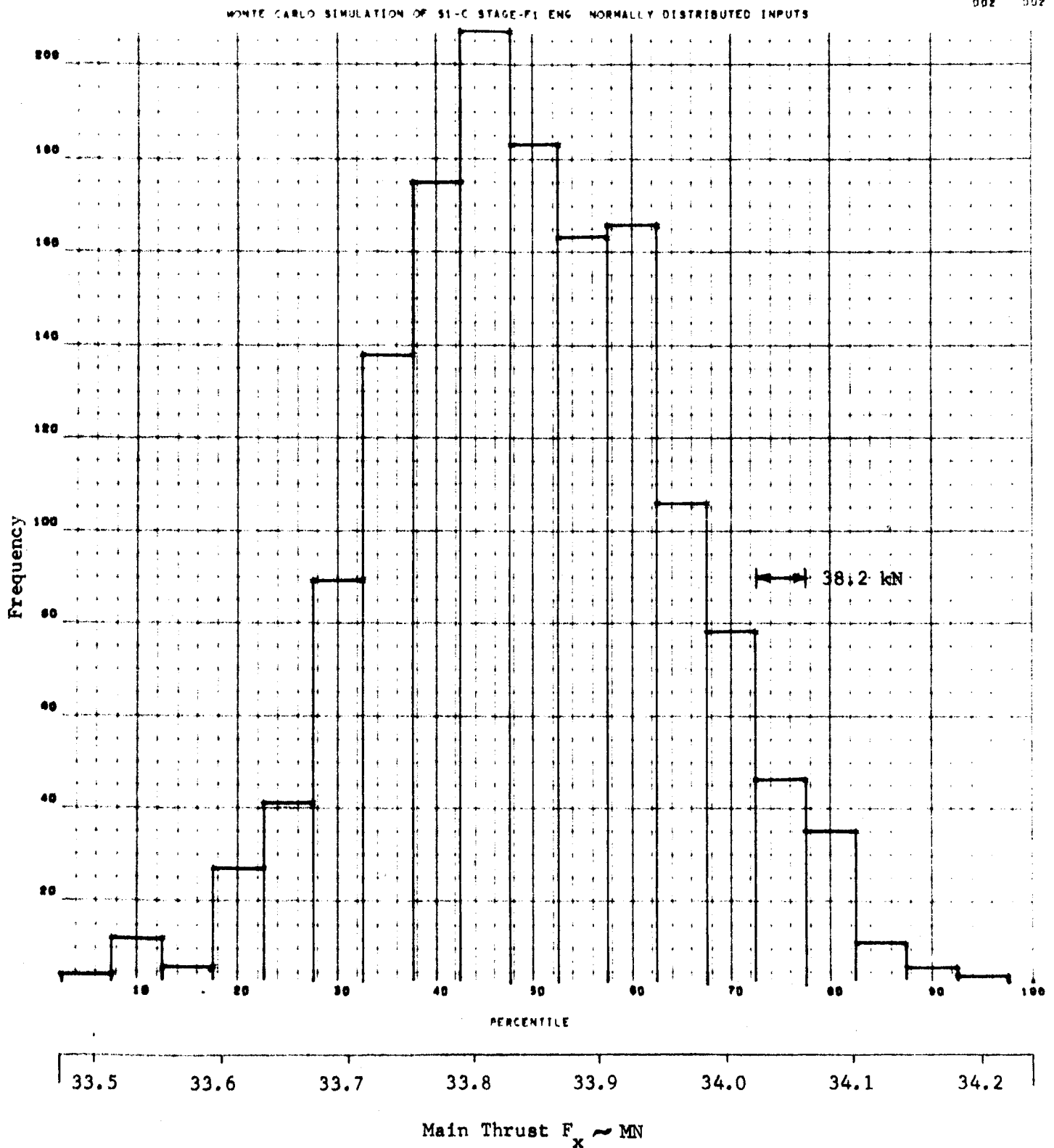


Figure 8-13. HISTOGRAMS FOR RESULTANT THRUST AND MOMENT VECTOR COMPONENTS, 1500 MONTE CARLO TRIALS, NORMALLY DISTRIBUTED INPUTS (CASE 1) S-1C STAGE. (a) MAIN THRUST COMPONENT

460260  
004 004

MONTÉ CARLO SIMULATION OF S1-C STAGE-F1 ENG NORMALLY DISTRIBUTED INPUTS

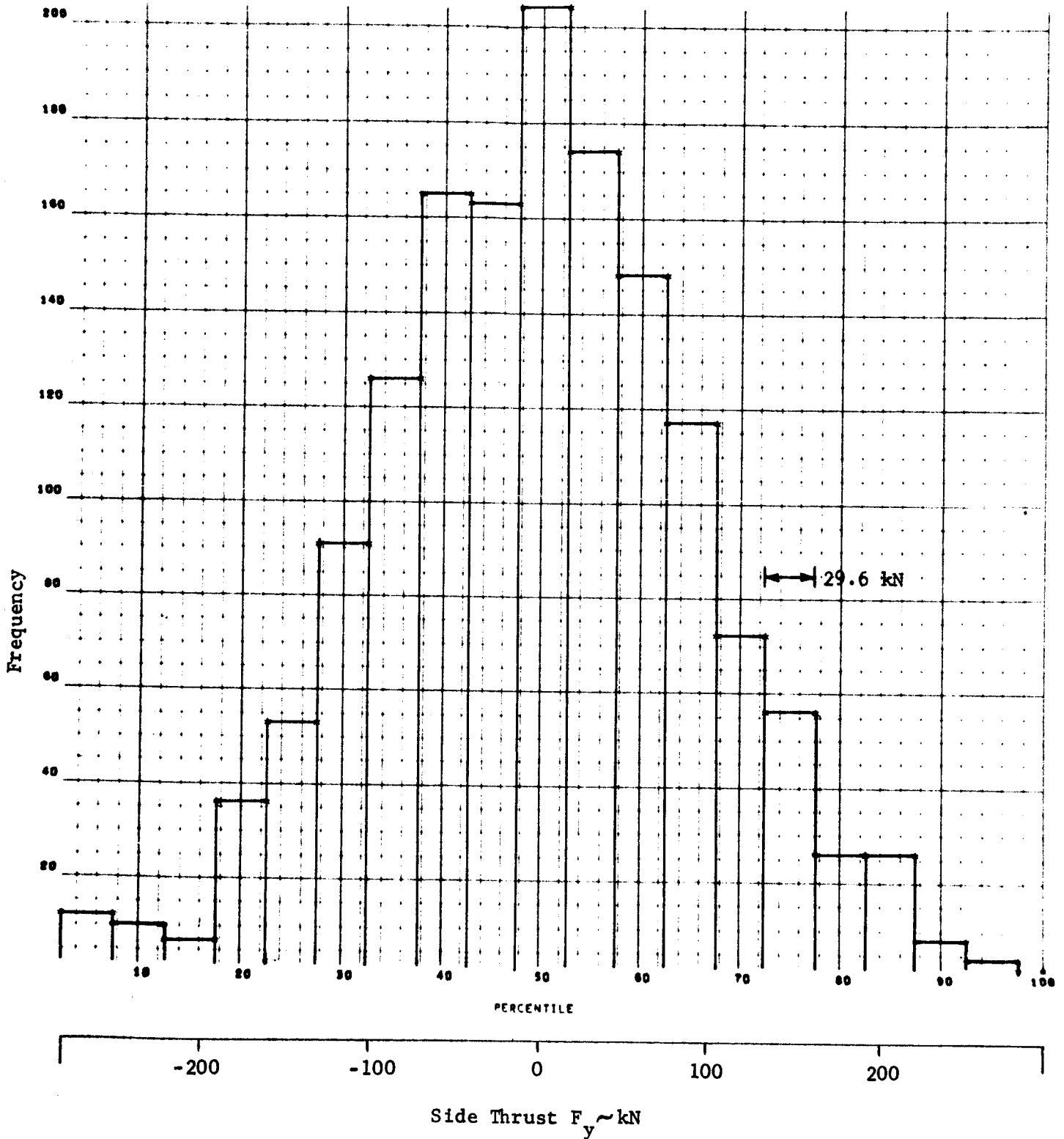


Figure 8-13(b). SIDE THRUST COMPONENT ALONG PITCH AXIS

460250  
006 006

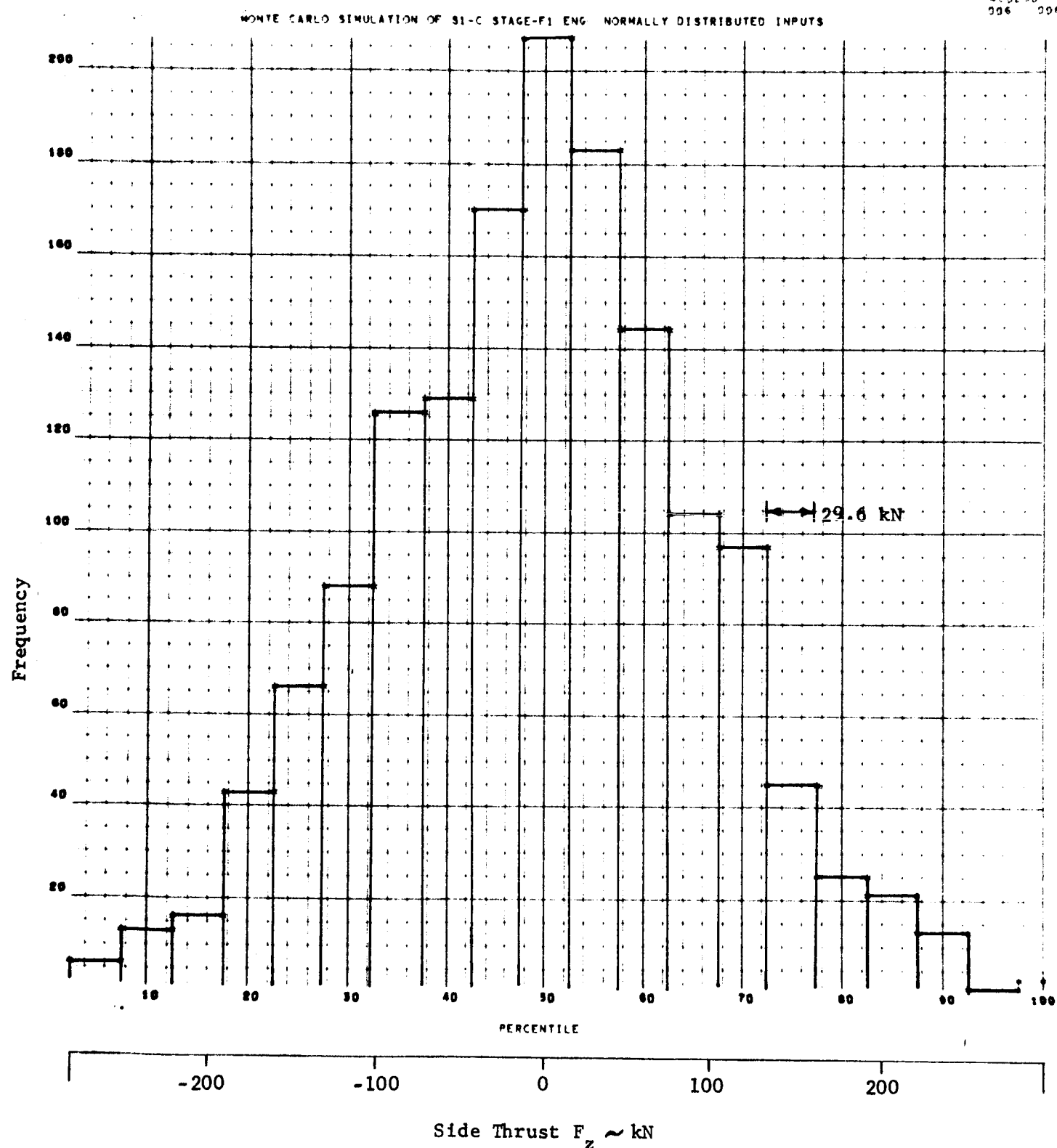


Figure 8-13(c). SIDE THRUST COMPONENT ALONG YAW AXIS



Monte Carlo Simulation of S1-C Stage-F1 Eng. Normally Distributed Inputs

460760  
000 000

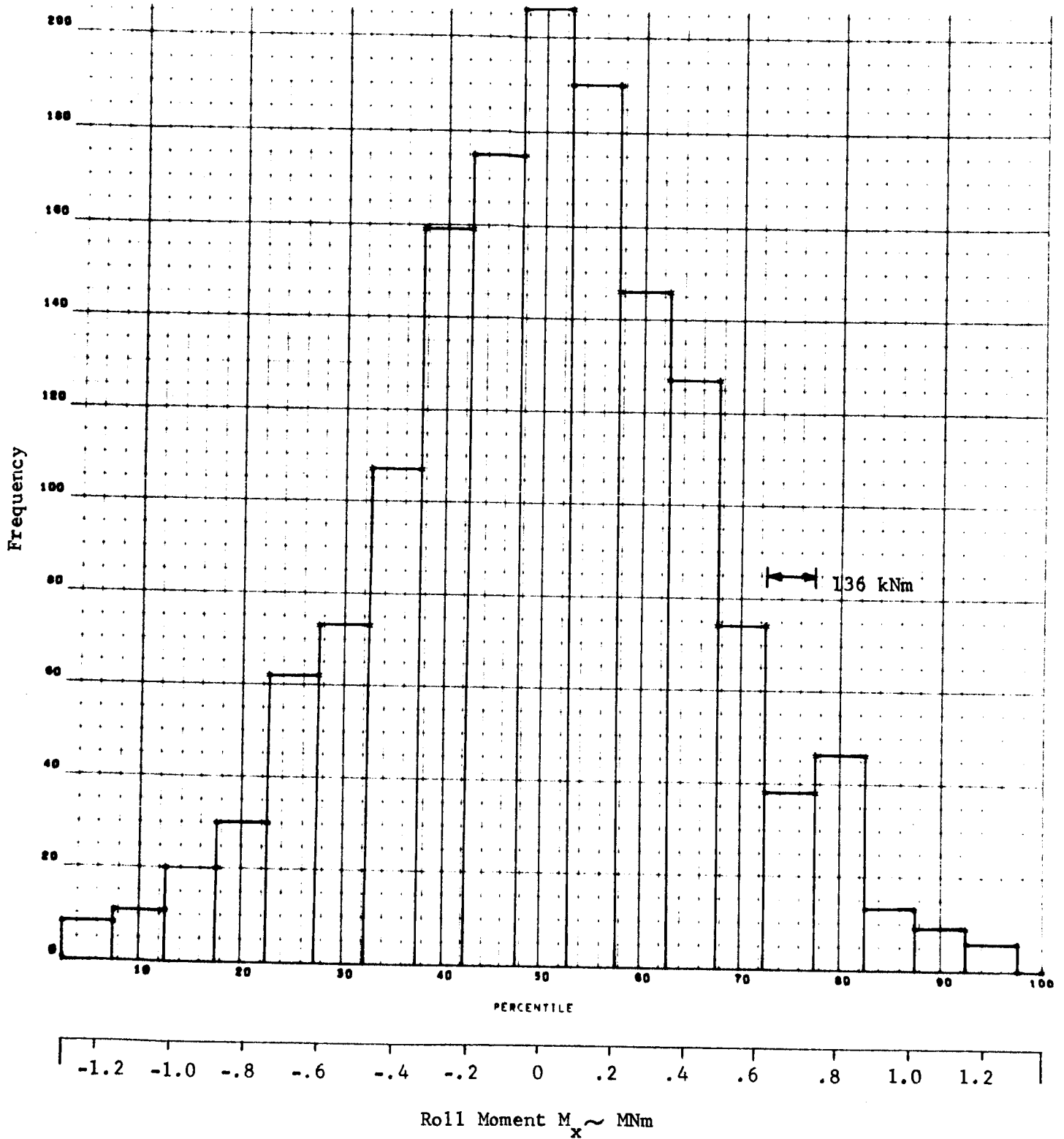


Figure 8-13(d). MOMENT ABOUT ROLL AXIS

473265  
010 010

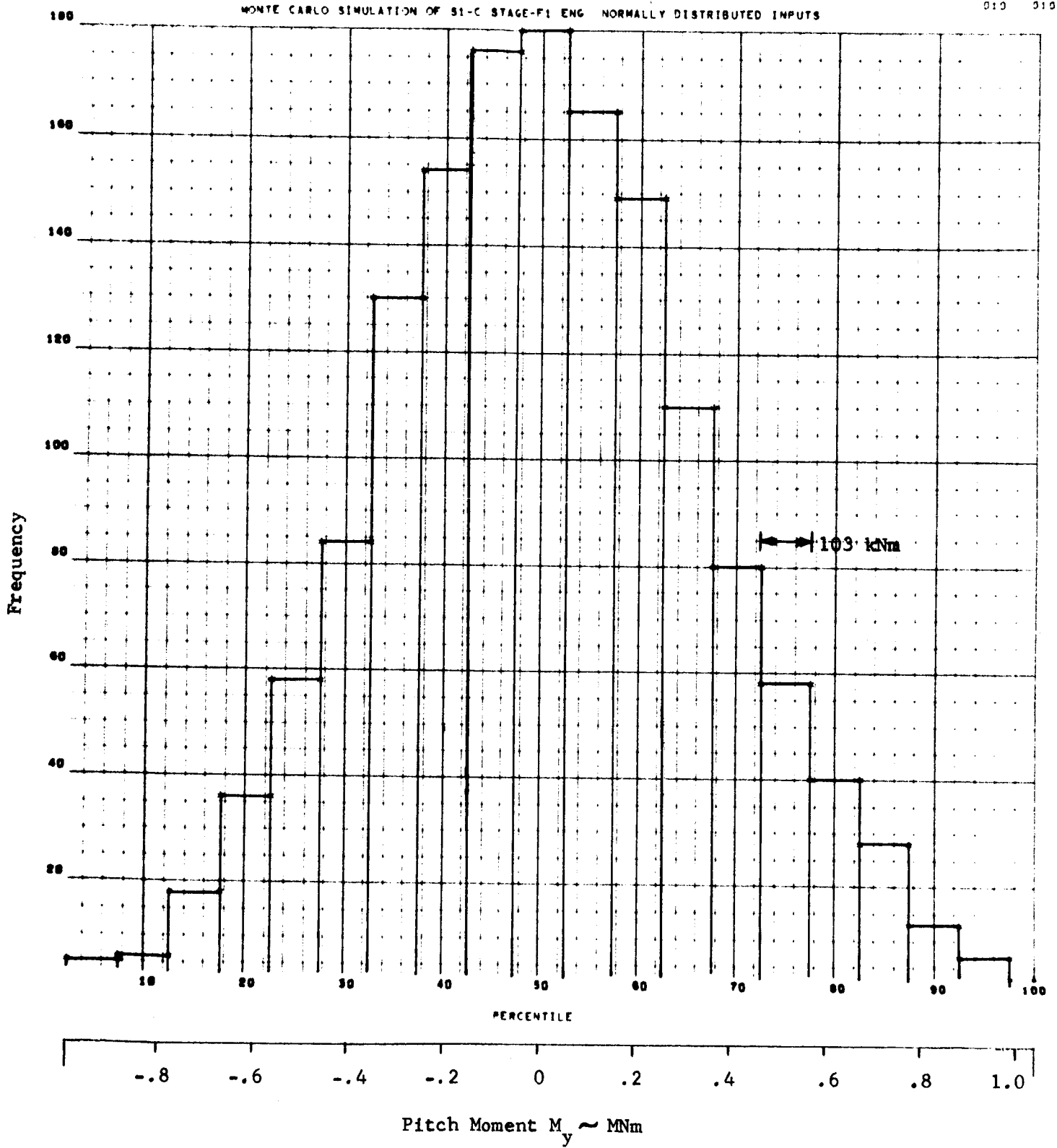


Figure 8-13(e). MOMENT ABOUT PITCH AXIS

460260  
012 012

MONTÉ CARLO SIMULATION OF S1-C STAGE-F1 ENG NORMALLY DISTRIBUTED INPUTS

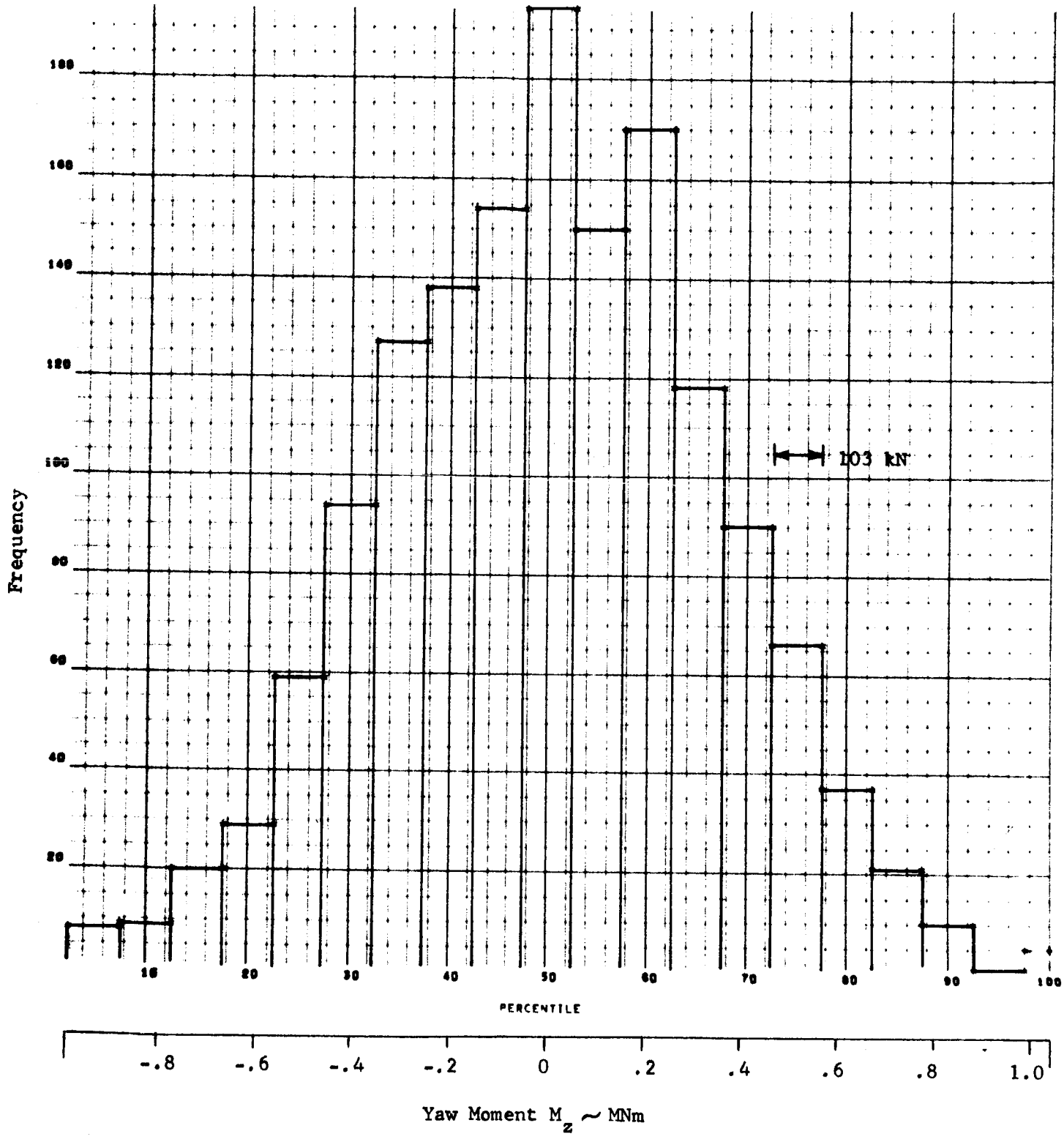


Figure 8-13(f). MOMENT ABOUT YAW AXIS

Table 8-20. MONTE CARLO SOLUTION FOR STATISTICAL PROPERTIES OF RESULTANT THRUST AND MOMENT VECTORS, S-IC STAGE, CASE 2

FORCE COMPONENT	MEAN N (lb)	STD. DEVIATION N (lb)	VARIANCE $N^2$ (lb <sup>2</sup> )
Fx	33855917. (7611113.)	119917. (26958.5)	$1.4380 \times 10^{10}$ ( $7.267 \times 10^8$ )
Fy	2338.47 (525.71)	97263.5 (21865.7)	$.94602 \times 10^{10}$ ( $4.7811 \times 10^8$ )
Fz	-2454.79 (-551.86)	96334.2 (21656.8)	$.92803 \times 10^{10}$ ( $4.6902 \times 10^8$ )
MOMENT COMPONENT	Nm (lb-in.)	Nm (lb-in.)	$N_m^2$ (lb <sup>2</sup> -in. <sup>2</sup> )
Mx	6397.3 (56621.)	431315.6 (3817459.)	$1.8603 \times 10^{11}$ ( $1.4573 \times 10^{13}$ )
My	11393.6 (100842.)	346079.2 (3063054.)	$1.1977 \times 10^{11}$ ( $.93823 \times 10^{13}$ )
Mz	-584.30 (-5171.5)	344928.2 (3052867.)	$1.1897 \times 10^{11}$ ( $.93200 \times 10^{13}$ )

Table 8-21. MONTE CARLO SOLUTION FOR STATISTICAL PROPERTIES OF RESULTANT THRUST AND MOMENT VECTORS, S-IC STAGE, CASE 3

FORCE COMPONENT	MEAN N (lb)	STD. DEVIATION N (lb)	VARIANCE $N^2$ (lb <sup>2</sup> )
Fx	33855864. (7611101.)	112326. (25252.1)	$1.2617 \times 10^{10}$ ( $6.3767 \times 10^8$ )
Fy	-1141.10 (-256.53)	92842.8 (20871.9)	$.86198 \times 10^{10}$ ( $4.3564 \times 10^8$ )
Fz	-6545.6 (-1471.5)	92288.6 (20747.3)	$.85172 \times 10^{10}$ ( $4.3045 \times 10^8$ )
MOMENT COMPONENT	Nm (lb-in.)	Nm (lb-in.)	$N_m^2$ (lb <sup>2</sup> -in. <sup>2</sup> )
Mx	21286.8 (188404.)	437968.0 (3876338.)	$1.9181 \times 10^{11}$ ( $1.5026 \times 10^{13}$ )
My	95734.3 (847319.)	349304.5 (3091601.)	$1.2201 \times 10^{11}$ ( $.95580 \times 10^{13}$ )
Mz	-249.05 (-2204.3)	332678.9 (2944452.)	$1.1067 \times 10^{11}$ ( $.86698 \times 10^{13}$ )

September 1966

460260  
002 002

## MONTE CARLO SIMULATION OF S1-C STAGE-F1 ENG UNIFORMLY DISTRIBUTED INPUTS

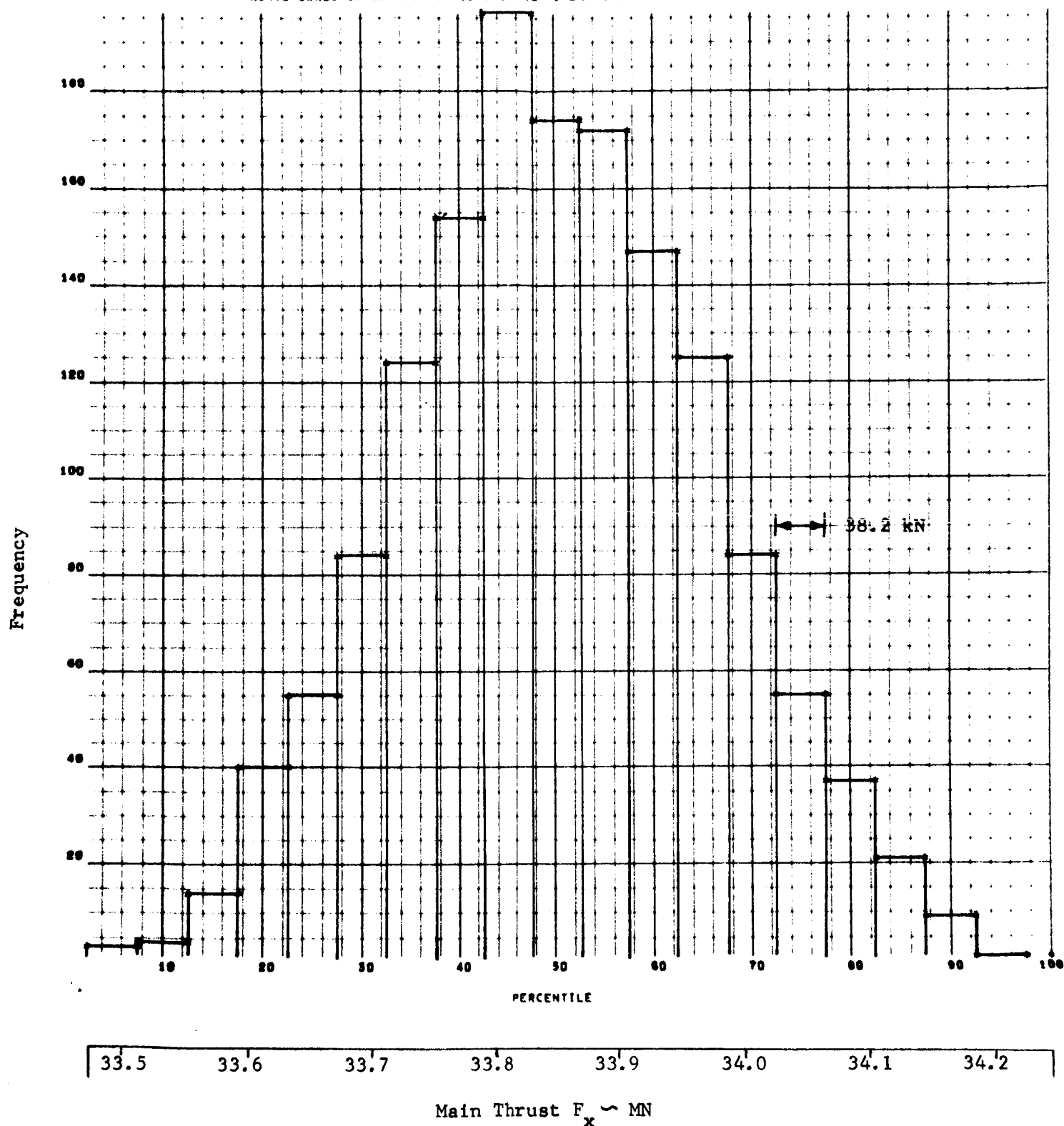


Figure 8-14. HISTOGRAMS FOR RESULTANT THRUST AND MOMENT VECTOR COMPONENTS  
1500 MONTE CARLO TRIALS, NORMALLY DISTRIBUTED INPUTS (CASE 2)  
S-1C STAGE. (a) MAIN THRUST COMPONENT

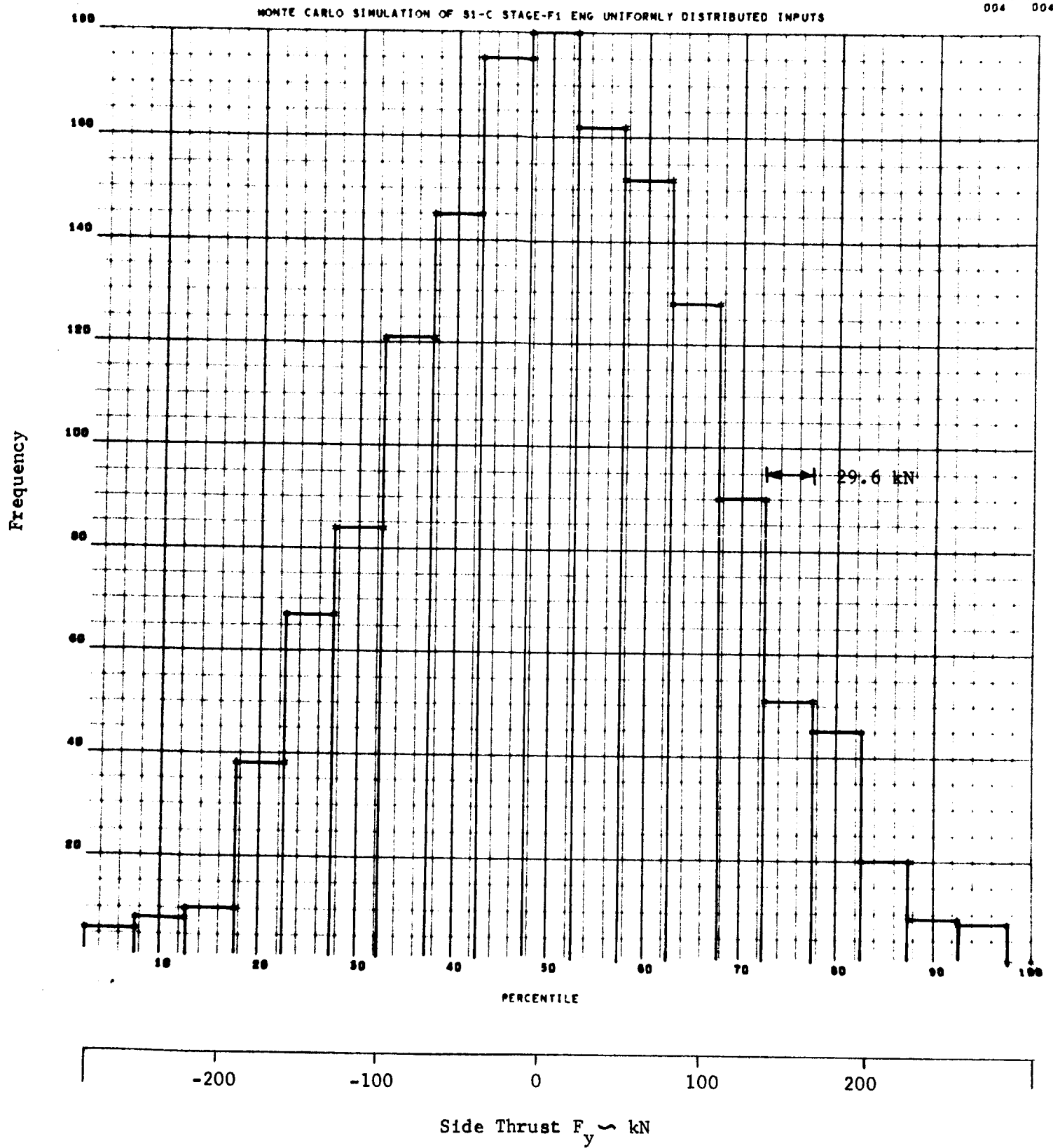


Figure 8-14(b). SIDE THRUST COMPONENT ALONG PITCH AXIS

MONTÉ CARLO SIMULATION OF S1-C STAGE-F1 ENG UNIFORMLY DISTRIBUTED INPUTS

460260  
006 006

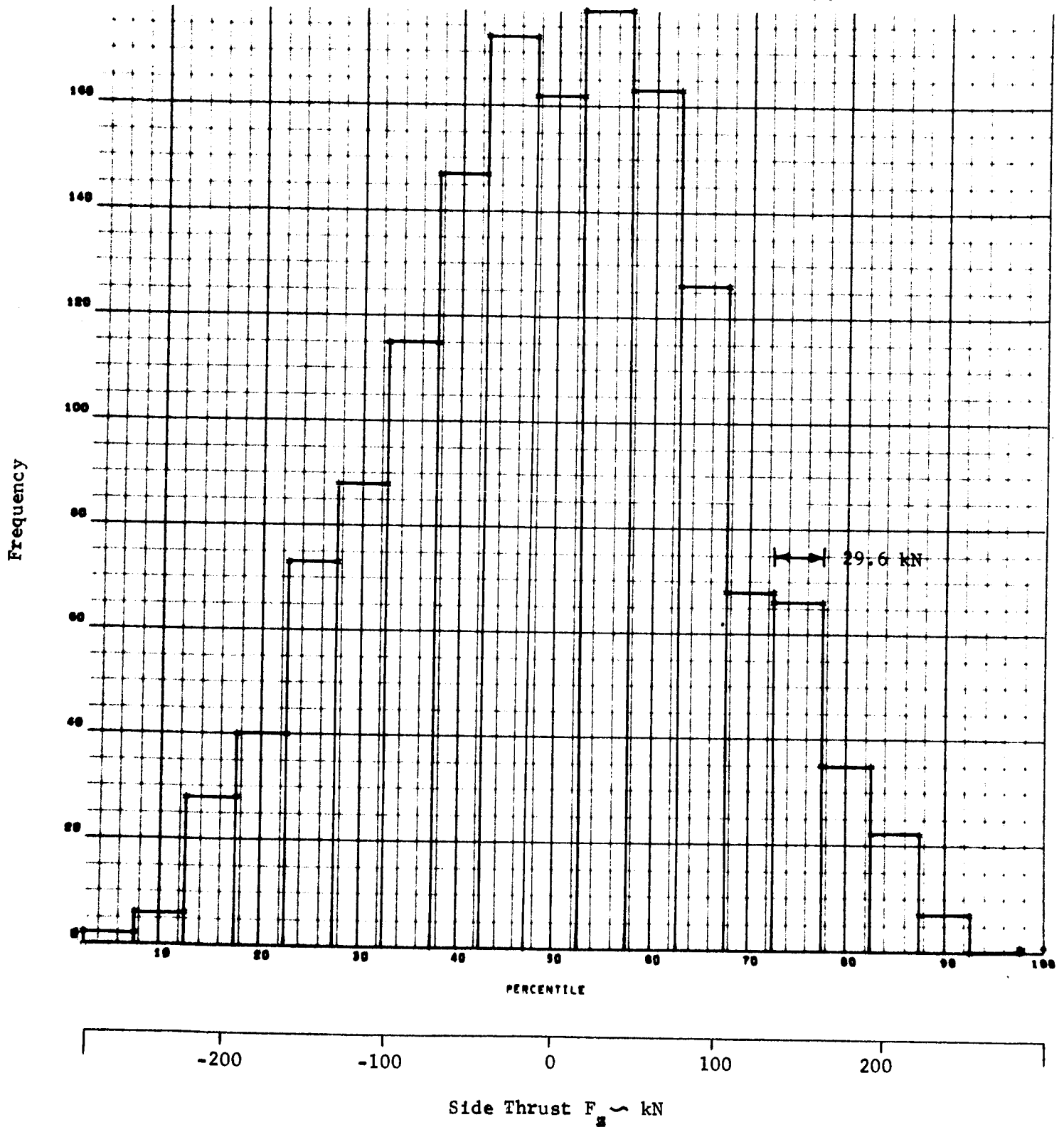


Figure 8-14(c). SIDE THRUST COMPONENT ALONG YAW AXIS

460260  
008 008

MONTE CARLO SIMULATION OF S1-C STAGE-F1 ENG UNIFORMLY DISTRIBUTED INPUTS

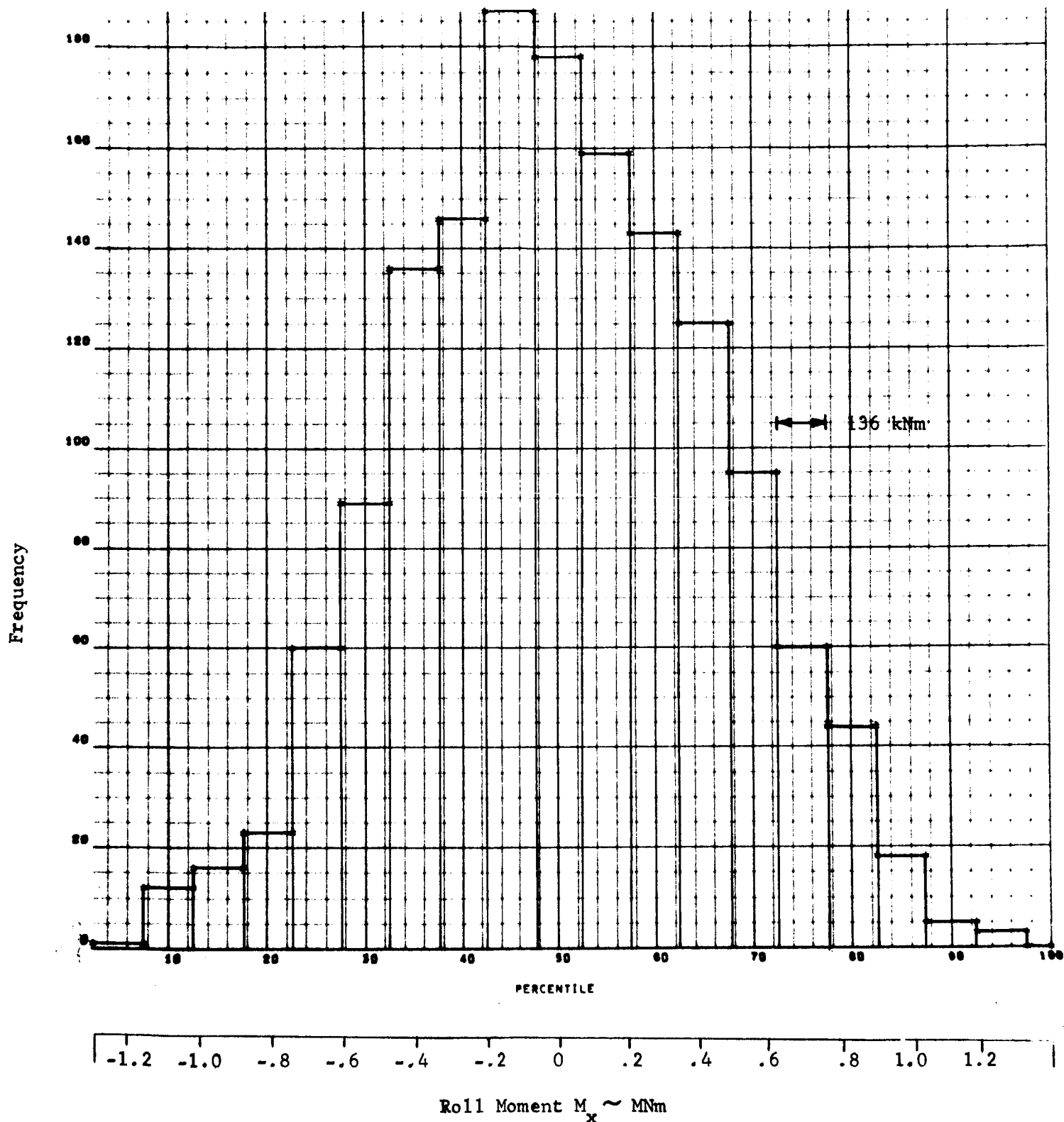


Figure 8-14(d). MOMENT ABOUT ROLL AXIS



460260  
010 010

MONTÉ CARLO SIMULATION OF S1-C STAGE-F1 ENG UNIFORMLY DISTRIBUTED INPUTS

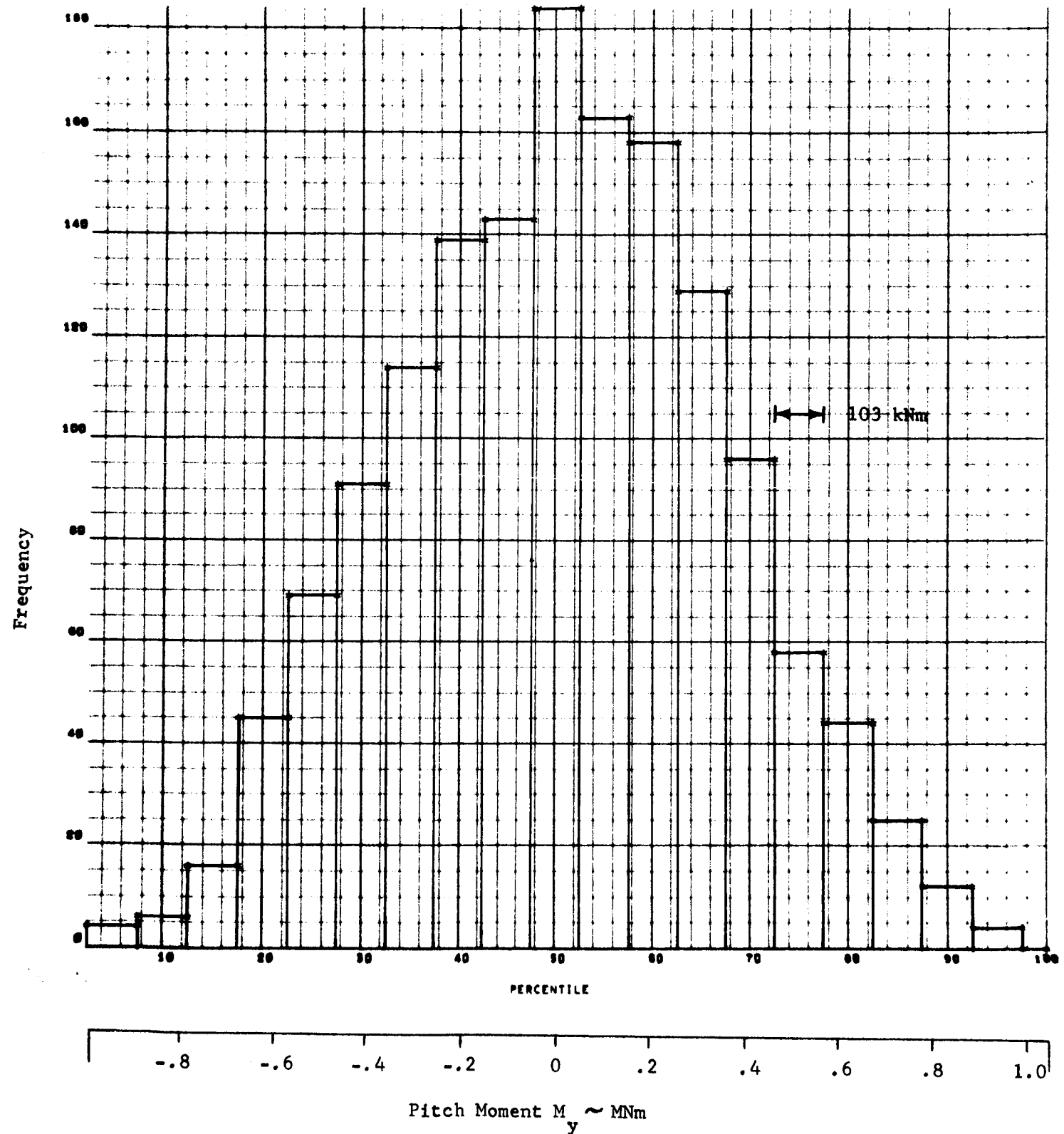


Figure 8-14(e). MOMENT ABOUT PITCH AXIS

MONTE CARLO SIMULATION OF S1-C STAGE-F1 ENG UNIFORMLY DISTRIBUTED INPUTS

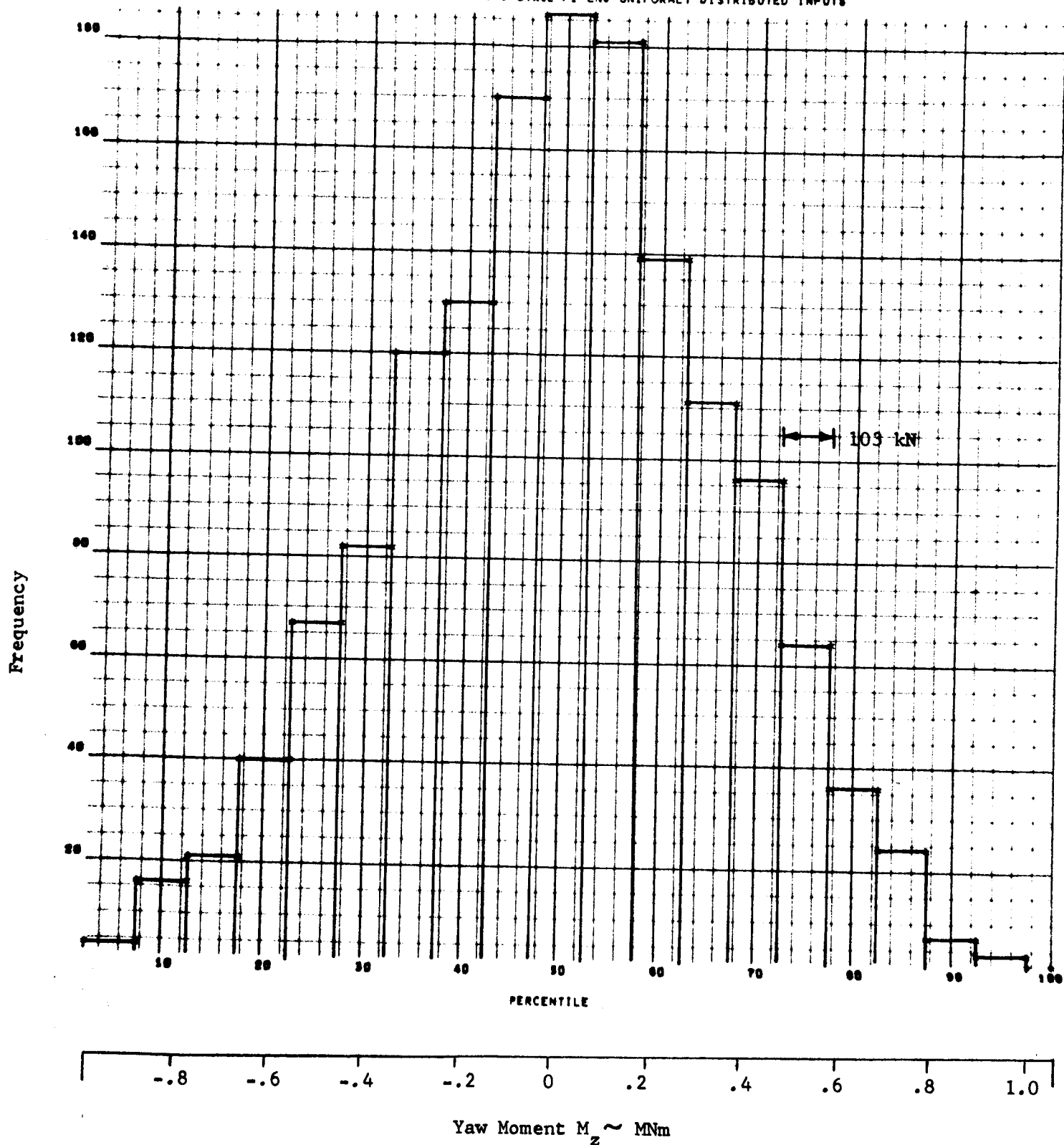


Figure 8-14(f). MOMENT ABOUT YAW AXIS

## 8.7 S-II AND S-IVB STAGES [20,21,22]

No statistical analysis was performed on the S-II and S-IVB stages. However, the geometry and tolerances of these stages were procured during the course of this study and are summarized in this subsection. Insufficient measurement data were available to allow a statistical analysis of either stage.

The S-II stage, second stage of the Saturn V vehicle, consists of one fixed J-2 center engine and four gimbaled J-2 peripheral engines equally spaced on a circle of radius 266.7 cm (105 in.) from the cluster center (Figure 8-15). Each outboard engine is canted one deg with respect to the stage centerline and is oriented with the actuator attach points away from the stage center (v-axes outward). The pertinent dimensions and stated tolerances are given in Table 8-22.

The S-IVB stage, powered by a single J-2 engine, is used as the second stage of the uprated Saturn I vehicle and as the third stage of the Saturn V vehicle. The J-2 engine is oriented such that the v-axis lies at an angle of 135 deg with respect to the y-axis of the stage (Figure 8-16). Tolerances for the stage are listed in Table 8-23.

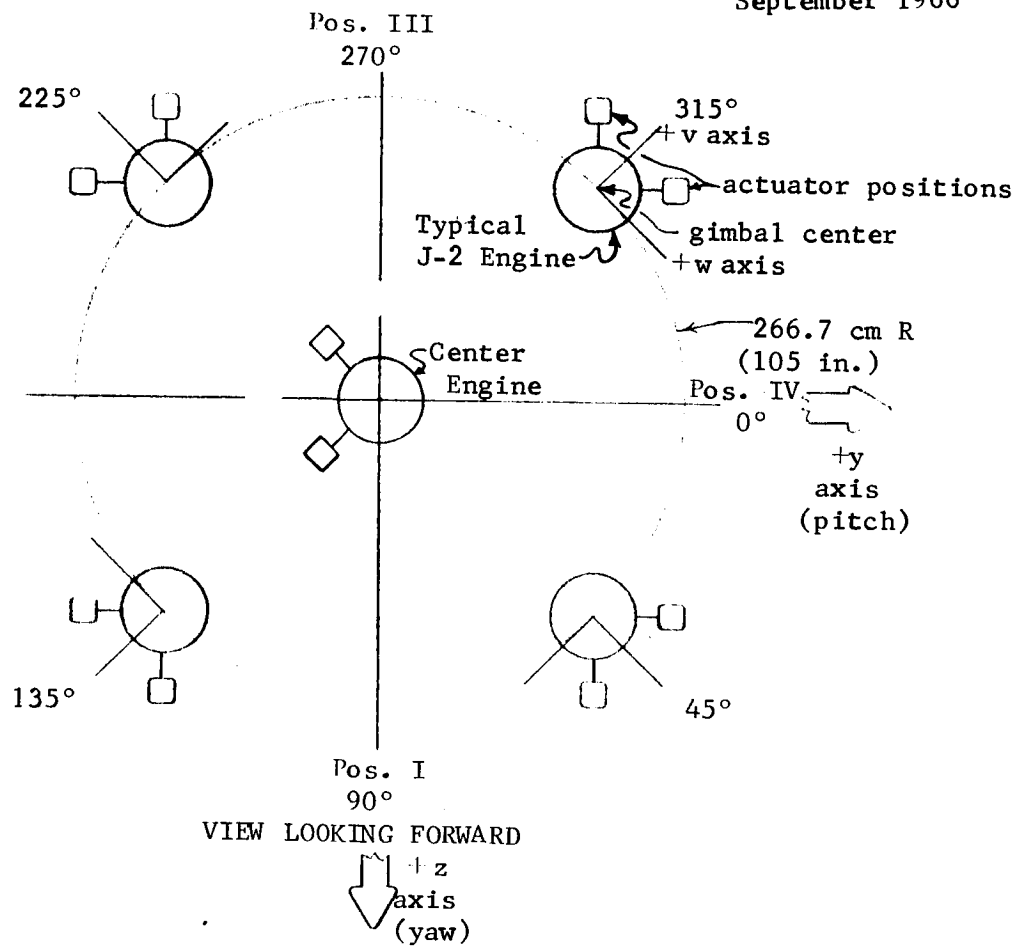


Figure 8-15. THRUST FRAME GEOMETRY, S-II STAGE

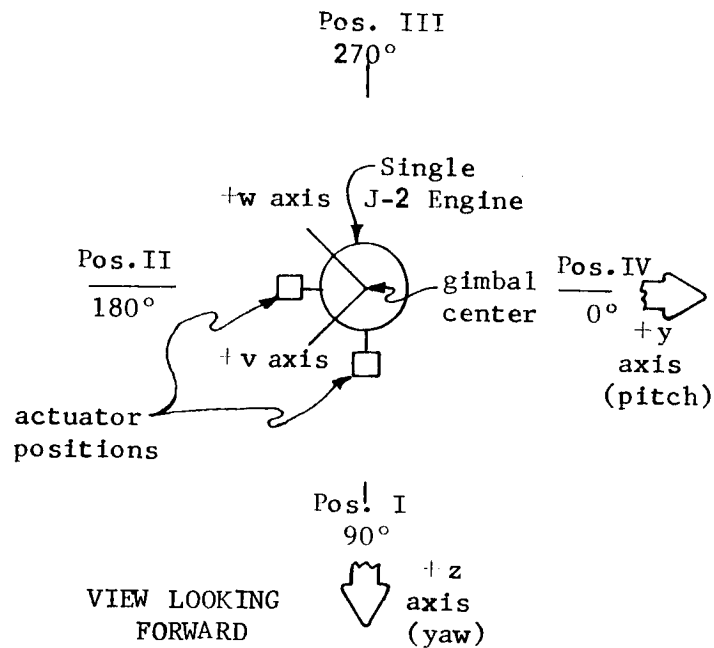


Figure 8-16. THRUST FRAME GEOMETRY, S-IVB STAGE

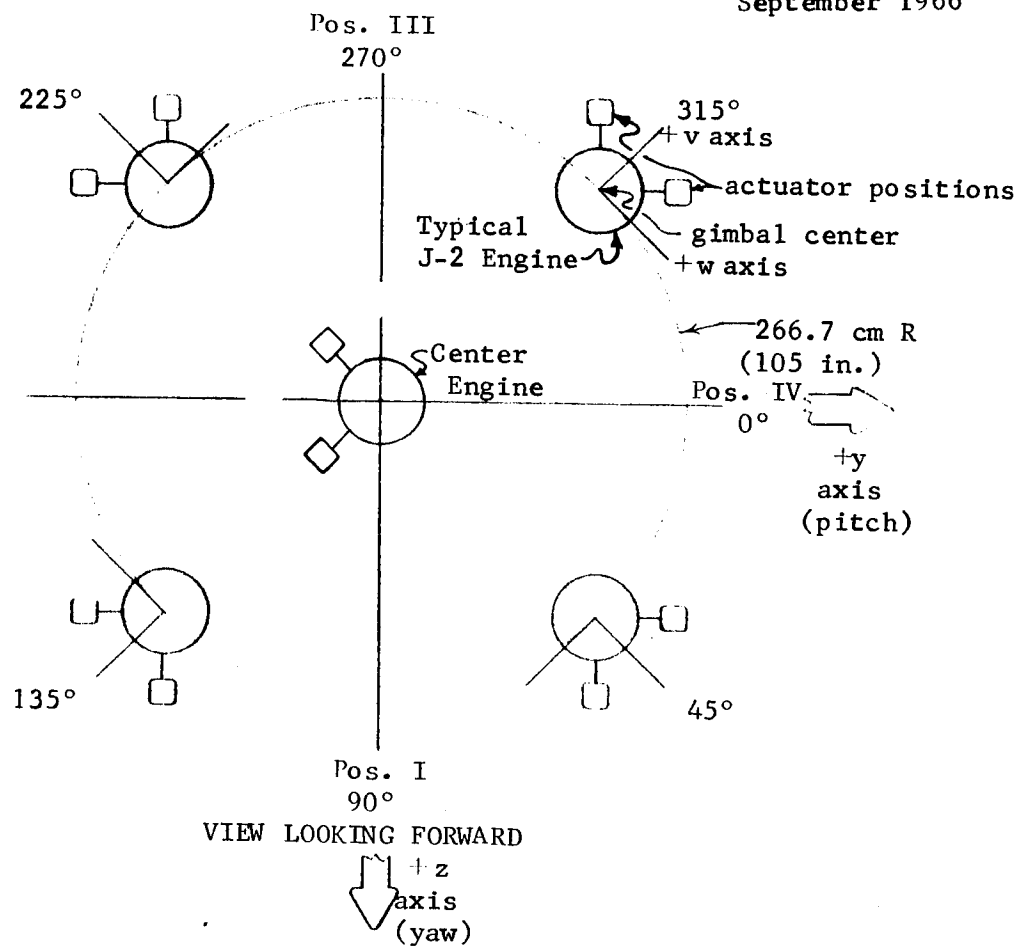


Figure 8-15. THRUST FRAME GEOMETRY, S-II STAGE

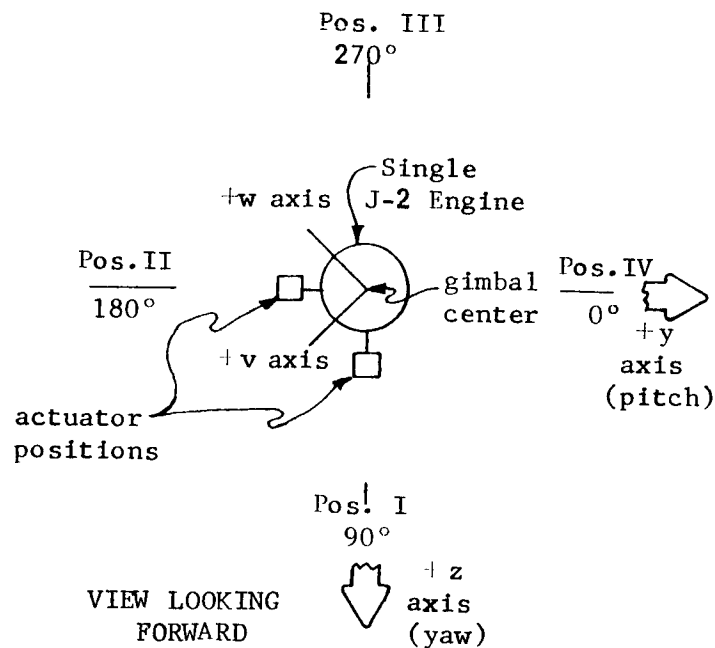


Figure 8-16. THRUST FRAME GEOMETRY, S-IVB STAGE

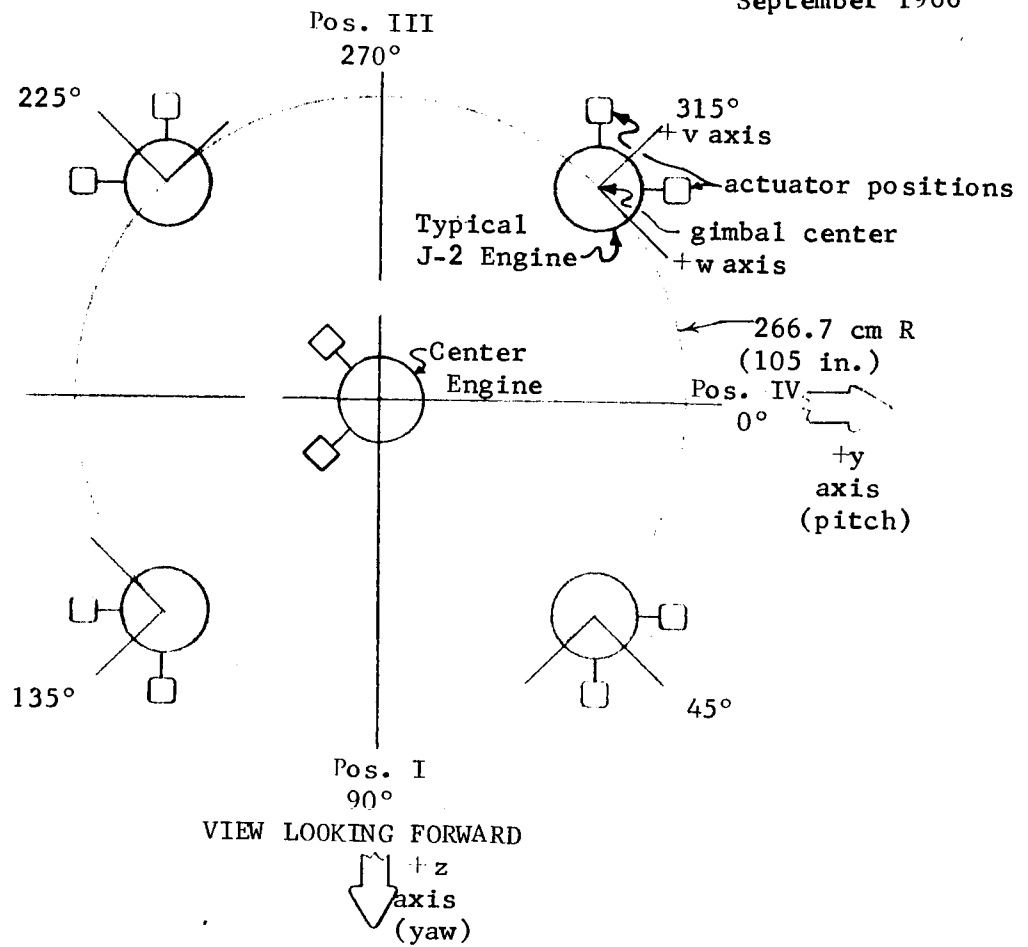


Figure 8-15. THRUST FRAME GEOMETRY, S-II STAGE

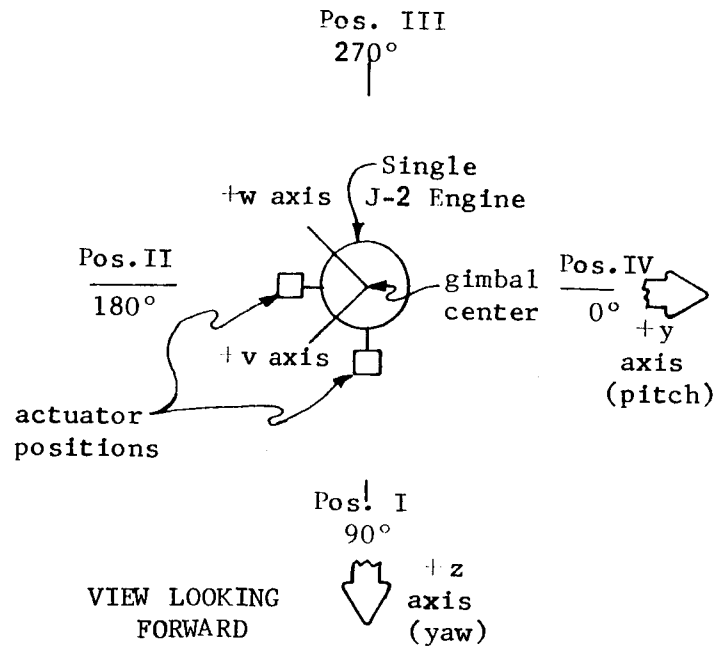


Figure 8-16. THRUST FRAME GEOMETRY, S-IVB STAGE

Table 8-22. NOMINAL VALUES AND TOLERANCES, ENGINE-TO-STAGE MOUNTING PARAMETERS, S-II STAGE

STAGE PARAMETER		CENTER ENGINE		PERIPHERAL ENGINES		
		NOMINAL	TOLERANCE		NOMINAL	TOLERANCE
GIMBAL CENTER DISPLACEMENT	x	0	$\pm .0762$ cm ( $\pm .030$ in.)	x	0	$\pm .0762$ cm ( $\pm .030$ in.)
	y	0	$\pm .1588$ cm ( $\pm .0625$ in.)	R	266.7 cm (105 in.)	$\pm .0762$ cm ( $\pm .030$ in.)
	z	0	$\pm .1588$ cm ( $\pm .0625$ in.)	$\theta$	45°, 135° 225°, 315°	$\pm 2^\circ$
ENGINE ANGULARITY	$\theta$	180°	--	XX	XXXX	XXXX
	$\Gamma$	0	--	$\Gamma$	1°	--
	$\delta$	0	22'	$\delta$	0	$\pm 22'$
	$\gamma$	0	22'	$\gamma$	0	$\pm 22'$

Table 8-23. NOMINAL VALUES AND TOLERANCES, ENGINE-TO-STAGE MOUNTING TOLERANCES, S-IVB STAGE

STAGE PARAMETER		NOMINAL	TOLERANCE
GIMBAL CENTER DISPLACEMENT	x	0	$\pm .0762$ cm ( $\pm .030$ in.)
	y	0	$\pm .635$ cm ( $\pm .250$ in.)
	z	0	$\pm .635$ cm ( $\pm .250$ in.)
ENGINE ANGULARITY	$\theta$	135°	--
	$\Gamma$	0	--
	$\delta$	0	$\pm 22'$
	$\gamma$	0	$\pm 22'$

## SECTION IX

### SUMMARY OF RESULTS

#### 9.1 GENERAL

This section summarizes the findings of the study and states the conclusions which may be drawn. The following subsections treat each of the major areas of investigation.

#### 9.2 CLASSICAL SOLUTION

- Existence

The study showed that it is possible to derive a classical probability solution to the problem of thrust vector misalignment. The solution can be made sufficiently general to apply to a wide range of engine clusters. However, a number of geometrical and statistical assumptions and restrictions are necessary to make the problem tractable.

- Form

The classical solution takes the form of a set of algebraic equations for the variances and covariances of the six thrust and moment components of an engine cluster. Each variance and covariance is expressed as an explicit function of input variances and covariances. Consequently, the classical solution infers that the output variances and covariances are independent of the input distribution shapes, provided the input variances and covariances remain fixed.



- Symmetry

The classical solution shows the existence of certain symmetry conditions. For a cluster of two engines, the line joining the two nominal gimbal points is a line of symmetry for the joint distribution of force or moment components in the gimbal plane. For a ring of three or more engines, circular symmetry exists for the joint distribution of forces or moments in the gimbal plane.

- Distribution Shapes

Except for the symmetry conditions just described, the classical solution yields no information concerning the shapes of the output distributions. However, clusters of three or more statistically identical engines tend toward normally distributed resultant thrust and moment vectors by virtue of the central limit theorem.

- Moments About Vehicle c.g.

The general solution can be extended to provide algebraic expressions for the variances and covariances of moments about a vehicle c.g. due to thrust misalignment. The c.g. location may be statistical but must be statistically independent of thrust misalignment.

### 9.3 STATISTICAL OPTIMIZATION

- Concept

The classical solution provides a means of optimizing certain cluster geometry parameters in the sense of minimizing thrust misalignment. In

September 1966

addition the classical solution can be used in optimizing the input tolerance budget on an existing cluster geometry.

- Cant Angle

An optimum cant angle exists which minimizes the variances of the pitch and yaw moments about the vehicular c.g. due to thrust misalignment in a ring of engines. However, canting of the engines may increase variances of side thrust.

- Clustering

Engines should be clustered as close to the cluster centerline as possible to minimize the variances of resultant moments.

- Center Engine

Inclusion of a center engine is advisable unless outweighed by the necessity of increasing the radius at which peripheral engines are located.

- Number of Engines

Clustering a number of small engines to achieve a given total thrust magnitude is advantageous if it is assumed that standard deviations of engine thrust and moment are proportional to rated engine thrust.

#### 9.4 MONTE CARLO SIMULATION

- Validity

The Monte Carlo simulation of thrust misalignment was accomplished with relatively few assumptions, and covers a wider range of cluster configurations than the classical solution.

- Multivariate Capability

The Monte Carlo program was designed to sample from multivariate input distributions of up to six dimensions and was verified for a bivariate distribution.

- Speed

The Monte Carlo program is extremely fast, typically requiring five minutes of IBM 7094 computer time for 1500 trials of the five-engine S-IC stage. Running time is dependent on number of engines, number of trials, and the dimensionality of input distributions.

- Double Precision

Double precision arithmetic was necessary to avoid errors due to machine roundoff, especially in handling random variables with means much larger than standard deviation.

## 9.5 ALIGNMENT REQUIREMENTS AND TECHNIQUES

The following general findings are based on examination of available documentation for the H-1, J-2, and F-1 engines and the stages on which they are used.

- Specification of Engine Thrust

Dynamic thrust generated by an engine is treated as a concentrated force vector. The position of the dynamic thrust vector is specified by two angularity components with respect to the engine centerline and two pierce

point displacement components with respect to the gimbal center. Geometric thrust vector position is specified in a similar manner. Gimbal center displacement from the engine centerline and thrust magnitude are also specified. Engine roll moment is not specified.

- Engine Adjustments

Two alignment adjustments are provided on each engine type investigated. A lateral thrust chamber adjustment is provided for correction of pierce point displacement error. Thrust vector angularity error is corrected by adjustment of actuator lengths.

- Engine Alignment Procedure

The purpose of engine alignment is to verify that the engine meets the alignment specification and, if it does not, to arrive at the necessary engine alignment adjustments. The production H-1 engine is optically aligned with no requirement to demonstrate dynamic thrust vector alignment. The J-2 engine is optically aligned and then statically test fired once to demonstrate the position of the dynamic thrust vector. No alignment changes are made based on the static test firings. The F-1 engine is dynamically aligned to null the average error of from two to four static test firings.

- Engine-to-Stage Alignment

Engine-to-stage alignment consists primarily of adjusting the actuator lengths of each engine to the lengths determined from engine alignment. Measured engine angularity with respect to the stage centerline has been preserved for some stages.

## 9.6 STATISTICAL ANALYSIS OF ENGINES AND STAGES

- Input Distributions

Sufficient measurement data were gathered to allow construction of distributions on the dynamic performance of the H-1, J-2, and F-1 engines, and on the distributions of engine mounting errors in the S-I stage.

- S-I and S-IC Solutions

Both classical and Monte Carlo solutions were obtained for resultant thrust and moment vectors of the S-I and S-IC stages. Reasonably close agreement was obtained between the two methods. In addition, the Monte Carlo simulation showed that uniform and normal input distributions with identical means and variances yield similar resultants.

## SECTION X

### RECOMMENDATIONS

#### 10.1 GENERAL

This section presents recommendations which can be made on the basis of findings from this study. Recommendations are divided into two categories, those pertaining to current alignment requirements and procedures and those pertaining to further theoretical studies which should be performed in the area of thrust misalignment.

#### 10.2 ENGINE AND STAGE ALIGNMENT

- Engine Roll Moment

None of the documentation on the three engines investigated in this study mentions roll moment generated about the engine centerline by the burning propellants. It is recommended that a dynamic engine test stand be instrumented to measure roll moment and that sufficient data be taken to furnish necessary statistical information. Specifications and requirements for demonstration of roll moment should be added to the model specification of any engine type showing a tendency to generate excessive roll moment. This would be especially important in single-engine stages such as the S-IVB, since in this case the engine roll moment is transmitted directly to the stage.

- Engine Logbooks

It is recommended that engine logbooks for engines receiving dynamic alignment tests clearly indicate the position of the measured thrust vector after final alignment. Logbooks examined under this contract were frequently confusing as to what adjustments, if any, were actually made to the engine.

Also, estimated measurement system accuracy and data reduction computer programs should be documented either directly in the logbook or in a referenced companion document.

All engine logbooks should be preserved in a central file by NASA for use in future statistical analysis.

- H-1 Engine

The production H-1 engine is optically aligned with no requirement for demonstration of the dynamic thrust vector position. As explained in the body of this report, such a procedure results in very accurate alignment of the geometric thrust vector but gives no information as to the dynamic thrust vector. It is therefore recommended that one of two possible procedural improvements be incorporated:

- (1) Perform sufficient dynamic alignment tests on the production H-1 engine to determine thrust vector position relative to the geometric thrust vector, or
- (2) Replace the present optical alignment procedure with a dynamic alignment procedure similar to that used with the F-1 engine.

- J-2 Engine

Acceptance test statistics on the J-2 engine indicate that production models have frequently exceeded the tolerance on pierce point displacement of the dynamic thrust vector. It is recommended that either the tolerance be loosened\* or that steps be taken to lower pierce point displacement errors.

\*Verbal information was obtained to the effect that pierce point displacement tolerance in the J-2 Model Specification is being relaxed to 0.4 in. from the present 0.25 in.

September 1966

If the tolerance is relaxed, it should be verified that the worst case moment about the gimbal center does not adversely affect the actuators or the stage on which the engine is used.

- F-1 Engine

The dynamic alignment procedure used for the production F-1 engine appears to give excellent results and no changes are recommended.

- Stage Alignment

Stage alignment procedures and specifications investigated appear basically sound aside from minor contradictions between assembly drawings and specifications, and no changes are recommended. However, this study revealed a serious deficiency in the area of stage alignment: a lack of available alignment data, especially on stages which have been manufactured by contractors. Of the stages investigated in this study (S-I, S-IB, S-IC, S-II, and S-IVB), sketchy alignment data were available on those S-I stages manufactured at MSFC, and little was available on any of the other stages. It is urged that immediate action be taken to collect and preserve data pertinent to thrust alignment on all future stages.

As a minimum the following geometrical quantities should be recorded at the time of post-static alignment:

1. pierce point displacement ( $R, \theta$ )
2. planar quality of pierce points ( $x$ )
3. angularity of thrust chamber centerline with respect to stage centerline ( $\delta, \gamma$ ).



Perhaps the simplest method for accomplishing this task would be to create a "stage logbook" similar to the engine logbook already in use. Stage contractors would be required to deliver a "stage logbook" along with each stage delivered. All such logbooks would be preserved in a running central file supervised by NASA. Logbooks would include all pertinent alignment measurements plus any procedural changes since alignment of the previous stage which might influence the statistical properties of the stage.

- Application to Current Flight Analysis and Prediction

Comparatively crude estimates of thrust misalignment are presently used for guidance and control system analysis and for calculation of flight vehicle trajectory dispersions. These estimates should be replaced by the more accurate results of the classical solution.

### 10.3 RECOMMENDED APPLICATIONS OF THE CLASSICAL SOLUTION

- Geometrical Optimization

The classical probability solution of thrust misalignment should be applied in optimizing the cluster geometry of stages presently in the initial design phase. Such an undertaking would serve the twofold purpose of improving the thrust alignment of the stage picked for analysis plus affording an opportunity to further extend and comprehend the optimization potential of the classical solution.

- Tolerance Optimization

The application of the classical solution to the problem of optimizing the input tolerance budget for an existing cluster geometry should be further

investigated. The feasibility of the Lagrange multiplier method proposed in subsection 5.2 should be determined by applying the method to existing Saturn stages. Alternate approaches such as linear programming could also be evaluated. The purpose would be to develop an analytical tool whereby input tolerances can be redistributed in the most economical way without degrading stage performance. If successful, such a scheme could result in substantial cost reduction in the manufacture of engines and stages.

#### 10.4 POSSIBLE EXTENSIONS TO THE CLASSICAL SOLUTION

- Uncertainty of Vehicle c.g. Location

As explained in Section IV, the classical solution can be used to calculate moments about a statistically located vehicle c.g., provided the statistical parameters of the c.g. location are known and are statistically independent of thrust alignment errors. However, no attempt was made in this study to determine the statistical nature of c.g. offset. It is suggested that a statistical analysis of c.g. uncertainty be performed in a similar manner to the thrust misalignment study.

- Time-Varying Solution

The classical solution as developed under this contract is applicable only to a stage in steady-state operation at a given flight time. It is recommended that the possibility of extending the classical solution to include the time-varying case be investigated.

SECTION XI REFERENCES

GENERAL REFERENCES

- [G1] Gantmakher, F. R. and Levin, L. M., The Flight of Uncontrolled Rockets, The McMillan Co., New York, 1964.
- [G2] Mechtly, E. A., SP-7012, The International System of Units, Physical Constants and Conversion Factors, NASA, Washington, D. C., 1964.
- [G3] Kaplan, Wilfred, Advanced Calculus, Addison-Wesley Publishing Co., Reading, Mass., 1956.
- [G4] Bradford, J., Echols, F., et al., TR-292-6-081, "Monte Carlo Simulation of the Resultant Thrust of Rocket Engine Clusters", Northrop Space Laboratories, Huntsville, Alabama, November 1966.

HARDWARE DATA REFERENCES

- [1] R-1141cS, H-1 Model Specification, Rocketdyne, 29 May 1959.
- [2] R-3620-1, H-1 Rocket Engine - Technical Manual, Rocketdyne, 10 June 1964.
- [3] RAO220-592, Rocket Engine Assemblies H1C and H1D Data Reduction and Engine Readjustment for Acceptance Test Process Specification, Rocketdyne, 24 September 1965.
- [4] 10M10017, Alignment Tolerance Block II, Saturn I Vehicles, MSFC Drawing.
- [5] 10M10017, S-I Stage Alignment, MSFC Drawing.
- [6] 10M03591, S-I Stage Alignment, Block II, MSFC Drawing.
- [7] QCI 01967, Optical Alignment, H-1 Rocket Engines to Vehicle Centerline, S-IB-4, Chrysler Corporation, 17 September 1964.
- [8] 10M04196, S-IB Stage Alignment, MSFC Drawing.
- [9] 10410031, Alignment Tolerance for Saturn Boosters, MSFC Drawing.
- [10] R-1420dS, F-1 Model Specification, Rocketdyne, 8 January 1959.
- [11] RA0620-007, Assembly and Adjustment Requirements for the F-1 Engine, Process Specification, Rocketdyne, 16 February 1965.
- [12] R-5557, F-1 Thrust Alignment Measuring System, Rocketdyne, 15 February 1964.
- [13] RAO220-167, F-1 Engine Acceptance Test Calibration and Adjustment Procedure, Rocketdyne, 21 August 1963.
- [14] 10M04146, S-IC Stage Alignment, MSFC Drawing.
- [15] R-ASTR-NFS-159-65, Thrust Alignment on S-IC, S-II, and S-IVB Stages, NASA-MSFC-Astrionics, 22 April 1965.
- [16] R-2158bS, J-2 Model Specification, Rocketdyne, 20 July 1960.
- [17] R-5845, J-2 Thrust Alignment Measurement Analysis, Rocketdyne, 14 September 1964.
- [18] RA-0201-095, J-2 Production Engine--General Outline of Specification, Process Specification, Rocketdyne, 4 February 1966.
- [19] NAO301-1002, Saturn II Stage--Engine Alignment Procedure and Requirements for, North American Aviation, 27 October 1965.
- [20] 10M04147, S-II Stage Alignment, MSFC Drawing.
- [21] 10M04148, S-IVB and Saturn V Stage Alignment, MSFC Drawing.

- [22] 10M04197, S-IVB Alignment Control (Saturn IB), MSFC Drawing.
- [23] R-3896, F-1 Rocket Engine Data Manual, Rocketdyne, 3 May 1966.
- [24] R-3825-1, J-2 Rocket Engine Data Manual Rocketdyne, 25 March 1966
- [25] RQA/M5, Optical Alignment (Basic), MSFC, November 1965.
- [26] 6-QHSI-MA-16, H-1 Engine Optical Alignment Test Procedure, Saturn I, Block II, MSFC, 26 April 1963.
- [27] RA0220-053, Rocket Engine Assembly (J2) 101716 and 103826 Thrust Alignment, Rocketdyne, 17 August 1964.
- [28] RA0220-510, J-2 Rocket Engine, Dynamic Thrust Alignment Process Specification, Rocketdyne, 15 November 1965.
- [29] R-TEST-SS-H79-66, H-1 Engine Firing Test Data Package, MSFC, 11 April 1966.
- [30] 6-QHSIC-AM-45, Alignment Test of F-1 Engine, MSFC, 8 February 1966.
- [31] IN-R-QUAL-66, Stage Alignment Test--S-IC-501, MSFC, 18 April 1966.
- [32] RA0220-601, F-1 Engine Acceptance Test Requirements and Procedures, Process Specification, Rocketdyne, 19 November 1965.
- [33] RA0201-050, Acceptance Test Instrumentation Requirements, Process Specification, Rocketdyne, 30 August 1965.
- [34] RA0201-051, Measuring Systems, Performance Analysis of, Process Specification, Rocketdyne, 12 May 1965.
- [35] RA0201-052, Calibration of Force Measuring Systems, Process Specification, Rocketdyne, 12 December 1961.
- [36] 60C30258, S-IB Stage Thrust Structure Assembly, MSFC.
- [37] 10416500, S-I Tail Section Assembly, ORD-ABMA Drawing.
- [38] 10411500, S-I Tail Section Barrell Assembly, ORD-ABMA Drawing.
- [39] M-QUAL-MM-3077-62, Manufacturing Analysis of Tail Section Assembly, Serial # Seven, SA-5 Vehicle, MSFC Drawing 30M01000, 13 August 1962.
- [40] IN-M-QUAL-61-7.1, Final Alignment Report--SA-1, MSFC, 16 August 1961.
- [41] ORDAB-DRMM, MEMO 3048-60, Manufacturing Analysis of Tail Section Assembly Drawing 10416500, Missile SA-1, ABMA, 16 June 1960.
- [42] 6-QHSI-MA-12, Alignment of the S-I Stage, MSFC.
- [43] M-QUAL-MM-3025-62, Manufacturing Analysis of the Barrel Assembly, Serial Number 7, for SA-5 Vehicle, MSFC, 2 May 1962.

- [44] 60B18054-1-900, Thrust Structure Assembly Data Package, SC501, Boeing Company, 23 June 1965.
- [45] 60B02800, Alignment--SIC Stage Control, MSFC Drawing.
- [46] J-2 Engine Alignment Experience Data Package, Rocketdyne Test Results, 23 July 1966.
- [47] F-1 Engine Alignment Experience Data Package, Rocketdyne Test Results, Undated.
- [48] IN-M-QUAL-62-9.1, Final Alignment Report--S-I-2, MSFC, 15 February 1962.
- [49] IN-M-QUAL 62-15.1, Final Alignment Report--S-I-3, MSFC, 13 September 1962.
- [50] IN-M-QUAL-62-17.7, Final Alignment Report--S-I-4, MSFC, 25 January 1963.
- [51] IN-M-QUAL 63-1.2, Final Alignment Report--S-I-5, MSFC, 16 July 1963.
- [52] IN-M-QUAL 63-2.16, Final Alignment Report--S-I-6, MSFC, 4 September 1963.
- [53] IN-M-QUAL 63-36.1, Alignment Test of H-1 Engines--S-I-8, MSFC, 28 May 1963.
- [54] ORDAB-DRMM (MEMO 3021-60), Manufacturing Analysis of Tail Section Assembly, Serial No. 1 Work Order SAT-595-3385 for Saturn Test Vehicle, ABMA, 10 February 1960.
- [55] M-QUAL-M-3003-61, Manufacturing Analysis of Tail Section Assembly, Drawing 10416500, Missile SA-2, MSFC, 17 January 1961.
- [56] M-QUAL-3024-61, Manufacturing Analysis of Tail Section Assembly, Drawing 10416500, Saturn Vehicle SA-D, MSFC, 11 April 1961.
- [57] M-QUAL-MM-3055-62, Manufacturing Analysis of Barrel Section Assembly, Serial Number Eight, SAD-5, MSFC, 28 June 1962.
- [58] M-QUAL-MM-3112-62, Manufacturing Analysis of the Barrel Assembly for SA-6, Serial Number 10, MSFC, 14 September 1962.
- [59] M-QUAL-MM-3137-62, Manufacturing Analysis of Tail Section Assembly, Serial Number 10, for SA-6 Vehicle, MSFC, 31 October 1962.
- [60] M-QUAL-MM-3002-63, Manufacturing Analyses of the Tail Section Assembly, SA-7, MSFC, 19 December 1962.
- [61] M-QUAL-MM-3157-62, Manufacturing Analysis of the Ring Assembly, Lower Thrust, for SA-9 Vehicle, Drawing 30 M02002-A, MSFC, 27 December 1962.
- [62] M-QUAL-MM-3053-63, Manufacturing Analysis of the Outrigger Assembly Thrust Support, Serial Number 3 for the SA-9 Vehicle, MSFC, 11 March 1963.
- [63] M-QUAL-MM-3087-63, Manufacturing Analysis of the Barrel Assembly, Serial Number Twelve, for SA-9 Vehicle, MSFC, 4 April 1963.

- [64] M-QUAL-MM-3188-63, Manufacturing Analysis of the Tail Section Assembly, Serial Number Twelve for the SA-9 Vehicle, MSFC, 30 July 1963.
- [65] 60B18054, Structural Assembly Thrust Structure, MSFC Drawing, 25 March 1964.
- [66] 60B32201, Structure Installation, Actuator Support and Retrorocket, MSFC, 15 November 1963.
- [67] 60B18054-1-919, Thrust Structure Assembly Data Package--SC502, Boeing Company, 15 March 1965.

## APPENDIX A

### DERIVATION OF COORDINATE TRANSFORMATIONS

#### A.1 GENERAL

This appendix contains the derivation of the coordinate transformations used in the classical solution and the Monte Carlo simulation. In addition to the general case of the canted peripheral engine, derivations for the special cases of an uncanted engine and a center engine are included. The coordinate systems and symbology used are defined in Section III of this report and will not be repeated here.

Figure A-1 shows a typical canted peripheral engine having six mounting errors: a three-dimensional error in gimbal point location and three small angle errors in orientation. The problem at hand is to find the coordinate transformation which replaces the actual force and moment vectors generated by the engine with equivalent force and moment vectors acting at the cluster origin. In addition it is necessary that the equivalent thrust and moment be expressed as vector components in the cluster coordinate system (xyz frame), and that the transformation must operate on a thrust and moment given in terms of engine coordinates (uvw frame).

In order to develop the required transformations, it is necessary to recall some rules governing the manipulation of force and moment vectors. Consider the rigid body shown in Figure A-2. Define two coordinate systems, xyz and  $x'y'z'$ , embedded in the body with vector displacement  $\vec{d}$  between their respective origins 0 and 0'. Let a vector force  $\vec{F}'$  and moment  $\vec{M}'$  act at point 0'. Now these vectors may be replaced by an equivalent force  $\vec{F}$  and moment  $\vec{M}$  acting at point 0, using the following relations:



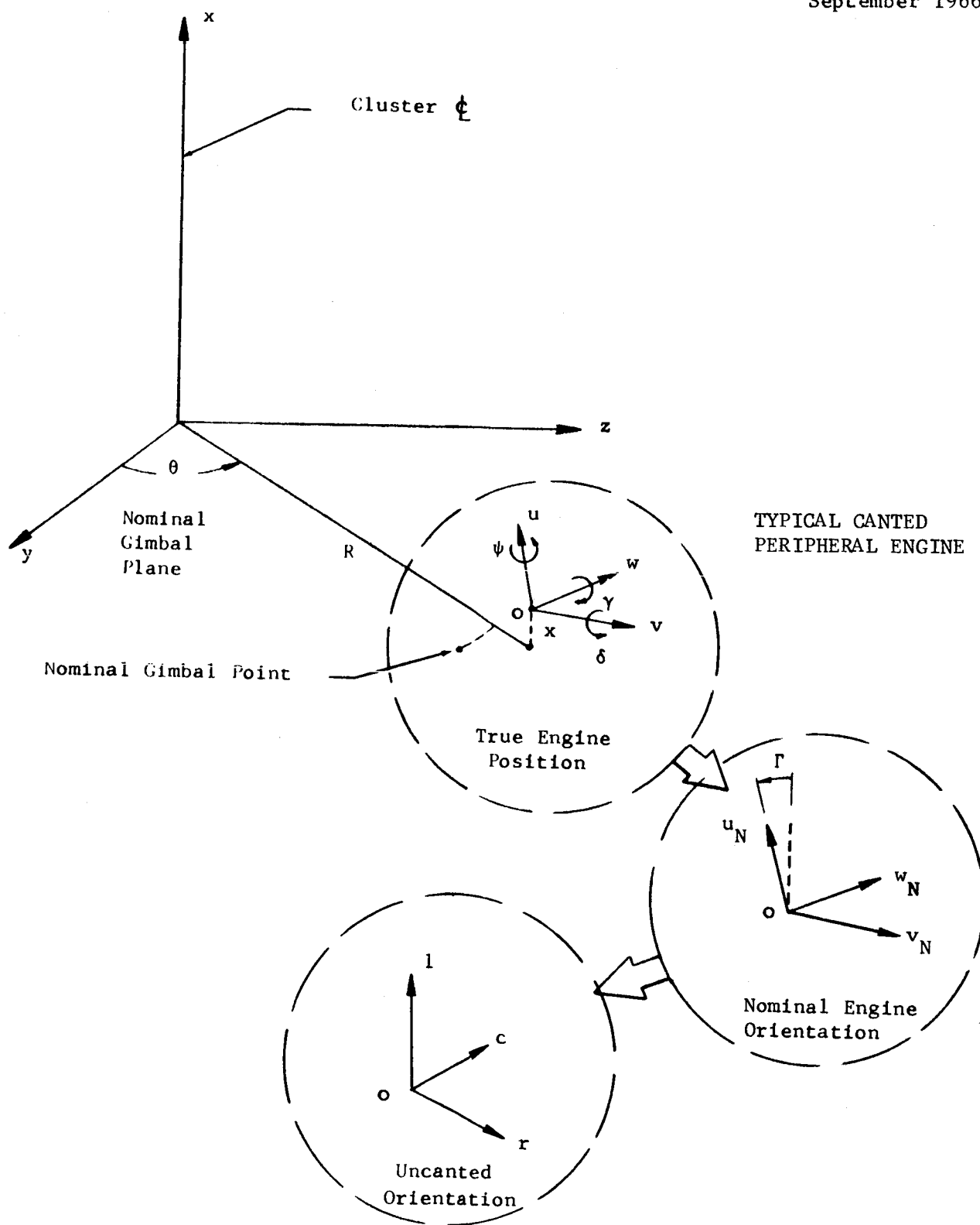


Figure A-1. COORDINATE AXES AND TRANSFORMATION SEQUENCE

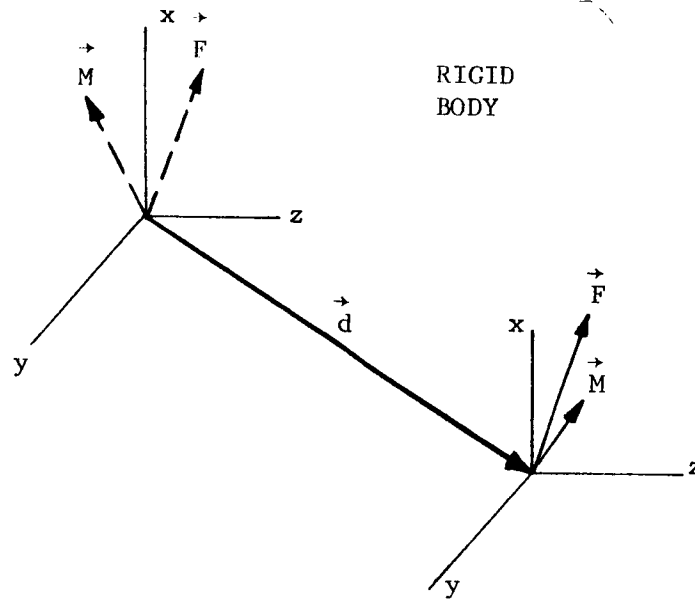


Figure A-2. TRANSFORMATION OF FORCES AND MOMENTS ACTING ON A RIGID BODY

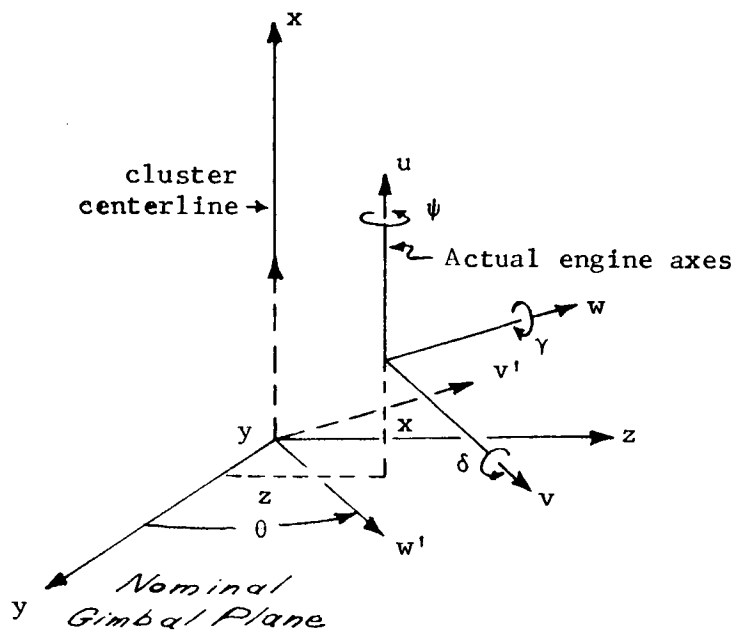


Figure A-3. TYPICAL CENTER ENGINE MOUNTING

$$\vec{F} = \vec{F}'$$

(A-1)

$$\vec{M} = \vec{M}' + \vec{d} \times \vec{F}'$$

These are the relations needed in deriving the required engine-to-cluster transformations, the primed vectors corresponding to engine thrust and moment, and the unprimed vectors corresponding to the equivalent force and moment acting at the cluster center due to that engine.

In actual practice the mechanics of the transformation shown in Figure A-2 are greatly simplified if the xyz and x'y'z' frames are parallel. Equations (A-1) then become

$$\vec{F} = \begin{bmatrix} F_x \\ F_y \\ F_z \end{bmatrix} \quad \text{where} \quad \begin{aligned} F_x &= F_{x'} \\ F_y &= F_{y'} \\ F_z &= F_{z'} \end{aligned} \quad (A-2)$$

$$\text{and} \quad \vec{M} = \begin{bmatrix} M_x \\ M_y \\ M_z \end{bmatrix} = \begin{bmatrix} M_{x'} \\ M_{y'} \\ M_{z'} \end{bmatrix} + \begin{bmatrix} d_x \\ d_y \\ d_z \end{bmatrix} \times \begin{bmatrix} F_{x'} \\ F_{y'} \\ F_{z'} \end{bmatrix} \quad (A-3)$$

$$\text{from which} \quad M_x = M_{x'} + d_y F_{z'} - d_z F_{y'}$$

$$M_y = M_{y'} + d_z F_{x'} - d_x F_{z'} \quad (A-4)$$

$$M_z = M_{z'} + d_x F_{y'} - d_y F_{x'}$$

Since the engine axes (in terms of which the engine force and moment vectors are given) are in general not parallel to the cluster axes, it is advantageous to derive the transformation in two steps: (1) Perform a rotation of coordinate axes to obtain the projections of the engine thrust and moment vectors on a coordinate system parallel to that of the cluster but centered at the

engine gimbal point. (2) Perform a translation of coordinate axes to obtain the equivalent force and moment vectors acting at the cluster center, using relations (A-2) and (A-4).

## A.2 ROTATION OF AXES

The required axis rotation is accomplished by rotating sequentially through the following axis orientations, all of which are centered at the actual engine gimbal point. (Refer to Figure A-1.)

- (1) uvw-frame: Actual engine axes (starting point),
- (2)  $u'_N v'_N w'_N$ -frame: Ideal engine orientation with  $v_N$ -axis inward  
(omitted if  $v_N$ -axis is outward),
- (3)  $u_N v_N w_N$ -frame: Ideal engine orientation with  $v_N$ -axis outward,
- (4)  $\ell rc$ -frame: Uncanted orientation (omitted if engine is already uncanted),
- (5)  $x'y'z'$ -frame: Parallel to cluster xyz-frame (end point for rotations).

### A.2.1 Small Angle Rotation

The first rotation, from uvw to  $u'_N v'_N w'_N$  consists of three small angle rotations  $\psi$ ,  $\delta$ , and  $\gamma$  about the u, v, and w axes, respectively. These angles may be thought of as the angles through which the engine would have to be rotated in order to assume its ideal orientation. Small angle approximations are made ( $\sin \alpha \approx \alpha$ ,  $\cos \alpha \approx 1$ , where  $\alpha$  is a small angle expressed in radians) and second-order terms are dropped so that the order of rotation is immaterial. These approximations are quite good for angles up to five degrees.

Let  $C$  be the desired transformation matrix. Then transformations are

$$\vec{F}_{u'N'v'N'w'N} = C \vec{F}_{uvw}$$

and

$$\vec{M}_{u'N'v'N'w'N} = C \vec{M}_{uvw}.$$

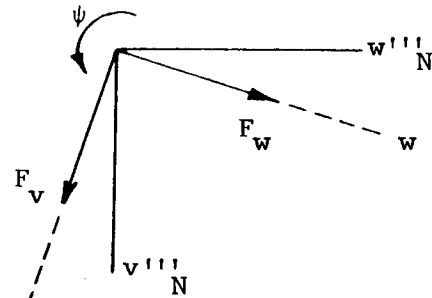
The intermediate rotations are as follows:

(1) Positive rotation  $\psi$ :

$$F_{u''''N} = F_u$$

$$F_{v''''N} = F_v + \psi F_w$$

$$F_{w''''N} = -\psi F_v + F_w$$



view looking in negative  $u$  direction

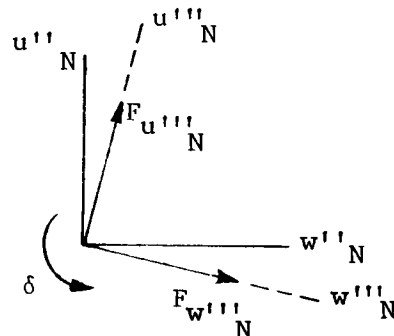
$$\therefore \begin{bmatrix} F_{u''''N} \\ F_{v''''N} \\ F_{w''''N} \end{bmatrix} = C_3 \begin{bmatrix} F_u \\ F_v \\ F_w \end{bmatrix} \quad \text{where } C_3 = \begin{bmatrix} 1 & 0 & 0 \\ 0 & 1 & \psi \\ 0 & -\psi & 1 \end{bmatrix} \quad (A-5)$$

(2) Positive rotation  $\delta$ :

$$F_{u''N} = F_{u''''N} - \delta F_{w''''N}$$

$$F_{v''N} = F_{v''''N}$$

$$F_{w''N} = \delta F_{u''''N} + F_{w''''N}$$



view looking in negative  $v'''$  direction

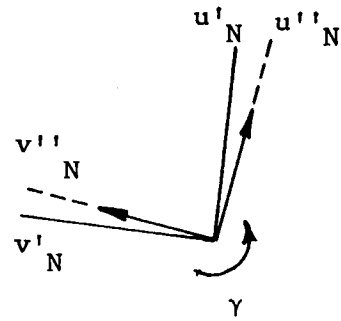
$$\therefore \begin{bmatrix} F_{u''N} \\ F_{v''N} \\ F_{w''N} \end{bmatrix} = C_2 \begin{bmatrix} F_{u''''N} \\ F_{v''''N} \\ F_{w''''N} \end{bmatrix} \quad \text{where } C_2 = \begin{bmatrix} 1 & 0 & -\delta \\ 0 & 1 & 0 \\ \delta & 0 & 1 \end{bmatrix} \quad (A-6)$$

(3) Positive rotation  $\gamma$ :

$$F_{u'N} = F_{u''N} + \gamma F_{v''N}$$

$$F_{v'N} = -\gamma F_{u''N} + F_{v''N}$$

$$F_{w'N} = F_{w''N}$$



view looking in negative  $w''_N$  direction

$$\therefore \begin{bmatrix} F_{u'N} \\ F_{v'N} \\ F_{w'N} \end{bmatrix} = C_1 \begin{bmatrix} F_{u''N} \\ F_{v''N} \\ F_{w''N} \end{bmatrix} \quad \text{where} \quad C_1 = \begin{bmatrix} 1 & \gamma & 0 \\ -\gamma & 1 & 0 \\ 0 & 0 & 1 \end{bmatrix} \quad (A-7)$$

By substitution the desired matrix is

$$C = C_1 C_2 C_3 = \begin{bmatrix} 1 & \gamma & 0 \\ -\gamma & 1 & 0 \\ 0 & 0 & 1 \end{bmatrix} \begin{bmatrix} 1 & 0 & -\delta \\ 0 & 1 & 0 \\ \delta & 0 & 1 \end{bmatrix} \begin{bmatrix} 1 & 0 & 0 \\ 0 & 1 & \psi \\ 0 & -\psi & 1 \end{bmatrix}.$$

Performing the indicated matrix multiplication,

$$C = \begin{bmatrix} 1 & \psi\delta + \gamma & \psi\gamma - \delta \\ -\gamma & 1 - \psi\delta\gamma & \delta\gamma + \psi \\ \delta & -\psi & 1 \end{bmatrix}.$$

Neglecting higher order terms the matrix reduces to

$$C \approx \begin{bmatrix} 1 & \gamma & -\delta \\ -\gamma & 1 & \psi \\ \delta & -\psi & 1 \end{bmatrix} \quad (A-8)$$

It may be verified that the order in which the rotations are performed is immaterial by showing that matrix C is unaffected by permuting  $C_1$ ,  $C_3$ , and  $C_3$  in the product.

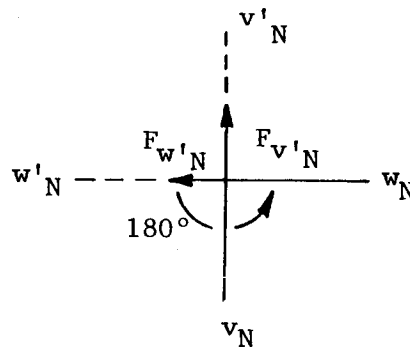
#### A.2.2 Rotation to Obtain $v_N$ -axis Outward

The conventional direction for the  $v_N$ -axis is to point away from the cluster centerline. In cases where cluster geometry dictates that this axis point inward, a  $180^\circ$  rotation of coordinates is performed about the  $u'_N$ -axis.

$$F_{u_N} = F_{u'_N}$$

$$F_{v_N} = -F_{v'_N}$$

$$F_{w_N} = -F_{w'_N}$$



view looking in negative  $u_N$  direction

$$\therefore \begin{bmatrix} F_{u_N} \\ F_{v_N} \\ F_{w_N} \end{bmatrix} = D_1 \begin{bmatrix} F_{u'_N} \\ F_{v'_N} \\ F_{w'_N} \end{bmatrix}$$

$$\text{where } D_1 = \begin{bmatrix} 1 & 0 & 0 \\ 0 & -1 & 0 \\ 0 & 0 & -1 \end{bmatrix} \quad (\text{A-9})$$

If the  $v_N$ -axis is already outward,

$$\begin{bmatrix} F_{u_N} \\ F_{v_N} \\ F_{w_N} \end{bmatrix} = D_2 \begin{bmatrix} F_{u'_N} \\ F_{v'_N} \\ F_{w'_N} \end{bmatrix}$$

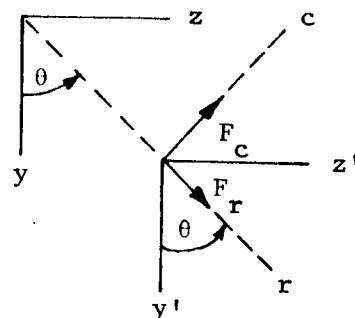
$$\text{where } D_2 = I = \begin{bmatrix} 1 & 0 & 0 \\ 0 & 1 & 0 \\ 0 & 0 & 1 \end{bmatrix} \quad (\text{A-10})$$

September 1966

$$F_{x'} = F_{\ell}$$

$$F_{y'} = F_r \cos \theta - F_c \sin \theta$$

$$F_{z'} = F_r \sin \theta + F_c \cos \theta$$

cluster  
centerview looking in negative  $\ell$  direction

$$\therefore \begin{bmatrix} F_{x'} \\ F_{y'} \\ F_{z'} \end{bmatrix} = G \begin{bmatrix} F_{\ell} \\ F_r \\ F_c \end{bmatrix} \quad \text{where} \quad G = \begin{bmatrix} 1 & 0 & 0 \\ 0 & \cos \theta & -\sin \theta \\ 0 & \sin \theta & \cos \theta \end{bmatrix} \quad (A-13)$$

### A.3 TRANSLATION OF AXES

The second step in the transformation is to obtain the equivalent force and moment vectors acting at the cluster center, given the vectors acting at the gimbal point in terms of the  $x'y'z'$  frame. Using equations (A-2) and (A-4)

$$\begin{bmatrix} F_x \\ F_y \\ F_z \end{bmatrix} = I \begin{bmatrix} F_{x'} \\ F_{y'} \\ F_{z'} \end{bmatrix}$$

$$\begin{bmatrix} M_x \\ M_y \\ M_z \end{bmatrix} = I \begin{bmatrix} M_{x'} \\ M_{y'} \\ M_{z'} \end{bmatrix} + H \begin{bmatrix} F_{x'} \\ F_{y'} \\ F_{z'} \end{bmatrix},$$

where

$$H = \begin{bmatrix} 0 & -d_z & d_y \\ d_z & 0 & -d_x \\ -d_y & d_x & 0 \end{bmatrix}.$$



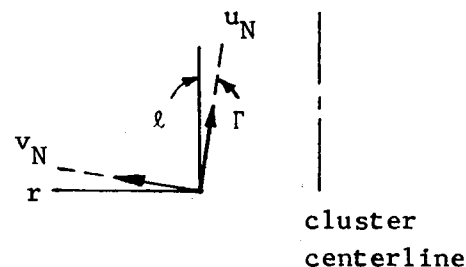
### A.2.3 Cant Angle Rotation

If the engine is canted, a rotation about the  $v_N$ -axis equal to the nominal cant angle  $\Gamma$  must be performed to obtain the vector projections in the  $\ell$ -rc-frame.

$$F_{\ell} = F_{u_N} c\Gamma + F_{v_N} s\Gamma \quad (\text{see note})$$

$$F_r = -F_{u_N} s\Gamma + F_{v_N} c\Gamma$$

$$F_c = F_{w_N}$$



view looking in negative  $w_N$  direction

$$\therefore \begin{bmatrix} F_{\ell} \\ F_r \\ F_c \end{bmatrix} = E_1 \begin{bmatrix} F_{u_N} \\ F_{v_N} \\ F_{w_N} \end{bmatrix} \quad \text{where} \quad E_1 = \begin{bmatrix} c\Gamma & s\Gamma & 0 \\ -s\Gamma & c\Gamma & 0 \\ 0 & 0 & 1 \end{bmatrix} \quad (\text{A-11})$$

If the engine is uncanted,

$$\begin{bmatrix} F_{\ell} \\ F_r \\ F_c \end{bmatrix} = E_2 \begin{bmatrix} F_{u_N} \\ F_{v_N} \\ F_{w_N} \end{bmatrix} \quad \text{where} \quad E_2 = I = \begin{bmatrix} 1 & 0 & 0 \\ 0 & 1 & 0 \\ 0 & 0 & 1 \end{bmatrix} \quad (\text{A-12})$$

### A.2.4 Theta Rotation

The last rotation of coordinates necessary to obtain a coordinate frame parallel to that of the cluster is a rotation through angle  $\theta$  about the  $\ell$ -axis.

NOTE:  $s \theta = \sin \theta$

$c \theta = \cos \theta$

From Figure 8-1 it is observed that

$$d_x = x$$

$$d_y = R \cos \theta$$

$$d_z = R \sin \theta, \text{ from which}$$

$$H = \begin{bmatrix} 0 & -R \sin \theta & R \cos \theta \\ R \sin \theta & 0 & -x \\ -R \cos \theta & x & 0 \end{bmatrix} \quad (A-14)$$

#### A.4 TOTAL TRANSFORMATION FOR A PERIPHERAL ENGINE

The total transformation for each type of peripheral engine may now be obtained by successive substitution into the approximate expressions previously derived.

##### A.4.1 Canted Peripheral Engine, $v_N$ -axis Outward

(1) Force vector:

$$\vec{F}_{xyz} = A \vec{F}_{uvw}$$

$$= I G E_1 D_2 C \vec{F}_{uvw}$$

$$\begin{bmatrix} F_x \\ F_y \\ F_z \end{bmatrix} = \begin{bmatrix} 1 & 0 & 0 \\ 0 & \cos \theta & -\sin \theta \\ 0 & \sin \theta & \cos \theta \end{bmatrix} \begin{bmatrix} c\Gamma & s\Gamma & 0 \\ -s\Gamma & c\Gamma & 0 \\ 0 & 0 & 1 \end{bmatrix} \begin{bmatrix} 1 & \gamma & -\delta \\ -\gamma & 1 & \psi \\ \delta & -\psi & 1 \end{bmatrix} \begin{bmatrix} F_u \\ F_v \\ F_w \end{bmatrix}.$$

From matrix multiplication

$$[A] \begin{bmatrix} c\Gamma - \gamma_s\Gamma & \gamma_c\Gamma + s\Gamma & \psi_s\Gamma - \delta_c\Gamma \\ -c\theta(\gamma_c\Gamma + s\Gamma) - \delta_s\theta & c\theta(c\Gamma - \gamma_s\Gamma) + \psi_s\theta & c\theta(\delta_s\Gamma + \psi_c\Gamma) - s\theta \\ -s\theta(\gamma_c\Gamma + s\Gamma) + \delta_c\theta & s\theta(c\Gamma - \gamma_s\Gamma) - \psi_c\theta & s\theta(\delta_s\Gamma + \psi_c\Gamma) + c\theta \end{bmatrix} \quad (A-15)$$

(2) Moment vector:

$$\begin{aligned} \vec{M}_{xyz} &= A \vec{M}_{uvw} + B \vec{F}_{uvw} \\ &= I G E_1 D_2 C \vec{M}_{uvw} + H I G E_1 D_2 C \vec{F}_{uvw} \\ &= A \vec{M}_{uvw} + H A \vec{F}_{uvw} \end{aligned}$$

$$\therefore B = H A = \begin{bmatrix} 0 & -R s\theta & R c\theta \\ R s\theta & 0 & -x \\ -R c\theta & x & 0 \end{bmatrix} A$$

$$[B] = \begin{bmatrix} \delta R & -\psi R & R \\ \begin{bmatrix} R s\theta(c\Gamma - \gamma_s\Gamma) \\ x[s\theta(s\Gamma + \gamma_c\Gamma) - \delta_c\theta] \end{bmatrix} + \begin{bmatrix} R s\theta(\gamma_c\Gamma + s\Gamma) \\ x[s\theta(\gamma_s\Gamma - c\Gamma) + \psi_c\theta] \end{bmatrix} & \begin{bmatrix} R s\theta(\psi_s\Gamma - \delta_c\Gamma) \\ -x[s\theta(\psi_c\Gamma + \delta_s\Gamma) + c\theta] \end{bmatrix} \\ \begin{bmatrix} R c\theta(\gamma_s\Gamma - c\Gamma) \\ -x[c\theta(\gamma_c\Gamma + s\Gamma) + \delta_s\theta] \end{bmatrix} & \begin{bmatrix} -R c\theta(s\Gamma + \gamma_c\Gamma) \\ x[c\theta(c\Gamma - \gamma_s\Gamma) + \psi_s\theta] \end{bmatrix} & \begin{bmatrix} R c\theta(\delta_c\Gamma - \psi_s\Gamma) \\ x[c\theta(\delta_s\Gamma + \psi_c\Gamma) - s\theta] \end{bmatrix} \end{bmatrix} \quad (A-16)$$

#### A.4.2 Canted Peripheral Engine, $v_N$ -axis Inward

(1) Force vector:

$$\begin{aligned} \vec{F}_{xyz} &= A \vec{F}_{uvw} \\ &= I G E_1 D_1 C \vec{F}_{uvw} \end{aligned}$$

$$A = \begin{bmatrix} 1 & 0 & 0 \\ 0 & c\theta & -s\theta \\ 0 & s\theta & c\theta \end{bmatrix} \begin{bmatrix} c\Gamma & s\Gamma & 0 \\ -s\Gamma & c\Gamma & 0 \\ 0 & 0 & 1 \end{bmatrix} \begin{bmatrix} 1 & 0 & 0 \\ 0 & -1 & 0 \\ 0 & 0 & -1 \end{bmatrix} \begin{bmatrix} 1 & \gamma & -\delta \\ -\gamma & 1 & \psi \\ \delta & -\psi & 1 \end{bmatrix}$$

$$[A] = \begin{bmatrix} c\Gamma + \gamma s\Gamma & \gamma c\Gamma - s\Gamma & -\psi s\Gamma - \delta c\Gamma \\ c\theta(\gamma c\Gamma - s\Gamma) + \delta s\theta & -c\theta(c\Gamma + \gamma s\Gamma) - \psi s\theta & c\theta(\delta s\Gamma - \psi c\Gamma) + s\theta \\ s\theta(\gamma c\Gamma - s\Gamma) - \delta c\theta & -s\theta(c\Gamma + \gamma s\Gamma) + \psi c\theta & s\theta(\delta s\Gamma - \psi c\Gamma) - c\theta \end{bmatrix} \quad (A-17)$$

(2) Moment Vector:

$$\begin{aligned} \vec{M}_{xyz} &= A \vec{M}_{uvw} + B \vec{F}_{uvw} \\ &= I G E_1 D_1 C \vec{M}_{uvw} + H I G E_1 D_1 C \vec{F}_{uvw} \\ &= A \vec{M}_{uvw} + H A \vec{F}_{uvw} \end{aligned}$$

$$\therefore B = H A = \begin{bmatrix} 0 & -R s\theta & R c\theta \\ R s\theta & 0 & -x \\ -R c\theta & x & 0 \end{bmatrix} A$$

$$[B] = \begin{bmatrix} -\delta R & \psi R & -R \\ R s\theta(c\Gamma + \gamma s\Gamma) + x[s\theta(s\Gamma - \gamma c\Gamma) + \delta c\theta] & R s\theta(\gamma c\Gamma - s\Gamma) + x[s\theta(\gamma s\Gamma - c\Gamma) - \psi c\theta] & -R s\theta(\psi s\Gamma + \delta c\Gamma) + x[s\theta(\psi c\Gamma - \delta s\Gamma) + c\theta] \\ -R c\theta(\gamma s\Gamma + c\Gamma) + x[c\theta(\gamma c\Gamma - s\Gamma) + \delta s\theta] & R c\theta(s\Gamma - \gamma c\Gamma) - x[c\theta(c\Gamma + \gamma s\Gamma) + \psi s\theta] & R c\theta(\delta c\Gamma + \psi s\Gamma) + x[c\theta(\delta s\Gamma - \psi c\Gamma) + s\theta] \end{bmatrix} \quad (A-18)$$

#### A.4.3 Uncanted Peripheral Engine, $v_N$ -axis Outward

(1) Force vector:

$$\begin{aligned} \vec{F}_{xyz} &= A \vec{F}_{uvw} \\ &= I G E_2 D_2 C \vec{F}_{uvw} \end{aligned}$$

$$A = \begin{bmatrix} 1 & 0 & 0 \\ 0 & c\theta & -s\theta \\ 0 & s\theta & c\theta \end{bmatrix} \begin{bmatrix} 1 & \gamma & -\delta \\ -\gamma & 1 & \psi \\ \delta & -\psi & 1 \end{bmatrix}$$

$$[A] = \begin{bmatrix} 1 & \gamma & -\delta \\ -\delta s\theta - \gamma c\theta & c\theta + \psi s\theta & \psi c\theta - s\theta \\ \delta c\theta - \gamma s\theta & s\theta - \psi c\theta & \psi s\theta + c\theta \end{bmatrix} \quad (A-19)$$

(2) Moment vector:

$$\vec{M}_{xyz} = A \vec{M}_{uvw} + B \vec{F}_{uvw}$$

$$\vec{M}_{xyz} = I G E_2 D_2^C \vec{M}_{uvw} + H I G E_2 D_2^C \vec{F}_{uvw}$$

$$= A \vec{M}_{uvw} + HA \vec{F}_{uvw}$$

$$\therefore B = HA = \begin{bmatrix} 0 & -Rs\theta & Rc\theta \\ Rs\theta & 0 & -x \\ -Rc\theta & x & 0 \end{bmatrix} A$$

$$[B] = \begin{bmatrix} \delta R & -\psi R & R \\ Rs\theta + x(\gamma s\theta - \delta c\theta) & \gamma Rs\theta + x(\psi c\theta - s\theta) & -\delta Rs\theta - x(\psi s\theta + c\theta) \\ -Rc\theta - x(\gamma c\theta + \delta s\theta) & -\gamma Rc\theta + x(c\theta + \psi s\theta) & \delta Rc\theta + x(\psi c\theta - s\theta) \end{bmatrix} \quad (A-20)$$

#### A.4.4 Uncanted Peripheral Engine, $v_N$ -axis Inward

(1) Force vector :

$$\vec{F}_{xyz} = A \vec{F}_{uvw}$$

$$= I G E_2 D_1^C \vec{F}_{uvw}$$

$$A = \begin{bmatrix} 1 & 0 & 0 & 1 & 0 & 0 & 1 & \gamma & -\delta \\ 0 & c\theta & -s\theta & 0 & -1 & 0 & -\gamma & 1 & \psi \\ 0 & s\theta & c\theta & 0 & 0 & -1 & \delta & -\psi & 1 \end{bmatrix}$$

$$[A] = \begin{bmatrix} 1 & \gamma & -\delta \\ \delta s\theta + \gamma c\theta & -c\theta - \psi s\theta & -\psi c\theta + s\theta \\ -\delta c\theta + \gamma s\theta & -s\theta + \psi c\theta & -\psi s\theta - c\theta \end{bmatrix} \quad (A-21)$$

(2) Moment vector:

$$\vec{M}_{xyz} = A \vec{M}_{uvw} + B \vec{F}_{uvw}$$

$$\begin{aligned} \vec{M}_{xyz} &= I G E_2 D_1 C \vec{M}_{uvw} + H I G E_2 D_1 C \vec{F}_{uvw} \\ &= A \vec{M}_{uvw} + H A \vec{F}_{uvw} \end{aligned}$$

$$\therefore B = H A = \begin{bmatrix} 0 & -R s\theta & R c\theta \\ R s\theta & 0 & -x \\ -R c\theta & x & 0 \end{bmatrix} A$$

$$[B] = \begin{bmatrix} -\delta R & \psi R & -R \\ R s\theta - x(\gamma s\theta - \delta c\theta) & \gamma R s\theta - x(\psi c\theta - s\theta) & -\delta R s\theta + x(\psi s\theta + c\theta) \\ -R c\theta + x(\gamma c\theta + \delta s\theta) & -\gamma R c\theta - x(c\theta + \psi s\theta) & \delta R c\theta - x(\psi c\theta - s\theta) \end{bmatrix} \quad (A-22)$$

#### A.4.5 Center Engine

Derivation of the transformations for a center engine is based on the coordinate system shown in Figure A-3. The small angle orientation errors and the angle  $\theta$  have the same rotation matrices as for a peripheral engine. A center engine is of course uncanted and the idea of " $v_N$ -axis inward" is not applicable. The gimbal point is ideally located at

September 1966

the cluster origin and the errors in locating the gimbal point are in terms of rectangular coordinates (x,y,z) rather than the cylindrical coordinates used for peripheral engines.

From these observations the force and moment transformations may be written directly.

(1) Force vector:

$$\begin{aligned}\vec{F}_{xyz} &= A \vec{F}_{uvw} \\ &= I G C \vec{F}_{uvw}\end{aligned}$$

$$A = \begin{bmatrix} 1 & 0 & 0 \\ 0 & c\theta & -s\theta \\ 0 & s\theta & c\theta \end{bmatrix} \begin{bmatrix} 1 & \gamma & -\delta \\ -\gamma & 1 & \psi \\ \delta & - & 1 \end{bmatrix}$$

$$[A] = \begin{bmatrix} 1 & \gamma & -\delta \\ -\delta s\theta - \gamma c\theta & c\theta + \psi s\theta & \psi c\theta - s\theta \\ \delta c\theta - \gamma s\theta & s\theta - \psi c\theta & \psi s\theta + c\theta \end{bmatrix} \quad (A-23)$$

(2) Moment vector:

$$\begin{aligned}\vec{M}_{xyz} &= A \vec{M}_{uvw} + B \vec{F}_{uvw} \\ \vec{M}_{xyz} &= I G C \vec{M}_{uvw} + H I G C \vec{F}_{uvw} \\ &= A \vec{M}_{uvw} + H A \vec{F}_{uvw}\end{aligned}$$

$$\therefore B = HA = \begin{bmatrix} 0 & -z & y \\ y & 0 & -x \\ -z & x & 0 \end{bmatrix} A$$

$$[B] = \begin{bmatrix} z(\gamma c\theta + \delta s\theta) + y(\delta c\theta - \gamma s\theta) & -z(c\theta + \psi s\theta) + y(s\theta - \psi c\theta) & z(s\theta - \psi c\theta) + y(c\theta + \psi s\theta) \\ z + x(\gamma s\theta - \delta c\theta) & \gamma z - x(s\theta - \psi c\theta) & -\delta z - x(c\theta + \psi s\theta) \\ -y - x(\gamma c\theta + \delta s\theta) & -\gamma y + x(c\theta + \psi s\theta) & \delta y + x(-s\theta + \psi c\theta) \end{bmatrix} \quad (A-24)$$



## DERIVATION OF CLASSICAL SOLUTION

## B.1 GENERAL

In this appendix a closed-form solution is derived which may be utilized to determine the distribution of moments and forces generated by random errors in an engine cluster. The transformation equations derived in Appendix A are used to relate the random errors to the resultant forces and moments. A solution is first derived for the contribution of the  $i^{\text{th}}$  peripheral engine to the variances and covariances of the resultant force and moment vectors; then by summing over  $N$  engines, where  $N \geq 2$ , a solution is derived for the variances and covariances of the resultant vectors due to a ring of  $N$  peripheral engines. In addition to the general case of a ring of peripheral engines, derivations for the special case of a center engine are included as well as a treatment of the case of a multi-ring cluster.

## B.2 FUNDAMENTALS OF TRIGONOMETRY AND PROBABILITY THEORY

In deriving the classical solution there is a need for some basic properties of the expectation operator, denoted by the symbol  $E[ ]$ , and the variances and covariances of random variables.

The following properties exist for any constant  $k$  and any random variables  $x$  and  $y$ .

$$E[k] = k \quad (B-1)$$

$$E[k \cdot x] = kE[x] \quad (B-2)$$

$$E[x \cdot y] = E[x] \cdot E[y] \quad \text{if } x \text{ and } y \text{ are independent} \quad (B-3)$$

$$E\left[\sum_{i=1}^n x_i\right] = \sum_{i=1}^n E[x_i] \quad (B-4)$$

$$\text{Var}[x] = \sigma_x^2 = E[x^2] - E[x]^2 \quad (\text{B-5})$$

$$\text{Cov}[x, y] = \sigma_{xy} = E[x \cdot y] - E[x] \cdot E[y] \quad (\text{B-6})$$

$$\text{Var} \left[ \sum_{i=1}^n x_i \right] = \sum_{i=1}^n \text{Var}[x_i] \quad \text{if } x_i \text{ and } x_j \text{ are independent for } i \neq j \quad (\text{B-7})$$

From the above properties, an expression for the  $\text{Cov} \left[ \sum_{i=1}^n x_i, \sum_{j=1}^n y_j \right]$  may be derived as follows:

$$\begin{aligned} \text{Cov} \left[ \sum_{i=1}^n x_i, \sum_{j=1}^n y_j \right] &= E \left[ \sum_{i=1}^n x_i \cdot \sum_{j=1}^n y_j \right] - E \left[ \sum_{i=1}^n x_i \right] \cdot E \left[ \sum_{j=1}^n y_j \right] \\ &= \sum_{i=1}^n \sum_{j=1}^n E[x_i y_j] - E[x_i] \cdot E[y_j] \quad \text{by (B-4)} \\ &= \sum_{i=1}^n \sum_{j=1}^n \text{Cov}[x_i, y_j] \quad \text{by (B-6)} \end{aligned}$$

and if  $x_i$  and  $y_j$  are independent for  $i \neq j$ , then

$$\text{Cov} \left[ \sum_{i=1}^n x_i, \sum_{j=1}^n y_j \right] = \sum_{i=1}^n \text{Cov}[x_i, y_i] \quad (\text{B-8})$$

In summing components for  $N$  equally spaced engines, there is also a need for identities for trigonometric functions of the following forms:

$$\sum_{k=1}^N c \left[ \frac{2\pi \cdot k}{N} \right], \quad \sum_{k=1}^N s \left[ \frac{2\pi \cdot k}{N} \right]$$

$$\sum_{k=1}^N c^2 \left[ \frac{2\pi \cdot k}{N} \right], \quad \sum_{k=1}^N s^2 \left[ \frac{2\pi \cdot k}{N} \right], \quad \text{and}$$

$$\sum_{k=1}^N c \left[ \frac{2\pi \cdot k}{N} \right] \cdot s \left[ \frac{2\pi \cdot k}{N} \right],$$

Consider Euler's identity,

$$e^{ix} = c[x] + i s[x].$$

Now

$$\sum_{k=1}^N \{c[k \cdot x] + i s[k \cdot x]\} = e^{ix} + e^{2ix} + \dots + e^{Nix} = S_n$$

$$e^{ix} S_n = e^{2ix} + e^{3ix} + \dots + e^{(N+1)ix}$$

$$e^{ix} S_n - S_n = e^{ix} (e^{Nix} - 1)$$

$$S_n = e^{ix} \frac{(e^{Nix} - 1)}{(e^{ix} - 1)} \quad (B-9)$$

Now, multiplying both numerator and denominator of equation (B-9) by  $e^{-\frac{1}{2}ix}$  gives

$$S_n = \sum_{k=1}^N c[k \cdot x] + i s[k \cdot x] = \frac{e^{(N + \frac{1}{2})ix} - e^{\frac{1}{2}ix}}{e^{\frac{1}{2}ix} - e^{-\frac{1}{2}ix}} \quad (B-10)$$

Therefore,

$$\sum_{k=1}^N c[k \cdot x] + i s[k \cdot x] = \frac{c[(N + \frac{1}{2})x] + i s[(N + \frac{1}{2})x] - c[\frac{1}{2} \cdot x] - i s[\frac{1}{2} \cdot x]}{2i s[\frac{1}{2} \cdot x]} \quad (B-11)$$

Equating real and imaginary parts, the result is

$$\sum_{k=1}^N c[k \cdot x] = \frac{s[(N + \frac{1}{2})x]}{2s[\frac{1}{2} \cdot x]} - \frac{1}{2} \quad (B-12)$$

$$\sum_{k=1}^N s[k \cdot x] = \frac{c[\frac{1}{2} \cdot x] - c[(N + \frac{1}{2})x]}{2s[\frac{1}{2} \cdot x]} \quad (B-13)$$

The desired identities may now be obtained by proper substitution in equations (B-12) and (B-13).

Let  $x = \frac{2\pi}{N}$  in equation (B-12). Then

$$\sum_{k=1}^N c\left[\frac{2\pi \cdot k}{N}\right] = \frac{s[2\pi + \pi/N]}{2s\left[\frac{\pi}{N}\right]} - \frac{1}{2}$$

$$\sum_{k=1}^N c\left[\frac{2\pi \cdot k}{N}\right] = \frac{s[2\pi] \cdot c\left[\frac{\pi}{N}\right] + c[2\pi] \cdot s\left[\frac{\pi}{N}\right]}{2s\left[\frac{\pi}{N}\right]} - \frac{1}{2}$$

$$\therefore \sum_{k=1}^N c\left[\frac{2\pi \cdot k}{N}\right] = \begin{cases} 1, & N=1 \\ 0, & N>1 \end{cases} \quad (B-14)$$

Let  $x = \frac{2\pi}{N}$  in equation (B-13). Then

$$\begin{aligned} \sum_{k=1}^N s\left[\frac{2\pi \cdot k}{N}\right] &= \frac{c\left[\frac{1}{2}\left(\frac{2\pi}{N}\right)\right] - c\left[2\pi + \frac{\pi}{N}\right]}{2s\left[\frac{\pi}{N}\right]} \\ &= \frac{c\left[\frac{\pi}{N}\right] - [c[2\pi]c\left[\frac{\pi}{N}\right] - s[2\pi]s\left[\frac{\pi}{N}\right]]}{2s\left[\frac{\pi}{N}\right]} \\ &= \frac{s[2\pi] s\left[\frac{\pi}{N}\right]}{2s\left[\frac{\pi}{N}\right]} \end{aligned}$$

$$\therefore \sum_{k=1}^N s\left[\frac{2\pi \cdot k}{N}\right] = 0, \text{ for all } N \quad (B-15)$$

To obtain the expression for  $\sum_{k=1}^N c^2\left[\frac{2\pi \cdot k}{N}\right]$  it is necessary to make use of the basic trigonometric identity of the form  $c^2[x] = \frac{1}{2} + \frac{1}{2} c[2x]$ . Then

$$\sum_{k=1}^N c^2\left[\frac{2\pi \cdot k}{N}\right] = \sum_{k=1}^N \left\{ \frac{1}{2} + \frac{1}{2} c\left[\frac{4\pi \cdot k}{N}\right] \right\}$$

or

$$\sum_{k=1}^N c^2\left[\frac{2\pi \cdot k}{N}\right] = \frac{N}{2} + \frac{1}{2} \sum_{i=1}^N c\left[\frac{4\pi \cdot k}{N}\right] \quad (\text{B-16})$$

Now, to evaluate  $\sum_{k=1}^N c\left[\frac{4\pi \cdot k}{N}\right]$ , let  $x = \frac{4\pi}{N}$  in equation (B-12). The result is

$$\begin{aligned} \sum_{k=1}^N c\left[\frac{4\pi \cdot k}{N}\right] &= \frac{s\left[4\pi + \frac{2\pi}{N}\right]}{2s\left[\frac{2\pi}{N}\right]} - \frac{1}{2} \\ &= \frac{s[4\pi] c\left[\frac{2\pi}{N}\right] + s\left[\frac{2\pi}{N}\right] c[4\pi]}{2s\left[\frac{2\pi}{N}\right]} - \frac{1}{2}, \end{aligned}$$

and substituting in (B-16) the result is

$$\begin{aligned} \sum_{k=1}^N c^2\left[\frac{2\pi \cdot k}{N}\right] &= \frac{N}{2} + \frac{1}{2} \left\{ \frac{s[4\pi] c\left[\frac{2\pi}{N}\right] + s\left[\frac{2\pi}{N}\right] c[4\pi]}{2s\left[\frac{2\pi}{N}\right]} - \frac{1}{2} \right\} \\ \therefore \sum_{k=1}^N c^2\left[\frac{2\pi \cdot k}{N}\right] &= \begin{cases} 1, & N = 1 \\ 2, & N = 2 \\ \frac{N}{2}, & N > 2 \end{cases} \quad (\text{B-17}) \end{aligned}$$

Similarly for  $s^2\left[\frac{2\pi \cdot k}{N}\right]$

$$\sum_{k=1}^N s^2\left[\frac{2\pi \cdot k}{N}\right] = \frac{N}{2} - \frac{1}{2} \sum_{k=1}^N c\left[\frac{4\pi \cdot k}{N}\right]$$

or

$$\sum_{k=1}^N s^2\left[\frac{2\pi \cdot k}{N}\right] = \begin{cases} 0, & N = 1, 2 \\ \frac{N}{2}, & N > 2 \end{cases} \quad (\text{B-18})$$

The identity for  $\sum_{k=1}^N s\left[\frac{2\pi \cdot k}{N}\right] c\left[\frac{2\pi \cdot k}{N}\right]$  may be developed in a similar manner as follows:

$$\begin{aligned}
 \sum_{k=1}^N s\left[\frac{2\pi \cdot k}{N}\right] c\left[\frac{2\pi \cdot k}{N}\right] &= \frac{1}{2} \sum_{k=1}^N s\left[\frac{4\pi \cdot k}{N}\right] \\
 &= \frac{1}{2} \frac{c\left[\frac{2\pi}{N}\right] - c[4\pi]c\left[\frac{2\pi}{N}\right] + s[4\pi]s\left[\frac{2\pi}{N}\right]}{2s\left[\frac{2\pi}{N}\right]} \\
 &= \frac{1}{2} s[4\pi] .
 \end{aligned}$$

$$\therefore \sum_{k=1}^N s\left[\frac{2\pi \cdot k}{N}\right] c\left[\frac{2\pi \cdot k}{N}\right] = 0 \quad \text{for all } N \quad (B-19)$$

Summarizing from equations (B-14) through (B-19), the results are

$$\sum_{k=1}^N c\left[\frac{2\pi \cdot k}{N}\right] = \begin{cases} 1, & N = 1 \\ 0, & N > 1 \end{cases} \quad (B-20)$$

$$\sum_{k=1}^N s\left[\frac{2\pi \cdot k}{N}\right] = \begin{cases} 0, & N \geq 1 \end{cases} \quad (B-21)$$

$$\sum_{k=1}^N c^2\left[\frac{2\pi \cdot k}{N}\right] = \begin{cases} N, & N = 1, 2 \\ \frac{N}{2}, & N > 2 \end{cases} \quad (B-22)$$

$$\sum_{k=1}^N s^2\left[\frac{2\pi \cdot k}{N}\right] = \begin{cases} 0, & N = 1, 2 \\ \frac{N}{2}, & N > 2 \end{cases} \quad (B-23)$$

$$\sum_{k=1}^N s\left[\frac{2\pi \cdot k}{N}\right] \cdot c\left[\frac{2\pi \cdot k}{N}\right] = 0, \quad N \geq 1 \quad (B-24)$$

Now, let  $\theta_1$  be the positive counter-clockwise angle between the y-axis and the radius vector to the first engine. Assuming each of  $N$  engines are equally spaced, the angle between the y-axis and a radius vector to the  $k^{\text{th}}$  engine is given by

$$\theta_k = \theta_1 + \frac{2\pi (k - 1)}{N} .$$

The identities (B-20) through (B-24) then reduce to

$$\begin{aligned}
 \sum_{k=1}^N c[\theta_1 + \frac{2\pi(k-1)}{N}] &= \sum_{k=1}^N [c\theta_1 c \frac{2\pi(k-1)}{N}] - s\theta_1 s[\frac{2\pi(k-1)}{N}] \\
 &= c\theta_1 \sum_{k=1}^N c[\frac{2\pi \cdot k}{N}] + c[0] - c[2\pi] - s\theta_1 \sum_{k=1}^N s[\frac{2\pi \cdot k}{N}] + s[0] - s[2\pi] \\
 &= c\theta_1 \sum_{k=1}^N c \frac{2\pi \cdot k}{N} - s\theta_1 \sum_{k=1}^N s \frac{2\pi \cdot k}{N} \cdot \\
 \therefore \sum_{k=1}^N c[\theta_1 + \frac{2\pi(k-1)}{N}] &= \begin{cases} c\theta_1, N = 1 \\ 0, N > 1 \end{cases} \quad (B-25)
 \end{aligned}$$

In a similar manner,

$$\sum_{k=1}^N s[\theta_1 + \frac{2\pi(k-1)}{N}] = s\theta_1 \sum_{k=1}^N c[\frac{2\pi \cdot k}{N}] + c\theta_1 \sum_{k=1}^N s[\frac{2\pi \cdot k}{N}]$$

or

$$\sum_{k=1}^N s[\theta_1 + \frac{2\pi(k-1)}{N}] = 0, N \geq 1 \quad (B-26)$$

$$\begin{aligned}
 \sum_{k=1}^N s^2[\theta_1 + \frac{2\pi(k-1)}{N}] &= \frac{N}{2} - \frac{1}{2} \sum_{k=1}^N c[2\theta_1 + \frac{4\pi(k-1)}{N}] \\
 &= \frac{N}{2} - \frac{1}{2} c[2\theta_1] \sum_{k=1}^N c[\frac{2\pi(k-1)}{N}] + \frac{1}{2} s[2\theta_1] \sum_{k=1}^N s[\frac{4\pi(k-1)}{N}] \\
 &= \frac{N}{2} - \frac{1}{2} c[2\theta_1] \sum_{k=1}^N c[\frac{4\pi \cdot k}{N}] + \frac{1}{2} s[2\theta_1] \sum_{k=1}^N s[\frac{4\pi \cdot k}{N}]
 \end{aligned}$$

or

$$\sum_{k=1}^N s^2[\theta_1 + \frac{2\pi(k-1)}{N}] = \begin{cases} s^2\theta_1, N = 1 \\ 2s^2\theta_1, N = 2 \\ \frac{N}{2}, N > 2 \end{cases} \quad (B-27)$$

In a similar fashion,

$$\sum_{k=1}^N c^2 \left[ \theta_1 + \frac{2\pi(k-1)}{N} \right] = \frac{N}{2} + \sum_{k=1}^N c^2 \theta_1 + \frac{4\pi(k-1)}{N}$$

or

$$\sum_{k=1}^N c^2 \left[ \theta_1 + \frac{2\pi(k-1)}{N} \right] = \begin{cases} c^2 \theta_1, & N = 1 \\ 2c^2 \theta_1, & N = 2 \\ \frac{N}{2}, & N > 2 \end{cases} \quad (B-28)$$

and,

$$\begin{aligned} \sum_{k=1}^N s \left[ \theta_1 + \frac{2\pi(k-1)}{N} \right] \cdot c \left[ \theta_1 + \frac{2\pi(k-1)}{N} \right] &= \frac{1}{2} \sum_{k=1}^N s \left[ 2\theta_1 + \frac{4\pi(k-1)}{N} \right] \\ &= \frac{1}{2} s[2\theta_1] \sum_{k=1}^N c \left[ \frac{4\pi \cdot k}{N} \right] + \frac{1}{2} c[2\theta_1] \sum_{k=1}^N s \left[ \frac{4\pi \cdot k}{N} \right] \end{aligned}$$

or

$$\sum_{k=1}^N s \left[ \theta_1 + \frac{2\pi(k-1)}{N} \right] \cdot c \left[ \theta_1 + \frac{2\pi(k-1)}{N} \right] = \begin{cases} s\theta_1 \cdot c\theta_1, & N = 1 \\ 2s\theta_1 \cdot c\theta_1, & N = 2 \\ 0, & N > 2 \end{cases} \quad (B-29)$$

### B.3 GENERAL ASSUMPTIONS

The nominal means of all errors are as follows:

- (1) Orientation errors:  $E[\delta] = E[\gamma] = E[\psi] = 0$ ,
- (2) Engine force components:  $E[F_v] = E[F_w] = 0$ ,  $E[F_u] = \mu_{F_u}$ ,
- (3) Gimbal mounting errors (peripheral engine):  $E[x] = 0$ ,  $E[R] = R_o$ ,  
 $E[\theta] = \theta_o$ ,
- (4) Gimbal mounting errors (center engine):  $E[x] = E[y] = E[z] = 0$ .



#### B.4 SYMMETRY ASSUMPTIONS FOR EACH ENGINE RING

- (1) Nominal engine centers are equally spaced and are the same distance from the center.
- (2) Engines have the same nominal thrust.
- (3) Covariance matrices of corresponding errors for different engines in the same ring are equal.
- (4) Cant angles for engines in the same ring are equal.

#### B.5 INDEPENDENCE ASSUMPTIONS

- (1) All engines within a ring are independent.
- (2) Each ring of engines is independent.
- (3) The force components of each engine are independent.
- (4) Orientation and gimbal point displacement errors are independent.
- (5) Orientation and engine thrust errors are independent.
- (6) Gimbal point displacement and engine thrust errors are independent.

#### B.6 APPROXIMATIONS

An approximation is made concerning the small angle  $\Delta\theta$ , where  $E[\Delta\theta] = 0$ , such that  $\cos \Delta\theta \approx 1$  and  $\sin \Delta\theta \approx \Delta\theta$ . Utilizing this small angle approximation, the following expressions may be obtained for  $E[\sin^2\theta]$ ,  $E[\cos^2\theta]$ , and  $E[\sin\theta\cos\theta]$ .

$$s\theta = s[\theta_o + \Delta\theta] = s\theta_o c\Delta\theta + c\theta_o s\Delta\theta$$

$$\approx s\theta_o + \Delta\theta c\theta_o .$$

$$\therefore E[s\theta] = s\theta_o \quad \text{where} \quad E[\Delta\theta] = 0 .$$

September 1966

$$s_{\theta}^2 \approx s_{\theta_0}^2 + \Delta\theta^2 c_{\theta_0}^2 + 2\Delta\theta s_{\theta_0} c_{\theta_0} - \Delta\theta^2 s_{\theta_0}^2$$

$$E[s_{\theta}^2] \approx s_{\theta_0}^2 + E[\Delta\theta^2] c_{\theta_0}^2 + 2E[\Delta\theta] s_{\theta_0} c_{\theta_0} - E[\Delta\theta^2] s_{\theta_0}^2.$$

Now,

$$\sigma_{\Delta\theta}^2 = \sigma_{\theta}^2 = E[\Delta\theta^2] - E^2[\Delta\theta] = E[\Delta\theta^2].$$

$$\therefore E[s_{\theta}^2] \approx s_{\theta_0}^2 + \sigma_{\theta}^2 (c_{\theta_0}^2 - s_{\theta_0}^2) \quad (B-30)$$

In a similar manner expressions may be obtained for  $E[c_{\theta}^2]$  and  $E[s_{\theta}c_{\theta}]$  as follows:

$$E[c_{\theta}^2] \approx c_{\theta_0}^2 + \sigma_{\theta}^2 (s_{\theta_0}^2 - c_{\theta_0}^2) \quad (B-31)$$

$$E[s_{\theta} \cdot c_{\theta}] \approx (1 - 2\sigma_{\theta}^2) s_{\theta_0} c_{\theta_0} \quad (B-32)$$

#### B.7 CONTRIBUTION OF $i^{\text{TH}}$ PERIPHERAL ENGINE

The random errors are related to the resultant forces and moments according to the following equations:

$$\vec{F}_{xyz} = [A] \cdot \vec{F}_{uvw} \quad (B-33)$$

$$\vec{M}_{xyz} = [A] \cdot \vec{M}_{uvw} + [B] \cdot \vec{F}_{uvw} \quad (B-34)$$

where  $[A]$  and  $[B]$  denote the matrices shown in detail in Appendix A.

The contribution of the  $i^{\text{th}}$  peripheral engine to the variances and co-variances of the resultant forces and moments may now be derived employing equations (B-5), (B-6), (B-33), and (B-34) as follows:

$$\text{Var}[\vec{F}_{xyz}] = E[( [A] \cdot \vec{F}_{uvw} )^2] - E^2[[A] \cdot \vec{F}_{uvw}] \quad (B-35)$$

$$\text{Var}[\vec{M}_{xyz}] = E[( [A] \cdot \vec{M}_{uvw} + [B] \cdot \vec{F}_{uvw} )^2] - E^2[[A] \cdot \vec{M}_{uvw} + [B] \cdot \vec{F}_{uvw}] \quad (B-36)$$

In the interest of brevity, only the derivation of the contribution to the variance of  $F_y$  will be shown. However, the same general method may be applied to obtain the contributions to the other variances and covariances of the resultant forces and moments.

From the coordinate transformations developed in Appendix A,  $F_y$  is given by the following equation:

$$F_{y_1} = F_u \cdot (-\gamma c \theta c \Gamma - c \theta s \Gamma - \delta s \theta) + F_v \cdot (-\gamma c \theta s \Gamma + c \theta c \Gamma + \psi s \theta) + F_w \cdot (\delta c \theta s \Gamma + \psi c \theta c \Gamma - s \theta) \quad (B-37)$$

Then, from the properties given in equations (B-1) through (B-4),  $E[F_{y_1}]$  is given by

$$E[F_{y_1}] = E[F_u] \cdot E[-\gamma c \theta c \Gamma - c \theta s \Gamma - \delta s \theta] + E[F_v] \cdot E[-\gamma c \theta s \Gamma + c \theta c \Gamma + \psi s \theta] + E[F_w] \cdot E[\delta c \theta s \Gamma + \psi c \theta c \Gamma - s \theta],$$

and since

$E[F_u] = \mu_{F_u}$ ,  $E[F_v] = E[F_w] = 0$ , and  $E[\gamma] = E[\delta] = E[\psi] = 0$ , the above equation reduces to

$$E[F_{y_1}] = -\mu_{F_u} c \theta_o s \Gamma \quad (B-38)$$

Now from equation (B-37),  $Fy_i^2$  is given by

$$\begin{aligned} Fy_1^2 &= Fu^2(-\gamma c \theta c \Gamma - c \theta s \Gamma - \delta s \theta)^2 + Fv^2(-\gamma c \theta s \Gamma + c \theta c \Gamma + \psi s \theta)^2 \\ &+ Fw^2(\delta c \theta s \Gamma + \psi c \theta c \Gamma - s \theta)^2 \\ &+ 2 Fu \cdot Fv(-\gamma c \theta c \Gamma - c \theta s \Gamma - \delta s \theta)(-\gamma c \theta s \Gamma + c \theta c \Gamma + s \theta) \\ &+ 2 Fu \cdot Fw(-\gamma c \theta c \Gamma - c \theta s \Gamma - \delta s \theta)(\delta c \theta s \Gamma + \psi c \theta c \Gamma - s \theta) \\ &+ 2 Fv \cdot Fw(-\gamma c \theta s \Gamma + c \theta c \Gamma + \psi s \theta)(\delta s \theta c \Gamma + \psi c \theta c \Gamma - s \theta) . \end{aligned}$$

And, noting that the force components are independent, the  $E[F_y^2]$  may be written as follows:

$$\begin{aligned}
 E[Fy^2] = & E[Fu^2] \cdot E[\gamma_c^2 \theta_c^2 \Gamma + c^2 \theta_s^2 \Gamma + \delta_s^2 \theta^2 + 2\gamma_c^2 \theta_s \Gamma c \Gamma] \\
 & \oplus \\
 & -2\gamma \delta s \theta c \theta c \Gamma + 2\delta s \theta c \theta s \Gamma] \\
 & + E[Fv^2] \cdot E[\gamma_c^2 \theta_s^2 \Gamma + c^2 \theta c \Gamma + \psi_s^2 \theta^2 - 2\gamma_c^2 \theta_s \Gamma c \Gamma] \\
 & \oplus \\
 & -2\gamma \psi s \theta c \theta s \Gamma + 2\psi s \theta c \theta c \Gamma] \\
 & + E[Fw^2] \cdot E[\delta_c^2 \theta_s^2 \Gamma + \psi_c^2 \theta c^2 \Gamma - s^2 \theta^2 + 2\delta \psi c^2 \theta s \Gamma c \Gamma] \\
 & \oplus \\
 & -2\delta s \theta c \theta s \Gamma - 2\psi s \theta c \theta c \Gamma] .
 \end{aligned}$$

Now, from equations (B-1) through (B-7) and (B-30) through (B-32), the above equation reduces to

September 1966

$$\begin{aligned}
E[Fy_i^2] = & (\sigma_{Fu}^2 + \mu_{Fu}^2) \{ (c_{\theta_o}^2 + \sigma_{\theta}^2 s_{\theta_o}^2) (\sigma_{\gamma}^2 c_{\Gamma}^2 + s_{\Gamma}^2) \\
& + \sigma_{\delta}^2 (s_{\theta_o}^2 + \sigma_{\theta}^2 c_{\theta_o}^2) + 2\sigma_{\gamma\delta} (1 - \sigma_{\theta}^2) s_{\theta_o} c_{\theta_o} c_{\Gamma} \} \\
& + \sigma_{Fv}^2 \{ (c_{\theta_o}^2 + \sigma_{\theta}^2 s_{\theta_o}^2) (\sigma_{\gamma}^2 s_{\Gamma}^2 + c_{\Gamma}^2) + \sigma_{\psi}^2 (s_{\theta_o}^2 + \sigma_{\theta}^2 c_{\theta_o}^2) \\
& \oplus -2\sigma_{\gamma\psi} (1 - \sigma_{\theta}^2) s_{\theta_o} c_{\theta_o} s_{\Gamma} \} \\
& + \sigma_{Fw}^2 \{ (c_{\theta_o}^2 + \sigma_{\theta}^2 s_{\theta_o}^2) (\sigma_{\delta}^2 s_{\Gamma}^2 + \sigma_{\psi}^2 c_{\Gamma}^2 + 2\sigma_{\delta\psi} s_{\Gamma} c_{\Gamma}) \\
& + s_{\theta_o}^2 + \sigma_{\theta}^2 c_{\theta_o}^2 \}
\end{aligned} \tag{B-39}$$

The expression for  $\text{Var}[Fy_i]$  may now be written using equations (B-5), (B-38), and (B-39)

$$\begin{aligned}
\text{Var}[Fy_i] = & E[Fy_i^2] - E^2[Fy_i] \\
= & (\sigma_{Fu}^2 + \mu_{Fu}^2) \{ (c_{\theta_o}^2 + \sigma_{\theta}^2 s_{\theta_o}^2) (\sigma_{\gamma}^2 c_{\Gamma}^2 + s_{\Gamma}^2) \\
& + \sigma_{\delta}^2 (s_{\theta_o}^2 + \sigma_{\theta}^2 c_{\theta_o}^2) + 2\sigma_{\gamma\delta} (1 - \sigma_{\theta}^2) s_{\theta_o} c_{\theta_o} c_{\Gamma} \} \\
& + \sigma_{Fv}^2 \{ (c_{\theta_o}^2 + \sigma_{\theta}^2 s_{\theta_o}^2) (\sigma_{\gamma}^2 s_{\Gamma}^2 + c_{\Gamma}^2) + \sigma_{\psi}^2 (s_{\theta_o}^2 + \sigma_{\theta}^2 c_{\theta_o}^2) \\
& \oplus -2\sigma_{\gamma\psi} (1 - \sigma_{\theta}^2) s_{\theta_o} c_{\theta_o} s_{\Gamma} \} \\
& + \sigma_{Fw}^2 \{ (c_{\theta_o}^2 + \sigma_{\theta}^2 s_{\theta_o}^2) (\sigma_{\delta}^2 s_{\Gamma}^2 + \sigma_{\psi}^2 c_{\Gamma}^2 + 2\sigma_{\delta\psi} s_{\Gamma} c_{\Gamma}) \\
& + s_{\theta_o}^2 + \sigma_{\theta}^2 c_{\theta_o}^2 \} - \mu_{Fu}^2 c_{\theta_o}^2 s_{\Gamma}^2
\end{aligned} \tag{B-40}$$

## B.8 VARIANCES AND COVARIANCES FOR A RING OF PERIPHERAL ENGINES

In order to derive expressions for the variances and covariances of the resultant forces and moments due to a ring of peripheral engines, the equations obtained as shown in subsection B.7 may be summed over  $N$  engines, where  $N \geq 2$ .

September 1966

For purposes of illustration only the expression for  $\text{Var}[F_y]$  will be derived, noting again that the same technique may be applied to obtain the expressions for the remaining variances and covariances.

From equation (B-7), the following equation for  $\text{Var}[F_y]$  may be written, since all engines in a ring are assumed to be independent.

$$\text{Var} \left[ \sum_{i=1}^N F_{y_i} \right] = \sum_{i=1}^N \text{Var}[F_{y_i}] \quad (\text{B-41})$$

Then, applying the trigonometric identities developed in subsection B.2 to equation (B-40),  $\text{Var}[F_y]$  due to a ring of 2 peripheral engines may be written as

$$\begin{aligned} \text{Var}[F_y] = & 2\{(\sigma_{Fu}^2 + \mu_{Fu}^2)\{(c_{\theta_1}^2 + \sigma_{\theta}^2 s_{\theta_1}^2)(\sigma_{\gamma}^2 c_{\Gamma}^2 + s_{\Gamma}^2) \\ & + \sigma_{\delta}^2(s_{\theta_1}^2 + \sigma_{\theta}^2 c_{\theta_1}^2) + 2\sigma_{\gamma\delta}(1 - \sigma_{\theta}^2)s_{\theta_1}c_{\theta_1}c_{\Gamma}\} \\ & + \sigma_{Fv}^2\{(c_{\theta_1}^2 + \sigma_{\theta}^2 s_{\theta_1}^2)(\sigma_{\gamma}^2 s_{\Gamma}^2 + c_{\Gamma}^2) + \sigma_{\psi}^2(s_{\theta_1}^2 + \sigma_{\theta}^2 c_{\theta_1}^2) \\ & \oplus -2\sigma_{\gamma\psi}(1 - \sigma_{\theta}^2)s_{\theta_1}c_{\theta_1}s_{\Gamma}\} \\ & + \sigma_{Fw}^2\{(c_{\theta_1}^2 + \sigma_{\theta}^2 s_{\theta_1}^2)(\sigma_{\delta}^2 s_{\Gamma}^2 + \sigma_{\psi}^2 c_{\Gamma}^2 + 2\sigma_{\delta\psi}s_{\Gamma}c_{\Gamma}) \\ & + s_{\theta_1}^2 + \sigma_{\theta}^2 c_{\theta_1}^2\} - \mu_{Fu}^2 c_{\theta_1}^2 s_{\Gamma}^2\} \quad (\text{B-42}) \end{aligned}$$

where  $\theta_1$  is the positive counter-clockwise angle between the y-axis and the radius vector to the first engine.

$\text{Var}[F_y]$  due to a ring of 3 or more peripheral engines may be written as

$$\begin{aligned} \text{Var}[F_y] = & \frac{N}{2} \{ (\sigma_{Fu}^2 + \mu_{Fu}^2)(1 + \sigma_\theta^2)(\sigma_\gamma^2 c_\Gamma^2 + s_\Gamma^2 + \sigma_\delta^2) \\ & + \sigma_{Fv}^2(1 + \sigma_\theta^2)(\sigma_\gamma^2 s_\Gamma^2 + c_\Gamma^2 + \sigma_\psi^2) \\ & + \sigma_{Fw}^2(1 + \sigma_\theta^2)(\sigma_\delta^2 s_\Gamma^2 + \sigma_\psi^2 c_\Gamma^2 + 2\sigma_\delta\psi s_\Gamma c_\Gamma + 1) \\ & - \mu_{Fw}^2 s_\Gamma^2 \} \end{aligned} \quad (B-43)$$

In summary, the following general statements can be made concerning the process of summation in order to determine the variances and covariances of the resultant forces and moments due to a ring of N peripheral engines.

- (1) If the expression for the variance or covariance due to the  $i^{\text{th}}$  peripheral engine contains no trigonometric functions of  $\theta_0$ , then the variance or covariance due to a ring of N engines, where  $N \geq 2$ , may be obtained by multiplying the entire expression by N.
- (2) If  $N = 2$  and the expression contains sine or cosine functions of  $\theta_0$ , replace  $\theta_0$  by  $\theta_1$ , and multiply the entire expression by 2. Set to zero all terms multiplied by either  $s\theta_1$  or  $c\theta_1$ , but not both.
- (3) If  $N > 2$  and the expression contains sine or cosine functions of  $\theta_0$ , replace  $s^2\theta_0$  and  $c^2\theta_0$  by  $\frac{N}{2}$ . Set all terms multiplied by  $s\theta_0$ ,  $c\theta_0$ , or  $s\theta_0 c\theta_0$  to zero.

## B.9 CENTER ENGINE

In order to derive the variances and covariances due to a ring consisting of one center engine, the transformation equations for a center engine developed in Appendix A are used to relate the random errors to the resultant forces and

moments. The expressions for the variances and covariances are then derived in exactly the same manner as outlined in subsection 8.2.7 and will not be included here.

#### B.10 MULTI-RINGED CLUSTERS

For the case of a stage with multiple rings of engines, it is possible to derive the variances and covariances associated with each ring by the techniques of the preceding sections. Then from equations (B-7) and (B-8)

$$\text{Var} \left[ \sum_{i=1}^N X_i \right] = \sum_{i=1}^N \text{Var}[X_i] \quad \text{if } X_i \text{ and } X_j \text{ are independent for } i \neq j$$

and

$$\text{Cov} \left[ \sum_{i=1}^N X_i, \sum_{j=1}^N Y_j \right] = \sum_{i=1}^N \text{Cov}[X_i, Y_i] \quad \text{if } X_i \text{ and } Y_j \text{ are independent for } i \neq j.$$

Since it is assumed that the rings are independent, expressions for the variances of the resultant forces and moments produced by a multiringed cluster may be obtained as follows:

$$\text{Var} \left[ \sum_{i=1}^{NR} \vec{F}_{x_i y_i z_i} \right] = \sum_{i=1}^{NR} \text{Var} [\vec{F}_{x_i y_i z_i}] \quad (\text{B-44})$$

$$\text{Var} \left[ \sum_{i=1}^{NR} \vec{M}_{x_i y_i z_i} \right] = \sum_{i=1}^{NR} [\text{Var} \vec{M}_{x_i y_i z_i}] \quad (\text{B-45})$$

where NR denotes the number of rings.

In a similar manner, expressions for the covariances may be obtained by adding the covariance contributions due to each ring.